Potential of Müller glia derived extracellular vesicles for retinal neuroprotection

WILLIAM DAVID BENJAMIN LAMB

Thesis submitted in partial satisfaction of the requirements for the degree of Doctor of Philosophy at the UCL Institute of Ophthalmology

University College London

September 2020

Supervisors: Professor Astrid Limb and Professor Sir Peng T Khaw

Declaration

I, William Lamb, confirm that the work presented in this thesis is my own. Where the information has been derived from other sources, I confirm that this has been indicated in the thesis.

August 2020

Acknowledgements

My prolonged experience as a student has taught me that supervisors come in many different varieties. As such, I know that I have been deeply fortunate to have Prof. Astrid Limb as mine. I am enormously grateful for her guidance and mentorship over the past four years, for being so generous with her time, and to have had the benefit of her expertise for the duration of my project.

I would like to thank my friends and colleagues in the Müller lab: Karen Eastlake, Rachel Wang, Erika Aquino, Josh Luis, and Celia Murray-Dunning, from whom I've learned so much and who've made my time as a PhD student so enjoyable. I'd like to apologise to each of them for four years of coffee grinding, apple crunching, and over-enthusiastic air conditioning.

I am greatly indebted to my second supervisor, Prof. Sir Peng Khaw, for his support and for his advice on the wider implications of my research, and Dr. Yann Bouremel for his friendship, enthusiasm, and French lessons.

I would like to thank Dr. Matt Hayes for sharing his knowledge and advice on all things imaging, and Prof. Gareth Williams at the School of Pharmacy for his kind assistance with EV characterisation.

I'm hugely grateful to Santen for funding my project, and for providing me with four years filled with unforgettable experiences, and plentiful opportunities to develop as a researcher and as a communicator of scientific ideas.

Finally I'd like to thank my parents for their constant support, and Lily – who didn't help much with the research but makes all aspects of life outside the lab significantly more enjoyable.

Abstract

Müller glia cells retain progenitor-like characteristics in the adult human eye and can partially restore visual function upon intravitreal transplantation into animal models of glaucoma. Based on observations that this effect does not depend on cell replacement of the degenerated retina, efficacy is thought to depend upon the cell transfer of neuroprotective agents to retinal ganglion cells (RGC).

In an attempt to identify candidate molecules, this work first characterised the ability of Müller glia to synthesise and secrete a range of neurotrophic growth factors. Since certain pro-inflammatory cytokines are known to be upregulated in the glaucomatous eye, this study also investigated the modulatory effects of exogenous cytokines on the expression of neurotrophin genes and proteins.

Recently it has been demonstrated that cells can communicate through the release of nano-sized membrane-bound organelles called extracellular vesicles (EV). These contain bioactive molecules that induce functional changes when internalised by recipient cells. Small and large sub-populations of EV (sEV and lEV) were purified from Müller glia cultures and their contents were characterised, revealing the enrichment of characteristic proteins and several RNA species.

Of particular interest are the findings of small non-coding microRNAs (miRNA) present in the sEV, that directly regulate gene expression through silencing of mRNA. Sequencing of miRNAs recovered from small EV subsets indicated preferential enrichment with transcripts that target genes involved in cell growth and survival, including PTEN, the master inhibitor of the AKT/mTOR pathway. On this basis, a putative mechanism for the neural pro-survival effects induced by neurotrophic factors previously ascribed to Müller glia was suggested.

Labelling of EV with a lipophilic dye confirmed the direct internalisation of these vesicles into primary RGC in culture. Since vesicle uptake has been shown to be cell type specific, it seems likely that Müller glia derived EV express membrane molecules that facilitate this internalisation, making them appealing for use as vehicles for the delivery of neuroprotective molecules to retinal neurons. Finally, Müller EV function was tested *in vivo* using a NMDA-model of RGC depletion. Adult rats receiving intravitreal delivery of $3x10^9$ small EV showed significantly improvement in RGC function when compared to vehicle control, as determined

by the negative scotopic threshold response (nSTR) of the dark-adapted electroretinogram (ERG).

Taken together, the data presented in this thesis suggests that EV represent a significant part of the neuroprotective Müller cell signalling activity, likely in addition to the release of neurotrophic growth factors. EV enriched in neuroprotective molecules may represent a more stable, and less immunogenic alternative to whole cell transplantation, particularly given their minute size and low toxicity profiles. This work provides new insight into the neuroprotective secretome of Müller glia, adding further support to previous studies demonstrating their potential utility in a cell-based glaucoma therapy.

Impact statement

Glaucoma is the most common retina neurodegenerative disease in the world, affecting approximately 64 million people, corresponding to 3.5% of the global population aged 40-80 years. Current strategies to treat glaucoma can slow the progression of optic nerve damage, but do not completely halt it, and cannot regenerate damaged tissue or restore function. Currently, stem cells are being investigated as a possible treatment for glaucoma because they have the potential to protect the optic nerve from further damage and even induce recovery of retinal function. A sub-population of Müller glia act as retinal-specific stem cells and can induce significant recovery of retina function following transplantation in animal models of glaucoma. This has been shown to be achieved by the release of neuroprotective molecules that are received by target cells in the host tissue, although the precise mechanisms of these signals are yet to be fully revealed.

It is hypothesised that extracellular vesicles (EV) - nano-sized membrane bound organelles released by eukaryotic cells - might constitute a significant component of this neuroprotective ability. The work presented in this thesis demonstrated that small EV secreted by Müller glia contain non-coding RNA molecules capable of moderating the expression of genes in recipient cells. Of particular relevance was the discovery that many of the genes targeted by these small RNAs encode proteins directly involved in the survival and plasticity of neurons, suggesting a highly plausible mechanism of therapeutic effect. Fluorescent labelling of these vesicles showed that they can be internalised by retinal neurons as well as non-neuronal retinal cells. Importantly, the current research showed a significant recovery of retinal function following injection of these EV into the vitreous of rats with degenerated retinal ganglion cells, which was comparable to the effect recorded following transplantation of the whole cells themselves.

This study is the first to investigate the nature of vesicle released by Müller glia cells, and the first to provide evidence that these organelles play a role in the communication of neuroprotective molecules to retinal ganglion neurons. This research also developed an efficient, reproducible, and scalable methodology for

collecting and purifying EV from Müller glial cells which will be valuable for future studies in the development of cell-based therapies to treat retinal degenerative diseases. The findings presented here deepen our understanding of glial – neuron interactions in the retina, and suggest a new mechanism by which Müller glia stem cells elicit neuroprotective effects following transplantation. Since EV are stable, non-immunogenic and non-replicative, those harvested from Müller cells may represent a novel therapeutic strategy for the treatment of retinal neurodegenerative conditions, bypassing many of the practical challenges that have thus-far hindered the translation of whole cell transplant to the clinic.

Table of contents

List of figures

Chapter1

Chapter 2

glaucoma therapy

List of result tables

Chapter 4

Chapter 1: General introduction and objectives

Introduction

Structure and function of the retina

The retina is a multi-layered sensory tissue that lines the back of the eye. It constitutes the third and innermost layer of the eye and consists of a coat of light-sensitive cells 0.4mm thick that lines the posterior two-thirds of the eye. The boundary between the ciliary body and the retina begins at the ora serrata, a serrated junction. At the centre of the tissue is a second boundary, the Porus Opticus, a small oval shaped area marking the entrance into the optic nerve. The optical elements within the eye focus an image onto the retina, initiating a cascade of chemical and electrical events that are ultimately received and communicated to the central nervous system (CNS) via the optic nerve. This is a paired cranial nerve located nasally and on the same plane as the anatomical centre of the retina. The optic nerve head itself is free from overlying retinal tissue, and typically measures approximately 1.75 mm vertically and 1.5 mm horizontally (Hildebrand and Fielder 2011).

The retina itself can be divided into two main sections, the neural retina (NR) and the retinal pigment epithelium (RPE). Adhered directly to the vascular choroid, the RPE is a multifunctional monolayer of hexagonal cells; densely packed with melanin pigment granules that acts as a barrier to indiscriminate diffusion between the vasculature of the choroid and the nerve cells of the retina. The RPE also plays several key roles in the maintenance and function of the retina and it's light sensitive neurons (known as photoreceptors) and includes: formation of the blood-retinal barrier, supply of nutrients to the neural retina, absorption of stray light, regeneration of visual pigment, and recycling of shed outer segments of photoreceptors (Strauss 2005).

Attached to the RPE is the first of three layers of retinal neurons, consisting of two types of photoreceptor cells known as rods and cones which are both

structurally equivalent but have specialised morphologies (fig. 1). Light enters a photoreceptor through its inner segment, and then passes into the outer segment where it is absorbed by photopigment molecules, initiating a process by which visible electromagnetic radiation is converted to nervous signal. As a sensory input, light intensity varies continuously and rapidly. When the neuron is in its resting state, the outside of the cell has an electrical potential that is 70 mV higher than that inside the cell, the resting potential. An increase of light intensity leads to photons isomerising light-sensitive 11-cis retinal in the visual pigment of a photoreceptor, which triggers the phototransduction cascade (Yau, Lamb et al. 1977). The signal is then amplified, leading to hyperpolarisation of the membrane potential through closing of cyclic-GMP gated ion channels, forcing the cell to reduce release of the excitatory neurotransmitter glutamate. Absence of signal triggers photoreceptors to increase release of glutamate, raising the membrane potential and thus initiating membrane depolarisation (Garharta and Lakshminarayananb 2015).

In the human and primate retina, the photoreceptor layer is built around an avascular zone called the central fovea which is densely packed exclusively with cone photoreceptors for high spatial, temporal and spectral resolution. Meanwhile, the more numerous rod photoreceptors are concentrated at the periphery of the retina, where their elongated architecture allows for a large area of light absorption, making them specifically adapted to produce signal in scotopic environments. Despite having very little sensitivity to colour and reduced resolution as a result of multiple cell convergence on single interneurons, the rods are capable of signalling in luminance as low as 0.03 cd/m^2, reaching full saturation at ~ 3 cd/m^2 (Kim, Lee et al. 2015).

The synaptic body of the photoreceptors is the portion that subsequently connects with neuronal cells, the horizontal and bipolar cells, which represent the next stages in the vision chain. Neural signals from the photoreceptor cells are conveyed to the bipolar cells directly or indirectly via horizontal cells, which in turn synapse with other bipolar cells or other adjacent horizontal cells (fig. 1). There

are two types of bipolar cells, both of which respond to glutamate neurotransmitter. The “ON”-center bipolar cells will depolarize and become active, whereas the “OFF”-center bipolar cells will hyperpolarize and become silent. The axons of ON-centre bipolar cells terminate in the inner half of the inner plexiform layer (IPL), where they synapse with dendrites from neurons of the third retinal layer: the retinal ganglion cells (RGCS). Similarly, OFF-centre BCs synapse with RGCs at the outer half of the IPL. RGCs are the output neurons of the retina, and they receive input from bipolar cells at ribbon synapses, via AMPA-type glutamate receptors (Jones, Pedisich et al. 2014) . ON-RGCs are excited by stimuli brighter than the “background”, while OFF- RGCs are excited by stimuli that are darker than the background (Wässle 2004). This arrangement provides a spatial processing of the visual input received from photoreceptors, and is the basis for the separate sensations of black and white (Sterling, Smith et al. 1995).

Ganglion cell dendrites branch in the IPL, but their somata are located in the ganglion cell layer, whilst their axons form the outermost strata of the retina; the nerve fibre layer (NFL) (fig. 1). At the optic disc, RGC axons converge, become myelinated, and form the optic nerve which exits the sclera through the lamina cribosa (Garharta and Lakshminarayananb 2015). Here, they continue as a series of fascicles separated by columns of astrocytes and vascular connective tissue septa. This intraorbital segment of the optic nerve extends from the eyeball to the orbit, where it becomes enveloped in meninges consisting of three layers: dura mater (outer), arachnoid (center), and pia mater (inner).

Beyond the NFL and directly adjacent to the vitreous humour is a 10μm-thick transparent boundary, formed by astrocytes and the end feet of Müller glia cells, known as the internal limiting membrane (ILM). This is primarily composed of collagen fibres, fibronectin, laminin and glycosaminoglycans (Pichi, Lembo et al. 2014). Wollensack and Spoerl identified the ILM as the most significant contributor to the biomechanical strength and plasticity of the retinal tissue, with mean strength reducing by 53% following it’s surgical removal (Wollensak and Spoerl 2004). The ILM represents the outermost boundary of the neural retina.

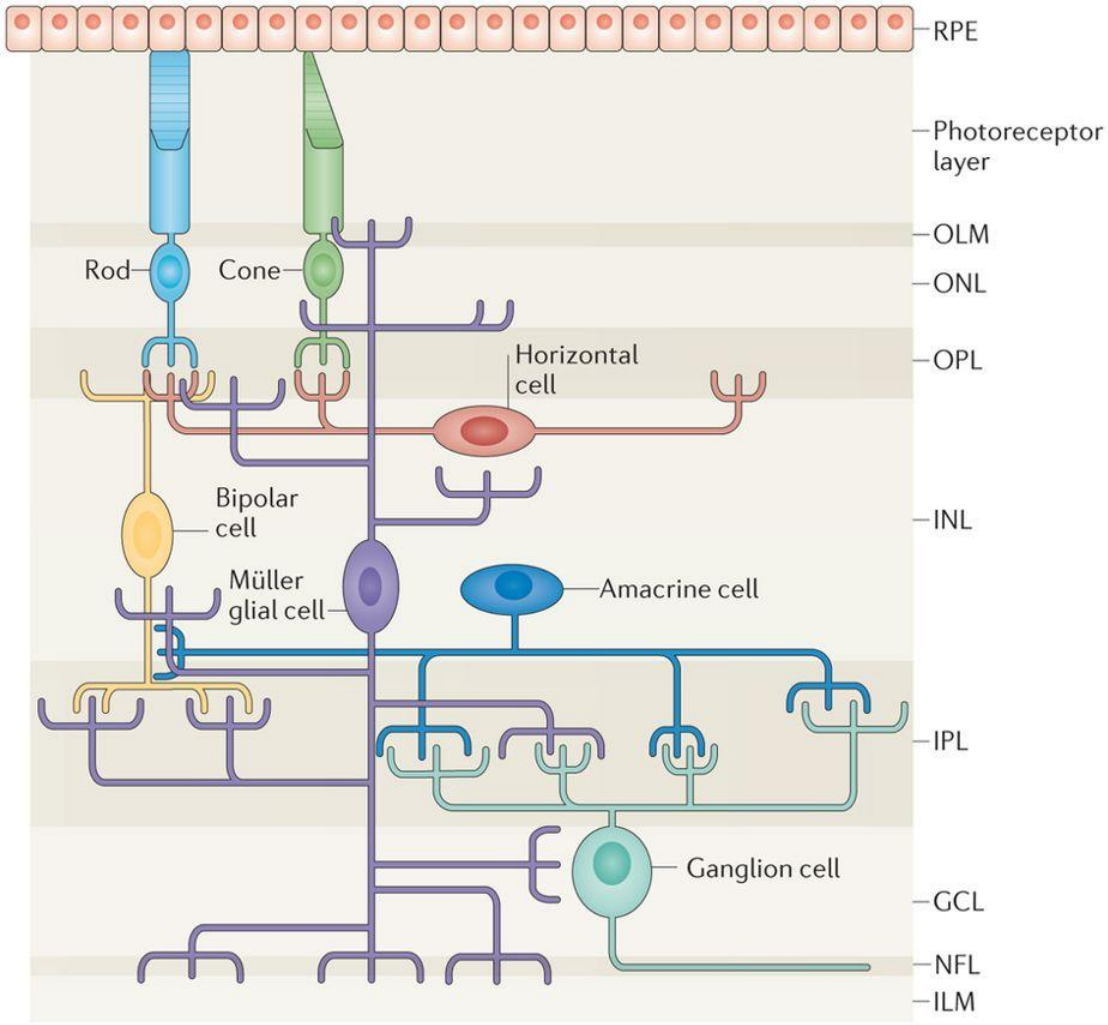

Figure 1. ***The organisation of the neural retina*** *(Goldman 2014). The nerve fibre layer (NFL) is comprised of RGC axons, which synapse with the amacrine and bipolar neurons of the inner nuclear layer (INL) at the inner plexiform layer (IPL). These cells, along with the horizontal cells, also interact with the photoreceptors that make up the outer nuclear layer (ONL) at the outer plexiform layer (OPL). The Muller glia span the entire thickness of the retina, their cell bodies positioned within the INL and their end-feet contributing towards the structures of the inner limiting membrane (ILM) and the outer limiting membrane (OLM). Beyond the OLM, the photoreceptor outer segments make contact with the pigmented cells of the retinal pigment epithelium (RPE).*

Retinal development

The retina originates from an outgrowth of the diencephalon during embryonic development (Wilson and Houart 2004). Development of the retina involves regulation of transcriptional and translational control, which is governed by intrinsic or environmental mechanisms. In humans, the process occurs between 7 and 18 weeks of gestation, and commences when a region within the ectoderm germ layer, specifically involving the anterior neural plate becomes specified as the eye field, which is characterized by the expression of a highly conserved combination of transcription factors: Rx, Six3, Six6, Pax6, Tll, Lhx2, and Tbx3 (Zuber, Gestri et al. 2003). The eye field also experiences repression of Wingless (Wnt1) and bone morphogenetic protein (BMP), through Noggin inhibition, whilst production of basic fibroblast growth factor (bFGF) and insulin-like growth factor (IGF) is enhanced (Pera, Wessely et al. 2001, Delaune, Lemaire et al. 2005). Following the induction of expression of these factors, this region separates to give origin to distinct retinal compartments, and the lateral walls of the anterior neural ectoderm evaginate to form optic vesicles. Within these vesicles are neuroblasts, multipotent retinal progenitor cells (RPCs) that have the capacity to differentiate into each of the seven types of cells born during ocular organogenesis: six types of neurons and Müller glial cells (Rodgers, Huffman et al. 2018).

The formation of the mature retina involves an evolutionary conserved production of neurons and glia by the retinal progenitors. The birth order of retinal neurons is highly conserved across species, and controlled by the synergistic action of combinations of transcription factors which yields specification to the retinal progenitor population at birth (Andreazzoli 2009). First generated are the ganglion cells, followed by horizontal cells and cone photoreceptors. Next comes differentiation of amacrine cells, rod photoreceptors, and bipolar cells, and finally Müller glia (Fuentealba, Rompani et al. 2015). The different retinal neurons are all derived from the same population of progenitors that pass through various proliferative states, gradually specifying into lineage-restricted precursor cells, which maturate into the terminally differentiated neurons during the later stages of organogenesis. Progenitors are elongated and span the final width of the

retina, while their nuclei are positioned within the central domain of what will become the retinal microenvironment. Early progenitor cells divide in a neurogenic mode, in which one daughter cell replenishes the progenitor pool, the other exits the cell cycle and differentiates into an early post-mitotic neuron. At this time, interkinetic nuclear migration, the apical–basal movement of the cell nuclei, influences selection of progenitors for cell cycle exit based on apical–basal polarized signals (Baye and Link 2007). The order by which they are generated is highly conserved, and appears to be regulated through a combination of intrinsic epigenetic alterations to the progenitor cells, combined with extrinsic changes in the signalling environment (Lonfat and Cepko 2017).

Once early RGCs are generated, they commence differentiation into mature ganglion morphologies by developing radial extensions towards the inner basal layer in a process dependent on the POU domain protein Brn-3b (Gan, Wang et al. 1999). These extensions anchor the soma into the inner lamina, whilst axonal outgrowths extend adjacent to the progenitor end feet, towards the eventual optic nerve. The later stages of retinogenesis are responsible for the production of late-born post-mitotic neurons, as well as the glial population. The late progenitors are responsible for the generation of bipolar and amacrine cells, and are similar in structure to young Müller glia, which retain an elongated bipolar morphology. In the mammalian retina, it has been suggested that the Müller glia here provide a scaffold by which “columnar units” of retinal neurons arise by migration of groups of pre-neurons along a common Müller (precursor) cell (Reichenbach, Ziegert et al. 1994).

The non-Müller glial cells, astrocytes and oligodendrocytes share a separate but common progenitor, and migrate into the retina from the brain via the optic nerve (Stone and Dreher 1987). The microglia are the last cells recruited to the retina, and are derived from myeloid precursors in the yolk sac that invade the optic nerve through the vitreous and optic nerve (Reese 2011). On conclusion of this migration and differentiation, the two plexiform-synaptic layers are formed, which separate the three nuclear layers of the retina and create the final retinal mosaic ultrastructure.

Müller glia cells and their role in the retina

First identified by Heinrich Müller in 1851, Müller glia are the principal and most abundant glial cells of the retina, comprising approximately 5% of the total cell count (Strettoi and Masland 1995). The elongated bipolar morphology of these cells is such that they span radially across the entire thickness of the retina, with the soma positioned in the INL, where they intertwine themselves between the cell bodies of the retinal neurons. In this manner, the Müller form architectural support structures throughout the retina, maintaining physical interactions with neural cells through functional processes that extend in a similar fashion to the radial glial cells of the CNS (Bringmann and Wiedemann 2012). The junctions forming the outer limiting membrane are between Müller cells themselves, as well as between Müller glia and photoreceptors, which form robust desmosomes or adherens junctions. Whilst certain species have gap junctions allowing passage of small biomolecules and ions or tight junctions at this site (Miller and Dowling 1970). These have not been recognised in higher order mammals (Reichenbach and Robinson 1995). No specialized junctions are present at the inner limiting membrane which is formed by the Müller glia basal endfoot, although the endfoot membrane is involved in exchange of molecules and biological signals between Müller cells and the vitreous via specific membrane proteins. Müller glial distal or apical processes project to the outer limiting membrane with microvilli extending into the subretinal space. These processes are enriched with organelles; golgi complexes, microtubules, multi-vesiculated bodies (MVB), and densely packed mitochondria. The highly specialized nature of Müller morphology and function means that they are enriched in many proteins that constitute their specific markers, which allow them to be distinguished from other cells of the retina and CNS. These include the filament proteins vimentin and glial fibrillary acid protein (GFAP), cytosol -associated glutamine synthetase, cellular retinaldehyde-binding protein (CRALBP), and glutamate-aspartate transporter (GLAST) (Reichenbach and Bringmann 2010).

As the sole macroglial cell type of the retina, Müller cells have multiple roles in the maintenance of retinal homeostasis, with responsibilities equivalent to those typically shared between the concerted action of oligodendrocytes, astrocytes,

and ependymal cells in the wider CNS (Reichenbach and Robinson 1995, Newman and Reichenbach 1996). Their highly specialized architecture and regular pattern throughout the retina allows these cells to form a functional, and anatomical link between retinal neurons, and the various compartments with which they must exchange molecules; the RPE and subretinal space, the retinal vasculature, and the vitreous body (Newman and Reichenbach 1996). In this way, Müller glia play a key role both the creation and maintenance of the neuroretinal architecture, and the support of neuronal survival and information processing (Newman and Reichenbach 1996).

That the Müller glia are essential for the maintenance of retinal structure and function can be evidenced from reports that selective Müller destruction causes retinal dysplasia, photoreceptor apoptosis and, ultimately, retinal degeneration and RPE proliferation (Dubois-Dauphin et al., 2000). Over the previous 30 years, the full scope and intricacies of the role of these remarkable cells in the healthy, as well as the diseased retina, has begun to be elucidated. *In vitro* and *in vivo* investigations have demonstrated the full extent of symbiotic metabolic coupling between neurons and glia cells (Tsacopoulos and Magistretti 1996). These reports have demonstrated that Müller cells are the primary site of retinal glucose metabolism, and glucose uptake during neuronal activity, as well as that energy substrates lactate/pyruvate can be mobilized from glial cells to then be oxidized in photoreceptors (Poitry-Yamate, Poitry et al. 1995). The view that emerges from similar studies highlights a pivotal role for the Müller glia in the coupling of neuronal activity to energy metabolism, and in the transfer of blood-borne glucose into metabolic products that can fuel neurons (Tsacopoulos and Magistretti 1996).

Müller glia have a key role in the formation of the blood-brain barrier, and the regulation of retinal blood flow. This is achieved through the transportation and subsequent release of neuronal potassium from the glia endfeet onto retinal arterioles, which are highly sensitive to changes in K^+ concentration (Paulson and Newman 1987, Tout, Chan-Ling et al. 1993). In a similar fashion, Müller glia are also responsible for the maintenance of ion and water homeostasis of the retinal

tissue. Under normal conditions, water accumulates in the retinal tissue for various reasons, including the uptake of nutrients from the blood and as a by-product of oxidative metabolism (Nagelhus, Horio et al. 1999). Müller dehydrate the retina through osmotically driven, transcellular currents of potassium ions which is facilitated through the enrichment of K^+ and aquaporins in their distal membranes

In addition to the maintenance of retinal homeostasis, Müller are integral to the proper synaptic activity of their associated neurons. Müller cells regulate this activity through the uptake and metabolism of extracellular neurotransmitters, including glutamate and γ-aminobutyric acid (GABA) (Bringmann, Grosche et al. 2013). Glutamate uptake by Müller cells is important to prevent the neurotoxic effects of glutamate as demonstrated by the neurodegenerative results of retinal glutamate transporter blockage (Izumi, Shimamoto et al. 2002). The uptake and metabolism of these neurotransmitters is also linked to various other functions of Müller glia cells. These include: protection against oxidative stress, metabolic support of photoreceptors and neurons, modulation of synaptic neurotransmitter activity, Ca^{2+} dependent release of gliotransmitters, and production of glutamine via the glutamine synthetase enzyme (Pow and Crook 1996).

Independent of their homeostatic role, Müller glia are similarly integral to photoreceptor function. Müller glia appear to mediate the light transfer through the vertebrate retina with minimal distortion and low loss. In this way, the Müller directly contribute to vision by acting as optical fibres, which assist in guiding light to photoreceptors (Franze, Grosche et al. 2007). This is possible due their specific optical properties; Müller cells have a highly specialised extended funnel shape, a higher refractive index than their surrounding tissue, and are oriented along the direction of light propagation. These features contribute to providing a ‘low-scatter’ passage for light from the retinal surface to the photoreceptor cells (Franze, Grosche et al. 2007). Ablation of Müller cells *in* vivo leads to photoreceptor disruption and apoptosis, hinting at the key role they play in maintaining their viability (Shen, Fruttiger et al. 2012). Müller glia are also

responsible for phagocytizing and recycling the cone chromophore, and regenerating their pigment (Wang and Kefalov 2011). A process mediated through the production of enzymes involved in the recycling of this pigment; 11-*cis* ROL and CRALBP, and the chromophores required by cone cells for the visual cycle.

Müller glia as adult stem cells

Although glial cells were originally considered to be end products of neural differentiation, with an origin very different from that of the neurons that they support, studies have since shown that some glial cells function as primary progenitors or neural stem cells (Kriegstein and Alvarez-Buylla 2009). In teleost fish, Müller cells act as radial-glial-like neural stem cells, and play a neuronal guidance role (Bernardos, Barthel et al. 2007). During normal adult growth, the Müller nuclei in the inner nuclear layer of the retina undergo self-renewing mitotic divisions, generating a rod progenitor that migrates along the radial fibres of the Müller glia into the photoreceptor layer of the outer nuclear layer. Here, the progenitor proliferates, and differentiates exclusively into rod photoreceptors (Raymond and Hitchcock 2000, Bernardos, Barthel et al. 2007).

In fish, the Müller glia are also the source of comprehensive regeneration in response to retinal damage (Hitchcock, Myhr et al. 1992, Mensinger and Powers 1999, Sherpa, Fimbel et al. 2008). In fish, Müller glia undergo reprogramming that enables regeneration in response to various retinal injuries, including those caused by mechanical damage (Fausett and Goldman 2006), intense light (Vihtelic and Hyde 2000), application of chemicals (ouabain and NMDA) (Fimbel, Montgomery et al. 2007), and even specific expression of toxic genes in neural sub-populations (Montgomery, Parsons et al. 2010). Regardless of the insult, Müller in the immediate vicinity of the damage become activated, leading to their partial dedifferentiation, a process that has been demonstrated to depend on Wnt signalling (Ramachandran, Zhao et al. 2011). These activated Müller express retinal progenitor and stem cell markers, re-enter the cell cycle undergoing interkinetic nuclear migration, and divide once in an asymmetric, self-renewing

division to generate a retinal progenitor (Goldman 2014). This daughter cell proliferates rapidly to form a compact neurogenic cluster surrounding the Müller glia; these multipotent retinal progenitors then migrate along the radial fibre to the appropriate lamina to replace missing retinal neurons (Thummel, Kassen et al. 2008).

Although mammalian Müller glia have some characteristics that are intrinsically different to those of their fish counterparts, it is also evident that certain regenerative properties are evolutionarily conserved, and these cells have a stem cell-like potential that may be dormant under the constraints of the non-neurogenic mammalian retinal environment (Das, Mallya et al. 2006). Although no evidence of spontaneous regeneration has been detected in the mammalian retina, Müller glia do respond to injury and disease by altering their morphology, biochemistry and physiology, in a process commonly referred to as reactive gliosis (Bringmann, Iandiev et al. 2009). In some instances this response may include proliferation, although the precise triggers are still poorly understood (Pasha, Münch et al. 2017). After injury, gliotic Müller cells can protect neurons from further damage and preserve tissue function via the secretion of beneficial antioxidants and neurotrophic factors (Honjo, Tanihara et al. 2000, Bringmann, Pannicke et al. 2006). However, prolonged gliosis is considered detrimental because it interferes with retinal homeostasis and the ability of Müller glia to support retinal neurons, ultimately contributing to neurodegeneration (Bringmann, Pannicke et al. 2006). For example, vascular endothelial growth factor (VEGF) secreted by activated Müller glia can enhance neuron survival, while also exacerbating disease progression by inducing vascular leakage and neovascularization (Bai, Ma et al. 2009).

Evidence for the stem cell like properties of glial cells in mammals is provided by studies investigating the role of radial glia in the development of the mouse brain. Here, these cells have been shown to play a neural-stem cell role, repopulating both the neural cell populations as well as the glial population itself (Merkle, Tramontin et al. 2004). In adult tissue, the same radial glial cells give rise to adult

subventricular zone stem cells that continue to produce neurons throughout adult life. Other pools of glia within the CNS have also shown neural stem cell traits. Bergmann glia housed in the cerebellum of adult mice express the neural stem cell markers Sox1 and Sox2 (Sottile, Li et al. 2006). Müller cells morphologically and biochemically resemble radial glia, and there is direct evidence for their dormant stem cell-like characteristics and neurogenic potential in higher vertebrates. This is illustrated in a study in which a subset of Müller that had been retrospectively enriched from the rat retina were found to form self-renewing neurospheres of proliferating multipotent progenitors in culture (Das, Mallya et al. 2006). These had the potential to generate all three basic cell types of the CNS, as well as the potential to generate retinal neurons, both in vitro and in vivo (Das, Mallya et al. 2006). The authors determined that the activation of Wnt and Notch pathways in activated Müller glia mediated this neurogenic potential, as is the case elsewhere in the CNS (Androutsellis-Theotokis, Leker et al. 2006, Michaelidis and Lie 2008).

Like most adult stem cells, human Müller glia appear to be multipotent and therefore tissue specific and restricted to producing different retinal cell subtypes. Immortalised cells cultured in vitro express progenitor markers Sox2, Pax6, Chx10 and Notch1, and are able to differentiate into a variety of retinal neurons, which in turn express distinctive neural markers (Lawrence, Singhal et al. 2007). These include; peripherin, a marker of photoreceptors, Protein Kinase, a marker of bipolar cells, calretinin, a marker of both amacrine and horizontal cells along with Brn3b; an early marker of committed RGC precursors (Lawrence, Singhal et al. 2007, Bhatia, Jayaram et al. 2011, Singhal, Bhatia et al. 2012). Together, this data further clarifies the progenitor-like characteristics of Müller glia, raising the potential for their use as a tool in stem-cell based therapies for diseases affecting the neurons of the eye.

Retinal neurodegeneration

Retinal degeneration is a pathophysiological feature of diseases affecting the posterior segment of the eye. According to the latest estimates from the World Health Organisation (Flaxman, Bourne et al. 2017), retinal degenerative

conditions account for >20 million of the world's blind population. In developed countries such as the United Kingdom, where blindness caused by cataract is rare, degenerative diseases like glaucoma, diabetic retinopathy and age-related macular degeneration are more prominent. In most optic neuropathies, vision loss occurs due to progressive neuronal atrophy and dysregulation, and resulting interruption to visual phototransduction. In certain pathological conditions neurodegeneration is secondary to, or exacerbated by, problems with the ocular vascular system. Either through abnormal angiogenesis or increased permeability of vessels, resulting in leakage or macular oedema (Nentwich and Ulbig 2015). Regardless of underlying cause, the final common pathway of these diseases appears to include a particular type of metabolic stress, leading to insufficient supply of nutrients to the respective target structures in the retina or optic nerve. Currently, pharmacological interventions used to treat these disorders are aimed at slowing their progression, but in many cases, progression cannot be halted, and patients may go on to develop total and permanent visual loss. There is a need therefore, for new therapeutic strategies capable of preventing, or even reversing damage to the retina and restoring sight.

Glaucoma

Glaucoma is an optic neuropathy involving structural damage of the optic nerve, death of retinal ganglion cells (RGCs), and defects of the visual field. The optic nerve, formed by the clustering of axons from RGCs located in the ganglion cell layer of the retina, carries visual impulses from the eye to the brain (Vrabec and Levin 2007). When optic nerve damage or deterioration disrupts the transfer of information, vision loss occurs. In advanced glaucoma cases the optic nerve head takes on an excavated appearance, thought to be caused by death of the ganglion cells and subsequent loss of their axons (Bengtsson 1976).

The primary injury to axons is the result of various interdependent factors, chief among which are elevated intraocular pressure (IOP), structural changes due to ageing, and high blood pressure. Cell death can also follow changes in the extracellular milieu surrounding the damaged neurons. In particular, there is a

secondary, slower, progressive injury in which the neighbouring neurons are affected by trans-synaptic degeneration (Vrabec and Levin 2007). This hypothesis may explain why IOP lowering therapy is often ineffective in preventing the progression of visual impairment in patients with glaucoma (Kong, Gibbins et al. 2019).

Open angle glaucoma (OAG), the most common form, is a chronic and progressive optic nerve disease that is likely to be affected by multiple genetic and environmental factors (Weinreb, Leung et al. 2016). Excessive fluid pressure develops within the eye due to various reasons including blockage of drainage ducts, and narrowing or closure of the angle between the iris and cornea. In the glaucomatous retina these are proceeded by the appearance of structural damage at the optic nerve head, including neuro-retinal rim thinning, cupping of the optic disc, and sectoral retinal nerve fibre layer (NFL) thinning, which indicates the pathological progression of the disease (Weinreb, Leung et al. 2016). Electroretinogram (ERG) is normal in glaucoma, indicating non-involvement of photoreceptor and bipolar/Müller's cells (Ventura and Porciatti 2006). These observations are supported by histopathological studies showing that, in glaucoma, retinal ganglion cells and axons die, while no other neurons are visibly affected. The death of RGCs represents, therefore, the final common pathway in glaucomatous optic neuropathy (Quigley, Addicks et al. 1981, Quigley, Nickells et al. 1995, Guo, Moss et al. 2005)

Apoptosis of retinal ganglion cells

Ganglion cell death in the context of glaucoma has been well characterised in both experimental models and clinical cases (Quigley, Nickells et al. 1995, Okisaka, Murakami et al. 1997). In both cases, it was observed that RGCs died with the distinct morphologic and biochemical features characteristic of apoptosis: inter-nucleosomal DNA fragmentation, chromosome clumping, cell shrinkage and membrane compartmentalization and blebbing, followed by complete fragmentation of the cell into large membrane bound compartments called apoptotic bodies (Fink and Cookson 2005). In contrast to necrosis, which

is a form of traumatic cell death resulting from acute injury, apoptosis is a highly regulated and active process that results in an orderly self-destruction, and follows a final common pathway regardless of the initiating trigger.

There is currently no consensus on the precise sequence of events that stimulate RGC apoptosis in the glaucomatous retina. A range of mechanisms have been proposed, but the some of the outstanding issues in glaucoma pathogenesis including whether the primary site of RGC damage is in the cell soma, or axons are still unresolved, as are the intricacies of the relationship between raised IOP and disease progression. Despite this, the use of new and better models of optic nerve injuries and experimental glaucoma have allowed insight into some of the key interactions underlying RGC apoptosis including neurotrophin insufficiency (Pease, McKinnon et al. 2000), amplification of free radical generation by stressed neurons (Nguyen, Alexejun et al. 2003), glutamate excitotoxicity from dysfunctional glia (Vorwerk, Gorla et al. 1999), and increased secretion of pro-inflammatory cytokines by activated glia (Tezel 2008).

The role of neurotrophic factor deprivation in glaucoma pathology

One of the more well established mechanisms underlying the pathogenesis of RGC loss is the obstruction of transport of key neurotrophic factors along axons at the optic nerve head (Knox, Eagle et al. 2007, Fahy, Chrysostomou et al. 2016). The dimensions of the RGC axon are such that it is limited in terms of machinery to synthesize the proteins and organelles required for cell survival and metabolic balance. As a result, the majority of these components are manufactured in the cell body and transported in an anterograde manner toward the distal synapse, by a series of kinesin-dependent molecular motors (Li, Jung et al. 2012). Meanwhile, retrograde transport allows for the clearance of waste metabolites and misfolded or aggregated proteins, as well as the delivery of trophic signals from the distal axon to the cell body (Nuschke, Farrell et al. 2015). Blockage and obstruction of axonal transport by ischaemia or increased IOP appears to be an initial step along the pathway ultimately culminating in glaucomatous RGC death,

as evidenced by studies tracking radiolabelled neurotrophins and their receptors in *in vivo* models of elevated IOP (Pease, McKinnon et al. 2000, Quigley, McKinnon et al. 2000).

The dependence of RGCs on neurotrophic factors is evident during optic nerve development, where RGCs extend neurites along the visual pathway towards neurotrophin-secreting targets in the brain (Meyer-Franke, Kaplan et al. 1995). During this process, projections that do not receive sufficient growth factor signalling are culled through the activation of apoptosis pathways, to ensure proper formation of the optic nerve. This relationship appears to be maintained in the adult tissue, where RGCs receive ongoing survival signals delivered in a retrograde fashion from targets in the CNS (Iwabe, Moreno-Mendoza et al. 2007).

It is logical therefore, that interruption to this delivery and withdrawal of neurotrophin support plays a major role in axonal loss in the glaucomatous retina, but it is unlikely to be the only cause of RGC degeneration. Clinical conditions do exist in which RGCs survive despite the longstanding loss or reduction in axonal transport, for example papilledema. In addition, even prolonged delivery of brain-derived neurotrophic factor (BDNF) and its tropomyosin receptor kinase (TrkB) to axotomized RGCs is unable to keep RGCs alive long-term, implying the contribution of secondary apoptotic factors (Di Polo, Aigner et al. 1998).

Stem cell-based therapies for glaucoma treatment

If diagnosed during early stages, retinal degenerative conditions like glaucoma can often be controlled or delayed by existing surgical and pharmacological interventions. However, these treatments do not restore lost neural function and are of limited effectiveness in many patients due to aggressive disease, unresponsiveness to treatment or late detection. There is therefore the need to establish new therapies to prevent blindness and restore vision. The transplantation of stem cells, may be one such strategy, as suggested by studies undertaken in experimental models of glaucoma-like disease.

Initially, work in the field of stem-cell therapeutics raised hopes that degenerated neural tissue could simply be replaced by grafted pluripotent cells, however the synaptic remodeling of neural circuits observed during retinal degeneration results in a complex disruption of the neural network in which integration of transplanted cells quickly proved challenging (Jones, Watt et al. 2003). It has been suggested that some residual plasticity exists in early stage disease, which may offer a window for transplantation-based approaches; although here the replacement of unidirectional neurons like photoreceptors, is potentially more feasible than the replacement of RGCs in glaucoma, which involve complex afferent inputs and distant synapses (MacLaren and Pearson 2007). The first studies involving transplantation to repair damage to retinal tissue involved the grafting of full foetal retina (Aramant and Seiler 1991), or cells dissociated from new-born retina (del Cerro, Notter et al. 1989), and although these studies report some level of integration into host tissue, no evidence of functional recovery was found. Recent developments in the field of stem cell biology, including the establishment of pluripotent stem cell lines, have inspired new strategies for the use of these cells for retinal protection and recovery from neurodegeneration.

Originally, stem cell-based strategies proposed the delivery of cells to damaged tissues either in suspension, or attached to biomaterial substrate scaffolds (Tomita, Lavik et al. 2005, Sodha, Wall et al. 2011, McHugh, Saint-Geniez et al. 2013). The therapeutic benefit of these interventions was presumed, therefore, to rely on the migration, *in* situ differentiation, and subsequent integration of these cells into the degenerated host architecture. Evidence supporting this hypothesis in the eye was initially provided by *in vivo* experiments involving the transplant of photoreceptors tagged with green fluorescent protein (GFP), which were found to be able to integrate into the host retina by forming synaptic connections and improve visual function (MacLaren, Pearson et al. 2006, West, Pearson et al. 2008, Homma, Okamoto et al. 2013). However, it was subsequently demonstrated that the GFP signals observed in the host retina were not as a result of transplanted cell integration, but due instead to biomaterial exchange between donor and host photoreceptors (Pearson, Gonzalez-Cordero et al. 2016, Ortin-Martinez, Tsai et al. 2017). This exchange was further confirmed by a study

showing that following transplantation of tdTomato labelled cells into the subretinal space of Nrl-eGFP mice, double fluorescent labelling of host cells could be detected (Santos-Ferreira, Llonch et al. 2016). Together, these reports suggest that the therapeutic benefits commonly reported following the transplant of pluripotent cells into degenerated tissue are as a result of their ability to provide trophic support to remaining and partially damaged cells. In this way, grafted cells could be considered as potential "factories" for the production and release of pro-survival signals such as neurotrophic factors and antioxidants that are capable of protecting retinal neurons and preserving their function.

Given this paracrine mechanism of action, various cell sources have been explored for their ability to improve visual function in experimental models of retinal degeneration through the release of pro-survival molecules. Rat and human bone marrow-derived MSCs (BMSC) that had been induced to secrete high levels of BDNF, GDNF and VEGF, and transplanted into the vitreous, exert a marked neuroprotective effect in rat eyes after optic nerve transection (Levkovitch-Verbin, Sadan et al. 2010). The efficacy of BMSC transplantation has also been attributed to secretion of platelet-derived growth factor (PDGF-AA) (Mead and Scheven 2015). Based on this collective evidence, neuroprotective factors produced by long-lived stem cells transplanted into the glaucomatous eye may have the potential to maintain and repair retinal function in a sustained fashion, possibly by releasing active neurotrophins and antioxidant molecules, or by releasing extracellular vesicles (cellular organelles) containing active regulatory molecules that promote neural repair and protection upon their uptake by damaged neurons.

Strategies for retinal neuroprotection

Reduction of IOP is currently the only therapy approved by regulatory agencies for the treatment of glaucoma. Reducing IOP helps prevent glaucoma in individuals at risk, however in many patients visual field loss due to loss of RGCs continues despite pressure reduction. Neuroprotection is the term used to

describe any intervention intended to slow or prevent the death of neurons, and has been a long-standing objective of clinical and basic neuroscience for the treatment of neurodegenerative conditions in the eye and throughout the CNS. In the context of glaucoma, neuroprotection refers specifically to therapies designed to protect the optic nerve and prevent death of RGCs directly, as opposed to interventions based upon the disease process. Because functional injury to the RGCs appears to precede the onset of structural damage (Fortune, Bui et al. 2004), it is likely that a recovery would restore their function. This may be achieved either by attenuating the hostility of the glaucomatous environment, or supplying the cells with molecules or agents that allow them to overcome cytotoxic conditions.

The pathophysiology of glaucoma is such that a number of physiological events converge to induce RGC loss: IOP elevation, ischemia, oxidative stress, neurotrophic growth factor deprivation and glutamate neurotoxicity. These variable mechanisms equate to a wide potential for neuroprotective targets and in recent years, researchers have investigated a number of compounds that can protect RGCs via targeting the aforementioned pathways. These include delivery of neurotrophins and anti-apoptotic genes by viral vector overexpression (Martin, Quigley et al. 2003, Malik, Shevtsova et al. 2005), inhibition of the generation of amyloid β (Clark, Wang et al. 2006), inhibition of glutamate receptor (Guo, Salt et al. 2006, Yücel, Gupta et al. 2006), use of free radical scavengers (Parisi, Centofanti et al. 2014), blockade of apoptosis with overexpression of an inhibitor (Ju, Kim et al. 2009), and use of a TNF α inhibitor (Bae, Lee et al. 2016). Despite promising data demonstrating the successful attenuation of RGC loss in mammalian glaucoma models, none of these has yet been definitively translated into a clinical treatment. As is typical of chronic neurodegenerative conditions, there are several factors that contribute to the challenges glaucoma presents for effective neuroprotective treatment. These include the long and gradual disease course and the variability in progression rate between patients, which greatly hinders the ability of researchers to determine that a change in outcome or improvement in progressive worsening, has been achieved.

Neurotrophic factors

A wealth of data collected from studies using a wide range of glaucoma models suggest neurotrophins and neurotrophic factors to be strongly neuroprotective, whilst promoting axon regeneration and enhancing neuronal cell function. In addition, it is known that blockade of axonal transport induced by IOP elevation leads to deficits of the levels and availability of these factors and subsequent RGC death, and that expression of BDNF and NGF in serum is significantly reduced in early and moderate forms of the disease (Oddone, Roberti et al. 2017). Given this promise, as well as the regenerative capabilities of neurotrophin-mediated interventions already observed in preclinical models of other neurodegenerative diseases, neurotrophic factors offer an attractive neuroprotective option to pursue in glaucoma.

In rats, adeno-associated viral delivery of bFGF and BDNF can promote RGC survival following glutamate insult (Schuettauf, Vorwerk et al. 2004), whist CNTF treatment significantly reduces RGC loss in a laser-photocoagulation model (Ji, Elyaman et al. 2004) as well as in a mouse optic-nerve crush model (Müller, Hauk et al. 2009). There is also very compelling evidence for RGC neuroprotection by nerve growth factor (NGF), both experimentally and in the clinic. Treatment with recombinant NGF delivered via eye drops in 3 patients with advanced glaucoma improved all parameters of visual function after 6 months (Lambiase, Aloe et al. 2009), and is currently undergoing clinical trial in a cohort of 60 patients with POAG (NCT02855450). Currently in phase II clinical trial is an implantable polymeric device developed by Neurotech Pharmaceuticals (Cumberland, Rhode Island, USA), which contains a genetically modified human cell line that secretes CNTF, allowing for a sustained and long-term delivery to the retina (NCT02862938). This approach may hold great promise for circumventing some of the barriers to long-term sustained delivery of neuroprotective agents to the retinal neurons (Williams and Tao 2009).

The neurotrophin family

Although several different classes of neurotrophic growth factors have been investigated for their efficacy in models of neurodegeneration, considerable emphasis has been placed upon the neurotrophin family, as it is known that obstruction to the retrograde transport of BDNF to RGC soma is a characteristic feature of raised IOP (Quigley, McKinnon et al. 2000). In addition, immunolocalization studies suggest that the BDNF receptor, TRKB, accumulates in the optic nerve head (Pease, McKinnon et al. 2000).

Key to the control of survival, prosper, and maintenance of neurons throughout the CNS and neural retina, the neurotrophin family of growth factors consists of nerve growth factor (NGF); brain-derived neurotrophic factor (BDNF); neurotrophin 3 (NT-3); and neurotrophin 4 (NT-4). Each derived from a common ancestral gene, the neurotrophins are highly conserved, trophic and mitogenic secreted proteins that play a role in the development, differentiation, connectivity and survival of neurons (West, Pruunsild et al. 2014). The regulatory influence of neurotrophins is mediated through two independent classes of receptors: the Trk family of high-affinity tropomyosin-kinase receptors initiate pro-survival signals, while the lesser understood low-affinity p75 receptor appears to propagate pro-apoptosis signals (Chao and Hempstead 1995, Casaccia-Bonnefil, Gu et al. 1999). The Trks are transmembrane proteins that feature several structural motifs shared with other tyrosine kinase receptors; including an intracellular kinase domain and immunoglobulin-like domains in their extracellular domains (Patapoutian and Reichardt 2001). TRK receptor activation of downstream survival signalling pathways include both extracellular signal-regulated kinases (ERK) and AKT.

The p75 receptor is the archetypal member of the TNF superfamily of receptors (Baker and Reddy 1998). This 27-strong group is comprised of type I membrane proteins sharing extracellular cysteine-rich domains, with a more variable region in the intracellular portion responsible for protein-protein interactions. Each neurotrophin binds with high-affinity to its cognate Trk receptor, while all

neurotrophins bind to p75 with low affinity. Recently it has been postulated that secreted pro-neurotrophins can also bind to P75 with high affinity (Fahnestock, Michalski et al. 2001). While p75 signalling is complex, it is generally considered to include the downstream activation of JUN N-terminal kinases (JNK), and is coupled to the mitochondrial apoptotic pathway (Lebrun-Julien, Morquette et al. 2009).

Neurotrophin genes are expressed as large (130kDa) pro-polypeptides that undergo extensive post-transcriptional processing (García, Forster et al. 2002). There is some debate in the literature as to whether the neurotrophins, particularly NGF, are released in pro or mature forms, with the general consensus that it is likely to be a combination of both, in an activity-dependent manner (Bruno and Cuello 2006). (Fahnestock, Michalski et al. 2001). Soluble neurotrophins dimerize, assuming a characteristic elongated shape, as a result of the association of two pairs of antiparallel beta strands which are maintained by a large cysteine knot motif (West, Pruunsild et al. 2014). These structural motifs are highly conserved among different members of the family, despite their unique signalling specificity.

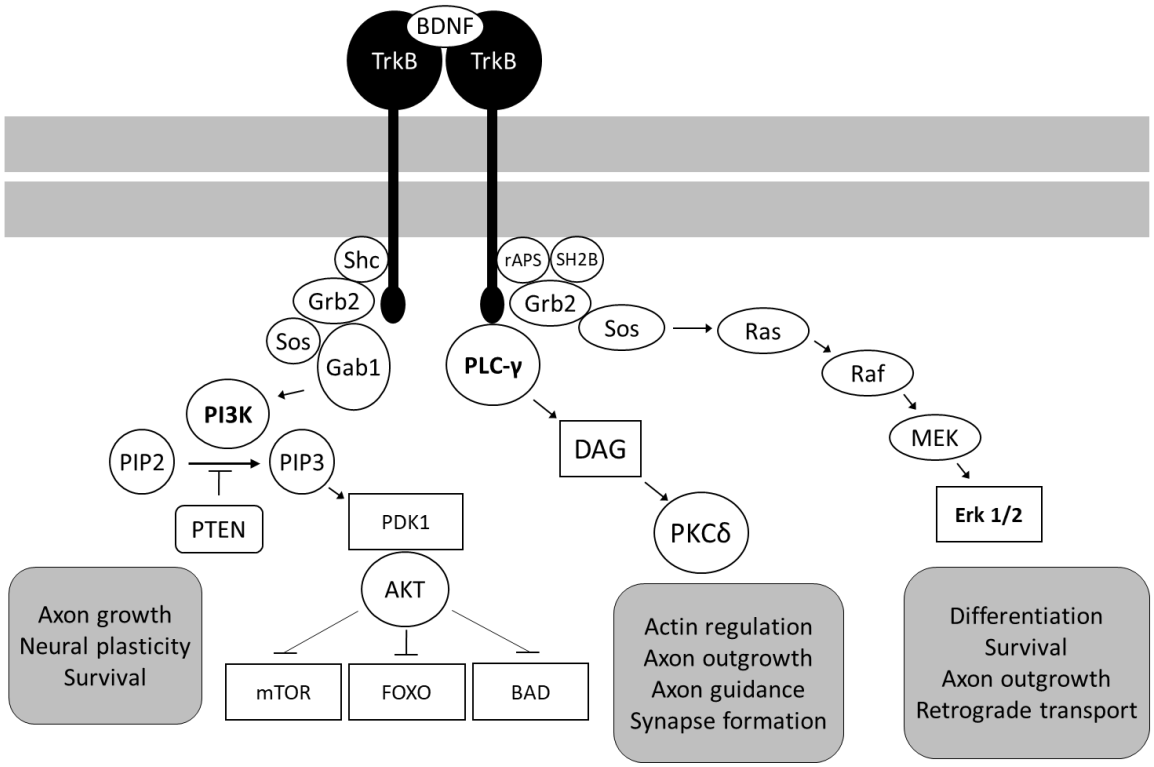

Figure 2. ***Growth and survival signalling cascades excited through neurotrophin and neurotrophic factor ligand binding.*** *Binding of a neurotrophin (e.g. BDNF) to it's high-affinity Trk receptor leads to dimerization of the two receptor monomers, and subsequent phosphorylation of their kinase domains. Once the receptor is activated, numerous cell survival and outgrowth cascades are initiated including MAP kinase, PI3K-akt, and PLCγ .*

Nerve growth factor

NGF was first identified almost 60 years ago with the discovery that a humoral agent produced by some mouse malignant tumours would, when implanted into the chick embryo, markedly upregulate the growth of (sensory and sympathetic nerve cells (Cohen and Levi-Montalcini 1957). NGF is the archetypal and prototypic neurotrophin, with properties and functions that define the neurotrophic family of growth factor polypeptides that exercise critical influence in key developmental events in the nervous system, from regulation of growth, to modulation of cell apoptosis, maintenance, proliferation, as well as the survival of certain target neurons. NGF signals with high-affinity through the TrkA receptor, and plays a pivotal role during the development, maintenance, and regeneration

of sensory neurons in the PNS and cholinergic neurons of the CNS, both in development and throughout adulthood (Roberti, Mantelli et al. 2014). NGF-sensitive neurons appear to express both the high- and low-affinity NGF receptors, despite the fact that these pathways are typically considered antagonistic. In reality, TrkA and p75 signalling appears to be synergistic, independent, or antagonistic in a manner that has not been reported for TrkB or TrkC (Freund-Michel, Bertrand et al. 2006).

In the eye, NGF and TrKA are typically expressed in the anterior segment; the vitreous, iris, ciliary body, cornea, and lens (Bonini, Aloe et al. 2002). During retina development, NGF and TrKA are highly expressed and influences neuronal outgrowth, survival, and selective apoptosis. In the retina under normal conditions, NGF is produced and utilized by the Müller glia, and in an autocrine fashion, the RGCs and bipolar neurons.

NGF is upregulated, and apparently therapeutic, in models of retinal injury or disease. Following peripheral nerve injury, macrophages infiltrate the nerve and release cytokines, which induce the synthesis of NGF in Schwann cells and fibroblasts within the injured nerve (Raff, Barres et al. 1993). Following optic nerve transection and ischaemic injury, it has been demonstrated that intravitreal injection of recombinant NGF inhibits RGC apoptosis in the rabbit, and that while exogenous application of NGF reduces retinal damage in a model of ocular hypertension, NGF antibody appears to exacerbate it (Lambiase, Centofanti et al. 1997). More recently, topical application of NGF to the eyes of rats with elevated intraocular pressure and glaucoma-type symptoms has been reported to rescue deficits in basal level NGF and TrkA in brain visual centres, and recombinant NGF eye drops are currently undergoing clinical trial (Sposato, Parisi et al. 2009, Groth 2018).

Brain-derived neurotrophic factor

BDNF shares approximately 50% amino acid sequence homology with NGF, and

despite being the second member of the neurotrophin family to be revealed, is the most widely expressed and well-characterized member in the mammalian nervous system (Barde, Edgar et al. 1982). BDNF signals with high affinity through the TrkB receptor, both of which are highly abundant throughout the CNS during development, where it has been associated with the differentiation, maturation, and survival of neurons, as well as synapse formation (Henderson 1996). Postpartum, BDNF levels increase dramatically in the brain, and robust, sustained expression of the factor appears to be essential for the suppression of apoptotic pathways and the ongoing prosperity of neural tissue (Katoh-Semba, Takeuchi et al. 1997). In adult mammals, the highest levels of BDNF mRNA and protein are found in the hippocampus, amygdala, cerebral cortex and hypothalamus, although there are very few compartments where BDNF transcripts are not detected (Webster, Herman et al. 2006).

The importance of sustained BDNF signalling through adulthood can be interpreted from its associations with a range of neurodegenerative disorders. To date, decreased BDNF has been implicated in the pathology of Alzheimer's disease, dementia, Parkinson's disease, type 2 diabetes mellitus, schizophrenia, chronic stress, and Huntington's disease (Phillips, Hains et al. 1991, Ferrer, Goutan et al. 2000, Howells, Porritt et al. 2000, Murakami, Imbe et al. 2005, Krabbe, Nielsen et al. 2007, Lee, Lange et al. 2011).

BDNF has also been associated with retinal degeneration, specifically in the context of glaucoma. Developing sensory and sympathetic neurons undergo apoptosis when deprived of retrograde BDNF and TrkB delivery, which has also been postulated as a mechanism of RGC depletion in experimental glaucoma (Oppenheim 1991, Pease, McKinnon et al. 2000). Studies have also highlighted the role of BDNF signalling in the preservation of retinal homeostasis during both normal and glaucoma-like states in heterozygous mouse mutants. Compared to wild-type, reduced BDNF mutants had functional, morphological and molecular degenerative changes in the inner retina caused by age as well as upon exposure to experimental glaucoma caused by increased intraocular pressure (Gupta, You

et al. 2014).

Understandably, these associations have generated considerable interest in the potential of exogenous or endogenous BDNF as a therapeutic, both in the retina and in the wider CNS. A host of literature supports the efficacy of BDNF as neuroprotective and potentially neurotrophic agent. The application of exogenous BDNF to the superior colliculus reduces developmental cell RGC death, and the addition of recombinant and endogenous factor to primary RGCs prolongs their survival in culture to isolated RGC prolongs their survival in culture (Castillo Jr, Del Cerro et al. 1994, Ma, Hsieh et al. 1998, Rohrer, LaVail et al. 2001). Multiple studies indicate that intravitreal injection of BDNF prolongs survival or rescues damaged RGC survival *in vivo* (Mey and Thanos 1993, Ikeda, Tanihara et al. 1999, Mo, Yokoyama et al. 2002)

Neurotrophins 3 and 4

Neurotrophins 3 and 4 (NT-3 and NT-4), are the most recently discovered and less scrutinized members of the neurotrophin family (Maisonpierre, Belluscio et al. 1990, Hallböök, Ibáñez et al. 1991). Whilst NT-3 signals through a third cognate Trk receptor, TrkC, NT-4 is a ligand for the TrkB receptor that it shares with BDNF (Lamballe, Klein et al. 1991). NT-3 has been demonstrated to promote the differentiation and support the survival of neuroblasts derived from the neural crest in early development (Zhou, Cameron et al. 1998). It also appears that the differentiation and survival of a subpopulation of large sensory neurons after their axons arrive at their targets is also dependent on presence of NT-3, and sympathetic neurons require NT3 for survival in the late developmental period (Tafreshi, Zhou et al. 1998). Unlike other members of the neurotrophin family, NT-3 also binds with low affinity to TrkA and TrkB which seems to be highly conserved and relevant to it's role in the mature nervous system (Ivanisevic, Zheng et al. 2007). For instance, during development NGF and NT-3 act in a co-ordinated manner to select TrkA-expressing sympathetic neurons (Tessarollo, Tsoulfas et al. 1997). In addition, the sympathetic neurons from NGF and NT-3 null mice die when expressing high TrKA and negligible TrkC (Glebova and Ginty 2005).

NT4 is the most recently discovered neurotrophin in mammals and its biological role is not fully understood (Hallböök, Ibáñez et al. 1991). While neurotrophin genetic knockout typically proves lethal during early postnatal development, NT-4 null mice show minor cellular deficits and develop normally to adulthood, suggesting that the action of NT-4 is not based upon essential neuron maintenance (Ibáñez 1996). NT4 knockout mice have recently been reported to require NT3 in early postnatal development and NT4 later in mature animals for survival of sensory neurons(Gillespie, Crair et al. 2000). NT-4 infusion into the visual cortex alters responses and blocks the effect of monocular deprivation in cat during the critical period. Even after responses to the deprived eye are adversely affected, NT-4 infusion is able to restore them (Gillespie, Crair et al. 2000). Little is known about the pattern of NT-3 and NT-4 expression in the healthy mammalian retina, however immunohistochemical investigation of high-IOP rat retina indicated a reduced signal for NT-4 at both the optic nerve head and the inner retinal layers, suggesting obstruction to it's delivery in the glaucomatous retina (Johnson, Deppmeier et al. 2000).

Neuroinflammation in the glaucomatous retina

An increasing body of literature implicates neuroinflammation, here defined as immune responses specifically relevant to the CNS, may be a key process in glaucoma progression (Xu, Chen et al. 2009, Soto and Howell 2014). In particular, *in vivo* models of ganglion cell degeneration involving artificially elevated IOP, suggest that inflammatory components may directly link increased IOP and ischemia with RGC loss (Tezel, Li et al. 2001, Nakazawa, Nakazawa et al. 2006, Li, Luna et al. 2007, Wang, McNatt et al. 2008). Investigation of the pathophysiological mechanisms at play in these models is hampered somewhat by a relatively long delay in RGC death following onset, and by considerable inter-individual variability. Adding further complexity is the fact that both ocular inflammation (uveitis), and the treatment of inflammatory conditions with steroids can lead to glaucoma as a result of obstruction in drainage structures in the anterior segment, which occurs secondary to ocular inflammation (Siddique,

Suelves et al. 2013, Baneke, Lim et al. 2016). Despite this, evidence does suggest that prolonged glial activation, and sustained release of pro-inflammatory cytokines in the glaucomatous retina may lead to a failure in the regulation of stress-induced immune response (Tezel 2013). Collectively, these studies suggest that innate immune cells, autoreactive T cells, autoantibodies, and excess complement attack have neurodegenerative activity in glaucoma and may be capable of harming RGC somas, axons, and synapses (Kuehn, Kim et al. 2006, Joachim, Reichelt et al. 2008, Wax, Tezel et al. 2008).

Inflammatory cytokines

Cytokines tumour necrosis factor alpha (TNFα) and transforming growth factor beta (TGFβ) are two neuroinflammation modulators for which there is strong evidence of involvement in glaucoma. Despite expression of the TGFβ gene being typically minimal in the healthy optic nerve, 70–100-fold greater TGFβ2 immunoreactivity has been reported in the glaucomatous optic nerve head, implying post-transcriptional regulation of TGF-β mRNA (Pena, Taylor et al. 1999). A subsequent study in primates supported these findings, adding that glaucomatous eyes had stronger expression of TGFβ1 and β2 in the glial cells surrounding the lamina cribrosa, concluding that TGFβ appears to contribute to the remodelling of lamina cribrosa in glaucoma (Fukuchi, Ueda et al. 2001). Significantly elevated levels of TGFβ are also characteristic of the anterior chamber of glaucomatous eyes, and presence of the cytokine has been shown to correlate with increased intraocular pressure. It is believed that this occurs through ECM remodelling interaction with the trabecular meshwork, leading to decreased aqueous humour outflow (Kirwan, Crean et al. 2004).

Tumour necrosis factor-alpha (TNFα) is a pro-inflammatory cytokine and inducer of apoptotic cell death through TNF receptor-1 (TNFR1) binding. Based upon observations that the expression of TNFα and its death receptor are increased in the glaucomatous retina (Tezel, Li et al. 2001) and the optic nerve head (Yan, Tezel et al. 2000), and that TNFα exposure leads to apoptosis of RGCs *in vitro* (Tezel and Wax 2000), it has been proposed as a putative mediator of

glaucomatous neurodegeneration. More direct evidence has been provided by the results of experiments in an induced ocular hypertension mouse model, where rapid upregulation of TNF-α was detected in the retina, preceding microglial activation, oligodendrocyte degeneration, and delayed apoptosis of RGCs (Nakazawa, Nakazawa et al. 2006). Interestingly, these effects were reproduced in healthy mice following intravitreal TNF-α application, whilst exogenous treatment with an anti-TNF-α-neutralizing antibody or genetic knockdown of TNF-α (or TNFR2), was sufficient to negate IOP-induced retinal damage.

In the glaucomatous eye, the glial cells, including Müller and astrocytes, are the main source of increased cytokines in the retina and optic nerve head (Yan, Tezel et al. 2000), although whether this action is designed to promote chronic neuroinflammation, or foster neuroprotection is unclear. Most inflammatory mediators produced by macroglia act on microglial cells, favouring chronic microglial activation and promoting neuronal apoptosis (Kettenmann, Hanisch et al. 2011). There is evidence to suggest this process may be reciprocal, as TNF-α produced by microglia has also been shown to intensify astrocyte activation and subsequent release of glutamate (Bezzi, Domercq et al. 2001). Glutamate released by activated microglia induces excitoneurotoxicity and contributes to neuronal damage in neurodegenerative diseases of the wider CNS, however low levels of TNF-α secreted by macroglia have also been shown to stimulate the secretion of NGF and glial cell line-derived neurotrophic factor (GDNF) in the same cells (Kuno, Yoshida et al. 2006). This data suggests that an autocrine loop involving TNF-α contributes to a neuroprotective response under inflammatory conditions. In support of this hypothesis is the fact that TNF-α released by activated microglia in the rat retina appears to stimulate astrocytes and Müller cells to produce neuroprotective factors, including NGF, following induction of hypertensive glaucomatous injury (Lee, Shin et al. 2014).

Secreted extracellular vesicles

Over the previous decade, secreted extracellular vesicles comprising of cytosol

enclosed within a lipid bilayer membrane have been identified as a previously underappreciated mode of intercellular communication. Although long considered merely a cellular waste disposal system, remarkable physiological and pathological effects have since been attributed to EV signalling, which appears to be mediated through the transfer of protein, lipid, and nucleic acid cargo to target cells.

The paradigm shift in the role of EV can be traced back to a 1996 publication presenting evidence for vesicles derived from the endocytic compartments of B lymphocytes, which presented MHC class II molecules and were capable of inducing an immune response (Raposo, Nijman et al. 1996). Shortly afterwards, Zitvogel et al (1998) published the first evidence of EV as a potential therapeutic agent by demonstrating that vesicles derived from dendritic cells and presenting MHC I and II proteins were capable of priming cytotoxic T lymphocytes for the eradication and suppression of murine tumours *in vivo* (Zitvogel, Regnault et al. 1998). The promise of these studies lead to the first phase I clinical trials of EV-based therapeutics in 2005, where 15 metastatic melanoma patients received four doses of autologous dendritic cell-derived EV, demonstrating the feasibility of large scale exosome production and the safety of EV administration (Escudier, Dorval et al. 2005).

Exosomes

Although there is currently no consensus on a universal nomenclature for cell-derived vesicles, the term is generally used to describe a subpopulation of small vesicles with a diameter of 40-150 nm, possessing of a low density gradient, and expressing upon their external membranes certain tetraspanins: CD81, CD63, CD9, and TSG101 (Kowal, Arras et al. 2016). The key distinguishing feature of exosomes from similar cell-derived vesicles is their multivesicular endosomal origin. Whilst larger ‘microvesicles’ arise from shedding of the external cellular membrane, exosomes are formed from inward budding of the early intraluminal vesicle membrane as part of the endocytic pathway.

Despite being first recognised in the 1940's, the true biological significance of cell-derived vesicles was not fully appreciated until the previous half decade, a point illustrated by the fact that in excess of 25 % of the > 5000 publications associated with the keywords "exosomes" or "extracellular vesicles" in NCBI's PubMed database were published between 2016 and 2018 (Chargaff and West 1946, Coordinators 2017). Key to the renewed interest in EV are recent reports indicating an ability to convey key messages as an important facet of intracellular communication (Denzer, Kleijmeer et al. 2000). As a result, EV are currently attracting enormous research interest, as the therapeutic potential of these particles is explored, including the possibility of identifying vesicles carrying novel biomarkers of disease, as well as a prospective delivery system for therapeutic agents. As enriched preparations of exosomes obtained using current methodologies do not necessarily discriminate between exosomes and other vesicle populations, limits to the full diversity of their signalling cargo are not yet fully understood. It is known that EV possess the capacity to transfer a range of specific proteins and lipids to target cells, and are capable of stimulating an array of functional changes. Of particular interest is the more recent discovery that certain populations are highly enriched in nucleic acids, particularly mRNAs and micro-RNAs, and are therefore capable of directly influencing the expression of proteins in target cells at the transcriptional level in a manner similar to that of an enveloped retrovirus (fig. 13) (Nolte-'t Hoen, Cremer et al. 2016).

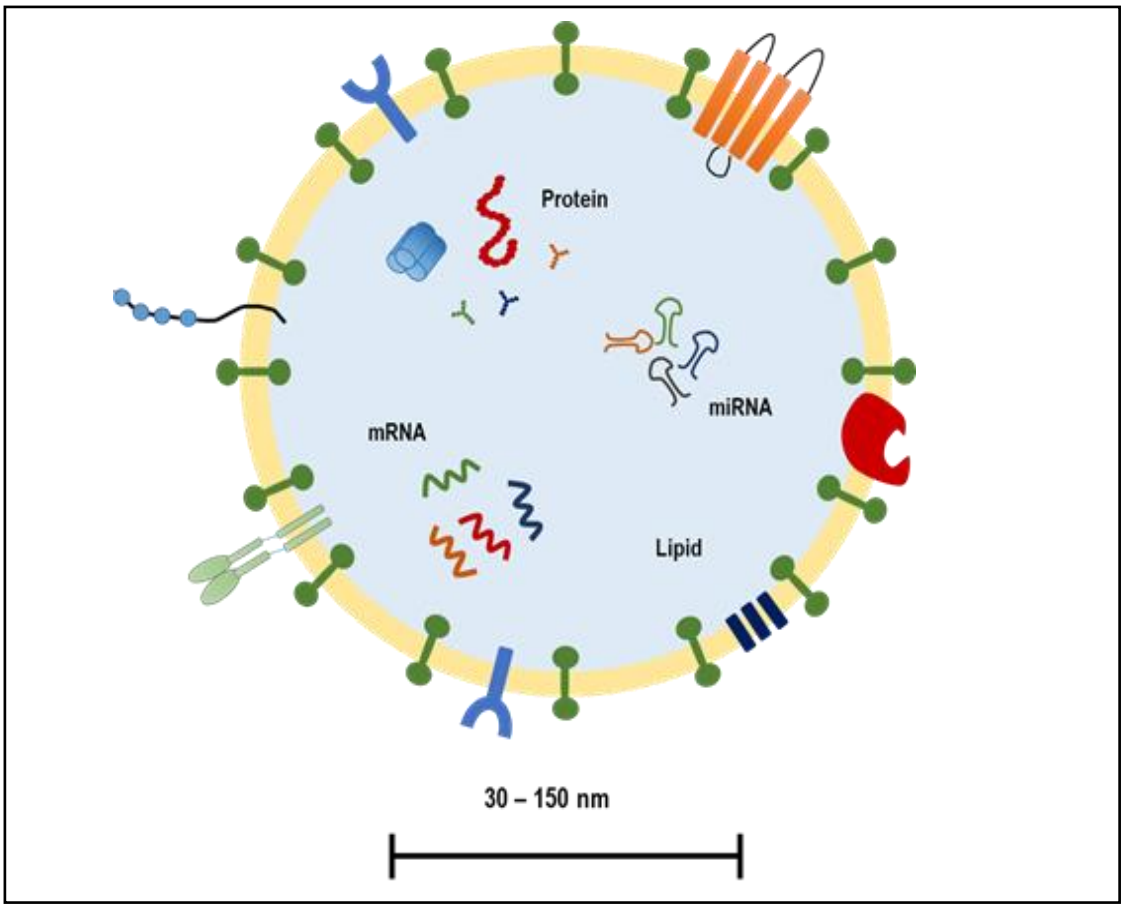

Figure 13. ***Schematic representation of an exosome****. A nano-sized vesicle delimited by a lipid-bilayer, and expressing upon its surface various transmembrane proteins, including tetraspanins CD9, CD63, and CD81. The vesicle lumen comprises of cell cytosol, in addition to ESCRT-associated proteins involved in exosome sorting and loading.*

Exosome biogenesis

Exosomes are derived from the endosomal system, and are formed as intraluminal vesicles (ILVs) in multivesicular bodies (MVBs). Endocytosis describes the process by which the cell internalizes molecules into large compartments from beyond the plasma membrane, before either recycling back to the cell surface or sorting for phagocytic degradation (Doherty and McMahon 2009). The endocytic transport pathway involves the *de novo* creation of a network of internal membrane compartments from the plasma membrane bilayer, with the purpose of internalising lipids and proteins, as well as associated extracellular fluid (Doherty and McMahon 2009). These compartments can be sub-classified into early, and late endosomes, as well as phagocytic lysosomes

(Doherty and McMahon 2009). Early endosomes are positioned near the cell surface where they fuse with incoming phagocytic and pinocytotic vesicles, and incorporate their content into compartments destined for recycling, degradation, or exocytosis. Contents destined for recycling are processed back to the cell surface for re-use, whilst the remainder undergo a series of transformations to become late endosomes. It is during this process that macromolecules fated to be degraded or exported, including proteins and nucleic acids from the trans Golgi network, are sorted into 30–100 nm vesicles that bud from the peripheral membrane into the late endosomal lumen. The distinctively 'multivesicular' appearance of late endosomes has led to them being referred to as multivesicular bodies (MVB) in the literature (fig. 14).

The invagination of the late endosomal membrane and subsequent formation of the ILVs represents the start of exosome biogenesis, a process ultimately completed by the fusing of MVBs with the external cellular membrane and wholesale release of vesicle contents. The formation of ILVs commences with the reorganization and enrichment of the endosomal membrane. Here, cell surface tetraspanin proteins, including CD9 and CD63, form networks with a range of subsidiary proteins to create tetraspanin enriched microdomains (TEMs) (Hemler 2003, Pols and Klumperman 2009). Secondary to the creation of TEMs, and essential for the formation of ILV and maturation of the late endosome, is the recruitment of the four endosomal sorting complexes required for transport (ESCRT) protein machinery: ESCRT-0, ESCRT-I, ESCRT-II, and ESCRT-III (Hurley 2010). ESCRT-0 binds to and clusters ubiquitinated cargo for delivery into MVBs, and recruits clathrin, ubiquitin ligases, and deubiquitinating enzymes (Ren and Hurley 2010). ESCRTs -I and -II co-assemble into a complex on endosomal membranes. In particular, ESCRT-II has a pivotal role in MVB biogenesis through bridging upstream ubiquitin-binding ESCRT complexes to the downstream ESCRT-III machinery involved in membrane scission (Babst, Katzmann et al. 2002). This complex is responsible for binding to lipids on the endosomal membrane, which then recruits ubiquitinated proteins to the endosome for packaging into ILV (Babst 2011). ESCRT-III is responsible for the final abscission of the budding vesicle, forming long filaments that wrap around the zone of membrane constriction, mediating cleavage through interactions with

the central spindle complex (Adell and Teis 2011). The abscission processes is aided by ALIX (also known as PDCD6IP), an associated protein that interacts with several ESCRT (TSG101 and CHMP4) proteins, and which is a key participant of the budding mechanism (Baietti, Zhang et al. 2012). The MVBs and their ILV content are either directed to the lysosome for proteolytic degradation, or towards fusion with the plasma membrane for subsequent release of the ILVs, that then become exosomes as they enter into the extracellular environment (fig. 14) (Reggiori and Pelham 2001). MVEs carrying the lysosomal-associated membrane proteins LAMP1 and LAMP2, tetraspanins CD63, CD9 and other molecules of late endosomes, can also fuse with the plasma membrane, where their contents are disseminated into the extracellular milieu (Eden, Burgoyne et al. 2016).

Although the characteristics of exosome biogenesis are well established, details of the molecular mechanisms that control the intracellular trafficking of MVBs and their fusion with the plasma membrane remain unclear. There is evidence that the highly conserved Rab family of small GTPases regulate many of the intracellular transport pathways associated with intercellular vesicle trafficking, including budding, motility, and fusion to acceptor membranes (Ali and Seabra 2005). RNA interference experiments have identified five Rab GTPases whose inhibition by shRNA result in decreased exosome secretion and morphological changes (Ostrowski, Carmo et al. 2010). Silencing of Rab27b has also been shown to radically alter MVB phenotype, whilst suppression of Rab27a increased the diameter of the ILVs, further emphasising their importance in vesicle biogenesis (Ostrowski, Carmo et al. 2010). Interestingly, silencing of these Rabs did not affect the regular secretory pathway of soluble proteins, presenting the possibility of manipulating exosome secretion *in vivo,* without disrupting other key cellular processes (Ostrowski, Carmo et al. 2010).

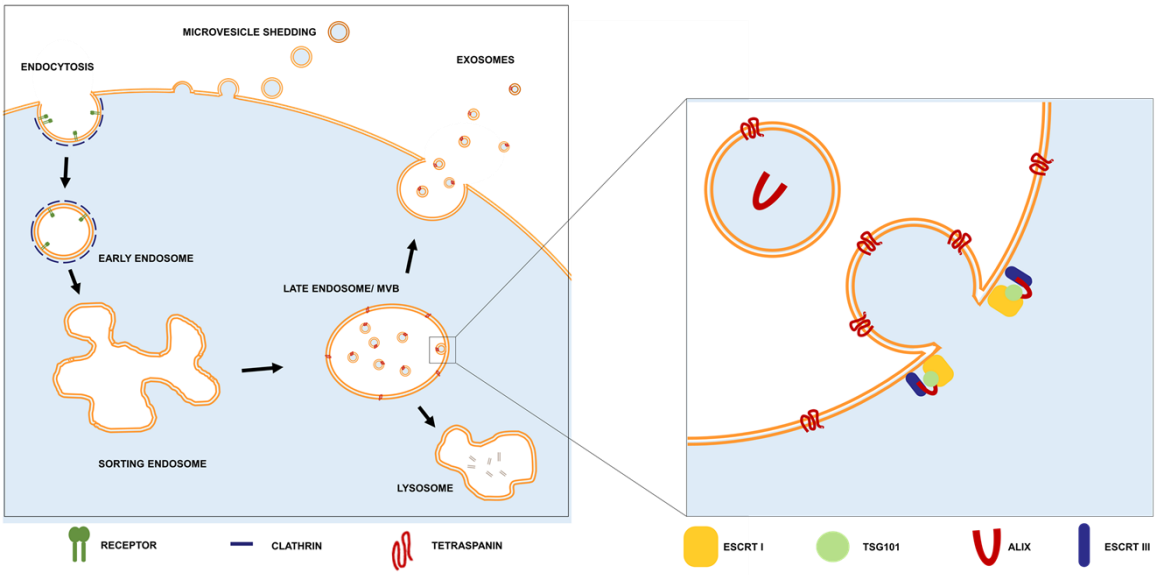

Figure 14. ***Biogenesis pathways of microvesicles and exosomes****. Microvesicles bud directly from the plasma membrane, whilst exosomes are formed through membrane invagination into endosomal compartments to form ILVs. These are released by fusion of MVBs with the plasma membrane.*

Shedding microvesicles

Microvesicles are heterogeneous, membrane-bound sacs, shed from the surface of myriad cell types. Initially referred to as “platelet dust”, discrete lipid-membrane vesicles were frequently observed in the intercellular space in electron micrographs, but were long considered to be merely artefacts relating to damage or apoptosis of surrounding cells (Wolf 1967). Understanding of the true nature of these structures began when the blebbing of vesicular material from plasma membrane was finally recognized in healthy eukaryotic cells (Beaudoin and Grondin 1991). Although structurally similar to MVB-derived exosomes, microvesicles are formed from outward budding and fission of the plasma membrane, and have a slightly different composition as a result. Whereas exosome size is limited by the internal volume of the endosome, microvesicles are more heterogenous, and are reported to be anywhere between 100 nm to many micrometres in diameter. Although disagreements over nomenclature and difficulty in discriminating between classes of EV in experimental preparations

have resulted in discrepancies in the literature, the majority of microvesicles appear to contain high levels of certain phospholipids, including phosphatidylserine, on their membrane outer leaflet and comprise various molecules from the parent cell including membrane constituents and cytoplasmic content (Théry, Zitvogel et al. 2002). Like exosomes, microvesicles have been shown to participate in intercellular communication, and have been shown to play a role in a diverse range of physiological processes including inflammation, vascular function, and tumour progression (Skog, Würdinger et al. 2008, Muralidharan-Chari, Clancy et al. 2010, Waldenström, Gennebäck et al. 2012).

Microvesicle Biogenesis

Microvesicle biogenesis occurs via the direct outward blebbing and pinching of the plasma membrane, releasing the nascent microvesicle into the extracellular milieu (fig. 14). Shed microvesicles originate from a separate and less well-characterised pathway than exosomes. A variety of poorly understood processes are necessary for the initiation and completion of membrane blebbing, including the redistribution of certain phospholipids and activation of cytoskeletal matrix proteins (Leventis and Grinstein 2010), which lead to the non-uniform distribution of glycerophospholipid clusters throughout the plasma membrane. The formation of these clusters is regulated by several types of transmembrane lipid transporter enzymes: scramblases, flippases and floppases, which facilitate the transfer of phospholipids between the inner and outer leaflet (Leventis and Grinstein 2010). The unequal distribution of these plasma membrane lipid components can result in changes to local membrane curvature consistent with the events of microvesicle budding (Yang, Gad et al. 2008). Ultimately, microvesicle budding and fission of plasma membrane is the result of a dynamic interplay between phospholipid redistribution and cytoskeletal protein contraction (Zwaal and Schroit 1997, Bevers, Comfurius et al. 1999).

Although no consensus yet exists, microvesicle formation appears to be induced by the translocation of phosphatidylserine from the plasma membrane inner leaflet to the outer, via the activity of aminophospholipid translocases (Bratton,

Fadok et al. 1997). There is also evidence to suggest that merely the accumulation of macromolecules, even those unrelated to the generation of membrane curvature, could influence bending of the plasma membrane by crowding in close proximity at the periphery of the cell (Stachowiak, Schmid et al. 2012). Here, lateral pressure is thought to be generated by protein-protein interactions which initiate membrane blebbing.

Regardless of initiating factor, budding is propagated by ADP-ribosylation factor 6 (ARF6). ARF6 initiates a signalling cascade that starts with the activation of phospholipase D (PLD), which then recruits the extracellular signal-regulated kinase (ERK) to the plasma membrane, which in turn phosphorylates and activates myosin light-chain kinase (MLCK), triggering the release of microvesicles (Donaldson 2003). The significance of ARF6's role in microvesicle biogenesis is such that, in a melanoma cell model, overexpression of the protein is sufficient to significantly upregulate microvesicle secretion, whilst production of smaller MVB-derived vesicles appears unchanged (Muralidharan-Chari, Clancy et al. 2009).

Interestingly, members of the ESCRT complexes involved in exosome biogenesis and excision have also been implicated in the formation of microvesicles. This was first observed in budding viruses, which hijack the TSG101 protein and ESCRT machinery to mediate exit of viral particles from the plasma membrane (Bieniasz 2009). In the context of microvesicles, TSG101 is recruited from the late endosomal membrane to the surface of cells by an accessory protein, the arrestin domain-containing protein 1 (ARRDC1), via it's arrestin domain (Nabhan, Hu et al. 2012).

Cellular uptake of extracellular vesicles

The current interest in the field of EV springs from the recognition of these organelles as important mediators of cell-to-cell communication. Via transfer of bioactive molecules, EV play an essential role in the maintenance of tissues and

integration of homeostasis, but also influence various pathological conditions (Stahl and Raposo 2019). Upon contact with tissue cells, EV must therefore interact with the target cell and either fuse directly or be subject to endocytosis. Whilst a large body of evidence exists relating to the processes of extracellular vesicle biogenesis, less is known about the mechanisms by which circulating vesicles are taken up by recipient cells, and how vesicles interact and are sorted after entry into the cells.

Numerous publications have provided evidence to suggest that EV are internalized into recipient cells. Indirect evidence can be found in studies reporting the transfer of nucleic acid EV cargos, the first of which demonstrated the presence of murine proteins in human mast cells following transfer of mouse exosomal RNA (Valadi, Ekström et al. 2007). Subsequent studies have utilised a luciferase reporter assay to allow visualization of EV transfer between cells (Montecalvo, Larregina et al. 2012), and EV-mediated delivery of siRNA has also been shown to downregulate target genes *in vitro* and *in vivo* (Cooper, Wiklander et al. 2014). Uptake studies based on the functional delivery of EV laden with luciferin substrate to luciferase expressing cells resulted in production of bioluminescence, suggesting that merging of the EV cytosol and the cytoplasmic compartment had occurred, either through membrane fusion at the plasma membrane or by uptake through other pathways followed by fusion with the endosomal membrane (Montecalvo, Larregina et al. 2012).

Direct evidence for internalisation of EV can be found from various studies involving visualization of EV uptake. Fluorescent lipophilic dyes like PKH26, PKH67, rhodamine B, DiL and DiD have been used to label EV membranes in a non-discriminate manner (Parolini, Federici et al. 2009, Imai, Takahashi et al. 2015, Kim, Haney et al. 2018). A more targeted approach involves the cloning of fluorescent conjugates like mCherry onto endosome-enriched proteins such as tetraspanin CD63, in EV-donor cells (Heusermann, Hean et al. 2016). There are however, limitations when using fluorescent protein conjugated EV labelling methods. Since EV markers are not similarly expressed in EV derived from all

cell-types, and often show heterogeneity in similar or different cell-types, the use of reporters conjugated to proteins enriched in EV is restricted to certain subpopulations of EV. Other groups have used membrane-permeable compounds to stain EV cytosolic lumen. These undergo esterification within EV lumen and fluorescence, allowing for their detection. Examples of these include carboxyfluorescein succinimidyl ester (CFSE) and 5(6)-carboxyfluorescein diacetate (CFDA) (Temchura, Tenbusch et al. 2008). Following labelling, subsequent entry of EV into recipient cells can be measured using methods such as flow cytometry and confocal microscopy (Wiklander, Bostancioglu et al. 2018), and cells may be washed briefly with a protease like trypsin prior to fixation in order to remove surface-bound EV, and ensure that signal detected refers to internalised organelles (Franzen, Simms et al. 2014). With any of these approaches, care must be taken and proper experimental controls used to ensure that internalised EV signal relates to the specific uptake of EV rather than artefacts arising from unbound dye, or free fluorescent protein. It should also be appreciated that almost all studies have relied on fluorescence microscopy, which has limited resolution for nano-scale objects because the wavelength of visible light is approximately 380-700 nm. As a result, single EV or clusters <390 nm in diameter cannot be distinguished. Although this should not affect the assessment of EV uptake in general but may affect the visualization and dynamic localization analysis of individual EV.

Endocytosis

EV uptake is a rapid process, labelled vesicles have been identified within cells as soon as 15 minutes after their initial application (Feng, Zhao et al. 2010). Although several mechanisms have been proposed for how EV convey their messages and are taken up by recipient cells, the majority of studies do suggest that extracellular EV are typically internalised into endosomal compartments (Morelli, Larregina et al. 2004, Montecalvo, Larregina et al. 2012). In support for this mechanism is the fact that EV uptake is reduced or absent at 4°C, and in cells fixed in paraformaldehyde. This implies that internalisation is an energy-dependent process as opposed to a result of passive membrane-fusion (Fitzner, Schnaars et al. 2011, Verdera, Gitz-Francois et al. 2017). Further evidence can

be found in studies demonstrating that restricting the endocytic pathway by Cytochalasin D depolymerization of actin filament networks, dramatically reduces EV internalisation (Escrevente, Keller et al. 2011).

Collectively, this data indicates that internalization of EV is an energy-dependent process, and requires a functioning cytoskeleton, both of which supports the endocytic pathway as the primary mechanism for EV uptake. Interestingly, attempts to prevent EV internalisation by inhibition of endocytic pathways, for example knockdown of dynamin2 protein in phagocytes, reduces but does not completely arrest uptake (Obregon, Rothen-Rutishauser et al. 2009, Feng, Zhao et al. 2010). This suggests that alternative or variable mechanisms may also play a role, and these are likely to be specific to different cell types. Endocytosis itself refers only to internalization through the *de novo* production of internal membranes from the plasma lipid bilayer and as such, is a general term encompassing a range of variable molecular pathways. Through the targeted inhibition of key components of these pathways in recipient cells, it has become clear that EV uptake can be mediated by several endocytic subdivisions including phagocytosis (Feng, Zhao et al. 2010), or macropinocytosis (Fitzner, Schnaars et al. 2011). Adding to the confusion are various reports claiming these interactions to be clathrin-mediated (Verdera, Gitz-Francois et al. 2017), clathrin-independent (Verdera, Gitz-Francois et al. 2017), or lipid Raft-mediated (Svensson, Christianson et al. 2013).

Phagocytosis and macropinocytosis

Phagocytosis refers to the receptor-mediated cellular engulfment of opsonized particles, including bacteria and apoptotic cell fragments, typically by specialized macrophages (Aderem and Underhill 1999). The process of internalization involves the progressive formation of invaginations surrounding the material destined for internalization and is generally employed for the uptake of large particles for lysosomal degradation. Interestingly, EV released by leukaemia cells have been shown to be taken up efficiently by macrophages, despite not being internalized by other cell types (Feng, Zhao et al. 2010). More direct evidence

for the involvement of phagocytosis is provided by studies demonstrating that inhibition of phosphoinositide 3-kinase (PI3K), an enzyme required for enabling membrane insertion into forming phagosomes, significantly reduces the internalisation of EV in a dose-dependent manner (Feng, Zhao et al. 2010). The same publication also reported that a fluorescent signal was detected in recipient dendritic cells after incubation with EV labelled with a phagosome tracer (pHrodo). The technical limitations associated with these findings, including specificity of the PI3K inhibitors and PI3K, which is also involved in macropinocytosis, as well as the tracer pHrodo's ability to distinguish phagocytosis compared to other low pH associated endosomal pathways, and emphasize the need for further validation of the phagocytosis-mediated EV uptake theory.

Macropinocytosis is a related mechanism of endocytic internalisation that involves the actin-dependent formation of invaginated membrane ruffles, resulting in large (>0.2 μM) intracellular vacuoles or "macropinosomes", which typically mature to late endosomes (Kerr and Teasdale 2009). Unlike phagocytosis, macropinocytosis is not regulated by cargo/receptor molecules co-ordinating the activity of effector molecules in the plasma membrane, but by activation of receptor tyrosine kinases, including EGFR and platelet-derived growth factor receptor (PDGFR). This leads to a global increase in actin polymerization at the cell surface, resulting in an elevation in actin-mediated ruffling and ultimately an increase in macropinosome formation (Kerr and Teasdale 2009). Thus far, the role of macropinocytosis in EV uptake is unclear. The alkalinizing drugs bafilomycin A, monensin and chloroquine have each been shown to inhibit microglial internalization of EV, which would be consistent with a role for the acidification of vacuoles characteristic of macropincytosis (Fitzner, Schnaars et al. 2011). More specific interference of macropinocytosis can be achieved by treatment with compounds that block Na+/H+ exchange, but while this resulted in a dramatically reduced internalisation of oligodendrocyte-EV by microglia (Fitzner, Schnaars et al. 2011) and HeLa cells (Verdera, Gitz-Francois et al. 2017), no change was found in uptake in an equivalent study in

macrophages (Feng, Zhao et al. 2010), or in target cells of the CNE1 line (Nanbo, Kawanishi et al. 2013).

Despite key differences between the subcategories of endocytic engulfment, there is significant crossover with regard to the involvement of associated cellular components. For example, the phospholipid phosphatidylserine (PS) has a role in both the phagocytic engulfment of apoptotic bodies (Fadok, Voelker et al. 1992), and in the mechanism by which some viruses enter cells by macropinocytosis (Shiratsuchi, Kaido et al. 2000). Although typically located in the inner leaflet of the plasma membrane, EV are enriched for PS on their outer membrane, which has been proposed as a potential facilitator of their uptake (Leventis and Grinstein 2010). Interestingly, negatively charged PS- or phosphatidylglycerol-loaded liposomes have been shown to suppress the cellular uptake of exosomes by macrophages, whilst uptake was not affected by phosphatidylcholine-containing liposomes. This data suggests that the negative charge of PS in exosomal membranes may be involved in their recognition and internalisation (Matsumoto, Takahashi et al. 2017). Incubation of macrophages with an antibody that masks TIM4, a receptor involved in PS-dependent phagocytosis, leads to attenuated uptake of EV (Feng, Zhao et al. 2010), as does treatment of dendritic cells with a competitive PS analogue (Morelli, Larregina et al. 2004). Finally, pre-treatment of vesicles with soluble annexin-V, which binds PS, inhibits internalisation of EV into microglia (Yuyama, Sun et al. 2012). It seems likely therefore, that despite uncertainty over precise mechanisms, phagocytic and macropinocytic uptake of EV may be part initiated by the PS presented on the outer leaflet of EV membranes.

It is also clear that certain uptake mechanisms involve interactions between EV-enriched proteins and membrane receptors on target cells that precede and facilitate endocytosis. Treatment of EV with proteinase K significantly reduced their internalisation into ovarian cancer cells (Escrevente, Keller et al. 2011). Several classes of proteins have been implicated, including tetraspanins, proteoglycans, integrins and lectins, and due to the abundance of tetraspanins

on EV membranes, and their role in cell adhesion as well as in cellular invasion by viruses, it has been proposed that EV internalisation requires similar interactions. In support of this theory is the fact that treatment of recipient cells with blocking antibodies against tetraspanins CD81 or CD9 can significantly reduce uptake of EV by dendritic cells (Morelli, Larregina et al. 2004). Interestingly, the same study reported a similar reducing effect following the treatment of dendritic cells with antibodies that mask the binding sites of the integrin CD11a, or its ligand ICAM-1, and integrins CD51 and CD61, highlighting the role of these transmembrane receptors.

Finally, it has been reported that cancer cell EV rely upon cell-surface heparan sulfate proteoglycans (HSPGs) for their internalization. Fluorescently labelled EV co-localise with internal vesicles containing GFP-linked HSPGs inside recipient cells (Christianson, Svensson et al. 2013), whilst treatment of cells with a heparan sulfate mimic halted EV uptake in a dose-dependent manner (Franzen, Simms et al. 2014). Further support for the role of this class of proteins in EV internalisation can be seen from the analysis of cells in which normal HSPG production has been artificially restricted, which showed a reduced capacity for EV uptake (Christianson, Svensson et al. 2013). In this study, the authors report that treatment of purified EV with heparinase did not influence their uptake, implying that it is cell-surface HSPG that is required for vesicle entry.

Clathrin mediated and clathrin-independent endocytosis

While phagocytosis is associated with specialized immune-phagocytes, clatherin-mediated (CME) and clatherin-independent endocytosis (CIE) are endocytic processes that occur in all cell types. The mechanism of CME involves cellular internalization of molecules through progressive assembly of clathrin-coated vesicles that contain a range of transmembrane receptors and their ligands. Epidermal growth factor receptor pathway substrate clone 15 (EPS15) is a component of clathrin-coated pits that is ubiquitously associated with AP-2

adaptor complex which is an integral component of the clathrin coat (Benmerah, Bayrou et al. 1999). Expression of a dominant-negative mutant of EPS15 inhibits CME and leads to a reduction in EV uptake (Feng, Zhao et al. 2010). Inhibition of essential components of the CME process, including the GTPase dynamin2 required for vesicle production, or treatment with chlorpromazine which prevents clathrin-coated pit formation at the plasma membrane, have been shown to decrease EV uptake, implying a role of CME in EV internalisation (Barrès, Blanc et al. 2010, Escrevente, Keller et al. 2011). Further evidence for the role of CME in vesicle uptake is provided by studies demonstrating that inhibition of dynamin2 in phagocytic cells arrested almost all EV internalisation (Feng, Zhao et al. 2010, Fitzner, Schnaars et al. 2011). Since dynamin2 is required for both CME and CDE, findings of decreased EV uptake following dynamin2-inhibition cannot be applied to distinguish between these endocytic pathways. These results do however suggest that CME plays at least some role in EV internalisation in certain cell types, but CIE, which includes endocytic subtypes like caveolin-dependent endocytosis (CDE), has also been found to be relevant for EV internalisation. A recent study demonstrated the involvement of CIE in EV uptake in HeLa cells using the small molecule inhibitors genistein and simvastatin, reporting a dose-dependent effect on exosome internalisation for both (Verdera, Gitz-Francois et al. 2017). The same group reported that EV intake was inhibited by siRNA-mediated knockdown of caveolin-1, flotillin-1, RhoA, Rac1 and PAK1, but not clathrin heavy chain, inferring that cellular entry by EV is governed by CIE, and macropinocytosis, but not CME.

Clinical trials involving extracellular vesicles for the treatment of neural disorders in the eye

Preclinical reports of EV therapy, particularly those secreted by various stem cell sources, are highly encouraging across a range of diseases, as well as in the modulation of immune responses in disorders such as GVHD and cancer. This has led to the development of multiple ongoing clinical trials that are actively recruiting patients. In the United States, the Food and Drug Administration (FDA)

have thus far approved clinical trials using EV as a treatment for sepsis (NCT02957279), ulcers (ClinicalTrials.gov Identifier: NCT02565264), and type 1 diabetes mellitus (NCT02138331).

The application of EV from various sources as a regenerative strategy for neural tissue is a relatively new concept, and the majority of studies are yet to be taken to the clinic. Based on pre-clinical studies of EV-mediated delivery of miR-124 promoting neurogenesis after ischemia (Yang, Zhang et al. 2017), a clinical trial based in Iran was planned for 2018-2019 using MSC-derived EV in the treatment of acute ischemic stroke (NCT03384433). The therapeutic efficacy of MSC-generated EV was to be examined in post-stroke phases 1 and 2, but the results of which are yet to be reported.

Two clinical trials relevant have been listed using EV in the context of blinding eye disease, one using serum EV miRNA as a biomarker in diabetic retinopathy which is currently recruiting (ClinicalTrials.gov Identifier: NCT03264976), and another using MSC-derived EV for the treatment of macular holes (ClinicalTrials.gov Identifier: NCT03437759). In the later, five patients with large and refractory macular holes were treated with either 50 µg or 20 µg MSC-EV in 20 µl PBS. Results of the study suggest that EV were capable of stimulating the closure of macular holes, although the report did not define a mechanism of action, and control groups were not included (Zhang, Liu et al. 2018). The intravitreal MSC EV therapy was well tolerated with only one patient experiencing an inflammatory reaction in response to a high EV dose, this was alleviated when the dosage was reduced.

Extracellular RNA

Ribonucleic acid (RNA) is a polymeric molecule required for the coding, regulation, and expression of genes. Despite the classical functions of RNA taking place intracellularly, it was demonstrated more than 70 years ago that RNA is also present in the external cellular environment, including human plasma

(Mandel and Metais 1948). More recently, small non-coding RNAs have been found to be ubiquitous in 12 different types of human body fluids (Weber, Baxter et al. 2010). The implications of these observations were not immediately clear, particularly as the extracellular environment is known to be abundant in ribonucleases (RNases), and it was uncertain as to how RNA molecules might be protected from degradation outside of the cell. The exogenous accumulation of transcribed or artificially synthesized RNA into human plasma leads to rapid degradation, however RNA species present in extracellular biological fluids appear to be stable (Tsui, Ng et al. 2002, Mitchell, Parkin et al. 2008). Since the discovery that extracellular vesicles (EV) associate with RNA species (Baj-Krzyworzeka, Szatanek et al. 2006, Ratajczak, Miekus et al. 2006), containment within membrane vesicles has been proposed as a mechanism by which RNA molecules could be protected from RNase decay (Raposo and Stoorvogel 2013).

Horizontal transfer of RNA between cells was first proposed in 1971, long before the first reports of secreted membrane vesicles (Kolodny 1971), however the discovery that certain EV are enriched in RNAs provided a potential mechanistic explanation by which functional nucleic acids could be transferred as a novel form of intercellular communication (Dinger, Mercer et al. 2008, Hunter, Ismail et al. 2008). Of particular interest were reports of EV presenting transmembrane proteins, which indicated the potential for specific interactions between certain EV ligands and specified cellular receptors. These reports were subsequently validated by publications revealing diverse roles in various physiological functions, through transfer of RNAs in processes such as cancer metastasis, insulin resistance, and neuroprotection (Mead, Amaral et al. 2018, Shurtleff, Temoche-Diaz et al. 2018). Intercellular communication via EV is a particularly intriguing prospect, since EV could deliver specific packages of RNAs and protein that could encode far more complex and precise messages than those imparted by signal transduction cascades induced by hormones or signalling factors. For example, transfer of a mRNA might allow for the targeted upregulation of one specific protein in the recipient cell, whilst transfer of short-non coding species could specifically downregulate translation of mRNA transcripts (Dinger, Mercer et al. 2008). The great potential of EV as natural delivery vectors for RNA-based

therapeutics was further highlighted by pioneering developments published in 2011 by Alvarez-Erviti et al, which demonstrated that engineered EV can be targeted to the brain and used for delivery of functional siRNA (Alvarez-Erviti, Seow et al. 2011).

The characterisation of RNAs in EV has progressed rapidly in recent years thanks to technical advances in the detection of low-abundance, complex nucleic acid samples. RNA populations in EV have been comprehensively examined using high-throughput RNA sequencing, and the majority further validated by highly sensitive RT-qPCR analysis (Nolte-'t Hoen, Buermans et al. 2012). In addition to protein-coding mRNAs, these populations have been reported to include many types of non-coding RNAs, including: long noncoding RNAs (lncRNAs), circular RNAs (circRNAs), small nucleolar RNA (snoRNAs), small nuclear RNAs (snRNAs), piwi-interacting RNAs (piRNAs), transfer RNA (tRNAs), ribosomal RNAs (rRNAs), and microRNAs (miRNA) (Carthew and Sontheimer 2009).

Despite these findings, there is still uncertainty and disagreement with regard to the specific composition of RNA-based EV cargo, much of which stems from a lack of clarity and consensus within the field with regard to nomenclature and characterisation of various vesicle sub-types. This has described in detail in the most recent statement from the *International Society for Extracellular Vesicles* (ISEV) (Théry, Witwer et al. 2018). Whilst several groups report the presence of large transcripts in RNA extracted from EV, others report a complete absence of mRNA and rRNA, particularly in endosome-derived exosome purifications, suggesting instead that these originate from contamination with large apoptotic compartments containing nuclear material (Crescitelli, Lässer et al. 2013). The characterisation of RNA purified from Müller glia derived EV previously reported in this thesis supports this theory, with small EV populations entirely lacking molecules above 200 nts in length. Instead, both EV populations analysed were proportionally enriched in small RNAs.

micro-RNAs (miRNAs) and their intracellular processing

Currently, the reference repository miRBase holds information about 1917 human precursors and 2656 mature miRNAs (release 22) (Kozomara, Birgaoanu et al. 2019). miRNAs and miRNA-target sites are highly conserved, suggesting that miRNAs have critical regulatory function in all living organisms. In total, >45,000 miRNA target sites within human 3′UTRs are conserved above background levels, and >60% of human genes have been under selective pressure to maintain pairing to miRNAs (Friedman, Farh et al. 2009). miRNAs are known to play a key role in the control of cell proliferation, differentiation, apoptosis and metastasis (Hwang and Mendell 2006, Li, Ren et al. 2017). They also act as the regulatory factors of diverse biological pathways including developmental timing control, and hematopoietic lineage differentiation in mammals (Ferreira, Calin et al. 2018). Recently, a wealth of studies have implicated miRNA dysregulation as a common feature in a range of neurodegenerative diseases (NDs), as well as carcinogenesis (Calin, Dumitru et al. 2002, Absalon, Kochanek et al. 2013, Peng and Croce 2016).

The primary transcript of a miRNA (pri-miRNA) gene encompasses a stem-loop precursor (pre-miRNA) that encloses the mature sequence. In the nucleus, the pri-miRNA molecule is cleaved at the base of the stem-loop structure by the RNAse III enzyme Drosha and its partner DGCR8, which form the microprocessor complex (Michlewski and Cáceres 2019). This cleavage appears to require an intact secondary structure of the pri-miRNA for efficient processing (Kim, Kim et al. 2016, Kwon, Nguyen et al. 2016). In this reaction, DGCR8 identifies the exact cleavage site in the 5’ and 3’ overhangs flanking the stem-loop, and the Drosha enzyme catalyses their excision. In addition to the canonical pri-miRNA processing pathway, several intronic pri-miRNAs have been identified that bypass Drosha/DGCR8, and are instead processed by the splicing machinery (Denli, Tops et al. 2004). In some instances miRNAs that are derived from small nucleolar RNA (snoRNA) in various species are processed directly by another RNAse III family member, DICER (Hutzinger, Feederle et al. 2009). This nuclear processing event results in the production of ~70 nt stem–loop precursor miRNAs, termed pre-miRNAs (Tsutsumi, Kawamata et al. 2011) , which are

subsequently exported to the cytoplasm via the export receptor Exportin5 (XPO5) and transporter complex Ran-GTP (Kim, Kim et al. 2016). Once in the cytoplasm, pre-miRNAs undergo a final processing event by the DICER endonuclease, giving rise to transitory small-RNA duplexes (Ha and Kim 2014).

Post-transcriptional gene silencing by miRNAs

One strand of the mature miRNA duplex is incorporated into the RNA-induced silencing complex (RISC) which includes Argonaute-2 (AGO2), Dicer enzyme, and Tar RNA binding protein (TRBP) (Kobayashi and Tomari 2016). AGO proteins contain two highly conserved RNA binding domains that bind and orientate the miRNA for interaction with the target. The guide miRNA strand dictates the target through pairing between nucleotides at positions 2-8 in the 5' end of the "seed" region, and complimentary sequences within the 3'UTR of target genes (Michlewski and Cáceres 2019). In most cases the passenger strand is degraded once the duplex has unwound (Ahmed, Ansari et al. 2009).

AGO–miRNA binding to the 3' UTR of mRNA transcripts can result in gene silencing both through repression of translation, and mRNA decay. Both modes of silencing are thought to be interconnected, with ribosome profiling assays suggesting that decay of transcripts is generally responsible for the majority (70-90%) of silencing activity (Guo, Ingolia et al. 2010). Such studies also indicate that whilst inhibition of translation can be rescued, mRNA degradation is irreversible, raising the possibility that interruption to the molecular cascade involved in mRNA degradation could allow for translation repression without mRNA decay (Bhattacharyya, Habermacher et al. 2006). These works and similar demonstrate that miRNA regulation is a dynamic process that appears to be able to respond rapidly to specific cellular needs.

Canonical miRNA/mRNA silencing can initiate the decay of mRNA via two different mechanisms. In the first, mRNA is cleaved within the base-paired region due to endonucleolytic activity of AGO proteins. The second involves recruitment

by AGO of a member of the glycine-tryptophan protein of 182 kDa (GW182) protein family (in humans known as trinucleotide repeat-containing gene 6A protein (TNRC6A), TNRC6B and TNRC6C). GW182 interacts with polyadenylate-binding protein (PABPC), thereby promoting mRNA deadenylation by recruiting the poly(A) nuclease 2 (PAN2)–PAN3 and carbon catabolite repressor protein 4 (CCR4)–NOT complexes Deadenylation promotes decapping by the mRNA-decapping enzyme subunit 1 (DCP1)–DCP2 complex, thereby making the mRNA susceptible to rapid degradation by 5'−3' exoribonuclease 1 (XRN1) (Eulalio, Huntzinger et al. 2008).

miRNA-mediated inhibition of mRNA translation is facilitated through AGO2, which competes with the family of translation initiation factors (eIF4A) for binding to the mRNA cap, blocking and interfering with their function (Ha and Kim 2014). There is not currently consensus on the precise mechanisms by which this is achieved, but some data indicates that the miRISC induces their dissociation from target mRNAs and thereby inhibits ribosome scanning and assembly of the eIF4F translation initiation complex (Qureshi and Mehler 2012). Other mechanisms of silencing involving premature termination of polypeptide synthesis via the blocking of ribosomal subunits have also been proposed (Huntzinger and Izaurralde 2011). A recent study performed in human and *D. melanogaster* cells reported that the AGO Trp-binding pockets that mediate GW182 binding are required for translation inhibition (Kuzuoğlu-Öztürk, Bhandari et al. 2016). GW182-mediated recruitment of CCR4–NOT may also lead to translation repression through recruitment of the RNA helicase DDX6 (Mathys, Basquin et al. 2014).

The role of miRNA in the CNS

Through negative regulation of gene expression, miRNAs are able to modulate diverse biological processes, including cell differentiation, proliferation, apoptosis and stress response. While the neuroprotective potential of miRNAs in retinal ganglion cells is still to be established, inspiration can be found in reports identifying neuroprotective miRNAs in the wider CNS. Overexpression of miR-

223 in hippocampal neurons regulates levels of the glutamate receptor subunits GluR2 and NR2B, inhibiting NMDA-induced calcium toxicity, and protecting the brain from neuronal cell death following transient global ischemia and excitotoxic injury (Harraz, Eacker et al. 2012). It has also been demonstrated that selected miRNAs have tissue-specific expression. For example, let-7g, miR-92b, miR-146b, miR-330, miR-384 and miR-551b are significantly more abundant in hippocampus compared to cortex (He, Zhang et al. 2007).

Interestingly, in the context of RGC protection, miRNAs have also been shown to play key roles in the development and function of the CNS. Due to non-specific binding that can occur beyond the “seed region”, a single miRNA species has the potential to silence a large number of potential mRNA targets. miRNA are therefore well positioned to modulate many biological mechanisms important for cellular growth, homeostasis and survival. During central nervous system (CNS) development, regulation of gene expression by miRNAs is tightly regulated by numerous factors including the post-transcriptional repression of specific genes by miRNAs (Cochella and Hobert 2012). Indeed, miRNAs mediate critical processes throughout the entirety of CNS development, as highlighted by the embryonic lethality of Dicer knockout mice before neurogenesis occurs (Meza-Sosa, Valle-García et al. 2012) (Bernstein, Kim et al. 2003). In addition, conditional deletion of Dicer in glial cells and in subsequent neuronal progeny during later embryonic stages, leads to abnormal cortical and cerebellar development (Kuang, Liu et al. 2012). The authors also reveal miR-9 as an essential miRNA component of the Notch1 signalling pathway fundamental to normal embryonic neurogenesis. Key roles for miRNA have been documented in a wide range of developmental processes including neural stem cell proliferation and differentiation (miR-31) (Meares, Rajbhandari et al. 2018), axon guidance (miR-9) (Shibata, Nakao et al. 2011), and the arborization of dendrites (miR-132) (Magill, Cambronne et al. 2010). Several miRNAs (miR-9, miR-124a/b, miR-135, miR-153, miR-183 and miR-219) have also been identified as highly conserved and specifically expressed in differentiating mammalian neurons, likely acting as effectors in processes associated with neuronal development and function (Sempere, Freemantle et al. 2004). Together, this data provides compelling

evidence for the necessity of regulatory global miRNA functioning for proper CNS development.

miRNAs have also been demonstrated to contribute towards the maintenance of homeostasis in the mature nervous system. For example, several publications implicate miR-26a in numerous neuronal processes through the targeted silencing of key members of intrinsic growth pathways. miRNA-26a is a physiological regulator of mammalian axon regeneration, through suppression of glycogen synthase kinase 3β (GSK3β) in adult mouse sensory neurons in vitro and in vivo (Jiang, Liu et al. 2015). In addition, miR-26a and 26b specifically target and repress translation of BDNF, one of the most important regulators of neuronal plasticity and neuron morphology (Caputo, Sinibaldi et al. 2011). There is also evidence implicating microRNA in the maintenance of glutamate homeostasis at the synapse. Neurite-enriched miR-218 stimulates translation of the GluA2 subunit of AMPA-type glutamate receptors and increases excitatory synaptic strength, whilst dopamine-regulated miR-181a has been reported to modify the GluA2 subunit in hippocampal neurons (Saba, Störchel et al. 2012, Rocchi, Moretti et al. 2019). Expression of miR-124 within peri-synaptic astrocytes indirectly leads to the upregulation of glutamate transporter excitatory amino acid transporter 2 (EAAT2), a protein required for the regulation of extracellular glutamate levels and synaptic activation (Morel, Regan et al. 2013). Interestingly, miR-124 has also been demonstrated important functions in microglia where they have been shown to suppress microglial activation and promote quiescence through deactivating macrophages via the C/EBP-α–PU.1 pathway (Ponomarev, Veremeyko et al. 2011).

Synaptic plasticity is also modulated by miRNAs. A subset of miRNA are localized to the neuronal synapto-dendritic compartment, where they act in the local regulation of protein synthesis and regulate plasticity as well as development (Schratt 2009). In particular, miR-134, miR-138, and miR-132 appear to regulate the morphology of dendritic spines, the primary sites of excitatory synaptic

transmission in the vertebrate brain (Wayman, Davare et al. 2008, Fiore, Khudayberdiev et al. 2009, Edbauer, Neilson et al. 2010).

There is strong evidence that the acquisition and consolidation of certain components of visual recognition memory is mediated by synaptic plasticity in the perirhinal cortex, since miRNAs can be activated in response to neuronal activity. It has also been hypothesised that they may offer an effective means of controlling the expression of genes involved in memory formation. In vivo, knockdown of miR-132 in the hippocampus leads to altered memory formation in rodents (Wang, Phang et al. 2013), emphasizing the essential role of miRNAs in regulating synaptic plasticity and subsequent learning and memory.

miRNA functions within the retina

In the context of glaucomatous neurodegeneration, several studies have aimed to establish the function and expression profile of specific miRNAs in the adult retina as well as during development, in the hope of identifying miRNAs and gene targets capable of regulating axon survival and regeneration (Andreeva and Cooper 2014). For example, miR24a is a regulator of the pro-apoptotic factors caspase9 and apaf1, and is required for correct retinal morphogenesis in Xenopus. Inhibition of miR-24a during development causes a reduction in eye size due to a significant increase in apoptosis (Walker and Harland 2009). In vitro studies on the effects of miR-96 overexpression or knockdown on the RGC-5 cell line, have shown that increased availability of miR-96 reduced cell survival through activation of caspase-24 (Wang and Li 2014).

Further data suggests that miR-9 regulates axon extension and branching in mouse cortical neurons through repression of Map1b translation, which acts a functional target for the BDNF-dependent control of axon extension and branching. It has been proposed that miR-9 links regulatory signalling processes with dynamic translation mechanisms, controlling Map1b protein levels and axon development (Dajas-Bailador, Bonev et al. 2012). *In vitro* miR-187 is a regulator

of apoptosis and proliferation in retinal ganglion cells via direct targeting of the Samd7 3'-UTR (Zhang, Wang et al. 2015). Proliferation of RGC-5 cells induced by exogenous TGF-β was shown to be enhanced in cells engineered to overexpress miR-187, and suppressed in those where the same miRNA was depleted. Although it has been demonstrated that RGC-5 cells are not RGC (Van Bergen, Wood et al. 2009), these cells have provided a tool for the investigation of this miRNA, and this data suggests that miRNAs have specific regulatory functions in the retina at a sub-cellular level, and the ability of carefully selected miRNAs to target multiple mRNAs that are altered in disease conditions makes these molecules interesting candidates as therapeutics, either in the form of miRNA mimics or through their delivery by vesicle vectors.

Mechanisms regulating miRNA sorting into EV

Based on current research, there are four potential modes for sorting of miRNAs into exosomes, although the underlying mechanisms remain largely unclear. The expression and activity of the neutral sphingomyelinase 2 (nSMase2) – dependent pathway appears to be directly proportional to the quantity of miRNA secreted into exosomes, but not the quantity of vesicles themselves, implying a crucial role in miRNA sorting (Kosaka, Iguchi et al. 2013). Also significant are short (4 nt) sequence motifs found to be over-represented in the 3′ section of certain miRNA clusters commonly enriched in exosomes. These motifs appear to initiate binding by the sumoylated heterogeneous nuclear ribonucleoprotein A2B1 (hnRNPA2B1), which controls their loading into exosomes. Directed mutagenesis of these motifs greatly reduces the quantity of exosomal-miRNA detectable (Villarroya-Beltri, Gutiérrez-Vázquez et al. 2013).

A further putative mechanism of selection is based upon 3' end post-transcriptional modifications. In human B cells, 3′ end adenylation of defined miRNA species was found to correlate with enrichment relative to exosomes, most likely due to this modification hindering their incorporation into vesicles. The authors also report a reverse behaviour for uridylated isoforms, which were greatly overrepresented in exosomes (Koppers-Lalic, Hackenberg et al. 2014).

Still unknown are the relative contributions of several miRNA associated proteins commonly detected with EV. Argonautes (AGOs) are important miRNA-processing proteins thought to play a role in the binding and stabilising of exosomal-miRNAs. AGO knockout downregulates enrichment of exosomes with certain preferentially exported miRNAs (Guduric-Fuchs, O'Connor et al. 2012). Another protein, ALIX, is involved in the ESCRT machinery responsible for the biogenesis of exosomes (Baietti, Zhang et al. 2012). Interestingly, knockout of ALIX in human liver stem cells does not reduce the quantity of exosomes released, but significantly decrease exosomal-miRNA expression levels, suggesting a central role in their packaging (Iavello, Frech et al. 2016). Similarly, Shurtleff et al. report that Y-box protein I (YBX1) is necessary for the sorting of miR-223 into vesicles, and has an important role in the secretion of miRNAs in exosomes by HEK293T cells (Shurtleff, Temoche-Diaz et al. 2016). In short, selection of miRNAs is not a binary process, but it appears that a complex interplay between various pathways and certain evolutionarily conserved motifs may increase the likelihood of a transcript's sorting into EV. Thus, the profile of miRNAs in EV appears to be specific, since particular repertoires of miRNAs are selectively sorted into vesicle compartments, while others are typically excluded. Additionally, EV can contain components that appear to reflect the nature and even the state of the producer cell, a characteristic that has been particularly well established in tumour-derived "oncosomes" (Zhang, Zhang et al. 2015).

The therapeutic potential of extracellular vesicles in the retina

EV naturally released may influence changes in target cells that either promote disease progression, for example assisting in the advancement of certain cancers, or induce some protective outcome (Oushy, Hellwinkel et al. 2018). These observations have led to the hypothesis that EV derived from cells with established therapeutic application, have the potential to transfer protective and trophic signals to degenerated cells and tissues, and so have attracted much attention as novel vectors for regenerative therapies. Over the previous decade

stem cell-derived vesicles have been shown to ameliorate pulmonary hypertension (Willis, Fernandez-Gonzalez et al. 2017); enhance tissue repair of the myocardium (Lai, Chen et al. 2011); promote hepatic regeneration in the liver (Tan, Lai et al. 2014); and encourage endogenous angiogenesis and neurogenesis after traumatic brain injury (Zhang, Chopp et al. 2015) amongst other functions.

A range of pluripotent stem cells, including human embryonic stem cells (hESC) and induced pluripotent stem cells (iPSC) have been investigated for their ability to repair or regenerate the retina in animal models of retina degeneration (Nazari, Zhang et al. 2015, Riera, Fontrodona et al. 2016, Shirai, Mandai et al. 2016). In addition, adult stem cells such as mesenchymal stem cells derived from the umbilical cord and bone marrow (BMSCs) (Lund, Wang et al. 2007, Park, Caballero et al. 2012, Mead, Logan et al. 2013) and human Müller stem cells (Singhal, Bhatia et al. 2012, Jayaram, Jones et al. 2014, Becker, Eastlake et al. 2016) have also been investigated. Most studies in the retina regenerative field have been aimed at replacing neurons, however, neural replacement by cell grafting has not been successfully achieved as this process requires integration of transplanted cells within the neural network. EV are increasingly being explored as potential therapeutic agents, both as natural delivery vectors or as improvements to cell based therapies. In recent years, EV have been identified in a wide range of cells and tissues, although there has been no investigation of their release from Müller glia. This is significant, because Müller glia with stem cell-like characteristics have been shown to mediate paracrine neuroprotective and functional improvements within the neural retina following transplantation into animal models of retinal degeneration, including glaucoma and retinitis pigmentosa.

EV derived from these cells therefore constitute an intriguing therapeutic prospect, in particular for the protection and repair of retinal neurons damaged in conditions like glaucoma, traumatic optic neuropathy and AMD. Recently it has been demonstrated that BMSC-derived exosomes confer neuroprotective signals to RGCs in rat models of glaucoma and optic nerve crush (Mead and Tomarev

2017, Mead, Amaral et al. 2018). Fluorescently labelled vesicles were shown to integrate into the rat ganglion cell layer following intra-vitreal administration, suggesting that unlike whole cells, EV can efficiently migrate through the inner limiting membrane. Important to this potential is the fact that EV are highly stable, are not themselves replicative, and are simple to produce and purify.

Background summary and general objectives of the thesis

Stem cell transplantation holds great promise as a potential treatment for currently incurable retinal degenerative diseases that cause poor vision and blindness, the chief of these being glaucoma. In addition to myriad functions in the healthy and diseased retina, Müller glia have stem cell characteristics that make them intriguing, tissue-specific candidates for cell-based therapies.

The beneficial effects reported from studies involving cellular transplant into animal models of retinal degeneration appear to be wholly reliant upon the ability of these cells to secrete neuroprotective signals, which are then received by target cells in the host tissue. This is particularly significant because the retinal ganglion neurons depend upon a constant supply of neurotrophin signalling for their survival (Quigley, McKinnon et al. 2000, Iwabe, Moreno-Mendoza et al. 2007), and Müller glia are thought to be the primary source of these factors in the retina.

In addition, a relatively novel and as-yet underappreciated method of cell signalling is by the release of nano-sized membrane-bound vesicles. Recent evidence suggests that these organelles represent a key component of the neuroprotective secretions of stem cells, raising the possibility of their use as an alternative or adjunct to whole cell transplant, potentially bypassing some of the challenges inherent in translating these therapies to the clinic.

On the above basis, the principle objectives of this PhD project were:

1. To characterise the nature of the molecules secreted by Müller glia *in vitro*, in order to evaluate their potential role in the neuroprotective secretome of these cells
2. To establish the expression and secretion of neurotrophic factors by Müller glia cells *in vitro,* as well as investigate how the presence of certain pro-inflammatory cytokines modulated that expression.
3. To clarify the role of extracellular vesicles in neuroprotective signalling by characterising subtypes released by Müller glia cells, and investigating their respective proteomic and nucleic acid contents.
4. To evaluate the therapeutic potential of Müller glia-derived vesicles in an animal model of RGC degeneration.

Chapter 2: Muller glia synthesis and secretion of neurotrophins

Introduction

Müller glia stem cells for retinal neuroprotection

The sophistication of cell transplantation derived from the earliest experiments involving embryonic retinae transplanted onto the neonatal rat brain showed axonal outgrowth into the superior colliculus (Hankin and Lund 1987, Hankin and Lund 1990). These initial studies led researchers to explore various cell sources to induce regeneration and preserve function in a range of pre-clinical models of retinal disease. Neural precursors derived from embryonic stem cells survived for 16 weeks following transplantation, migrated large distances, and appeared to integrate within the host retina (Banin, Obolensky et al. 2006). Meanwhile, umbilical cord tissue cells (Zhao, Li et al. 2011), and photoreceptor precursors (MacLaren, Pearson et al. 2006, Gonzalez-Cordero, Kruczek et al. 2017) have each been trialled in murine models of inherited retinal disease.

Since glaucoma culminates in the specific degeneration of the retinal ganglion cell neurons, attempts have also been made to target these cells for protection and regeneration, following their depletion. Several groups report the efficacy of bone marrow-derived mesenchymal stem cells (BMSCs) in rats following either laser-photocoagulation of the trabecular meshwork, or optic nerve crush (Johnson, Bull et al. 2010, Mesentier-Louro, Zaverucha-do-Valle et al. 2014, Hu, Li et al. 2017). In addition, transplantation of umbilical cord mesenchymal stem cells, oligodendrocyte precursors and olfactory bulb cells have each been shown to exert a neuroprotective effect on RGCs in rodents (Bull, Irvine et al. 2009, Collins, Li et al. 2017, Ji, Lin et al. 2018). Despite these promising preclinical results, significant challenges remain in translating therapies based upon these cells into the clinic. Increasingly, research focus has been placed upon the derivation of tissue-specific multipotent cells bearing characteristic phenotypes, which may be preferred for use in regenerative therapies (Lengner 2010, de Miguel-Beriain 2015).

Muller glia with stem cell characteristics have been identified in the adult human retina, previous work in our lab has investigated the therapeutic potential of the Müller in various animal models of glaucoma. We have shown that a population of Müller glia with stem cell characteristics is present in the adult human retina, and that they have the ability to grow indefinitely *in vitro* and can be encouraged to differentiate into cells with characteristic markers and functions of various retinal neurons (Lawrence, Singhal et al. 2007, Bhatia, Jayaram et al. 2011). Critically, Muller glia differentiated from iPSC-derived retinal organoids partially restore visual function in rats following NMDA-induced cytotoxicity, as determined by improvements in negative scotopic threshold response of the electroretinogram (Singhal, Bhatia et al. 2012, Eastlake, Wang et al. 2019). The proliferative ability of these cells, combined with their established neurotrophic properties, confer Müller glia an enormous potential for expansion and use in cell therapies.

Thus far, no evidence has been reported from studies of transplantation into the eye of stem cells replacing the degenerated structures of the host retina, or integrating into axon extension to the brain. The promising therapeutic benefits observed in these experiments is instead thought to rely upon their ability to secrete neuroprotective molecules into the retinal microenvironment, in particular neurotrophic growth factors. In support for this hypothesis, rat and human bone marrow-derived MSCs induced to secrete high levels of BDNF, GDNF and VEGF exert a marked neuroprotective effect in rat eyes after optic nerve transection (Levkovitch-Verbin, Sadan et al. 2010), and the efficacy of BMSC transplantation has been attributed to secretion of platelet-derived growth factor (PDGF-AA) (Mead and Scheven 2015). Whilst rodent Müller glia express and produce neurotrophins, and constitutively upregulate expression of NGF, BDNF, NT-3, and NT-4 when challenged by high concentrations of glutamate, little is known of the human Müller glia’s capacity to secrete these factors (Taylor, Srinivasan et al. 2003).

Chapter summary and objectives

The neurotrophin hypothesis of glaucoma neurotoxicity proposes that the obstruction of retrograde transport in the optic nerve head leads to deprivation of neurotrophin support to RGC, resulting in apoptotic cell death. Based on the evidence summarised above, neuroprotective signals produced by long-lived stem cells or cells with stem cell-like characteristics, can protect and preserve retinal function *in situ*. This hypothesis is attractive because these factors are known to promote neuronal survival and regeneration in many experimental paradigms.

Stem cell transplantation has been performed extensively in several experimental models of retinal degeneration, but cell-based therapies to regenerate the human neural retina are still far from being implemented in the clinic. It is logical therefore that successful identification of the specific efficacious signals produced, might allow the design of targeted therapies with the potential to bypass the need for invasive cell transplant.

Inflammatory cytokines such as TNF-α are comparatively enriched in the glaucomatous retina, and are thought to mediate RGC damage and apoptosis through glial cell interactions. In that context, the potential modulating influence of exogenous cytokine application on the production of neurotrophic factors in Müller glia may be significant for their therapeutic potential.

The objectives of this chapter were therefore as follows:

1. To identify candidate molecules produced by Müller glia that may be responsible for the neuroprotective ability of these cells.
2. To evaluate the potential modulating influence of exogenous cytokine application on the synthesis and secretion of neurotrophic factors in Müller glia.

Materials and methods

Müller Glia Cell Culture

The Müller glia cell line MIO-M1, derived from human cadaveric retina (Limb, Salt et al. 2002) was used in this study. Cells were cultured for up to 35 passages on T-75 culture flasks with Nunclon surfaces in Dulbecco's Modified Eagle medium (DMEM, 1X with GlutaMAX™, without sodium pyruvate; Gibco, Life Technologies, Carlsbad, CA, USA) supplemented with 10% fetal calf serum (FCS, Biosera, Boussens, France), 20 µg/mL penicillin and 20 µg/mL streptomycin (Gibco, Life Technologies). Cells were seeded at densities of $2x10^5$ cells in 5ml medium per T25 flask, or $0.75x10^5$ cells in 2mL medium per well in 6 well plates. To passage, confluent monolayers were detached once a week by addition of 1-2 ml of TrypLE™Express (Gibco, Life Technologies) to cell monolayers, following by incubation for 5 minutes at 37°C, 5% CO_2. Cells were then suspended in 5-10 ml of DMEM (as above), centrifuged at 1500 X g for 5 minutes at 22 °C, after which supernatants were aspirated, and cell pellets re-suspended in fresh media, before being seeded in culture flasks. Fully confluent monolayers were generated after 7 days and subcultured at a dilution of 1:4.

Cryopreservation

Cell pellets were suspended in freezing media composed of 40% FCS, 10% Dimethyl Sulfoxide (DMSO) (Sigma-Aldrich, UK) in DMEM. Suspensions were transferred to 1.5mL cryovials ($1x10^6$ cells/mL), and initially placed in an isopropanol freezing cassette at -80°C for 24 hours to ensure controlled cryopreservation, before extended storage in liquid nitrogen.

Culture of Müller glia derived from pluripotent stem cells (PSC)

Müller glia cells dissociated from retinal organoids formed by PSC were provided by Dr K. Eastlake from the Institute of Ophthalmology, and maintained in DMEM supplemented with 10% FCS, 20 µg/mL Epidermal Growth Factor (EGF; cat no 315-09, Peprotech; U.K.), and 20 µg /mL Fibroblast Growth Factor (FGF; Cat no 100-18B, Peprotech; U.K). Cultures were grown in T25 culture flasks coated with human fibronectin (Catalogue no. 356008, Corning®, USA) at a working concentration of 50µg/mL in extracellular matrix buffer consisting of 15mM $NaHCO_3$, pH 9.6.

Culture of Müller glia with cytokines

The human Müller glia cell line Moorfields/Institute of Ophthalmology Müller-1 (MIO-M1) was cultured for periods of 24 hours, 48 hours and 120 hours days in T25 flasks with DMEM supplemented with 2% FCS, and 1% penicillin/streptomycin. At the time of seeding, the cytokines tumour necrosis factor - alpha (TNF-α; Cat no 300-01A, Peprotech; UK), transforming growth factor-beta1 (TGF-β1; Cat no 100-21, Peprotech; U.K.), and heparin binding EGF-like growth factor (HB-EGF; cat no 100-47, Peprotech; *U.K.*) were added to the culture medium at concentrations previously established in the host laboratory. These were as follows: TNF-α 5ng/ml; TGF-β1 50ng/mL; and HB-EGF 50ng/mL. Cytokines were added to culture media at the time of seeding and were not replenished during the culture period.

Isolation of mRNA, reverse-transcription and polymerase-chain reaction (RT-PCR)

RNA isolation was conducted using the RNeasy Plus Mini Kit as per manufacturer protocol (Catalogue no. 74134; Qiagen, Germany). Following cell culture in the presence of cytokines, and at the time points indicated above, culture media was

removed from the flasks and monolayers were washed with sterile PBS, before being detached with a cell scraper. Cell pellets from T25 flasks were suspended in 350µL of RLT Plus Buffer containing β-mercaptoenthanol diluted at 1:100 and by Dr K Eastlake and Miss R Wang from the host laboratory. Cells were frozen overnight at -20°C for complete cell lysis and homogenisation. RNA extraction was then performed according to the manufacturer's instructions. Cell lysates were centrifuged at 2000rpm for 5 minutes at 4°C before being transferred to a gDNA Eliminator Spin Column to remove genomic DNA. Lysates were homogenised with 70% ethanol and loaded onto a RNeasy Mini Spin Column and contaminants were eluted by washing with the buffer RW1 and RPE (supplied). Concentrated RNA was eluted in 20µL of the supplied RNase-free water and the concentration was determined using a spectrophotometer (Nanodrop-1000, Thermo Scientific). RNA samples were stored at -80°C until use and thawed on ice prior to performing the assays.

For the reverse-transcription, 1µg of isolated RNA was made up to a volume of 9.5 µL with Ultrapure™ RNase-free water (Catalogue no. 10977-35, Invitrogen). 1µL of dNTP mix (Catalogue no. U151A; Promega; USA) and 1µL Oligo d(T)12-18 primer (Catalogue no. 18418-012; Life Technologies) were added to make a final volume of 11.5 µL. The mix was incubated for 5 minutes at 65°C, before cooling at 4°C for 1 minute. To this mix, 1µl 100mM DTT, 1µl SuperScript® IV reverse transcriptase (Catalogue no. 18090010; SuperScript® IV First-Strand Synthesis System; Life Technologies), 4µl of 5X SuperScript® IV Buffer and 0.5µl RNasin® Plus RNase inhibitor (Catalogue no. N2611; Promega) were subsequently added. After brief centrifugation, this mix was incubated at 55°C for 10 minutes, 80°C for a further 10 minutes, and finally chilled at 4°C. The cDNA product was stored at -20°C.

For amplification, 1.5 µL of cDNA were added to a reaction mix containing 10µL of GoTaq® Green Master Mix (Catalogue no. M712; Promega), 1µl of forward and 1µl of reverse primers (10µM), made to a final volume of 20 µL with DNase-free water. PCR cycling was carried out using a thermocycler (Mastercycler® Gradient; Eppendorf, UK). An initial incubation at 95°C for 6 minutes, was followed by a further incubation at annealing temperature for 1 minute, and an

extension step of 72°C for 1 minute. This was repeated for an appropriate number of cycles according to each primer pair used (see appendices). PCR reaction was terminated following a final extension phase at 72°C for 5 minutes, and then held at 4°C. PCR products were stored at -4°C overnight or immediately separated by agarose gel electrophoresis.

Gel electrophoresis

A 2% agarose gel containing 1 in 15,000 GelRed™ nucleic acid gel stain (10,000X in water; Cat no 41003; Biotium Inc., Hayward, CA, USA) was made, and 10µl of the PCR product were loaded into wells, in parallel to a 100bp DNA ladder (Cat no G210; Promega). Gels were run at 100V for 60 minutes, before being examined by UV trans-illumination. Genesnap Image Acquisition Software (www.syngene.com) was used to take images of the gel at optimum exposure, these were processed for band densitometry using ImageJ software (Java, USA). Data was exported to Graphpad Prism 5 (GraphPad Software Inc.; La Jolla, CA, USA).

Protein Isolation and electrophoresis

Whole cell lysates were isolated for protein expression analysis. After cells were grown under various experimental conditions, media was aspirated, cells were washed briefly with PBS and cells were then detached using a cell scraper. Cell pellets were resuspended in 100µl ice-cold radio Immunoprecipitation Assay (RIPA) lysis buffer (Cat no R0278; Sigma-Aldrich) containing 10µl of protease inhibitor cocktail (P8340, Sigma-Aldrich, UK), 0.5mM Dithiothreitol (DTT), 1mM Phenyl Methyl Sulphonyl Fluoride (PMSF) and 3mM Sodium Orthovanadate (Na3VO4). The suspension was then placed on ice for 5 minutes to allow cells to swell and lyse and then centrifuged for 5 minutes at 10,000 rpm to remove any cellular debris. The supernatant containing the proteins was collected and stored at -20°C. Total protein concentration of whole cell lysates was measured in duplicate using the Thermo Scientific Pierce™ BCA (Bicinchoninic Acid) Protein

Assay Kit (Cat no 23225; Life Technologies) as per manufacturer's instructions. Known increasing concentrations of bovine serum albumin were used as a reference protein in duplicate. Absorbance was measured immediately at 562nm in a Safire plate reader (Tecan; Mannedorf, Switerzland).

Protein gel electrophoresis was conducted using NuPAGE® (Life Technologies) electrophoresis and buffer reagents NuPAGE® (Life Technologies). Precast Nupage™ 4-12% Bis-Tris gels with 15 wells and MOPS / MES 1X Running Buffer were used in order to separate proteins of masses between 15kDa and 260kDa. The proteins analysed in the study were NGF (26kDa), BDNF (28kDa), NT-3 (30kDa), NT-4 (22kDa), (β-actin (42kDa), CD9 (25kDa), CD63 (26kDa), Alix (96kDa), and Calnexin (67kDa). Loading samples (15µl each) were prepared with 3.75µl of loading buffer (LDS 4X; Cat no NP0007; Life Technologies), 1.5µl of reducing agent (10X; Cat no NP0009; Life Technologies) and a maximum of 9.75µl of protein + ddH_20. Loading samples were boiled at 80°C for 10 minutes to denature proteins (with the exception of when probing for CD63, for which the antibody required non-reducing conditions). 5µl of pre-stained protein standard ladder (Broad Range 11-190kDa; Cat no P7706; New England Biolabs; Ipswich, MA, USA) was loaded in parallel with quantities of 5 or 10 µg of protein into gel wells for a total volume of 15uL. Gels were run for 50 minutes at 180V.

Semi-dry transfer of proteins and Immunoblotting

Poly VinyliDene Fluoride (PVDF) membranes (Immobilon-FL PVDF, 0.45 µm; Cat no IPFL00010; Merck Millipore; Darmstadt, Germany) were cut to size, soaked in methanol for 2 minutes and rinsed in distilled water before being immersed in 1X transfer buffer (20X; Cat no NP0006; Life Technologies). After separation, pre-soaked filter paper (Cat no 1703968; Bio-Rad Laboratories; West Berkley, CA, USA). was placed on the bottom platinum anode of the Trans-Blot® SD Semi-Dry Transfer Cell (Bio-Rad Laboratories), and pre-wet membrane placed on top. The gel was placed on top of the membrane, followed by a second pre-wet filter paper. The top cathode was secured in place and the transfer was ran at 25V for 30 minutes.

Western blot was used to confirm and compare expression of neurotrophic factors in Müller glia cell lysates, as well as the presence of extracellular vesicle-enriched markers in EV preparations using established methods (Eastlake, Heywood et al. 2017). PVDF membranes were blocked for one hour at 37°C, in blocking buffer consisting off Tris-buffered saline (TBS) with 0.1% Tween-20, 5% milk and 5% FCS. Primary antibodies were diluted in blocking buffer and membrane was incubated over-night at 4°C on a shaker. Membranes were washed at room temperature on a shaker, for three periods of 20 minutes, in TBS + 0.1% Tween-20 detergent. Membranes were incubated with horseradish peroxidase-conjugated secondary antibodies (Jackson ImmunoResearch Laboratories Inc.; PA, USA*),* diluted 1:5000 in blocking buffer for 1 hour at room temperature. This was followed by three washes as described above. Luminata western HRP substrate chemiluminescent solution (1mL) (Classico, Millipore Corporation; Billerica, MA, USA) was applied to the membrane for two minutes, before removal. The membrane placed in a cassette and the protein was visualised using Fuji X-ray film (Cat no AUT-300-040D; Thermo Fisher Scientific) developed in a dark room. Films were scanned, and the optical density of bands present was quantified using ImageJ. Data was exported and statistical analysis performed using Graphpad Prism 5 (GraphPad Software Inc.; La Jolla, CA, USA)

Enzyme-linked immunosorbent assay

Müller glia cell supernatants from MIO-M1 cells cultured with and without cytokines (5×10^5 cells cultured with 4 mL of serum free DMEM + 1% pen/strep for 48 h) were concentrated using an Amicon Ultra-15 centrifugal filter device with a 3 kDa molecular weight cut-off (#UFC9 005 24, BD Biosciences). Concentrates were measured for total protein content using the Pierce BCA protein assay kit (Thermo Scientific, Waltham, MA) to allow for normalisation after concentration. Volumes of concentrate equivalent to 30µg of total protein were quantitated for the presence of the neurotrophins NGF, BDNF, NT-3, and NT-4 using the Human Multi-Neurotrophin Rapid™ Screening enzyme linked immunosorbent assay kit (Biosensis®, Thebarton, Australia), according to the manufacturer instructions. Experiments were performed in triplicate, and absorbance was measured at 450

nm using a plate reader (Safire, Tecan, Maennedorf, Switzerland).

Gel/western blot imaging and Statistical Analysis

Images of RT-PCR gels and immunoblot membranes were quantified for densitometry of bands using ImageJ (Java, USA) software. Results were exported to Microsoft Excel and GraphPad Prism 5 (GraphPad Software Inc.; La Jolla, CA, USA) which were used for semi-quantitative comparison. Genes of interest were normalised to β-actin, used as a housekeeping control. Three biological replicates of each experiment were made. Results were expressed as means +/- standard error of the mean (SEM) at 95% confidence intervals. For experiments comparing two different conditions a paired, two tailed student's T test was used. A P value of <0.05 was considered statistically significant.

Results

Expression of genes and proteins coding for neurotrophins by adult-derived and PSC-derived Müller glia

RT-PCR and western blot analyses were used with the aim of clarifying the gene expression and production of neurotrophins in Müller glia cells. Expression of NGF, BDNF, NT3 and NT4 mRNA were detected in Müller of the MIO-M1 immortalised cell line, as well as in Müller cells isolated from retinal organoids derived from three different pluripotent stem cell lines (fig. 3, A). Next, antibodies directed to neurotrophin antigens were used to probe Müller cell lysates for the presence of the translated proteins. Enrichment of NGF and BDNF was detected in all cells investigated, whilst smaller signals were also detected for NT3 and NT4, confirming that Müller glia cells in culture transcribe and translate neurotrophin genes *in vitro* (fig 3, B).

Cytokine modulation of nerve growth factor expression

Semi-quantitative analyses of the expression of genes coding for NGF showed a significant upregulation in response to treatment with TNF-α at a concentration of 5ng/mL, and this response was found to be consistent at 24 ($p = 0.023$) and 48 hours post-treatment ($p=0.042$) (fig. 4). The trend for NGF upregulation continued at 120 hours post-treatment, although variation in mean expression between treated and untreated cells was not statistically significant ($p = 0.0793$). Supplementation of MIO-M1 cells with TGF-β1 (50ng/mL) or HB-EGF (50ng/mL) did not significantly modulate the expression of NGF mRNA at any time after activation by these two cytokines.

Cytokine modulation of brain-derived neurotrophic factor expression

Semi-quantitative RT-PCR revealed robust expression of the BDNF gene in MIO-M1 cell cultures (fig. 5). Supplementation of MIO-M1 cultures with the inflammatory cytokines TNF- α, TGF-β1 and HB-EGF resulted in significant downregulation of BDNF expression. This was evident at 24, 48, and 120 hours post-treatment with TNF- α (p= 0.045, p = 0.015, p = 0.017) as well as .TGF-β1 (50ng/mL) (p = 0.042, 0.025, 0.004), and HB-EGF (50ng/mL) (p = 0.02, 0.036. 0.009).

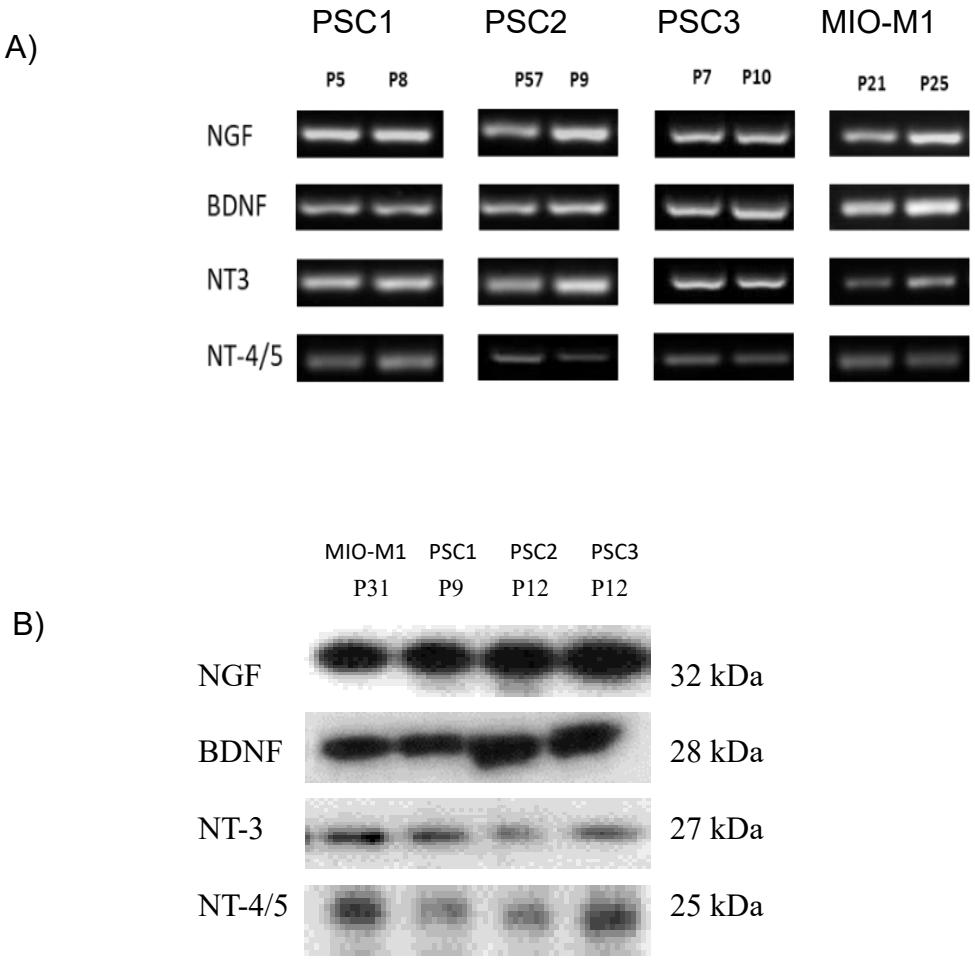

Figure 3. ***A) Expression of neurotrophin mRNA and protein in Müller glia cells****. Gel bands demonstrating expression of neurotrophin mRNA in human Müller glia derived from three pluripotent stem cell derived Müller cell lines (PSC1, PSC2 and PSC3) and the Müller cell line (MIO-M1).* ***B)*** *western blots presenting the expression of neurotrophins in 10 µg of whole cell protein lysates, with corresponding molecular weights.*

Cytokine modulation of neurotrophin 3 expression

As with NGF, semi-quantitative gene analysis identified a significant upregulation of the NT-3 gene in MIO-M1 cells cultured in the presence of TNF-α at a concentration of 5ng/mL (fig. 6). This response was consistent at 24 ($p = 0.04$), 48 ($p=0.035$) and 120 hours post-treatment with this cytokine ($p=0.007$). In contrast, treatment of MIO-M1 cells with either TGF-β1 (50ng/mL), or HB-EGF (50ng/mL), did not significantly modulate NT-3 gene expression.

Cytokine modulation of neurotrophin 4 expression

Semi-quantitative gene expression analysis identified a robust upregulation of NT-4 mRNA in MIO-M1 cell cultures in response to supplementation of media with TGF-β1 (50ng/mL), and this was statistically significant after 24, 48, and 120 hours culture with this cytokine ($p = 0.031, 0.046, 0.003$) (fig. 7). Treatment of MIO-M1 cells with either TNF-α (5ng/mL), or HB-EGF (50ng/mL), did not significantly modulate the expression of NT-4 mRNA in these cells.

Cytokine modulation of Glial cell line-derived neurotrophic factor

Finally, analysis of GDNF mRNA confirmed consistent expression in MIO-M1 Müller glia cultures (fig. 8). Semi-quantitative analyses revealed that mean expression of this gene following 24 and 48 hours post-supplementation was significantly upregulated in the presence of TGF-β1 (50ng/mL) ($p = 0.05, 0.025$). A trend for increased mRNA expression was also apparent following treatment of cells with TNF-α (5 ng/mL), and HB-EGF (50ng/mL), although this slight upregulation was not significant. These observations suggest that expression of this factor appears to be elevated in Müller glia in response to the presence of these three inflammatory cytokines.

NGF

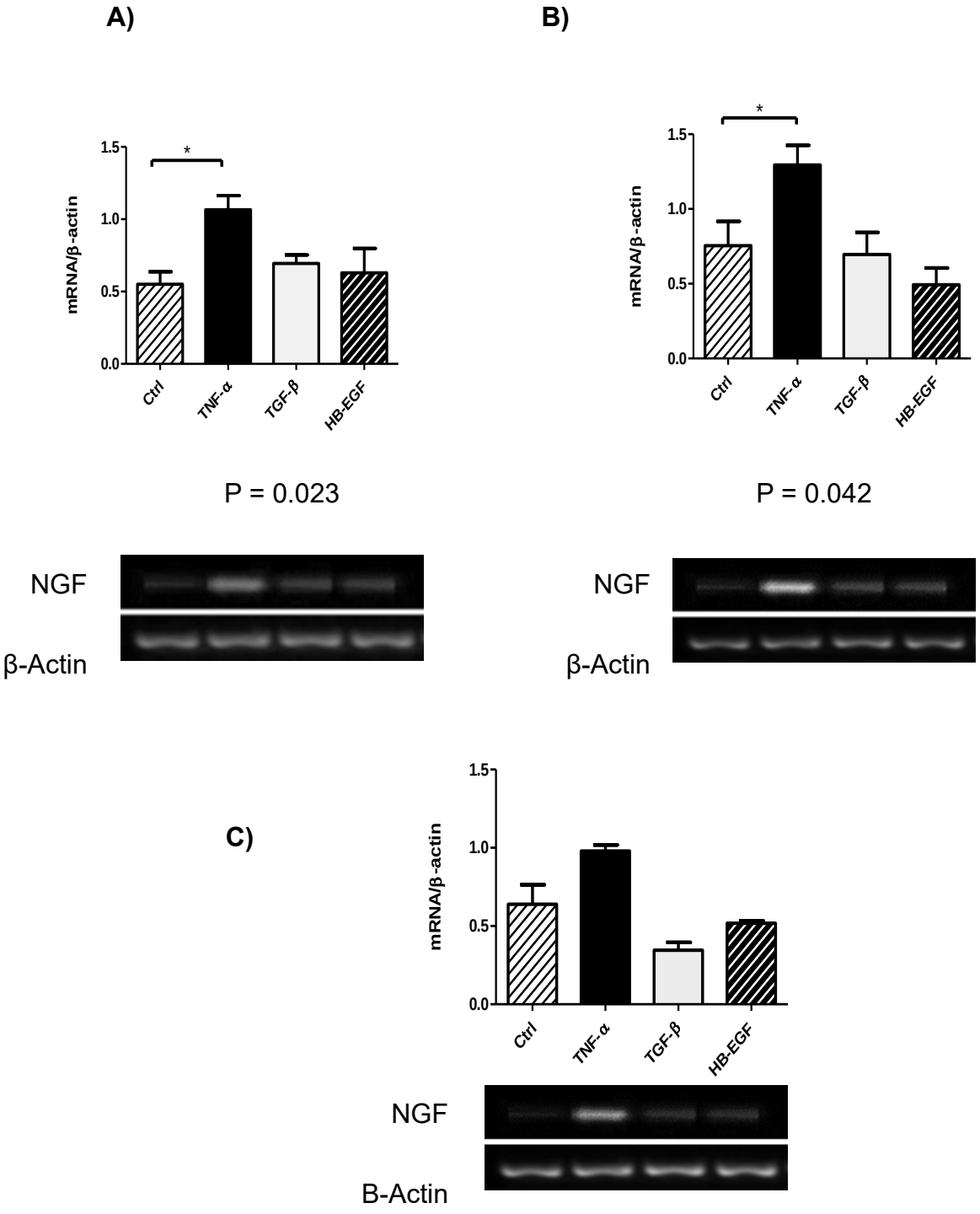

Figure 4. ***Expression of NGF mRNA****. Representative gel bands and histograms displaying expression of NGF normalised to β-actin (mean ± SEM), in MIO-M1 cells following incubation with cytokines for* ***A****) 24 hours,* ***B****) 48 hours, and* ***C****) 120 hours (n=4). * indicates significant difference (p = < 0.05) as determined by paired t-test.*

BDNF

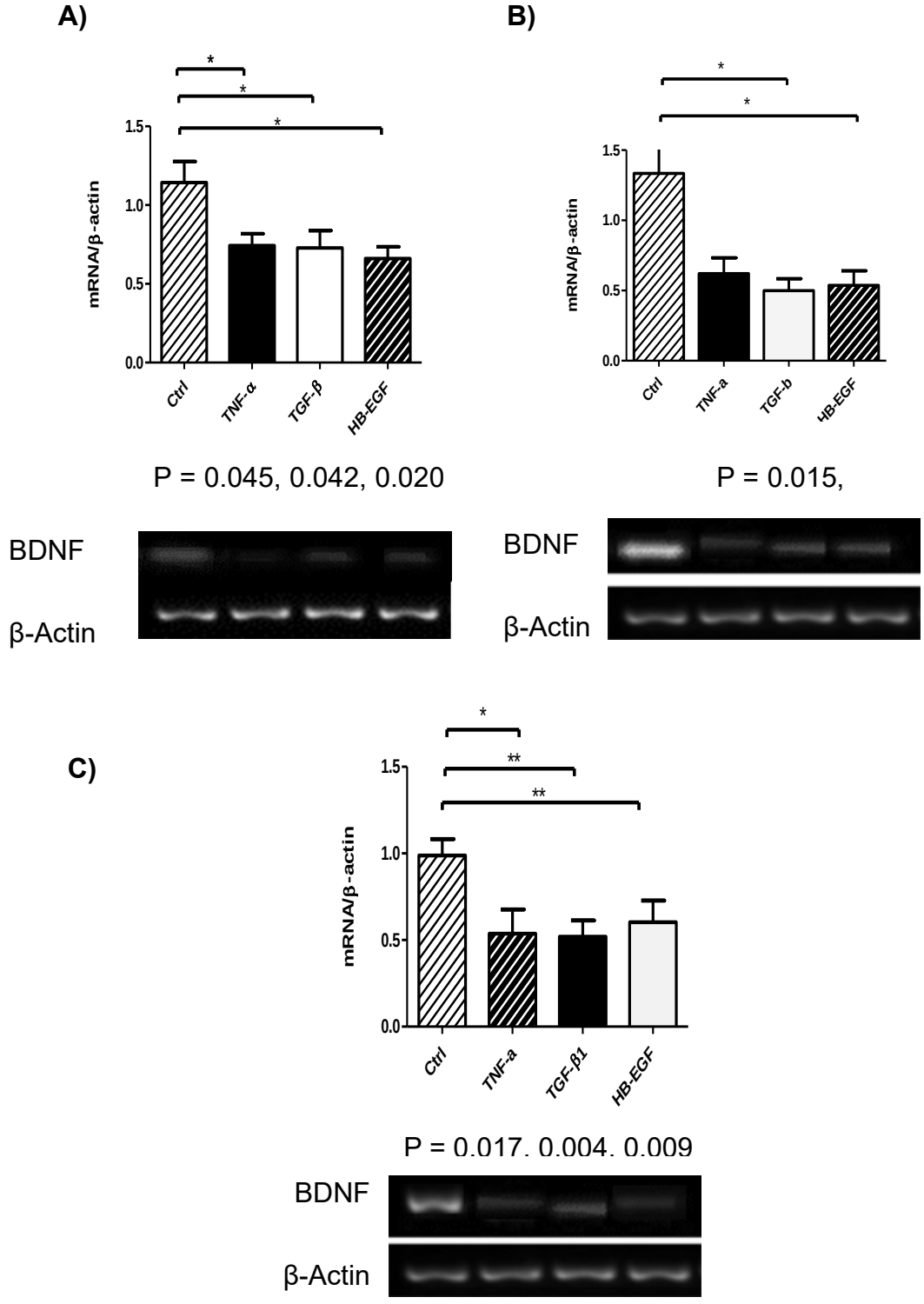

Figure 5. ***Expression of BDNF mRNA.*** *Representative gel bands and histograms displaying expression of* ***BDNF*** *normalised to β-actin (mean ± SEM), in MIO-M1 cells following incubation with cytokines for* ***A****) 24 hours,* ***B****) 48 hours, and* ***C****) 120 hours (n=4). * indicates significant difference (p = < 0.05) as determined by paired t-test.*

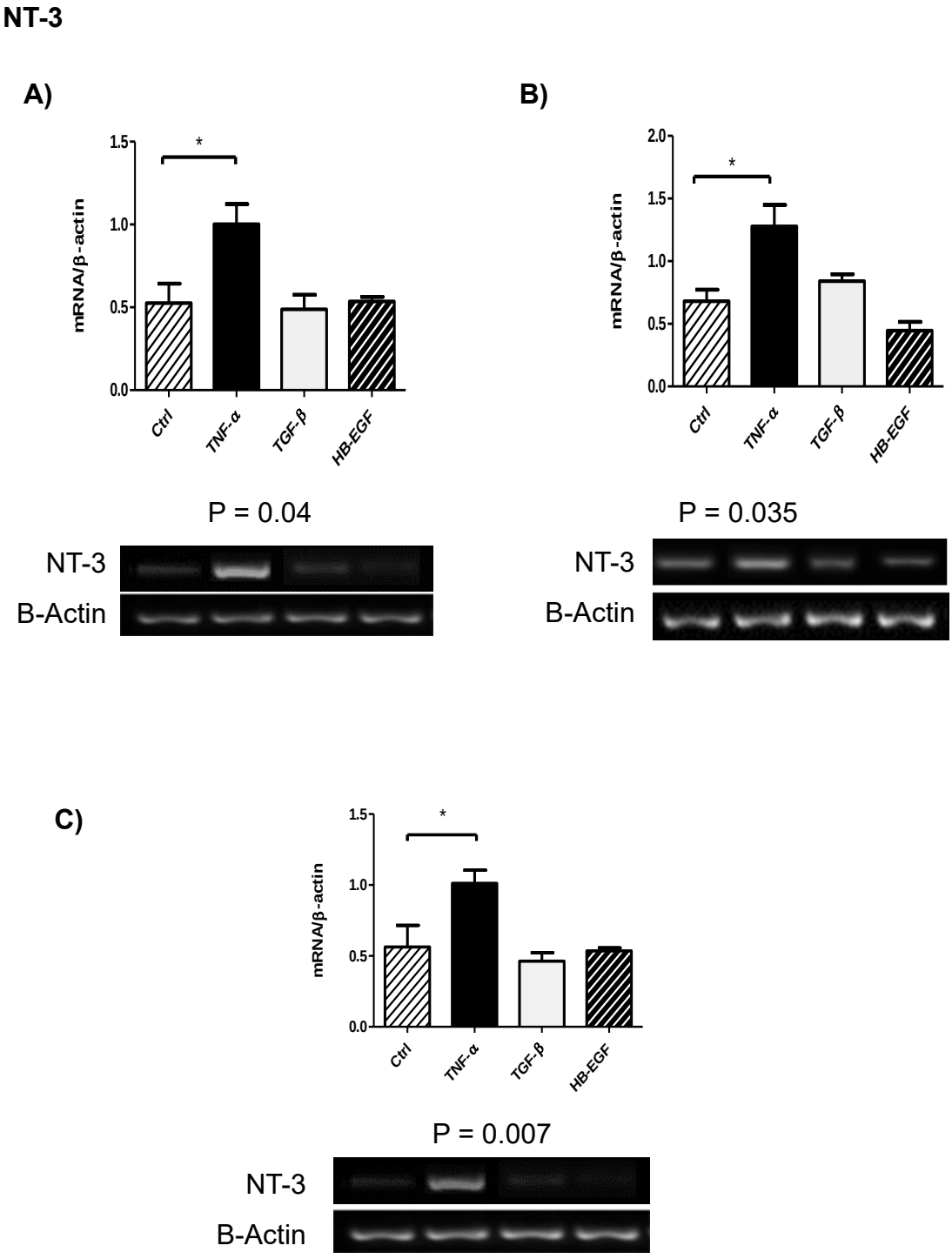

Figure 6. ***Expression of NT-3 mRNA.*** *Representative gel bands and histograms displaying expression of NT-3 normalised to β-actin (mean ± SEM), in MIO-M1 cells following incubation with cytokines for A) 24 hours, B) 48 hours, and C) 120 hours (n=4). * indicates significant difference (p = < 0.05) as determined by paired t-test.*

NT-4

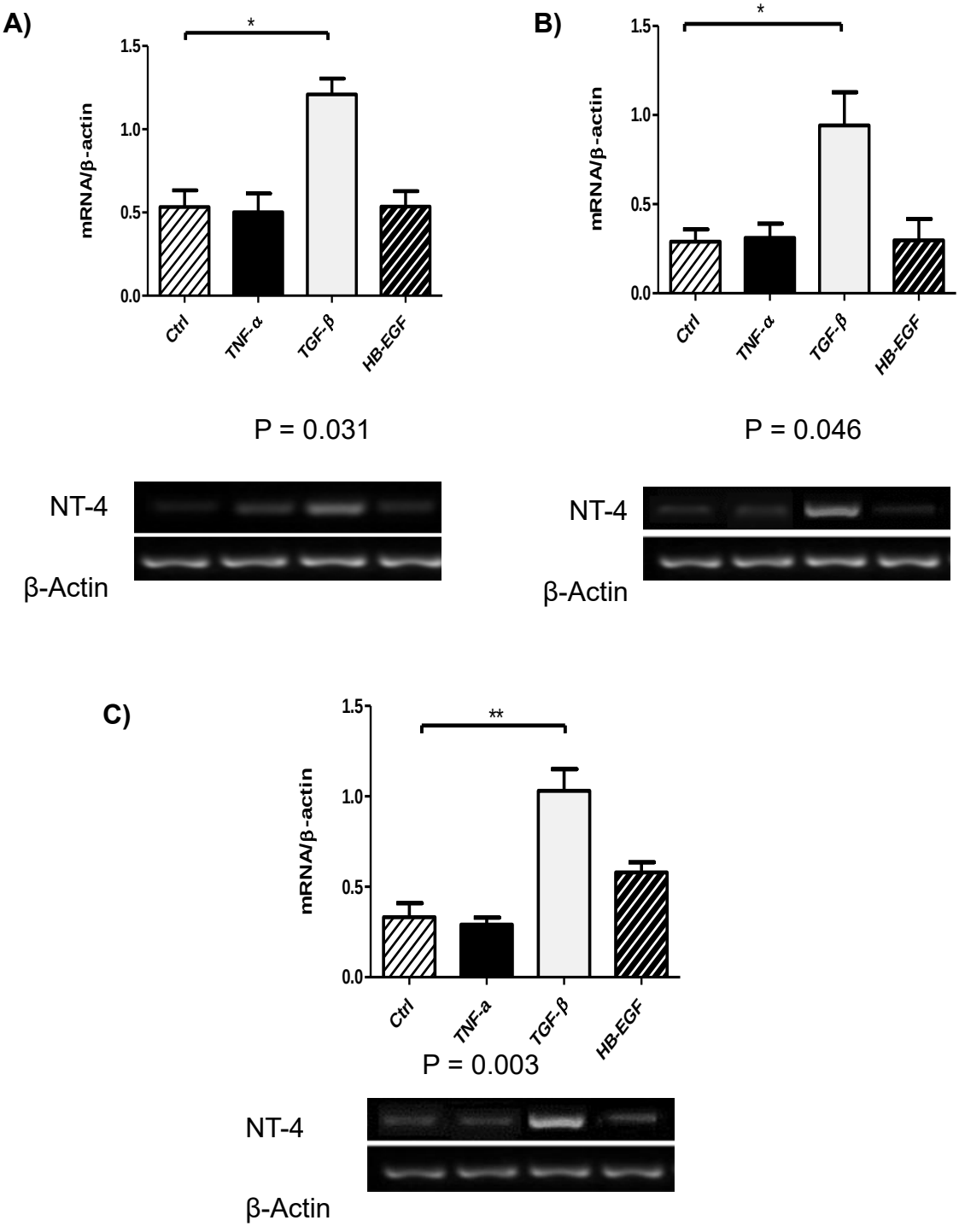

Figure 7. ***Expression of NT-4 mRNA.*** *Representative gel bands and histograms displaying expression of* ***NT-4*** *normalised to β-actin (mean ± SEM), in MIO-M1 cells following incubation with cytokines for* ***A****) 24 hours,* ***B****) 48 hours, and* ***C****) 120 hours (n=4). * indicates significant diference (p = < 0.05) as determined by paired t-test.*

GDNF

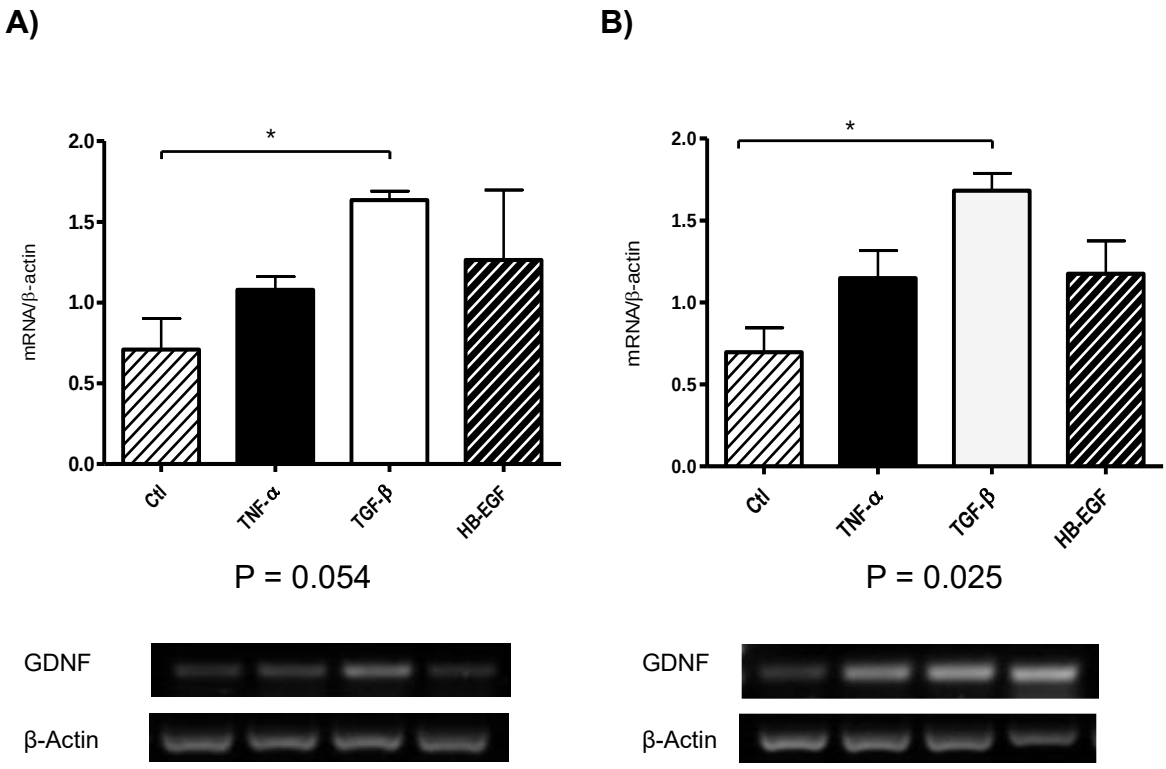

Figure 8. ***Expression of GDNF mRNA.*** *Representative gel bands and histograms displaying expression of GDNF normalised to β-actin (mean ± SEM), in MIO-M1 cells following incubation with cytokines for A) 24 hours, B) 48 hours (n=4). * indicates significant difference (p = < 0.05) as determined by paired t-test.*

Cytokine modulation of cell-associated and secreted proteins coding for neurotrophins in Müller glial cells

Western blot was used to identify the intracellular proteins coding for three neurotrophin proteins prior to maturation and release. Robust intracellular expression of the neurotrophin proteins NGF, BDNF and NT-3 was confirmed in MIO-M1 cell lysates. However, significant cytokine-modulation of intracellular NGF, BDNF and NT-3 proteins was not detected at the translational level in MIO-M1 cell lysates (fig. 9). GDNF protein was also expressed, and appeared to be upregulated intracellularly in the presence of both TNF-α (5ng/mL) and HB-EGF, although these results were variable. A significant and prolonged upregulation was detected following incubation with TGF-β1 (50ng/mL) ($p = 0.02, 0.028$) (fig.10, B).

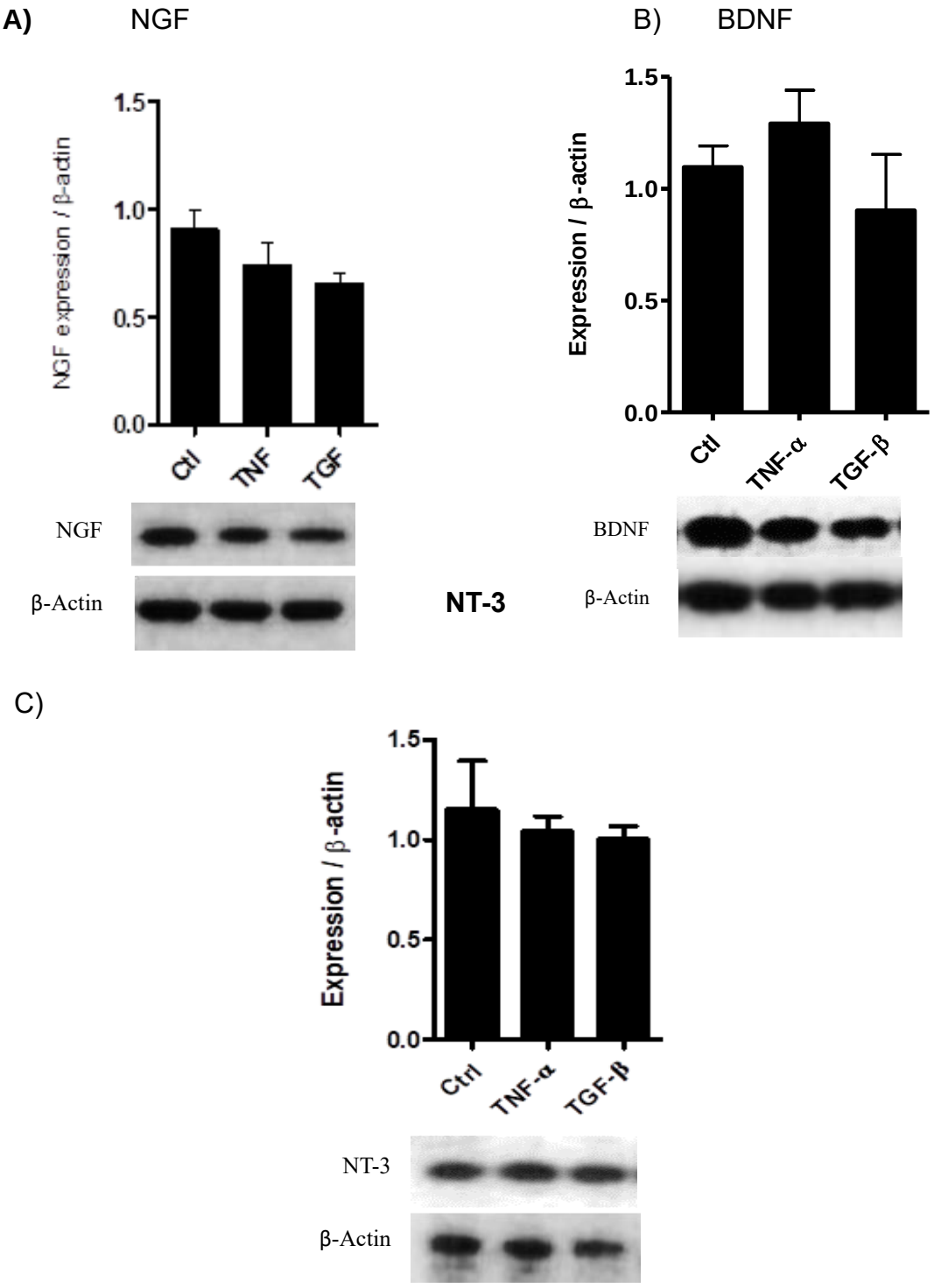

*Figure 9. Representative western blot bands and histograms from MIO-M1 cell lysates presenting relative expression of neurotrophic factor proteins to β-actin (mean ± SD; n=3), following 48 hours supplementation with TNF-α (5 ng/mL), and TGF-β1 (50 ng/mL). **A**) NGF, **B**) BDNF, **C**) NT-3*

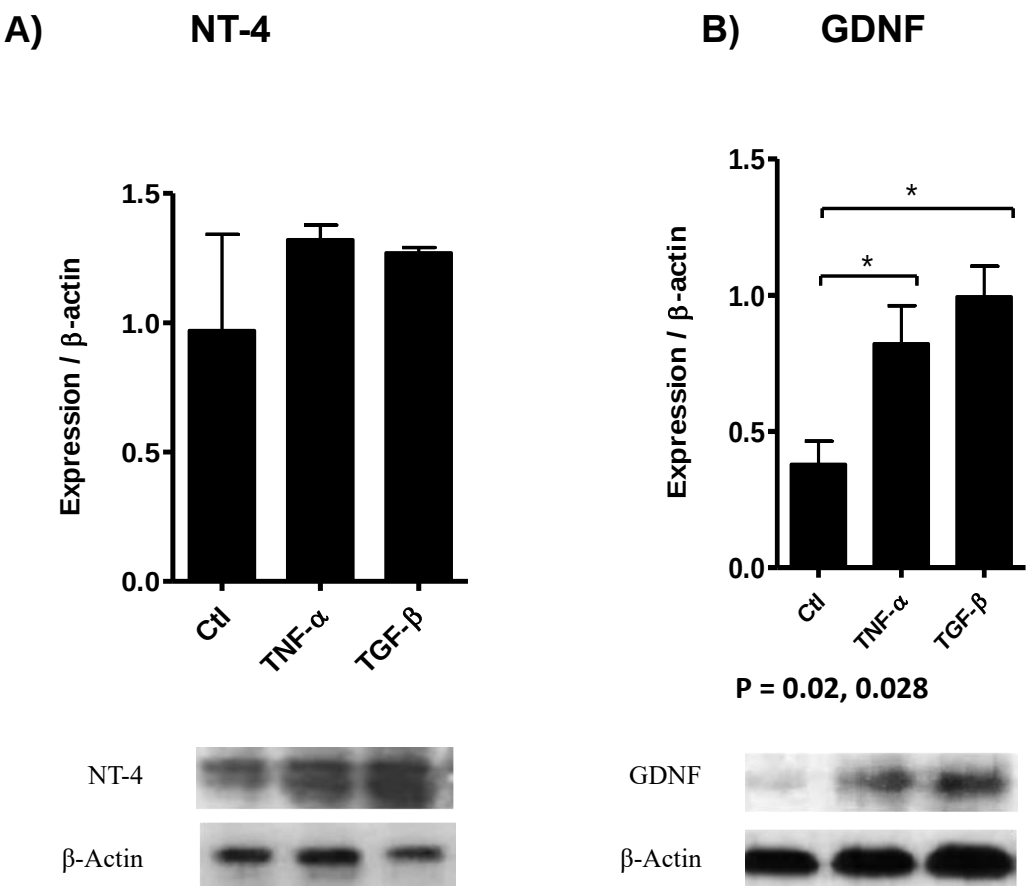

Figure 10. Representative western blot bands and histograms presenting relative expression of neurotrophic factor proteins to β-actin (mean ± SD; n=3), following 48 hours supplementation with TNF-α (5 ng/mL), and TGF-β1 (50 ng/mL). ***A****) anti-NT-4/5, B) anti-GDNF****.*** ** indicates significant difference (p = < 0.05) as determined by paired t-test.*

Müller glia secretion of neurotrophins

With the aim of confirming post-transcriptional secretion of neurotrophic factors, the concentrations of NGF, BDNF, NT-3, or NT-4 were quantified in Müller glia culture supernatants following 48-hour culture in the presence or absence of TNF-α or TGF-β1 (50ng/mL were used for both cytokines). On this basis, enzyme-linked immunosorbent assays (ELISA) (Biosensis® Pty Ltd, Thebarton, Australia) were used to assess the secreted active forms of these neurotrophins (fig. 11, 12). Culture supernatants from cells treated with TNF-α were found to contain significantly higher concentrations of NGF (p = 0.017) than control cell supernatants, however no significant variations in mean concentrations of BDNF, NT-3, or NT-4 were detected in the study (fig. 11, 12).

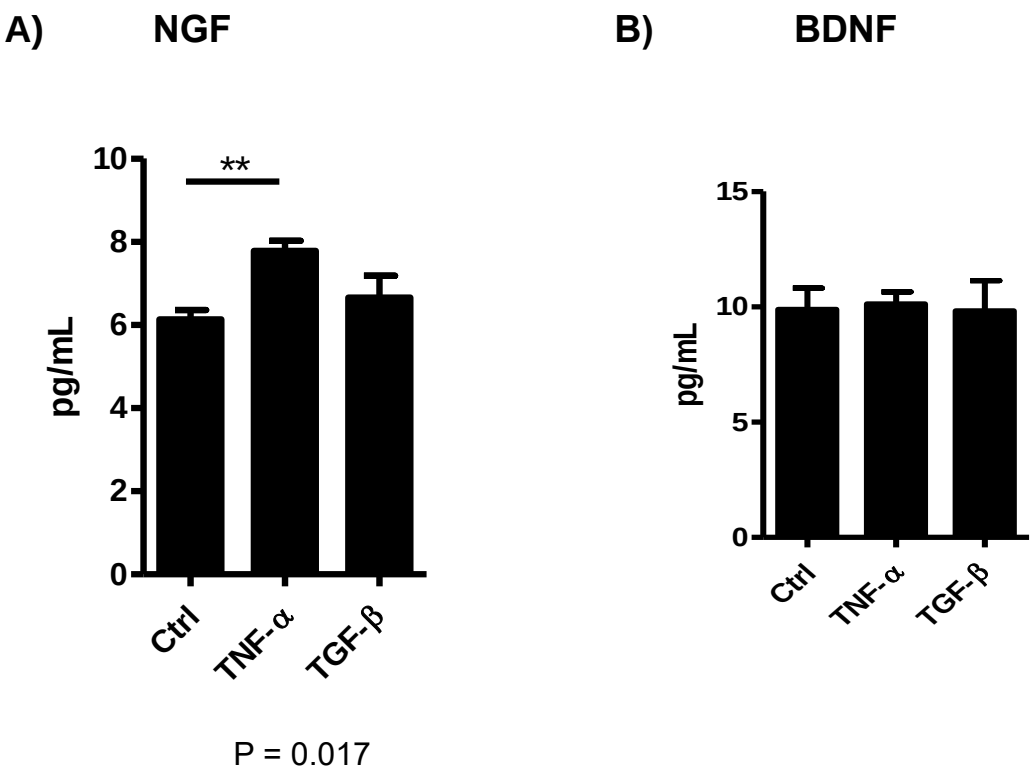

Figure 11. ***Histograms represent concentrations of neurotrophins detected by ELISA in MIO-M1 culture supernatants*** *(mean ± SEM), following 48 hrs of cytokine supplementation.* ***A****) NGF (n=6),* ***B****) BDNF (n=6). * indicates significant difference (p = < 0.05) as determined by paired t-test.*

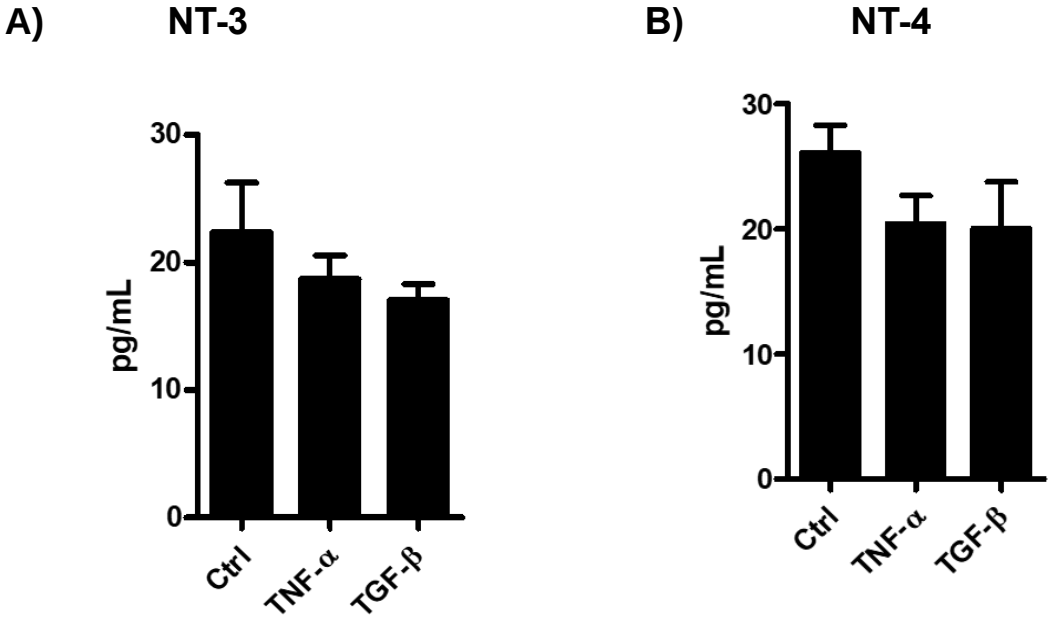

Figure 12. ***Histograms represent concentrations of neurotrophins detected by ELISA in MIO-M1 culture supernatants*** *(mean ± SEM), following 48 hrs of cytokine supplementation.* ***A****) NT-3 (n=6),* ***B****) NT-4 (n=6).*

Discussion

This study further confirmed the expression of mRNA coding for the neurotrophic factors GDNF, NGF, BDNF, NT3 and NT4 in human Müller glia. It was of interest that cytokines, including TGF-β1, TNF-α, and HB-EGF were shown to differentially modify the gene expression of these factors, which may be influenced *in vivo* upon the release of inflammatory cytokines caused by retinal degeneration (Bringmann and Wiedemann 2012). However, gene expression was not accompanied by changes in protein expression in all cases. TNF-α has been previously reported to upregulate NGF and GDNF mRNA in astrocytes, but not in Müller glia. The current study showed that Müller glia can upregulate mRNA expression of both mRNA and protein coding for this neurotrophin upon culture with TNF-α. It was also of interest that gene and protein expression of GDNF were upregulated by TGF-β1.

Implications of neurotrophic factor release by Müller glia cells

A wealth of data collected from experimental models of glaucoma demonstrate neurotrophins and neurotrophic factors to be strongly neuroprotective and capable of promoting axon regeneration and enhancing neuronal cell function. In addition, it is known that glaucomatous blockade of axonal transport induced by IOP elevation leads to deficits of the levels and availability of these factors and subsequent RGC death, and that expression of BDNF and NGF in serum is significantly reduced in early and moderate forms of glaucoma (Oddone, Roberti et al. 2017). Given the regenerative capabilities of neurotrophin-mediated interventions already observed in preclinical models of other neurodegenerative diseases, neurotrophic factors may offer an attractive neuroprotective option to pursue in glaucoma.

Because of their strategic location within the retina, Müller cells are in a position to influence all aspects of retinal function and neuronal activity. Indeed, Müller cells interact with most, if not all neurons in the retina in a symbiotic relationship (de Melo Reis, Ventura et al. 2008). It is logical therefore to suggest, that the production and release of neurotrophic factors constitutes a key component of the support and regulation that Müller glia and other macroglial cells provide to retinal neurons. By demonstrating that the secretome of Müller glia comprises of all four neurotrophins, this work provides new insight into the neuron supporting role of these cells during normal physiology, as well as suggesting the origin of the paracrine neuroprotective function in animal models of RGC disease. Indeed, it has been previously demonstrated that release of multiple neurotrophic factors from glial cells increases the long-term survival of developing RGCs in culture (Meyer-Franke, Kaplan et al. 1995), and that the exogenous addition of neurotrophic factors from glial cells significantly attenuates the degeneration of RGC after optic nerve damage in the rat (Yan, Wang et al. 1999). This also appears to be pivotal during retinal development, since survival of neonatal rat RGCs appears to depend upon factors produced by Müller glia, which appear to act both directly, and indirectly through other cells of the retina (Raju and Bennett 1986).

In situ, Müller glia span the thickness of the retina and thus have physical contact with neurons and other retinal cells (Reichenbach and Bringmann 2010). Early studies looked to evaluate the neurotrophic support provided by these cells to retinal neurons using co-culture assays, for example Müller cell co-culture with *ex vivo* RGC from the adult pig significantly enhances their survival and outgrowth, however it was not immediately evident whether physical contact between the cell types was required for their neuroprotective effect (García, Forster et al. 2002). Indeed, early works reported that Müller cells had a neurite-promoting effect on retinal ganglion cells only when there was direct cell-to-cell contact, and that soluble factors released by Müller did not induce significant neurite outgrowth (Raju and Bennett 1986). In providing evidence of the Müller's ability to synthesise and secrete neurotrophic factors, this thesis further supports a paracrine mechanism of intracellular support. In addition this data adds to

previously published works suggesting that RGC co-cultured with Müller glia were capable of blocking the excitotoxic effect of glutamate, even when there was no direct contact between the different cell types (Kawasaki, Otori et al. 2000).

It is important to note that while immortalised Müller glia from the adult human eye appear to continuously secrete neurotrophins in culture, as do Müller cells isolated from retinal organoids in the lab, this may not be true of Müller glia *in situ.* The fact that expression of these genes appear to be modulated by cytokines, suggests that their production may be dependent on upstream signalling, and so may represent a response to disease or injury. Alternatively, since the RGCs are known to require constant neurotrophin support during development and in adult tissue to avoid the initiation of apoptotic pathways (Quigley, Nickells et al. 1995), it is possible that Müller glia constitutively produce these factors in the healthy retina.

In addition to experiments demonstrating the neuroprotective effect of Müller glia cell transplant in animal models of RGC-depletion (Singhal, Bhatia et al. 2012, Eastlake, Wang et al. 2019) , unpublished data from our lab also supports the neuroprotective influence of factors released by Müller glia *in vitro.* Culture of primary RGC cells in media pre-conditioned by Müller significantly enhances survival and axon branching (unpublished). These observations are comparable with previous studies describing how conditioned medium from purified chick retinal Müller cells supports the survival of E10 sympathetic neurons (Reis, Cabral da Silva et al. 2002). In this way, Müller glia are analogous to other types of stem cells currently being considered for therapeutic application in the eye. For example, human neural progenitors have been shown to protect photoreceptors, maintain synaptic integrity and support horizontal cell survival when co-cultured with porcine retinal explants (Mollick, Mohlin et al. 2016). Similarly, co-culture of neural progenitors with rat and mice retina *in vitro* has been demonstrated to delay the degeneration of photoreceptors (Englund-Johansson, Mohlin et al. 2010). Profiling of conditioned media in this study indicated that the protective effect was likely to be a result of the secretion of a variety of growth factors.

Relationships between Müller glia cells and pro-inflammatory cytokines

The data reported here indicate that the addition of exogenous cytokines to Müller glia in culture was capable of modulating the expression of neurotrophin genes. Interestingly, equivalent variation in the quantities of neurotrophin protein being translated and secreted were not revealed by western blot or ELISA. While it is tempting to simply conclude that the variations in neurotrophin expression and secretion reported here are a direct result of cytokine initiated signalling pathways, care must be taken in their analysis. Müller glia themselves express low levels of TGF-β and TNF-α, and in addition, whilst neurotrophin release was measured by ELISA, the Müller cells themselves express tropomyosin-kinase receptors and respond to BDNF by upregulating production of other factors (Harada, Harada et al. 2002, Harada, Guo et al. 2011). It is probable therefore, that the underlying mechanisms responsible for the effects reported here are complex and indirect, likely involving the synthesis and release of numerous factors which then initiate further downstream responses in neighbouring cells.

Although this is the first study to report the upregulation of NGF by TNFα in Müller glia, the association between inflammatory stimuli and increased expression of NGF and other neurotrophic factors is well established in glial cells of the wider CNS (Gadient, Cron et al. 1990, Kuno, Yoshida et al. 2006). The process by which TGF- β regulates transcription of GDNF is less established and likely to be an indirect response. There is evidence of cooperation between GDNF and TGF-β signalling in neuronal cell cultures *in vitro*, however this effect has not been attributed to upregulation of the GDNF gene or its receptors. Instead TGF-β treatment is proposed to induce recruitment of the glycosyl-phosphotidylinositol-anchored GDNF receptor to the neuronal plasma membrane (GFRα1) (Peterziel, Unsicker et al. 2002), but there is no evidence of these mechanisms occurring in Müller glia, and would be worthy of investigation.

TGF-β1 has previously been demonstrated to stimulate the production of BDNF and reduce that of NT-3 in other cell types (Cai, Campana et al. 1999, Sometani,

Kataoka et al. 2001). It was of interest, therefore, that the present data indicated a significant and sustained downregulation of BDNF gene expression in MIO-M1 cultures in response to treatment with the pro-inflammatory cytokines TNF-a, TGF-β, and HB-EGF. This downregulation was not detected post-translationally within the cells (western blot analyses), or following release into the extracellular environment (ELISA tests). BDNF signalling through the high-affinity TrkB receptor has proven to have a neuroprotective effect in both the central and peripheral nervous systems, during a wide range of adverse conditions including glutamatergic stimulation, cerebral ischemia, hypoglycaemia, and neurotoxicity (Maisonpierre, Belluscio et al. 1990). Given the neuron-supporting function of the glia cells in the retina, it may seem counterintuitive that cytokine signalling would decrease production of this factor in Müller cells. It is important to note, however, that baseline expression and secretion of BDNF in untreated cells was high, and that Müller glia represent one of the major sources of this factor in the neural retina (Seki, Tanaka et al. 2005). Since RGCs have been shown to require constant supply of BDNF for survival, and increased concentrations of cytokines and decreased neurotrophin signalling are a feature of the glaucomatous retina (Ochiai and Ochiai 2002, Gupta, You et al. 2014), it is possible that impairment of BDNF production by Müller glia represents a feature of glaucomatous progression. Further studies clarifying the molecular mechanisms underlying this downregulation are required.

Although this report is the first to investigate a link between pro-inflammatory signalling and neurotrophins in Müller cells, there is some disagreement in the literature as to the modulatory effects of various inflammatory stimuli on BDNF production in glial cells of the CNS. In primary cultures of neonatal rat astrocytes, BDNF synthesis does not appear to be modified by TNF-α (Miklič, Jurič et al. 2004); however, other publications report marked upregulation of BDNF mRNA and protein in response to TNFR1 activation of NF-κB and C/EBPβ transcription factors (Saha, Liu et al. 2006). Associations between BDNF synthesis, and the EGF family of growth factors that includes TGF-β and HB-EGF are similarly ambiguous. HB-EGF is widely expressed in the central nervous system, and HB-EGF knockout mice have been shown to express significantly higher levels of

both BDNF and NGF in the cerebral cortex compared to wild type (Oyagi, Moriguchi et al. 2011). Although suggestive of a link between the two factors, the precise interactions underlying this association are yet to be understood. Given the conflicting reports, it is likely that the effect of this cytokine on neurotrophin production may be indirect, and depend upon the production and subsequent response to secondary factors in the culture systems studied.

This study showed a significant upregulation of the NT-3 gene in MIO-M1 cultures in response to supplementation with TNF-α and this response was observed for up to 120 hours post-treatment. A link between TNF-α signalling and modulation of NT-3 synthesis in glial Müller cells was also observed. There are, however, reports of a 2.5 fold increase in NT-3 production following treatment of surgical disc annulus cells cultured with interleukin 1-β (IL-1) (Gruber, Hoelscher et al. 2012). Both IL-1 and TNF-α exert influence through a common pathway mediator, TAK-1, which is upstream of the NF-kB transcription factor thought to be responsible for modulation of neurotrophin expression. It is therefore likely that a similar mechanism may be responsible for the effect observed in Müller cells, although further experiments evaluating the phosphorylation of TAK-1 following TNF-α treatment are required for clarity.

Semi-quantitative RT-PCR also revealed a consistent upregulation of the NT-4 gene expression in cells supplemented with TGF-β. There is insufficient evidence in the literature for a direct link between TGF-β signalling and NT-4 modulation but it was significant that in this study TGF-β appeared to upregulate the expression of NT-4, whilst downregulating BDNF. It seems probable that this association is the result of an attempt to maintain neurotrophin homeostasis in the retinal microenvironment, rather than a direct regulation of transcription. In contrast to TGF-β, although TNF-α treatment of Müller glia downregulated BDNF expression, it did not appear to influence the expression of NT-4 which was unchanged at each of the three time-points examined.

Despite mediating distinct neuronal functions, both NT-4 and BDNF act through the same high-affinity TrkB receptors present on both glia and neuron cells, with similar potency for receptor activation (Proenca, Song et al. 2016). Whereas BDNF is highly expressed throughout the CNS and appears to be a key regulator of normal neuronal plasticity, NT-4 is minimally expressed in normal physiology but may have a more potent neurotrophic influence. This can be interpreted from reports that mice with NT-4 knocked-in to replace BDNF have significantly higher numbers of sensory neurons than wild-type, and whilst BDNF allele homozygosity is necessary for the support of the nodose-petrosal ganglion complex in transgenic mouse models, a single NT-4 allele is sufficient (Erickson, Conover et al. 1996, Fan, Egles et al. 2000). In summary, these studies suggest complex interplay between the transcriptional regulation of the two factors, where the suppression of BDNF results in a compensatory up-regulation of NT-4 in order to satisfy demand for TrkB activation.

When examining intracellular protein levels by western blotting, the objective was to detect the protein either immediately post-translation, or during transit towards the cell surface membrane prior to release. Although each of the factors was detected in Müller glia cell lysates, cytokine modulation of these proteins (unlike that seen with the correspondent gene expression) was not significantly modified. It is possible that the lack of significant cytokine modulation detected by western blotting is due to both the inherent biological variation between individual cells in culture and the lack of sensitivity of the technique. In addition, each of the neurotrophins undergo extensive post-transcriptional modification, and this almost certainly influence quantification attempts by western blot analyses (Canossa, Griesbeck et al. 1997). The antibodies used to detect the four members of the neurotrophin family in these experiments identified proteins of a molecular weight corresponding to the mature form of the factor in question. As the neurotrophin family members are initially expressed in large, 3-protein complexes which are then processed, both intra and extra-cellularly, it is likely that western blots failed to detect a significant quantity of translated NTs present within the cell. These factors may explain the variability between mRNA and protein expression observed.

There are also several factors capable of explaining the failure to detect variations in concentration of secreted factors, aside from NGF, in extracellular media. Although the presence of secreted neurotrophins was confirmed in each Müller glia culture supernatant examined, protein levels were minimal (6 – 25 pg / mL), and towards the lower limit of sensitivity of the ELISA kits used (Biosensis™, Australia). The ELISA experiments included in this study were conducted on Müller-glia cell supernatants following 48 hours of incubation, and it is likely therefore, that the minimal concentrations of neurotrophin detected relate to the instability and short half-life of the factors following release into the culture medium. There is debate in the literature as to whether the NTs, particularly NGF are released in pro or mature forms, with the general consensus that it is likely to be a combination of both, in an activity-dependent manner (Bruno and Cuello 2006). *In vivo,* secreted pro-NTs undergo enzymatic processing in order to reveal the mature form, before undergoing enzymatic degradation by neuron-derived matrix metalloproteinases (Pang, Teng et al. 2004, Saha, Liu et al. 2006). It is unclear whether the proprietary antibodies used to detect NTs in the ELISA platform used in this study are capable of discriminating between mature, or precursor forms of the secreted protein. It is likely, therefore, that the above issues contributed to reducing the sensitivity of the experiments, and the more subtle variations in NT protein expression were drowned out by lack of sensitivity and specificity.

Conclusions

Müller glia with stem cell characteristics have been identified in the adult human retina, which can be expanded in vitro and transplanted into animal models of retina degeneration, causing a significant recovery of neural function following intravitreal or sub-retinal transplantation (Singhal, Bhatia et al. 2012, Jayaram, Jones et al. 2014). Moreover, Muller glia differentiated from PSC-derived retinal organoids partially restore visual function in rats following NMDA-induced cytotoxicity, as determined by improvements in the negative scotopic threshold response of the electroretinogram (Eastlake, Wang et al. 2019). The data

reported here demonstrates that Müller glia constitutively express neurotrophins and other neurotrophic factors which likely contribute to this paracrine neuroprotective effect. This is particularly relevant as deprivation of neurotrophic factor supply to the RGCs is known to contribute to their apoptosis in the glaucomatous retina.

While it may be tempting to simply oversaturate the retina with exogenous soluble neurotrophins, either through their direct application or by overexpressing these factors in target cells, this strategy typically provides only short-term improvements in RGC survival, and the effects are not additive (Chen and Weber 2004). The data presented here also indicates that the presence of certain inflammatory cytokines known to be upregulated in glaucoma is likely to influence the production of these neurotrophic agents, either directly or indirectly, and there is still much to be discovered regarding the underlying mechanisms influencing their synthesis and secretion. While the production and release of neurotrophins is likely to be key to the process by which transplanted Müller cells have been shown to ameliorate neurodegeneration and restore aspects of electroretinal response in animal models of RGC depletion, it is also likely that secondary sources of communication are involved in this process.

In addition to the secretion of soluble factors, cells are capable of communicating via the release and receipt of nano-sized membrane-bound vesicles, known as extracellular vesicles (EV). These contain cargos of proteins and nucleic acids capable of influencing sustained phenotypic alterations following their internalisation into recipient cells. Increasingly, the therapeutic potential of EV is being recognised for a range of conditions, often as an alternative or adjunct to stem-cell therapy, or direct treatment with recombinant factors. Unlike cells, soluble factors or oligo-based therapies, EV are highly stable for a long-term, they are non-replicative, and simple to produce and purify, making them a potentially effective platform for the treatment of a wide range of disease conditions (Choi, Kim et al. 2013). On this basis, further studies in this thesis have addressed the investigation of the nucleic and protein cargos of EV released by Müller glia.

Chapter 3: Characterisation of extracellular vesicles released by Müller glia cells

Introduction

Extracellular vesicle composition

As a field still very much in its infancy, in-depth nucleic acid characterization, proteomics and lipidomics studies are just starting to unravel the extent of EV composition and content. Exocarta, Vesiclepedia and similar public databases have sprung up to compile and keep track of publications, catalogue proteins, nucleic acids and lipids associated with EV, and to help make large-scale bioinformatic analysis feasible (Kim, Lee et al. 2015, Keerthikumar, Chisanga et al. 2016). Although EV subtypes share a general lipid-bilayer composition, the specific content of individual classes of vesicle is thoroughly dependent upon their cell source, biogenesis, and environmental conditions. Activation and transformed status of the cell, exposure to hypoxia, irradiation, or oxidative injury, shear stress exposure and exposure to activated components of the complement system, all appear to influence EV content cargo and rate of production (Beaudoin and Grondin 1991, Trajkovic, Hsu et al. 2008). The full characterisation of their cargo may allow the identification of clues to their biogenesis, targeting, and cellular effects. In certain cases, may also reveal their cellular origin and uncover new biomarkers for disease diagnosis and prognosis.

Proteins associated with extracellular vesicles

Rather than containing random samples of cellular components, EV harbour specific subsets of proteins, some of which are common between EV of different classifications, and some cell type specific. Although numerous analyses have highlighted proteins frequently found in EV preparations, it is becoming clear that these do not represent exosome-specific markers but merely proteins commonly enriched in EV. It has been suggested, that the relative proportions of these proteins may vary in different preparations of EV shed by different cell types; however, lack of nomenclature standardisation and standardization of purification methods are likely to be contributing factors to the differences observed (Kowal, Arras et al. 2016). As yet, these markers cannot be used to discriminate between

different classes of EV, as both, exosomes and shed microvesicles have many proteins in common (Lötvall, Hill et al. 2014).

For purposes of characterisation, the most commonly found proteins have shown to be involved in the biogenesis and formation of these vesicles (fig 3). Exosomes are therefore typically enriched in proteins associated with the late endosome. These transmembrane or lipid-bound proteins include tetraspanins (CD9, CD63, Cd81); integrins (β4, α6, fibronectin); and cell adhesion molecules (CAM). Also commonly reported are cytosolic components of the endocytic pathway including Alix, TSG101, various Rabs, annexins and chaperone heat shock proteins such as Hsp70 and Hsp90 (Théry, Boussac et al. 2001). Finally, there are various reports of vesicle co-isolation with extracellular proteins that bind specifically or non-specifically to EV membranes. These include: acetylcholinesterase, fibronectin, and soluble cytokines and growth factors (Lancaster and Febbraio 2005, Tomasoni, Longaretti et al. 2012, Robbins and Morelli 2014). Surface proteins have been shown to play important roles in EV-mediated communication. For example, tumour derived vesicles have been reported to bind chemokine receptors, CCR6 and CD44v7/8. When these are engulfed by monocytes, these factors induced activation of Akt, suppressing apoptosis (Baj-Krzyworzeka, Szatanek et al. 2006). EV are typically absent of proteins associated with non-endosomal intracellular compartments, including mitochondria, Golgi apparatus and ER. Absence of these non-EV-related proteins can thus serve as confirmation of EV purity following isolation.

A recent report comparing the full proteomic composition of exosomes and microvesicles purified from brain endothelial cells found that of a total of 1758 proteins identified, 544 were found exclusively in microvesicles, 206 were unique to exosomes, and 366 were shared between both vesicle subtypes (Dozio and Sanchez 2017). Proteins unique to shed vesicles were mitochondrial, endoplasmic and cytoskeletal related, whilst those present only in exosomes were those associated with endosomal compartments (as indicated above). A major role of EV is the promotion of intracellular signalling, and their ability to influence the behaviour of tissues. This has been attributed to their enrichment

with proteins specific to their cell of origin. For example, reticulocyte-EV have been reported to mediate disposal of transferrin receptor during erythrocyte maturation, whilst placenta-derived EV mediate immune suppression via expression of the Fas ligand, and tumour-derived EV promote metastasis via integrins (Pan and Johnstone 1983, Tong and Chamley 2015). Interestingly, the same study reported far greater similarity in the proteomic composition of microvesicles and parent-cells, compared to that of exosomes (Dozio and Sanchez 2017). This implies that many of those abilities may be attributed to shedding microvesicles, as well as the fact that the composition of exosomes are specific, and not a mere reflection of the cell. This also indicates the existence of specialized mechanisms that control the sorting of these molecules into exosomes.

Nucleic acids associated with extracellular vesicles

In addition to protein cargo, EV mediated communication is based upon the recognition that these organelles are enriched in various nucleic acid species. EV have an innate ability to transfer genetic information, and even regulate gene transcription in target cells, raising the possibility for their use as therapeutic agents (Lee, El Andaloussi et al. 2012).

The presence of DNA in EV has been described by a few groups, however there is still debate as to how DNA might be processed and packaged into certain types of EV and even whether reports of EV bound DNA are not merely artefacts of purification (Jin, Chen et al. 2016). Myoblast-derived exosomes have been reported to contain both mitochondrial, and chromosomal DNA (Guescini, Genedani et al. 2010), whilst genomic DNA in exosomes was noted in cell culture supernatant as well as in human and mouse biological fluids, including blood, seminal fluid, and urine. Interestingly, it is possible that the encapsulation of DNA within exosomes may confer enhanced stability to DNA when outside the cell (Jin, Chen et al. 2016).

Since the transfer of RNA-loaded vesicles plays a key role in cell-cell communication in many different contexts and pathologies (Zhang, Liu et al. 2010, Mittelbrunn, Gutiérrez-Vázquez et al. 2011, Hergenreider, Heydt et al. 2012, Halkein, Tabruyn et al. 2013), it is most likely that the primary mechanism of EV-mediated genetic transfer is through the delivery of various RNAs (Valadi, Ekström et al. 2007). Analysis of exosomes derived from human mast cell lines indicate that despite the presence of mRNAs, RNA found in exosomes were mainly small, non-coding microRNAs. Interestingly, further microarray and DNA–ChIP analysis revealed the presence of more than 270 gene transcripts that were only present in exosomes, and just 8% corresponded to those detected in parental cells. EV are, therefore, disproportionately enriched in RNA species compared to their parental cells, suggesting the existence of specific mechanisms for the sorting and loading of genetic material during biogenesis (Zomer, Vendrig et al. 2010).

In contrast to 3’ adenylated miRNA generally found in cells, EV-associated miRNAs are typically 3’ uridylated (Koppers-Lalic, Hackenberg et al. 2014). It has therefore been suggested that these 3′ post-transcriptional modifications are likely to be signals involved in the selection and sorting of miRNA into EV (Koppers-Lalic, Hackenberg et al. 2014). Other research focus upon interactions between proteins and specific sequence motifs present in miRNAs that may influence their localization into exosomes. Heterogenous nuclear ribonucleoprotein A2B1 (hnRNPA2B1) is a ubiquitous protein that has been previously shown to control the intracellular trafficking of specific mRNAs in neurons, as well of HIV-1 RNA (Lévesque, Halvorsen et al. 2006). In T cells, HnRNPA2B1 has been demonstrated to specifically bind exosomal miRNAs through the recognition of a selection of overrepresented motifs. This is supported by observations that miRNA loading into exosomes can be modulated by mutagenesis of the identified motifs, or suppression of hnRNPA2B1 expression levels (Villarroya-Beltri, Gutiérrez-Vázquez et al. 2013).

Associations between miRNA sorting and packaging have also been made with another RNA binding protein, argonaute 2 (AGO2), which is may form a complex

with ALIX, as well as proteins involved the neutral sphingomyelinase 2 (nSMase2) pathway (Iavello, Frech et al. 2016). Inhibition of these proteins has been shown to universally decrease miRNA present in EV (Kosaka, Iguchi et al. 2013). Taken together, these studies present evidence that nucleic acid loading into EV is not necessarily random, and may involve coordination between cis-acting elements in RNA sequence and specific proteins responsible for this activity.

Chapter summary and objectives

Work presented in the previous chapter established the synthesis and secretion of a range of neurotrophic factors by Müller glia cells *in vitro*. Although there is much evidence supporting the short-term neuroprotective benefits of these peptides in models of neurodegeneration, therapeutic strategies based upon increasing the availability of growth factors suffer from challenges such as flattening of response, and concerns over their stability in the protease-rich extracellular environment. While deprivation of neurotrophic factors is characteristic of the glaucomatous retina, even prolonged delivery of BDNF and TrkB receptor to axotomized optic nerve is unable to maintain RGCs long-term (Di Polo, Aigner et al. 1998). It is likely therefore, that neurotrophin secretion constitutes a part, but not all of the efficacy of Müller glia cell transplant, and it would be prudent to expand the search for additional paracrine signals.

The large-scale release and subsequent uptake of nano-sized EV represents a novel method of intracellular communication. These organelles are currently receiving renewed research interest owing to their ability to act as a vector for the transfer of therapeutic cargos to degenerated tissues in a range of disease models (Murphy, de Jong et al. 2019). Despite this, there is still uncertainty over the precise nature of these cargos, how they relate to their cell of origin, the mechanisms controlling their sorting into vesicles, and the particular vesicle subtypes responsible for efficacious responses. In Müller cells, the characterisation of these organelles represents the first step in the process of fully evaluating their therapeutic potential for retinal neurodegenerative conditions

The objective for this chapter was therefore:

1. To quantitatively and qualitatively define two subpopulations of Müller glia-derived EV with regard to size, morphology, proteomic-enrichment, and nucleic acid profile.

Materials and methods

Preparation of cell culture supernatants for isolation of extracellular vesicles

Müller glia cultures consisting of MIO-M1 cells from passages 15-30 were cultured to approximately confluency in T175 culture vessels as previously described in Chapter 2. Culture medium was aspirated, and monolayers were washed three times in warm, sterile phosphate buffered saline (PBS) to remove any trace of serum. Cells were then incubated in 20mL DMEM + 1% P/S in the absence of serum and phenol-red indicator for 48 hours. After removal, culture media from two T175 flasks (40mL) was pooled, and centrifuged at 300 x g for 10 minutes in order to pellet floating cells. After this centrifugation, culture supernatants were either processed immediately for EV isolation, or stored at -80°C until use.

Depletion of particles from Dulbecco's phosphate buffered saline for extracellular vesicle isolation

For all EV isolation experiments, 1 X sterile Dulbecco's Phosphate buffered saline (DPBS) (Gibco, cat. no. C14190500BT) was used as vesicle buffer. DPBS was depleted of particles by a round of high velocity ultracentrifugation, 100'000 X g for 6 hours, using a fixed-angle Ti45 rotor (Cat no 339160; Beckman Coulter, Brea, CA, USA) and an Optima® XE-90 preparative centrifuge (Beckman Coulter, Brea, CA, USA). The supernatant was removed and passed through a 0.22 µM syringe filter unit (Cat no F8148; Millex®, Merck, Darmstadt, Germany). Particle depletion was confirmed through NTA measurement, and transmission electron microscopy as detailed below.

Extracellular vesicle isolation by differential centrifugation

For isolation of “large EV” (fig. 15), conditioned culture supernatants from four T175 flasks was pooled into two 50mL falcon tubes, and centrifuged at 300 X g for 10 minutes at room temperature. After discarding the pellet, the supernatant was centrifuged a second time at 2000 X g, for a further 20 minutes. The supernatant was then passed through a syringe microfilter with a 0.8 µm pore size (Cat no 431221; Corning®, Fisher Scientific Co., Pittsburgh, PA, USA), before being transferred to 34mL polypropylene ultracentrifugation tubes (Cat no 326823; Beckman Coulter, Brea, CA, USA). Supernatant was then centrifuged at 12’000 X g for one hour at 4°C, using a swing-bucket SW32 Ti rotor (Cat no 369694; Beckman Coulter, Brea, CA, USA) and an Optima® XE-90 preparative centrifuge (Beckman Coulter, Brea, CA, USA). Supernatants were removed, and the pellets washed in 1mL of 1X sterile and particle-depleted DPBS. Preparations were combined, and subjected to a second round of centrifugation to pool particles. These were resuspended in 100uL of 1X DPBS, previously depleted of particles. For isolation of “small EV” (fig. 15). Supernatants from the final (12’000 x g) centrifugation step of the large EV purification were pooled, and passed through a 0.22 µm vacuum filter unit (Cat no CLS431174; Corning® , Fisher Scientific Co., Pittsburgh, PA, USA). Supernatants were then carefully loaded over 4 mL of 30% sucrose solution (prepared in 1 X DPBS), forming a gradient, and centrifuged at 120’000 x g, 4 °C for 90 min using a swing-bucket SW32 Ti rotor (Cat no 369694; Beckman Coulter, Brea, CA, USA) and an Optima® XE-90 preparative centrifuge (Beckman Coulter, Brea, CA, USA). The supernatant was then discarded, the sucrose layer recovered (~5 mL), and resuspended in 1 × DPBS before ultracentrifugation at 120’000 x g at 4 °C for 90 min to pellet down the small vesicles. Finally, the pellet was resuspended in 100 µL 1 × DPBS and stored at − 80 °C for further use.

Isolation of EV protein for Western blot analysis

EV preparations eluted from a total of five small or large EV pellets prepared as previously described, were separately combined by ultra-centrifugation (120’000

x G, 100 minutes, 4°C). Supernatants were removed, and pellets resuspended in 100 µL of ice cold RIPA lysis buffer containing 10µl of protease inhibitor cocktail, 0.5mM Dithiothreitol (DTT), 1mM Phenyl Methyl Sulphonyl Fluoride (PMSF) and 3mM Sodium Orthovanadate (Na3VO4). Solutions were emulsified by up-and-down pipetting, and vortexed before measurements of total protein concentration were made by BCA assay as described above. Identification of specific proteins present in the EV was analysed by western blotting as detailed previously in Chapter 2.

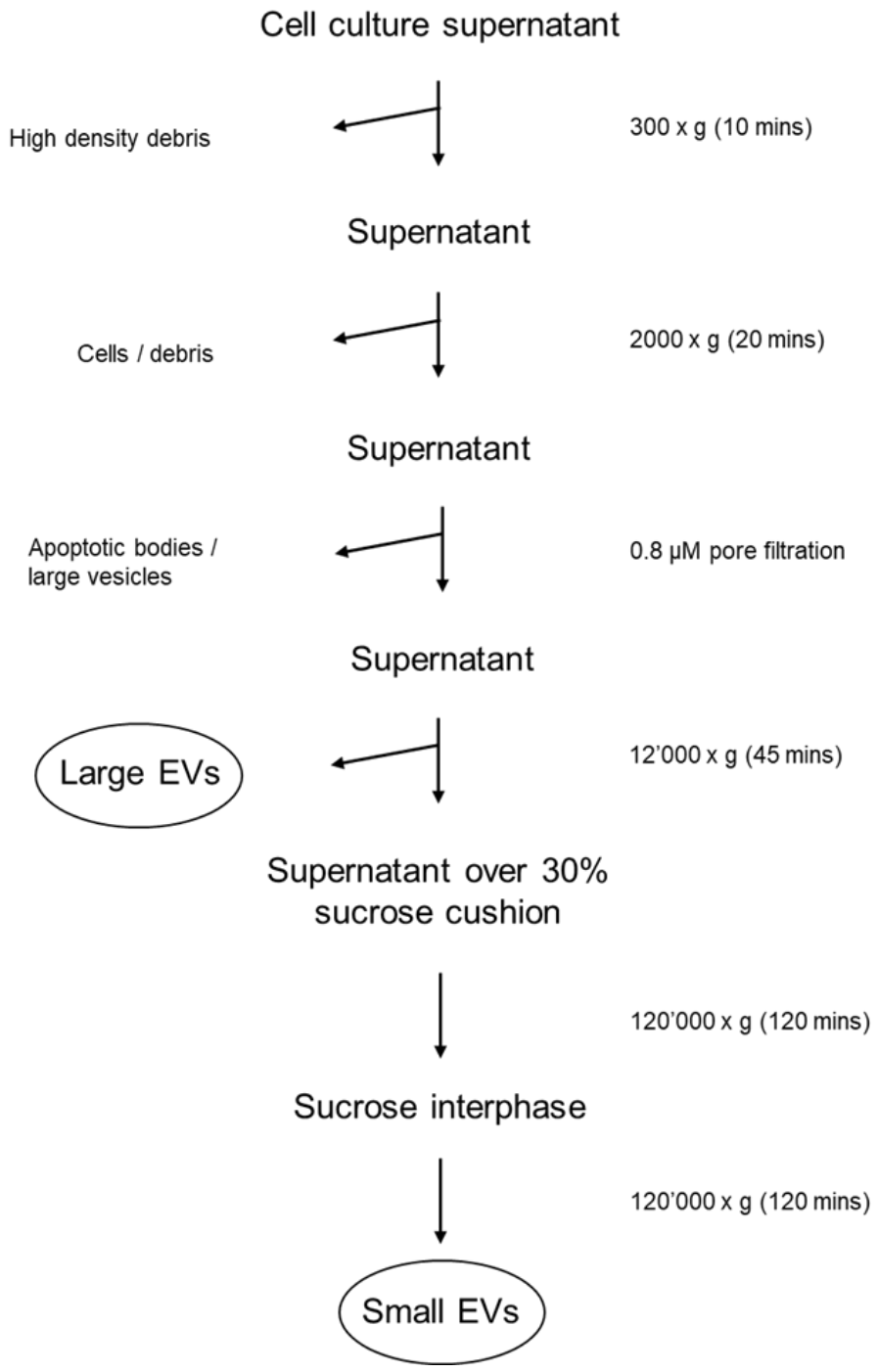

Figure 15. ***Flow chart summarizing EV purification methodology****.*

Size profiling of EV by Nanoparticle Tracking Analysis

Nanoparticle tracking analysis (NTA) estimates particle diameter by tracking EV diffusion due to Brownian motion, through a time series of pre-recorded video micrographs. It also allows for visualisation of scattered light from particles in solution by laser illumination. The number of particles imaged is controlled by the scattering cross-section, and by adjustments to the sensitivity and shutter speed settings of the camera. Estimates of EV diameter were made using a NanoSight LM10 system (NanoSight Ltd.,Minton Park, Amesbury, UK). EV preparations were diluted 1:100, 1:1000, and 1:5000 in sterile/particle-free DPBS 1X, in order to achieve concentrations of between $1x10^7$ and $1x10^9$ particles/mL required for accurate sampling (approximately 30–100 particles in the NanoSight video window field of view). The following software settings were employed and constant for all samples: detection threshold, 9–10; blur, auto; and minimum expected particle size, 10 nm. Temperature was maintained at 22°C. A 532-nm laser beam was applied to the 0.3-ml loaded suspension, and video-recorded for 60 s at a frame rate of 30 frames/s. After each measurement, the field of observation was advanced, for a total of three recordings. The video was then analysed using the NTA 3.2 software. The velocity of particle movement was measured to calculate particle size by applying the two-dimensional Stokes–Einstein equation (Filipe, Hawe et al. 2010). After tracking and analysis, descriptive sample characteristics were obtained, as well as estimates of total concentration. Raw data was exported to Excel, and summarised graphically as mean finite track length adjustment (FTLA) concentration by particle diameter, +/- 1 standard error of the mean. In addition, graphs were generated of total relative intensity of particles recorded against diameter.

Electron Microscopy

Transmission electron microscopy (TEM) was used to visualise EV preparations and cross sections of whole cells. EV purifications were thawed and adjusted to room temperature, as were preparations made from cell-free control media. 50 µL droplets were adsorbed onto formvar/carbon-coated grids (Formvar/Carbon

on 400 Mesh Copper; cat no AGS162, Agar Scientific Ltd., Essex, England) for 20 minutes, before 3 washes of 30 seconds in droplets of sterile, particle-free DPBS. EV were then fixed in 1% glutaraldehyde (v/v) solution (Cat no 340855; Merck, Darmstadt, Germany), for 10 minutes at room temperature, before a second round of washing. Negative staining was achieved by 15 minutes incubation in 2% uranyl acetate solution (w/v) (Cat no AGR1260A; Agar Scientific Ltd., Essex, England), after which excess stain was blotted, and grids allowed to air dry for 30 minutes. Imaging was conducted on a 100kV transmission electron-microscope (JEOL-101 TEM; JEOLUSA, MA, USA) with image capture by Gatan Orius digital camera. Micrographs were exported, and processed using ImageJ software where vesicles present were measured.

For imaging of whole cell sections, MIO-M1 monocultures were grown in 24-well tissue culture plates (Corning®, USA), before overnight fixation in a mixture containing 3% glutaraldehyde and 1% paraformaldehyde, buffered to pH 7.4 with 0.07 M sodium cacodylate-HCl. Monocultures were washed three times with cacodylate buffer (pH 7.4), and then osmicated for 2 hours in a 1% aqueous solution of osmium tetroxide. rinsed in deionized water, and dehydrated through ascending concentrations of ethanol (50%–100%, 10 minutes per step). After a final dehydration in 100% ethanol, wells were filled with Araldite resin and cured at 60°C. Ultrathin sections were made using a microtome (Ultracut S; Leica, Cambridge, UK), and contrasted sequentially with 1% uranyl acetate and lead citrate. Sections were viewed and photographed using a transmission electron microscope as previously described.

For imaging of vesicle budding by scanning electron microscopy, cells were cultured in 24-well plates coated with human fibronectin (Catalogue no. 356008, Corning®, USA) at a working concentration of 50µg/mL in extracellular matrix buffer consisting of 15mM NaHCO3, pH 9.6. Wells were fixed and dehydrated to 100% ethanol as previously described. After dehydration cells were critical point dried, sputter coated with gold, and imaged using a scanning electron microscope (6100SEM; JEOL), operating at 15 kV.

Isolation of extracellular vesicle total RNA and RNase degradation assay

To evaluate the sensitivity of EV-associated RNA to RNase degradation, small and large EV pellets were collected as previously described, and concentrations were determined by nanoparticle tracking analysis. From each, a quantity of 2e9 particles was diluted into 100 µL of particle-free DPBS, mixed gently by pipetting, and then halved into two 50 µL volumes. One half of each half EV sample was then incubated with RNase A enzyme (100 U/mL) (Invitrogen™, MA, USA) for 15 minutes at 37 °C, before addition of RNase Inhibitor (1 U/mL) (Invitrogen™, MA, USA) and a final incubation for 10 minutes at 37 °C. Untreated samples were incubated without enzyme for equivalent times as experimental controls.

After treatment, the Total Exosome RNA and Protein Isolation Kit (Invitrogen) was utilized for recovery of total RNA from both halves of large and small EV samples. Each sample was made up to 200 µL with DPBS, and combined with 205 µL of 2× denaturing solution, vortexed to lyse, and then incubated on ice for 5 min. After incubation, 410 µL of Acid-Phenol: Chloroform was added, and vortexed for 30 s to mix, before centrifugation for 5 min at 12,000 x g to separate the mixture into aqueous and organic phases.

Once centrifugation was complete, the upper (aqueous) phase was removed and transferred to a fresh tube. EtOH (1.25 volumes-100% purity) was added to the aqueous phase for each sample and then vortexed to mix. A volume of 700 µL of this preparation was placed onto a spin column cartridge in a collection tube, and spun at 10,000 x g for 15 s. RNAs bound to filter cartridge membranes were then washed once with 700 µL of wash solution 1, and twice with a 500 µL volume of wash solution 2/3 (centrifuged at 10,000 x g for 15 s for each). After washing, the filter was dried by an additional 1 minute centrifugation at 12,0000 x g.

The filter cartridge was transferred into a fresh collection tube and 25 µL of preheated (95 °C) nuclease-free water was applied to the centre of the filter.

Samples were centrifuged for 30 s at 10,000 x g to recover the RNA, then a second 25 µL volume of preheated (95 °C) nuclease-free water was applied to the centre of the filter and centrifuged for 30 s at 10,000 x g. After the second spin, the eluate containing the RNA was collected and concentrations of total RNA were quantified by NanoDrop UV spectrophotometer (Nanodrop-1000, Thermo Scientific), before storage at -80 °C .

High sensitivity screen-tape analysis

To compare size and quality of total RNA profiles recovered from EV and whole cells, samples were assessed by electrophoresis using the 2200 TapeStation system (Agilent), using High Sensitivity RNA ScreenTape (5067–5579) with High Sensitivity RNA ScreenTape Sample Buffer (5067–5580) and High Sensitivity RNA ScreenTape Ladder (5067–5581). The range of total RNA input was 500 – 10,000 pg/µL, and the total RNA integrity was estimated using the software RNA Integrity Number or RIN. Screentapes were analysed using the Tapestation Analysis Software. Peaks were identified using Agilent's proprietary statistical calculations integrated into the software. If peaks are identified, peak data is recorded as peak concentration (picogram per microliter).

Results

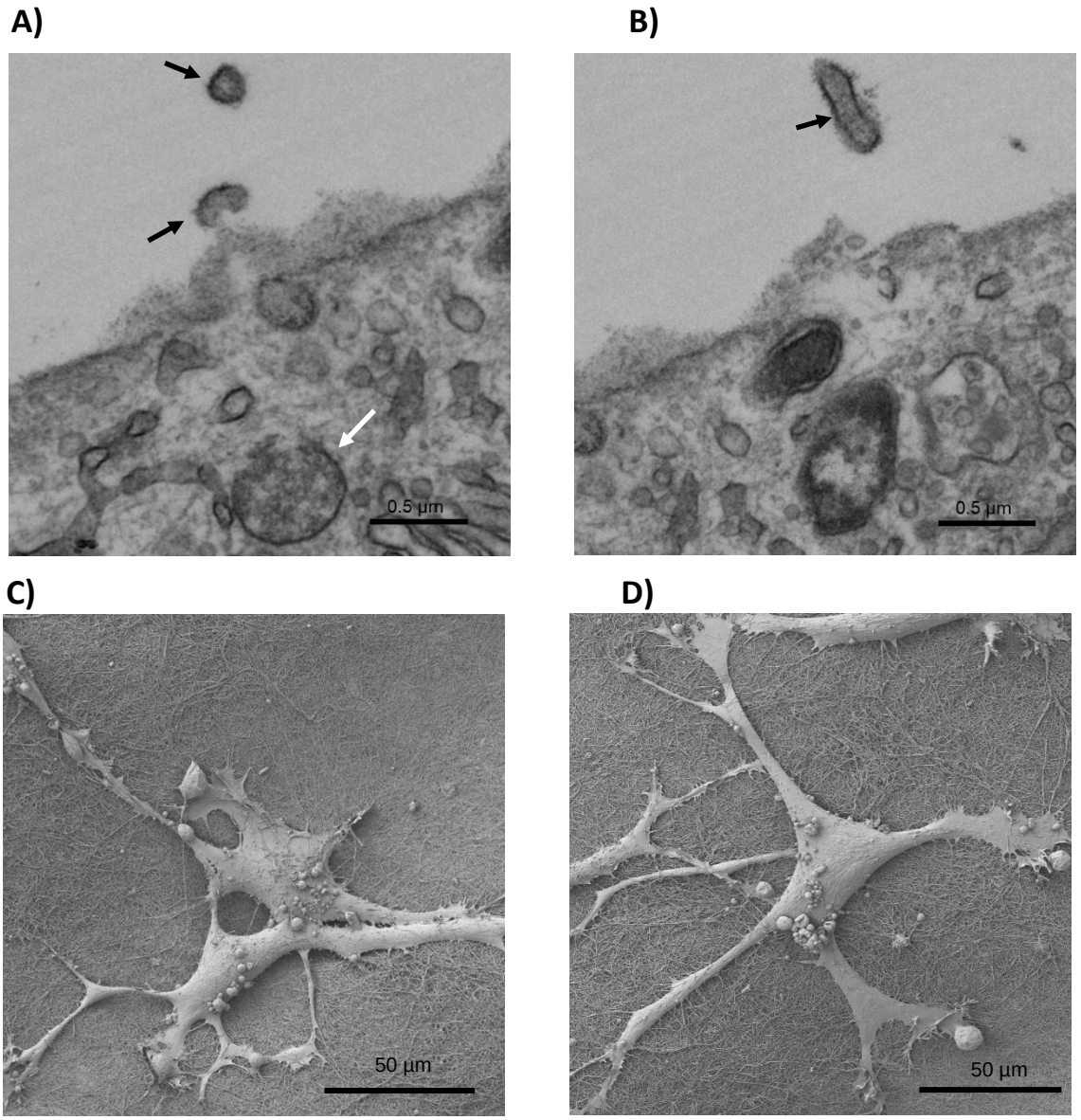

Figure 16. ***Electron micrographs demonstrating two mechanisms of vesicle production and release in vitro.*** *A and B) TEMs shows a MIO-M1 cell in cross-section. Indicated with by black arrows are microvesicles shedding directly from the cell surface membrane. White arrows identify the presence of multivesiculated late endosomes (MVBs), and evidence of their fusion with cell membranes and release of exosomes. C) and D), SEMs displaying Müller glia in culture, evident on cell surfaces are large microvesicles blebbing directly from the plasma membrane.*

Müller glia cell release of vesicles observed by electron microscopy

Scanning (SEM) and transmission (TEM) electron microscopy was utilised in order to image Müller glia cells from the MIO-M1 cell line. In micrographs of the cells in cross section it was possible to identify vesicle-filled membrane-bound internal compartments of approximately 500 nm in diameter, consistent with multivesicular bodies (MVBs). There was also evidence of these structures fusing with the external cell membrane and releasing their minute vesicle content, as well as larger membrane-bound organelles in the process of blebbing outward from the membrane, consistent with shedding microvesicles (fig. 16; A, B). Scanning electron micrographs of Müller glia on a collagen matrix indicate large scale blebbing of vesicles from plasma membranes in 3D. Vesicles are heterogenous and range from <1 – ~5 µm in diameter (fig. 16; C, D).

Characterisation of extracellular vesicle size by nanoparticle tracking analysis

Size distribution analyses of large and small vesicle purifications were made by NTA. Descriptive statistics comparing size profiles of small and large EV are summarized in figure 19. Preparations were heterogenous and highly polydisperse, containing particles ranging between ~100 and ~950 nm in diameter. Mean particle size was 312 nm, whilst the analyses predicted that 90% of particles in these populations were >167 nm, and that the modal particle diameter was 282 nm. Small EV were isolated from media prior processed for large EV. To ensure for homogeneity of samples, supernatants were passed through a 0.22 µm vacuum filter, before sedimentation through a 30% sucrose “cushion” at 120’000 x g. Analyses revealed that small EV samples purified in this way were less polydisperse, more homogenous and enriched in significantly smaller particles than large EV preparations. Small EV had a mean diameter of 150.2 nm, and a mode of 112.9 nm. 50% of particles present were under 127 nm, whilst 90% were below 209 nm, indicating a substantial homogeneity of the vesicle population collected (fig. 19).

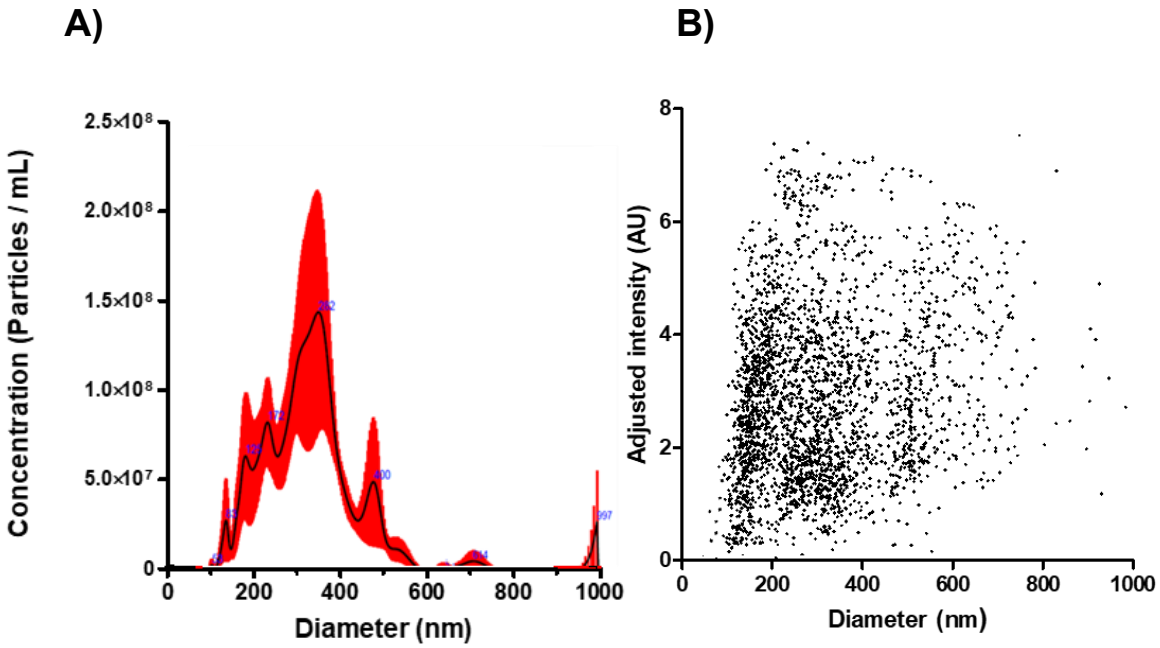

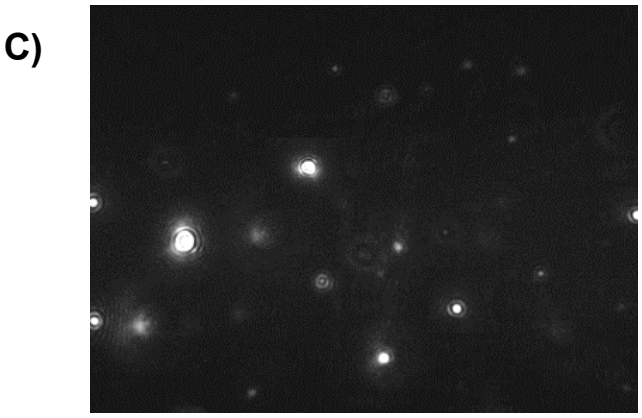

Figure 17. ***Diameter of particles present in large EV preparations characterised by Nanoparticle Tracking Analysis****. **A**) mean finite track length adjustment (FTLA) concentration by particle diameter +/- SEM. **B**) Adjusted intensity by particle diameter and (**C**) corresponding representative video frame*

A)

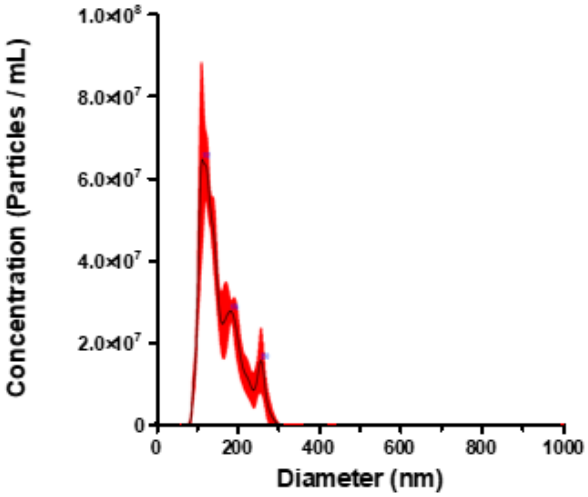

B)

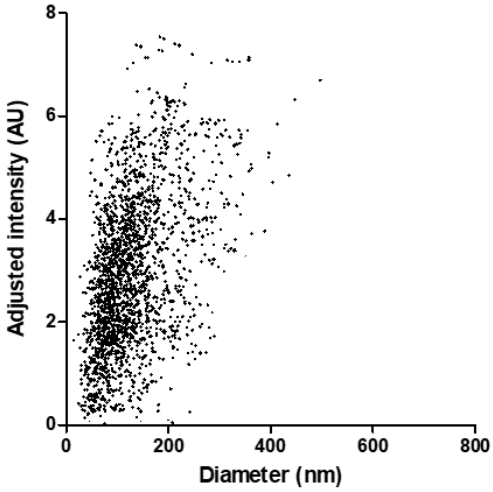

C)

Figure 18. ***Diameter of particles present in small vesicle preparations characterised by Nanoparticle Tracking Analysis****.* ***A****) Mean FTLA concentration by particle diameter +/- SEM.* ***B****) Adjusted intensity by particle diameter and (****C****) corresponding representative video frame*

A

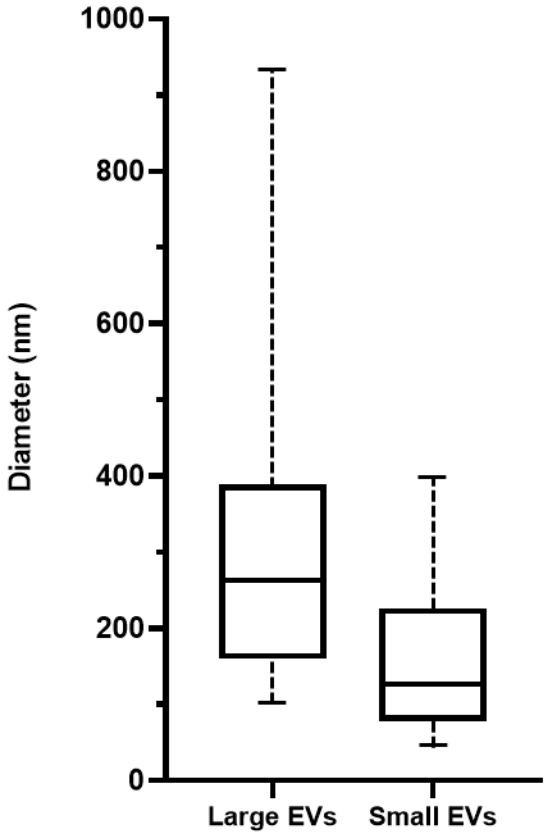

B

Preparation	Mean (±SE)	Mode (±SE)	Median (±SE)	SD (±SE)	D10 (±SE)	D90 (±SE)
Large EVs	312.4 (6.9)	282.1 (11.3)	237.3 (5.7)	107.4 (8)	167.7 (4.1)	398.2 (33.5)
Small EVs	150.2 (5.6)	112.9 (6.8)	126.6 (0.9)	66.8 (3.7)	78.4 (1.6)	208.9 (7.4)

Figure 19. ***Comparison of particle size profiles between small and large EV preparations.*** ***A****) Boxplot presenting differences in the mean size range of particles (n=3) isolated. Boxes span D10 to D90, with D50 presented as the mid-line.* ***B****) Table comparing descriptive characteristics of small and large EV preparations.*

Characterisation of proteins present in EV

Large, and small EV preparations were characterised for expression of proteins coding for exosome markers, using western blot analysis (fig. 20). EV protein lysates were blotted with antibodies against proteins known to be enriched in the membranes of endocytic compartments, and expression of these proteins was compared with an equivalent quantity (2 µg) of total protein taken from whole-cell MIO-M1 lysates. Small and large EV preparations were found to be enriched in tetraspanin protein CD9, whilst CD63 was detected only in small EV lysates. Tetraspanins were absent (CD63) or relatively under-expressed in whole cell protein. Small EV were also positive for ALG-2-interacting protein X (ALIX), a component of the ESCRT-3 complex and regulator of the endosomal transport pathway, whilst no signal was detected in equivalent protein concentrations of large EV, or MIO-M1 control protein. The reverse was true for the endoplasmic reticulum membrane markers Calnexin and Calreticulin, which were robustly expressed in whole cell lysates, whilst no signal was detected in EV preparations. A faint signal for cytoskeletal marker β-actin was detected in small EV samples, whilst a stronger signal was evident in protein lysates recovered from large EV. This protein was robustly expressed in whole cell lysates, as anticipated. No evidence of vesicle encapsulation was detected when blots were probed for four growth factors expressed by Müller cells: NGF, BDNF, GDNF, NT3.

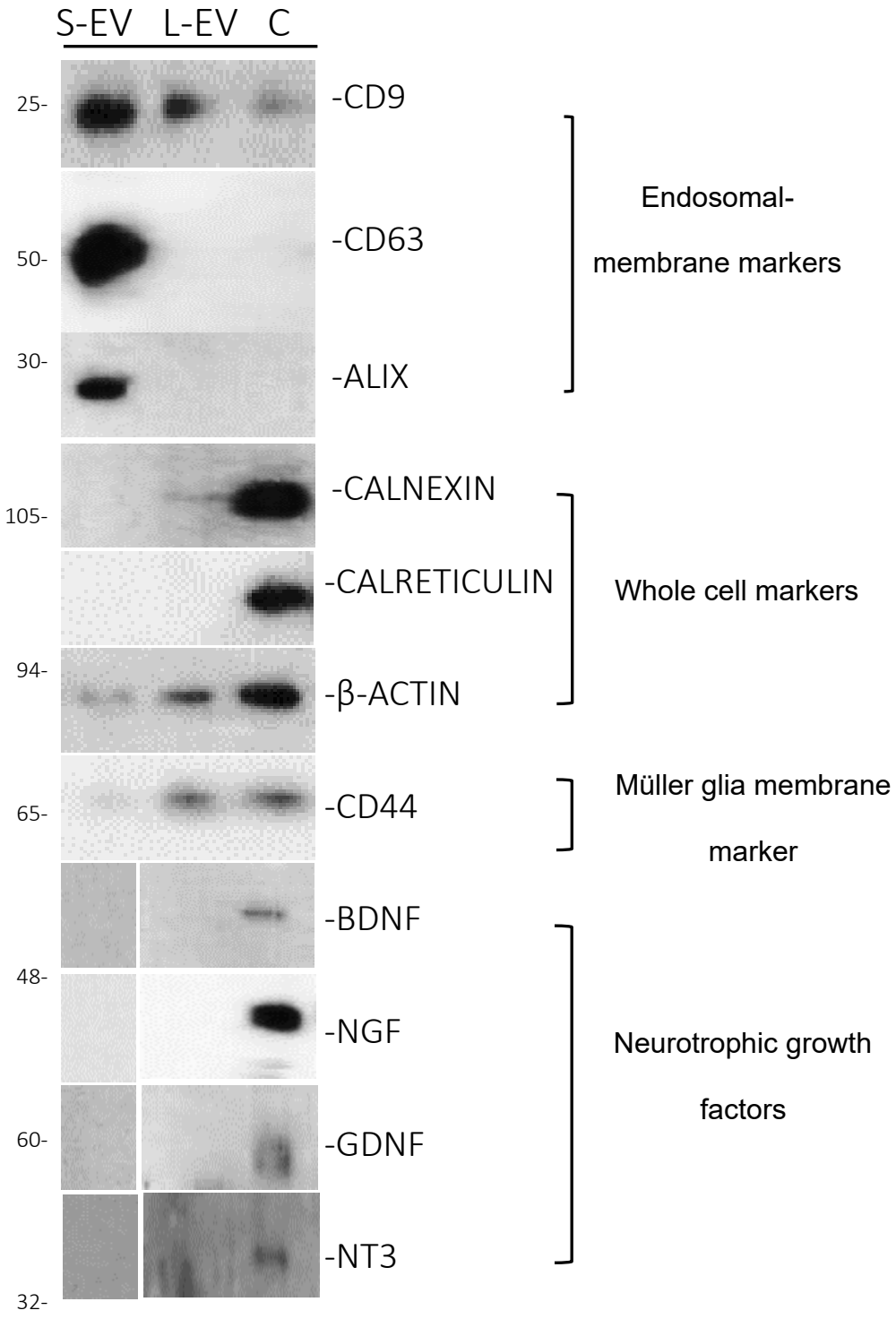

Figure 20. ***Western blot analyses of protein enrichment****. Large (L-EV) and small (S-EV) EV with whole cell lysates (CL) for their expression of endocytic membrane markers, endoplasmic reticulum, and cytoskeletal proteins . Also present are blots comparing detection of growth factor protein in EV preparations and whole cell lysates. Data are representative of three separate experiments.*

Electron microscopy of Müller glia-derived extracellular vesicles

Transmission electron micrographs were made by fixation and negative staining of vesicle pellets purified from Müller glia cells, and visualised between 20,000 and 40,000 magnification (fig. 21). Micrographs established the presence of a large quantity of spherical 3-dimensional objects, primarily rounded but occasionally possessing a biconcave morphology (fig 21; B, D. In some instances, EV appeared to be lysed or to have fused together (fig. 21; B-E). At increased magnification it was possible to identify evidence of a characteristic bi-layer membrane on individual vesicles, of approximately 5 nm diameter (fig. 21; A - E). Micrographs taken from fields of cell-free controls were absent of vesicle-type objects, confirming that the structures present were cell-derived (fig. 21; F).

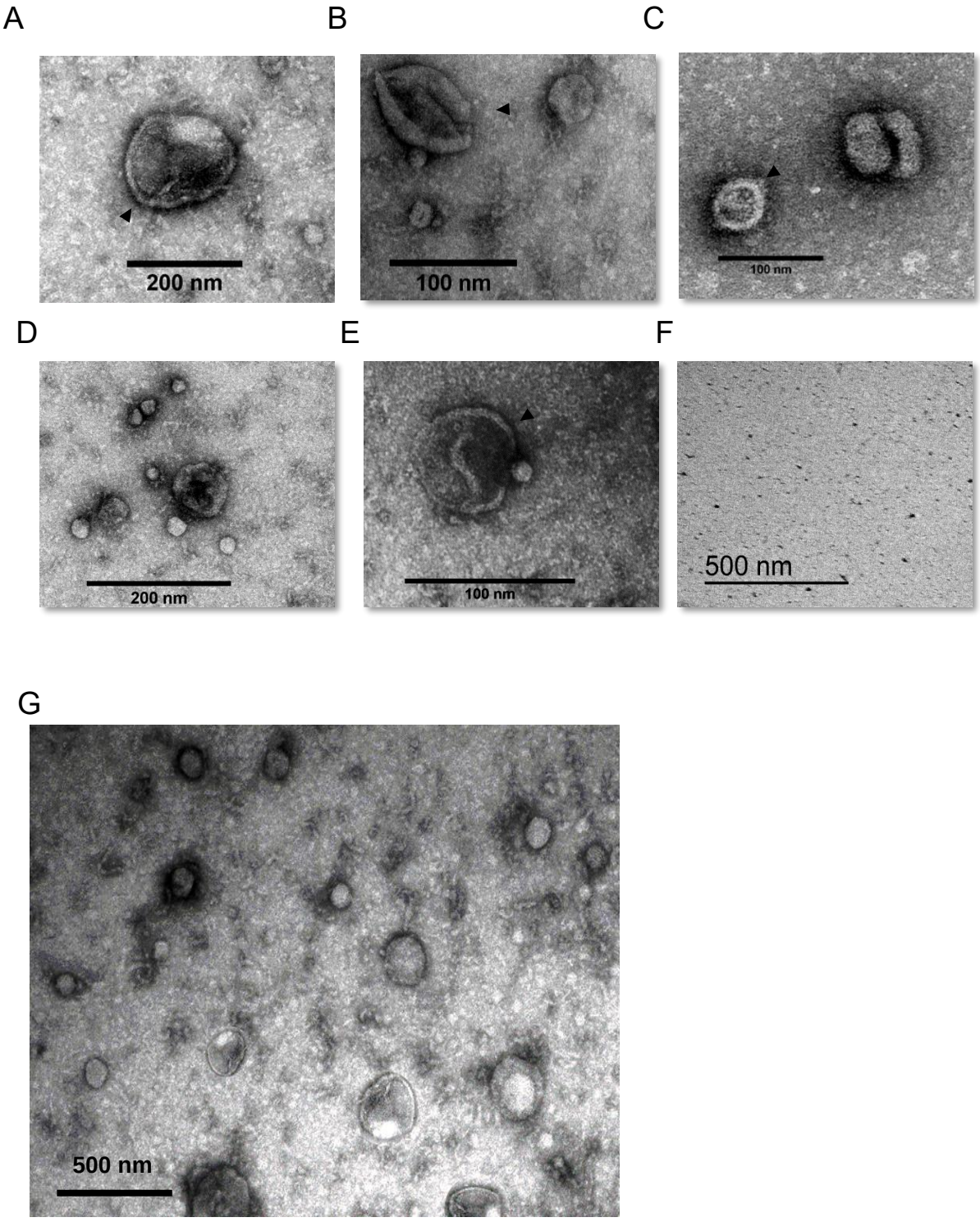

Figure 21. ***Transmission electron micrographs of a heterogenous Müller glia-derived EV population****. (**A**-**E**) Micrographs made at 40'000 x magnification show spherical and cup-shaped structures, 30–300 nm in diameter. Fields illustrate the size of vesicles and 'double-membrane' morphology. **F**) Cell-free controls were absent of vesicle-like structures. **G**) Full field micrograph made at 20,000 x magnification, representative of the diversity of vesicle diameter and morphology present in EV preparations.*

Müller glia-derived extracellular vesicles contain RNA

Initially, between 435 and 690 ng of total RNA was isolated from three pellets containing 1x 10^9 large EV, a larger quantity than the 190 – 420 ng recovered from an equivalent number of small EV. To confirm that RNA was confined inside EV, half of each EV preparation was treated with Rnase A (Promega, UK) in solution before RNA isolation. Nanodrop spectrophotometry of samples revealed no significant difference in RNA degradation between RNase-treated and control EV (fig. 22), suggesting that RNA was not associated with the external surface of EV or merely co-precipitating. Importantly, 800 ng of exogenous RNA added to exosomes was degraded by the added RNase. Following RNase treatment, large EV preparations returned an average of 503 ng of total RNA, a significantly higher quantity than was recovered from an equivalent number of small EV (215 ng), although these values were variable. For purposes of further characterization,10 ng of total RNA from each purification was evaluated by high sensitivity RNA screentape analysis.

RNA profiles in the large and small vesicular fractions were separated by high-sensitivity RNA ScreenTape analysis (Agilent Technologies, Palo Alto, USA). For purposes of comparison, the profile of Müller glia from each donor culture was also analysed (fig. 23). In whole cells, the dominant peaks correspond to the ribosomal RNA (rRNA) subunits 18S and 28S, although the electropherograms also indicate the presence of a comparatively small quantity of small RNAs between 25 and 200 nucleotides (nts) in length (fig. 23; A). The rRNA subunit peaks were absent or irregular in RNAs recovered from large EV purifications, although these were generally non-uniform and appeared to contain variable quantities of degraded RNAs (fig. 23; B). In contrast to whole cells, the dominant peak in large EV corresponded to small RNAs, with peaks between 50 and 75 nts in length. The same was true in samples isolated from small EV preparations, however these were more uniform and completely lacked rRNA subunits or long mRNA content identified in whole cells and large EV (fig. 23; C). In small EV, the dominant RNA peak appeared to surround the internal standard spike-in at 25 nts, suggesting enrichment in miRNA species.

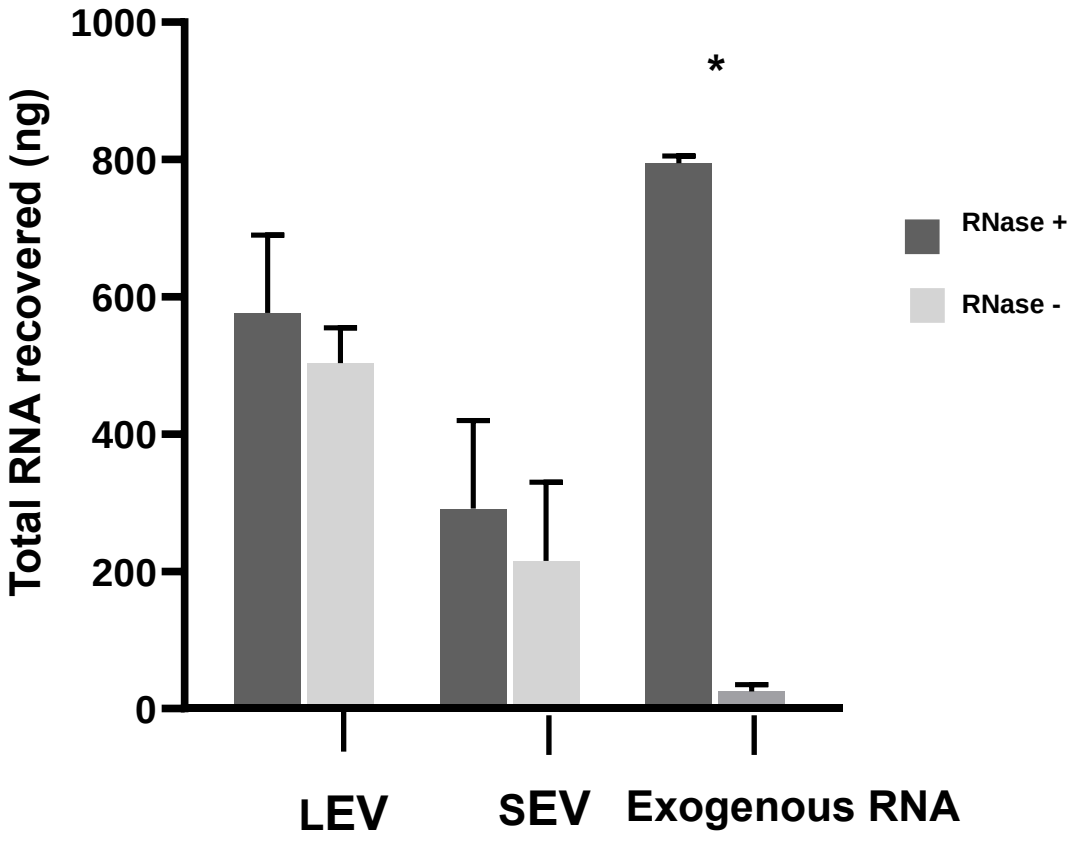

Figure 22. ***Comparing quantity of total RNA recovered from EV preparations pre-treated with RNase with those untreated****. Plots represent the mean of three replicates refined from equivalent quantities of purified EV. No difference in recovered RNA concentration was determined by nanodrop when comparing RNAse treated and non-treated samples, whilst a known quantity of free-RNA was significantly degraded p=<0.001.*

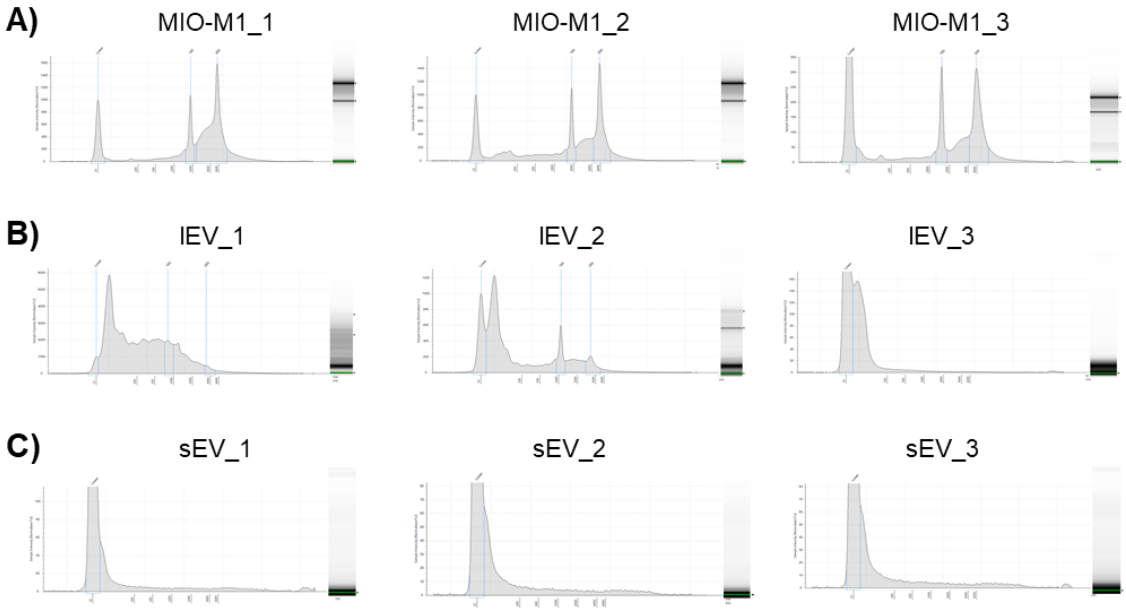

*Figure 23**. Electropherograms and corresponding gel images presenting the profile of RNAs recovered from large (lEV) and small (sEV) purifications, compared with donor MIO-M1 cells**. The short peak at 25 nt is an internal standard. (A) Whole cell samples had characteristic 18S and 28S ribosomal RNA (rRNA) peaks indicating the presence of non-degraded long RNA species. (B) rRNA was under-represented or lacking in large EV purifications, which were non-uniform and contained small non-coding RNAs 25 - 100 nts. (C) In small EV populations small RNA are dominant (20 – 30 nts), and no rRNA peaks or large transcripts were detected.*

Discussion

A differential ultracentrifugation protocol efficiently purifies vesicle sub-populations from Müller glia cell supernatants

Nanoparticle tracking (NTA) is currently the “gold standard” technique for sizing and quantifying nano-scale particles in suspension. In this study, NTA was used to characterize the size profiles of two different EV subsets, referred to as “large” and “small”, purified from Müller glia cell supernatants. Although care must be taken when interpreting data based entirely upon light-scatter based techniques like NTA, the diameters estimated for particles present in both preparations were consistent with those previously published for two categories of extracellular vesicles: MVB-derived exosomes (30 - 100 nm), and membrane-shed microvesicles (100 - 2000 nm) (Bobrie, Colombo et al. 2012). Analysis of large EV preparations indicated the presence of heterogenous, and polydisperse particle populations, ranging from 100 and 1000 nm in diameter. In particular, multiple size peaks were predicted between 200 – 500 nm (fig. 17). Importantly, >90% of particles present in large EV samples were over 150 nm in diameter. It is likely therefore, that these preparations were enriched with membrane-shed microvesicles, an observation supported by the fact that large EV protein lysates indicated the presence of a Müller cell membrane marker CD44, which was absent in small EV (fig. 20).

Measuring highly heterogenous samples using light-scattering techniques is challenging due to the inherent difficulty of sampling a stochastic process like Brownian motion over a finite period of time, which can affect resolution (Anderson, Kozak et al. 2013). The NTA software is able to correct for this when sizing a uniform and well-defined population, however this correction is not appropriate for the analysis of organic and diverse material like cellular vesicles, where assumptions about distribution cannot be made. Moreover, EV have a low refractive index compared to inorganic samples (latex or polystyrene beads for example), and it has been suggested that this could lead to an underestimation

of their size (Van der Pol, Coumans et al. 2014). With this in mind, the conclusions drawn from NTA analysis must be reinforced with secondary measuring techniques like electron microscopy. Analysis of sEV populations isolated through sequential steps of micro-filtration and ultracentrifugation onto a sucrose cushion (fig. 15), indicated the capture of significantly more homogenous populations than those isolated by the protocol used for large EV. Here, the majority of large particles were eliminated, and the mean population diameter reduced to 126 nm (fig. 18). These findings were largely in agreement with previously published reports suggesting that different preparative methods yield vesicles with varying characteristics (Tauro, Greening et al. 2012).

Since there is overlap in diameter and buoyant density between specific EV subtypes, assigning a vesicle to a particular biogenesis pathway by size alone is challenging. For this reason researchers working within the EV field are instead encouraged to describe EV populations by terms that refer to clearly defined characteristics. Although it is not accurate to describe the small EV purifications as exosomes, it is logical to say that the average size of particle present in this population is below that typically described for membrane-shed microvesicles. Coupled with the enrichment of endosomal membrane protein markers observed by western blot assays, it is accurate to say that the small EV preparations utilized in these experiments are “exosome-enriched”. Conversely, although there are particles <150 nm detected in large EV samples, 90% are above the maximum sizes reported for exosomes, and so it is also accurate to say that the large EV used in down-stream analyses in this work were “microvesicle-enriched”.

Electron micrographs confirm the presence of cell-derived vesicles

Analysis of electron micrographs showed that the diameter of the vesicles present in the EV preparations was surprisingly homogenous, with the majority sized between 30 and 200 nm. EV diameters appeared smaller than as estimated by

NTA, however, this study is not the first to report a discrepancy between vesicle sizes quantified under the electron microscope, and those predicted by distribution measurements. It is known that storage of preparations at 4°C and above appears to reduce the diameter of exosomes by as much as 60% after just two days (Sokolova, Ludwig et al. 2011). Although the preparations used in this study were stored at -20 °C, vesicles did spend several hours at room temperature during fixation and contrast staining, and it is possible that this contributed to the smaller particle size observed.

In general particles imaged were within size ranges predicted by light scattering techniques, although no vesicles measuring over 300 nm were identified in electron micrographs, despite significant concentrations of EV above that diameter predicted by nanoparticle tracking analysis. One factor likely to contribute to this discrepancy is the process of absorbing the sample onto the EM grid surface. Vesicles were applied at high concentration, and grids then washed extensively to remove those that are unbound. This process is known to bias selection of smaller particles, and so imaged EV are not necessarily representative of the original preparations (Théry, Amigorena et al. 2006). Variation may also be explained by the fact that since NTA predicts the hydrodynamic diameter of the EV in solution, small numbers of larger particles contribute disproportionally to light scattering than smaller particles in polydisperse samples, leading to a slight overestimation in diameter for the sample as a whole (Filipe, Hawe et al. 2010).

Electron micrograph analysis also allowed insight into the form, shape, and structure of isolated particles. In general vesicles appeared spherical, primarily rounded but occasionally possessing a biconcave ‘cup-shape’ morphology. While early studies did suggest that exosomes had the central depression identifiable in figure 21, this trait has since been shown to be an artefact of dehydration and contrast staining, and is not present in samples viewed by alternative imaging techniques like scanning-electron microscopy (Raposo, Nijman et al. 1996, Conde-Vancells, Rodriguez-Suarez et al. 2008).

The extensive and multistep sample preparations required for TEM are known to induce changes in EV morphology, evidence of this can be seen in the way that many of the structures were irregular in shape and appearing to have lysed. Analysis of electron micrographs did indicate the presence of a lipid-bilayer membrane structure, between 5 and 10 nm surrounding select vesicles (fig.21 A-D). Interestingly this bi-layer was more commonly evident on vesicles above 100 nm in size, and so more likely to be shed-vesicles rather than endosomal exosomes, although this is likely a result of the relatively low resolution of the image combined with the minuteness of the structures. Regardless, the presence of membranes confirms the cellular-origin of the particles present, and excludes the possibility of artifact or protein aggregate contamination.

Protein lysates of extracellular vesicles are enriched in endosomal-membrane markers

Small EV lysates were found to be enriched in two tetraspanin proteins, CD9 and CD63, neither of which were detected in equivalent quantities of cellular protein (2 µg). A weak signal also indicated the presence of CD9 in large EV preparations. According to the most recent proteomic data presented in the Vesiclepedia database (Pathan, Fonseka et al. 2019), vesicles of endosomal origin are highly enriched in tetraspanins (>120-fold enrichment compared to parental cells) which suggests an endoplasmic or “exosomal” origin for the small EV nanoparticles used in these experiments. The presence of CD9 in large EV may indicate a certain quantity of exosome-contamination, although care must be taken with interpretation, as many tetraspanins have also been reported to be widely distributed within the plasma membrane. For example, immuno-gold labelling of CD9 has been detected on larger, plasma membrane-derived microvesicles pelleted at 10,000 x g, as well as on lipoprotein conglomerates smaller than 50 nm that frequently co-pellet with exosomes (Bobrie, Colombo et al. 2012). CD9 may therefore be considered a non-specific EV marker, while CD63 appears to be localized exclusively to intracellular compartments, and may be more explicitly exosomes. The role of tetraspanins in the initiation of exosome biogenesis is relatively well established, however, the role that tetraspanins play

in the generation of microvesicle blebbing from the plasma membrane is less clear. There is evidence to suggest that certain tetraspanins enhance outer membrane curvature and vesicle fission, through interactions with the cytoskeletal matrix (Bari, Guo et al. 2011). Alternatively, the presence of CD63 but not CD9 in large EV may simply represent variability in the sensitivity and efficacy of the antibodies used, and the relative availability of antigen epitopes for each protein target.

Small EV preparations were also positive for ALG-2-interacting protein X (ALIX), an accessory of the endosomal sorting complex required for transport (ESCRT). Whereas tetraspanins are membrane bound, ALIX is a cytosolic protein known to be present in the internal compartment of endoplasmic vesicles (Baietti, Zhang et al. 2012). In vitro reconstitution experiments suggest that ESCRT-I and ESCRT-II together support budding processes and tentatively identify ESCRT-III as the complex that cleaves the buds to form intraluminal vesicles. ALIX interacts with several ESCRT (TSG101 and CHMP4) proteins and it is thought to participate in the budding and abscission processes, although the precise mechanism by which the protein becomes internalised into exosome lumens has not yet been confirmed. Interestingly, a 2016 study reported that ALIX knockdown did not influence the number of EV released by human liver cells, but did significantly decrease their miRNA composition. This suggests that ALIX plays a role in the packaging of miRNA into exosomes during biogenesis, rather than the creation of ILV (Iavello, Frech et al. 2016). Further clarification is required, but the ALIX signal reported in EV preparations in this study may indicate robust enrichment of extracellular miRNAs. Due to a lack of available EV protein controls the western blot assay is not quantitative. The comparative lack of endosomal markers detected in large EV compared to small EV lysates does, however, reinforce their respective enrichment in vesicles of plasma-membrane origin, rather than exosomes.

Whilst the presence of endocytic markers was confirmed in EV preparations, endoplasmic reticulum markers Calnexin, and Calreticulin were absent in large

and small EV, although robustly expressed in whole cell lysates. A significant challenge in the preparation of pure EV isolates from cell culture media is contamination with cytoplasmic debris from apoptotic cells that co-precipitate during centrifugation. While contamination of samples with apoptotic debris, including microsomes from the ER-compartment, can be minimized by using only cell cultures of high viability, a small quantity of dead or dying cells cannot be entirely avoided. As a result, ISEV guidelines stress the importance of confirming the absence of common non-EV contaminants in the isolated preparations. Calnexin and Calreticulin are multi-functional chaperones that bind transiently to nascent proteins, assisting in folding and assembly while retaining unfolded or unassembled N-linked glycoproteins in the endoplasmic reticulum (Lamriben, Graham et al. 2016). The absence of Calnexin and Calreticulin western blot signals in EV lysate indicates that the particles present are not of endoplasmic reticulum origin, and are therefore unlikely to have originated from the lysis of apoptotic cells.

Traces of the cytoskeletal marker β-actin were detected in large and small EV samples, whilst this protein was markedly observed in whole cell lysates. The Vesiclepedia database presents more than 70 studies reporting the presence of β-actin in various vesicle-enriched samples (Pathan, Fonseka et al. 2019). It is evident that despite the fact that exosomes are not possessing a cytoskeleton, a proportion of them do contain actin cargo. As a non-muscle cytoskeletal protein, β-actin is ubiquitously expressed and prevalent in the cell cytoplasm. Large vesicles formed by pinching-off of the cell plasma membrane may contain greater quantities of cytoplasm, including cytoskeletal proteins. Whilst the process of exosome biogenesis does not involve β-actin *per se*, transport of multi vesicular bodies to the plasma membrane is dependent on their interaction with actin and the microtubule cytoskeleton (Villarroya-Beltri, Baixauli et al. 2014). The low intensity of the signal observed in this study, implies that β-actin is not a primary constituent of the vesicles isolated. It is probable that the protein is limited to the cargo of membrane-shed EV, for which it would be expected that the relative intensity of the signal would decrease in more homogenous exosomal purifications, as was observed in small EV lysates (fig. 20).

Extracellular vesicles produced by Müller glia do not contain neurotrophic factors

As demonstrated in this study and in the literature, Müller glia cells within the retina or in culture express and secrete neurotrophic growth factors (Seki, Tanaka et al. 2005). Some evidence suggests that microvesicles shed from neurons and astrocytes contain growth factors, and are able to promote paracrine responses in target cells (Schiera, Proia et al. 2007, Proia, Schiera et al. 2008). More recently, HEK293 EV engineered to encapsulate NGF protein have been demonstrated to deliver this factor to neurons of the cortex following systemic delivery in a mouse stroke model (Yang, Wu et al. 2020). It was therefore hypothesized that the same growth factors may be encapsulated within Müller-derived EV, and that this may constitute a mechanism by which these are secreted and distributed to target neurons. Western blot analysis confirmed presence of the neurotrophins NGF, BDNF, and NT3, as well as GDNF in Müller cell lysates, but all of them were absent in EV preparations.

Whilst no data currently supports the loading of specific proteins into exosomes through the endocytic transport pathway, some evidence suggests that large microvesicles may contain proteins specific to the donor cell of origin. In particular this protein cargo has been associated with facilitating communication within the immune system (Gasser and Schifferli 2004), and within the tumour micro-environment (Minciacchi, You et al. 2015). Although no evidence of neurotrophic factor enrichment was detected in Muller-glia EV, it may be possible that the quantities of protein present in EV isolates were simply too low to for detection by traditional antibody-based capture techniques. More sensitive protein detection techniques like mass-spectrometry may be required to reveal the true extent of potential EV protein cargos. The data reported here does suggest, however, that growth factor ligands are unlikely to be specifically enriched in secreted EV, at least when compared to donor cells.

Interestingly, there is evidence for segregation of the neurotrophin receptor TRKB with small vesicles derived from glioblastoma cells, as well as reports of receptor EGFRv-III transfer via tumour microvesicles (Al-Nedawi, Meehan et al. 2008, Pinet, Bessette et al. 2016). The methodology utilized in these studies is not able

to differentiate between TRKB encapsulated within vesicle lumens, and membrane-bound receptor collected by EV shed from the cell plasma membrane. Nonetheless, it is possible that delivery of neurotrophin receptor to target neurons is a more efficient strategy to enhance neuroprotective signalling in the retinal microenvironment than the transfer of the ligand itself, where binding interactions are likely to be disrupted by the vesicle membrane. Despite these observations, research interest in EV has increasingly moved away from the potential transfer of proteins and focused instead on the exchange of genetic material, particularly various RNA species, which is now well established in a range of tissues and physiological contexts (Rufino-Ramos, Albuquerque et al. 2017).

Müller cell-derived EV contain small RNA species

It has been proposed that extracellular vesicles released by cells carry regulatory RNA molecules, thereby allowing for long distance cell-cell communication by genetic transfer. In order to ascertain the RNA content of EV released by Muller glia cells, small and large EV preparations were purified from three separate passages of MIO-M1 cells. To confirm that RNAs were confined within vesicle lumens rather than being membrane-associated, or simply co-precipitating with EV, half of each preparation was first treated with RNase A in solution, before recovery of RNA and quantification by nanodrop spectrophotometer. This treatment caused only a minor reduction in RNA concentration when comparing RNAse treated and non-treated samples. From this data, it can be deduced that the RNAs present were internalised within EV, and so protected by the vesicle membranes, as anticipated (fig. 22). These findings are comparable to previous studies, where it has also been observed that the addition of a membrane-disrupting detergent (Trizol) in combination with RNase leads to complete degradation of EV RNA (Valadi, Ekström et al. 2007). The ability of vesicle membranes to protect sensitive cargos against degradation adds weight to suggestions that membrane-vesicles may provide a stable vehicle for the transport of RNA through RNase rich extracellular environments (Cheng, Sharples et al. 2014, Hagiwara, Kantharidis et al. 2014).

As anticipated, RNA profiles of EV populations differed significantly from those observed in whole cells. Because mRNA typically comprises only 1-3% of total cytoplasmic RNA samples it is not readily detectable even with the most sensitive of methods. Ribosomal RNA makes up >80% of total RNA samples, with the majority of that consisting of the 18S and 28S rRNA species (Johnson, Abelson et al. 1977). Assessment of RNA by bioanalyzer is therefore based upon the assumption that rRNA quality and quantity reflect that of the underlying mRNA population.

Whilst cellular RNAs predominantly consist of rRNA subunits (fig. 23), and comparatively contain low quantities of small non-coding RNA, the reverse was true in profiles generated from EV samples, which were enriched in molecules <200 nts in length. Of the three sources, large EV produced the most variable and least consistent profiles. Although all three replicates contained small non-coding RNAs, samples 1 and 2 also appear to have a quantity of larger species present. Sample 2 has small rRNA peaks emerging around the 18s, while both have an irregular ”smeared” profile indicative of degraded long nucleic acid transcripts. The presence of these longer molecules may account for the increased quantity of RNA recovered from large EV compared to small.

The large EV purifications were heterogenous in size, and likely contain a mixture of vesicle subtypes: endosome-derived exosomes, membrane-shed microvesicles, and even large apoptotic bodies. Large EV samples were absent of protein markers of apoptosis in western blot studies (fig. 20), however the screentape analysis is a far more sensitive method of detection. Previous studies profiling the RNA composition of various EV subtypes report that the dominant RNA species present in apoptotic bodies is rRNA, and so it is possible that this inter-sample variation reflects variable contamination of the large EV with traces of apoptotic compartments, rather than specific loading of vesicles with longer transcripts (Crescitelli, Lässer et al. 2013).

All EV-sourced samples were enriched in small RNAs varying between 20 – 200 nts in length. In large EV, a separate peak contained RNAs between 50 and 100 nts, corresponding to sizes reported for transfer RNAs (tRNA) (76 – 90 nts) (Rich and RajBhandary 1976). Large EV enrichment in tRNA would be consistent with previously published experiments characterizing vesicle transcriptomes from various cellular sources, where tRNA has been reported to comprise anywhere between 5 and 90 % of the total EV RNA content (Bellingham, Coleman et al. 2012, Turchinovich, Drapkina et al. 2019). Interestingly, tRNAs have also been reported as the predominate RNA species present in cell culture media, although pre-treatment of each sample with RNAse would have been sufficient to degrade any unbound RNA.

The RNA profiles for the three small EV samples were consistent, each containing a complete lack of rRNA subunits, instead dominated by a peak that appeared to surround the internal standard spike-in at 25 nts, suggesting enrichment in miRNA species as anticipated. The profiles also indicate the presence of larger small RNA molecules in small EV samples, although the minimal quantities of total RNA present in these makes it difficult to separate these from the background noise of the electropherogram.

Conclusions

This study developed and refined a protocol for a detailed evaluation of extracellular vesicles released by Müller glia cells *in vitro.* Size-profile characterisation indicated that a protocol involving a combination of differential-gradient ultracentrifugation and micro-filtering is able to precipitate populations of organic, nano-sized particles with an average diameter corresponding to that of endosome-derived exosomes (~100 nm). A variation on the protocol allowed recovery of a second, more heterogenous population of large particle sizes suggesting enrichment in large membrane-shed microvesicles (~250 nm). Although assigning vesicles to a particular biogenesis pathway is challenging, the presence of endosomal membrane markers CD9, CD63 and ALIX in small EV isolates, as well as the Müller plasma membrane marker CD44 in large EV,

reinforced conclusions drawn from size profiling. The absence of cytoplasmic proteins and markers of apoptosis in EV population lysates suggested a lack of cell debris contamination. Vesicle size and morphology were validated by electron microscopy, which also revealed evidence of a characteristic lipid bi-layer membrane, confirming their cellular origin. Collectively, the current results satisfy ISEV requirements to claim the presence of cell-derived extracellular vesicles (Théry, Witwer et al. 2018). They also illustrate some of the difficulties inherent in characterization of nano-sized biological materials, and reinforce the need to confirm and compare data with secondary sizing techniques.

Recently, various therapeutic benefits recognised in EV derived from cellular sources have been attributed to their ability to act as a vector for the transfer of genetic material between cells. In particular, there is evidence that small non-coding RNAs contained within vesicles are capable of regulating the translation of specific gene targets and so moderate diverse signalling pathways. In a recent study “exosomes” derived from bone marrow stem cells delivered intravitreally to rats with raised IOP reduced thinning of the nerve fibre layer and promoted neuroprotection. Knockdown of AGO2 in donor cells, a protein critical for miRNA packaging and function, significantly attenuated these effects, leading the author’s to conclude that RGC neuroprotection may be miRNA-dependent (Mead, Amaral et al. 2018). This work echoes results from related experiments in other disease models. Application of MSC-derived exosomes improved cardiac function in post-MI mice in a manner that was dependent on the presence of miR-210 delivery and subsequent down-regulation of angiogenesis gene Efna3 (Wang, Chen et al. 2017). This data suggests that miRNAs represent interesting therapeutic candidates, and their encapsulation within EV offers the advantage of protection from degradation by extracellular ribonucleases, which could allow exosomal-miRNAs to exert their function at distant sites and in a prolonged manner (Cheng, Sharples et al. 2014).

In conclusion, large and small EV isolated from Müller glia cells were found to be comparatively enriched in small RNAs compared to donor cells. Given the current

interest in EV transfer of miRNA between cells, the identification and quantification of these RNA molecules will provide further insight into the neuroprotective effect that these cells have demonstrated in animal models of retinal degeneration.

Chapter 4: MicroRNA expression profiling of Müller glia Extracellular Vesicle subsets by Illumina sequencing

Introduction

miRNA delivery by extracellular vesicles

Valadi and colleagues were the first to identify the presence of mRNA and miRNA internalised within the lumens of EV, also recognizing that these were capable of functional transfer through the detection of translated proteins in recipient cell cultures (Valadi, Ekström et al. 2007). Subsequent analysis revealed distinct RNA profiles between exosomes, membrane-shed microvesicles and donor cells, with exosomes primarily enriched with small RNAs (>100 nts), whilst generally lacking large ribosomal RNA subunits. Among the various small RNAs present, miRNAs are proportionally more represented than in their parent cells (Goldie, Dun et al. 2014).

High-throughput sequencing of exosomal-miRNAs from prion-infected neurons determined that this miRNA signature is distinct from that of its cellular origin, and may also vary depending on the physiological condition of the cell (Bellingham, Coleman et al. 2012). These observations have been reinforced by more recent studies, including that of Lunavat et al. who compared miRNA enrichment between vesicle populations derived from the MML-1 melanoma cell line. The authors report that 23 out of the 252 miRNAs detected in total were identified only in exosomes, whilst 113 were common between EV sub-types and parental cells (Lunavat, Cheng et al. 2015). As these, and other profiling studies suggest, miRNAs may be not randomly incorporated into EV. It is possible that a sorting mechanism by which certain miRNAs are preferentially selected for loading appears to exist, several such pathways have been suggested although no true consensus has yet been found.

Potential of EV and micro-RNAs for glaucoma therapy

The paradigm shift in the role of EV as a potential therapeutic agent can be traced back to a 1996 publication presenting evidence for vesicles derived from the endocytic compartments of B lymphocytes, that presented MHC class II molecules and were capable of inducing an immune response (Raposo, Nijman et al. 1996). Shortly after, Zitvogel et al (1998) published the first evidence of EV as a potential therapeutic agent in demonstrating that MHC-positive vesicles derived from dendritic cells were capable of priming cytotoxic T lymphocytes for the suppression of murine tumours *in vivo* (Zitvogel, Regnault et al. 1998). The promise of these studies lead to the first phase I clinical trials of EV-based therapeutics in 2005, where 15 metastatic melanoma patients received four doses of autologous dendritic cell-derived EV, demonstrating the feasibility of large scale exosome production and the safety of exosome administration (Escudier, Dorval et al. 2005).

Several pre-clinical studies have examined the effects of exosomes and small-EV derived from cells with presumed therapeutic influence in a variety of disease models, including ocular pathologies. Periocular injection of EV purified from mesenchymal stem cell (MSC) supernatants significantly ameliorated experimental autoimmune uveoretinitis in rats. In this study the authors suggested that this effect was caused by inhibition of the migration of inflammatory cells and observed that the effect of EV was equivalent to that of their parent cells (Bai, Shao et al. 2017). Similarly, it has been demonstrated that intravenous small-EV injections in a mouse model of autoimmune uveitis attenuated retinal damage, which was accompanied by a reduction in inflammatory cell infiltration and cytokine production (Shigemoto-Kuroda, Oh et al. 2017).

In the context of neuroprotective signals derived from stem cells, many of the therapeutic benefits reported from exogenous application of stem cell-derived EV have been attributed to their ability to transfer short non-coding RNAs, capable of regulating gene expression at the transcriptional and post-transcriptional level

in target cells. For example, improved cardiac function in post-MI mice following the application of MSC exosomes was found to be dependent on the downregulation of the angiogenesis gene Efna3 (Wang, Chen et al. 2017). The authors determined that this inhibition was caused by miR-210, a specific miRNA highly enriched in MSC vesicles, as the therapeutic effect was largely lost in EV purified from miR-210 knockouts. In a similar study, transplantation of MSC-EV electroporated with miR-132 mimics into the ischemic hearts of mice markedly enhanced neovascularization in the peri-infarct zone, and preserved heart function (Ma, Chen et al. 2018).

Small BMSC EV injected intravitreally into rats following induction of elevated IOP, reduced thinning of the nerve fibre layer and promoted significant neuroprotection. Knockdown of AGO2, a protein critical for miRNA packaging and function, significantly attenuated these effects leading the authors to conclude that RGC neuroprotection is likely miRNA-dependent (Mead, Amaral et al. 2018). This work echoes results from related experiments in several other disease models, for example Wang et al. report the angiogenic promoting effects of cardiomyocyte exosomes in diabetic rats, determining that this effect was dependent on transfer of miR-320, and could be blocked by knockdown in parent cells (Wang, Huang et al. 2014). This data strongly suggests that exosomal miRNAs may represent interesting therapeutic candidates, with the advantage of protection from degradation by blood-derived ribonucleases, which could allow exosomal-miRNAs to exert their function at distant sites (Cheng, Sharples et al. 2014).

Chapter summary and objectives

The results of characterisation studies previously reported in this work suggest that both small and large EV derived from Müller glia cells are enriched in small RNA species (<200 nt). Recently, non-coding RNA, primarily miRNAs have been implicated in genetic transfer between cells, and are of particular interest due to their ability to regulate gene expression through targeted silencing of mRNA (Valadi, Ekström et al. 2007). Given that various Müller glia or Müller glia-like cells

confer a neuroprotective signalling response when transplanted into animal models of RGC-degeneration (Becker, Eastlake et al. 2016, Eastlake, Wang et al. 2019), it is logical that miRNAs potentially transferred via Müller-EV may represent a part of that action.

The objectives for this chapter were:

1. To characterise miRNA present within small and large EV, as well as in Müller glia donor cells, using high-throughput Illumina sequencing.

2. To use a bioinformatic pipeline to identify target mRNAs for the most abundant species detected, and to validate these by quantitative PCR.

3. To compare the miRNA expression profile between the different sources investigated to allow insight into the underlying mechanisms behind the loading and sorting of these molecules into secreted vesicles. Analysis of predicted functions for species particularly abundant in EV compared to donor cells, or vice versa, will allow the evaluation of their potential role in extracellular signalling or internal cellular processes.

Materials and methods

Isolation of RNA from EV released by Müller glia in culture

Total RNA samples were isolated from small and large EV pellets obtained by a differential ultracentrifugation / micro-filtration protocol (as described previously in Chapter 3) using the Total exosome RNA and protein isolation kit (Invitrogen). 200 μL of each vesicle sample (following incubation with ribonuclease enzyme as previously described) was combined with an equal volume of 2x denaturing solution, vortexed to lyse, and then incubated on ice for 5 min. After incubation, 400 μL of acid-phenol/chloroform was added, vortexed for 30–60 sec to mix, and then centrifuged for 5 min at 15,000 x g at room temperature to separate the mixture into aqueous and organic phases. After centrifugation, the aqueous upper phase was carefully removed and transferred to a fresh tube. A 1.25 volume of 100% EtOH was then added to the aqueous phase for each sample, before vortexing. A 700 μL volume of the mixture was transferred into a spin column placed within a collection tube, and then spun at 12,000 x g for 30 sec in order to immobilize RNAs onto the glass-fibre filter. Samples were washed once with 700 μL wash solution 1, and twice with 500 μL wash solution 2/3 by centrifugation at 12,000 x g for 15 sec. Next, the filter was dried by spinning for an additional 1 min at 12,000 g, before transfer into a fresh collection tube. Finally, 25 μL of preheated (95◦ C) nuclease-free water was applied to the centre of the filter. Samples were centrifuged for 30 sec at 10,000 g to recover the RNA from the column, before a second 10 μL volume of nuclease-free water was applied. After a second centrifugation at 12,000 x g, the eluate containing RNA was collected, concentration quantified by nanodrop spectrophotometer (Nanodrop-1000, Thermo Scientific) and stored at −20◦ C. After treatment, each sample was diluted to 2 ng/μL and 1 μL was analysed on the Agilent 2100 Bioanalyzer using the Agilent RNA 6000 Pico Kit (Series II) to determine the mass of RNA going into downstream analysis, as previously described.

Construction of small RNA libraries and sequencing

Prior to small RNA sequencing, the quality and quantity of total RNA were checked by 2200 TapeStation system (Agilent), using High Sensitivity RNA ScreenTape (5067–5579) with High Sensitivity RNA ScreenTape Sample Buffer (5067–5580) and High Sensitivity RNA ScreenTape Ladder (5067–5581). The range of total RNA input is 500 – 10,000 pg/µL, and total RNA integrity is estimated using the software RNA Integrity Number (RIN) algorithm, which provides a value describing the deterioration of the sample taking the ratio of 18S and 28S into account. Whole cell RNA samples pass quality control if RIN is >8. These are then used for downstream cDNA synthesis, and high-throughput sequencing. RIN was not considered for samples isolated from vesicles, as these generally lack ribosomal RNA.

Preparation of libraries and sequencing was conducted by the UCL genomics service at the UCL Institute of Child Health (UCL,London, UK). miRNA libraries were prepared using a QIAseq miRNA Library Kit (Qiagen, Manchester, UK) according to the Illumina small RNA sample preparation protocol. Briefly, 250 ng of total RNA from three whole cell passages, three small EV samples, and three large EV samples were converted into miRNA NGS libraries. Adapters containing unique molecular identifiers (UMIs) were ligated to the 3´ and 5´ ends of all miRNAs and single-stranded complementary RNA (cDNA) was synthesized by reverse transcription using primers containing an integrated UMI. During reverse transcription, a universal sequence was also added that is recognized by the sample indexing primers during library amplification. A clean up of the cDNA was performed using a streamlined magnetic bead-based method (QIAseq Beads; Qiagen). The cDNA samples were amplified by PCR (22 cycles) using indexing forward primers and a universal reverse primer. After library amplification, a second magnetic-bead based clean up of the miRNA library was performed. Library preparation quality control was checked using a Bioanalyzer 2100. The library pool was then sequenced in a NextSeq 500 sequencing instrument (Illumina, Inc. San Diego, CA) according to the manufacturer instructions in a

single-end read fashion with a read length of 75 bases. Raw data were demultiplexed and text-based FASTQ files storing sequence and quality scores for each sample were generated using the software bcl2fastq (Illumina Inc., San Diego, CA).

Small RNA sequencing analysis: Mapping and differential expression

Raw data in FASTA format was collected, and all downstream analyses were conducted by the author as illustrated in figure 24. The quality of the generated reads was assessed using the FASTQC tool, by studying their per base sequence quality plot, per base N content plot, adapter content plot and per sequence quality score plots (Andrews 2017). The adapter trimming was done using Cutadapt (Martin 2011). The quality of the generated reads was assessed using FASTQC by studying their per-base-sequence quality plot, per-base N content plot, adapter content plot, and per-sequence quality score plots.

Raw reads in FASTQ format were mapped to the miRbase database using Bowtie2 following adapter removal by Cutadapt and counts tables were obtained using the featureCounts function in R (Langmead and Salzberg 2013, Kozomara, Birgaoanu et al. 2019). The data was normalized by count per million (CPM) function in edgeR (Robinson, McCarthy et al. 2010). The number of samples above a minimum of 2.5 CPM were counted, and only transcripts present above that minimum in at least three libraries were retained. The pairwise differences in miRNA expression levels among the libraries from different sources were examined using the DESeq2 package (version 1.10.1) (Love, Anders et al. 2019). The false discovery rate (FDR) was controlled for at 5% using the Benjamini-Hochberg method for each pairwise comparison, and miRNA were considered differentially abundant when the log2-fold change was >2 or <−2. A summary of the microRNA sequencing data analysis pipeline used is presented in figure 24.

Statistical analysis software

Histograms, PCA, scatterplots, venn diagrams, and heatmaps were made using the ggplot2 and heatmap2 packages in R (distributed by CRAN). GraphPad Prism 8.0 (GraphPad prism, Prism 8 for Windows, version 8) was used to conduct statistical analyses not included in integrated pipelines.

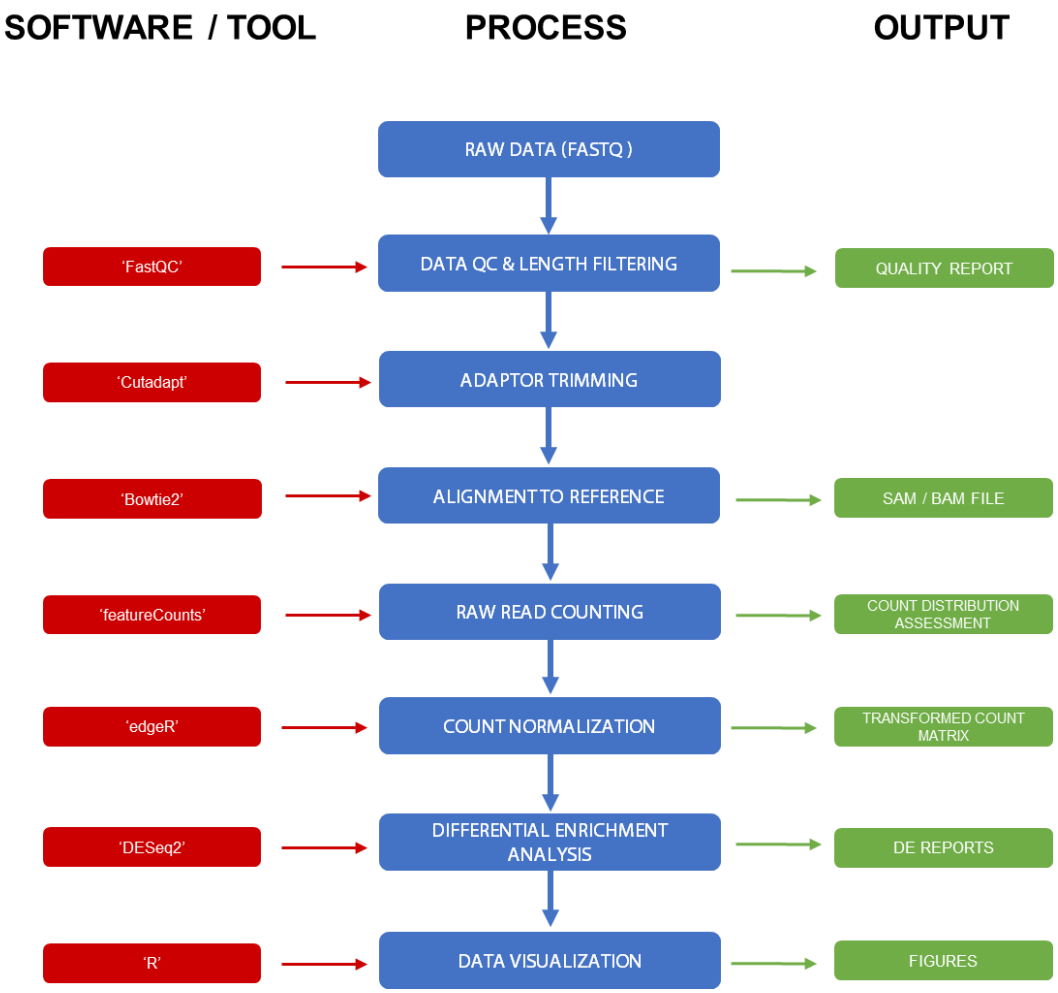

Figure 24. Flow chart illustrating the micro-RNA sequencing pipeline used for analysis of small RNA sequencing data

Pathway enrichment analysis

The web-based application DIANA-mirPath V3 was used to perform the enrichment analysis of predicted target genes by miRNAs in biological pathways (Vlachos, Zagganas et al. 2015). The algorithm microT-CDS was chosen to predict EV-derived miRNA targets, using the default microT threshold of 0.8. DIANA-mirPath performed an enrichment analysis of multiple miRNA target genes to all known KEGG pathways. The statistical significance value associated with the identified biological functions was calculated by the mirPath software (http://microrna.gr/mirpath). Biological pathways showing p-value less than 0.05 were considered as significantly enriched.

GO biological process analysis was performed using the Ingenuity® software (Ingenuity Systems, USA; http://analysis.ingenuity.com). miRNA target filters were applied to significant, differentially expressed miRNAs (adjusted p value ≤0.05 in all three statistical methods) and mRNA target lists were generated based on highly predicted or experimentally observed confidence levels using the Tarbase index of experimentally supported miRNA:mRNA interactions. Core expression analyses were performed with default criteria to determine the most significant functional associations (biological and canonical pathways) of mRNAs targeted by dysregulated miRNAs

Spiking of internal miRNA standard and reverse transcription

For qPCR validation of miRNA of interest in EV and whole cell samples, a total of 3 µL synthetic *Caenorhabditis elegans cel-miR-39* (Norgen Biotek Corporation, Canada; cat. 59000) was added to each sample as a spiking control prior to extraction of RNA (Selth, Townley et al. 2012). Total RNA samples recovered as previously described in Chapter 3 were reverse-transcribed into cDNA using the microScript microRNA:cDNA Synthesis Kit (Norgen Biotek Corporation, Canada;

cat. number 54410). A poly (A) tail was first added to the RNA template, followed by cDNA synthesis using a specific adapter primer. For each sample, 10 μL of 2x Reaction Mix and 1 μL of microscript microRNA enzyme mix were added to 500ng of total RNA, and diluted to a volume of 20 μL in nuclease-free water. The cDNA synthesis reaction was then incubated in a thermocycler (Mastercycler® Gradient; Eppendorf) at 37 °C for 30 minutes, 50 °C for 30 minutes, and 70 °C for 15 minutes, before being cooled on ice and finally stored at -20 °C until required.

Quantitative real-time PCR for validation of microRNA sequencing

A subset of four miRNA were chosen for validation of sequencing results. Two of which had been identified as enriched in small EV compared to whole cells (hsa-miR-21-5p, hsa-miR-29b-5p), one was predicted to be unchanged between the RNA sources (hsa-miR-10a-5p) and one that was relatively depleted in small EV (hsa-miR-767-3p). SYBR-based qRT–PCR was performed using miRNA specific primers designed using the mIRPrimer2 software (Busk 2014) (see supplementary table 2). For quantification of gene expression, real-time PCR was conducted using SYBR Fast Universal qPCR Master Mix (Applied Biosystems™; cat. 4309155) on the QuantStudio™ 6 Flex Real-Time PCR System (Applied Biosystems™). For each reaction, 5ng of cDNA template was diluted to a volume of 8 μL in nuclease-free PCR-grade water on ice. 10 μL of 2X PCR mix containing SYBR green was added, as was 1 μL (5 μm) of specific forward primer and an equivalent quantity of specific reverse primer. For quantification of the cel-miR-39 internal control transcript, a gene specific forward primer was used in combination with a universal reverse primer (Norgen Biotek Corporation, Canada; cat. number 54410). Prior to loading, plates were centrifuged to homogenise the reaction mix and bring it down to the bottom of the well. The thermo cycling conditions were set as follows: 50 °C for 2 minutes, 94 °C for 10 minutes, followed by 40 cycles of 94 °C for 15 seconds and 60 °C for 30 seconds and 72 °C for 45 seconds. Fluorescent signal emitted between 60°C and 72°C of each cycle was recorded.

At the end of the run, the threshold cycle (Ct) value was exported from the QuantStudio™ 6 Flex Real-Time PCR software (v1.1). Ct values represent the number of cycles at which the amplified PCR product reaches a threshold level of detection, each reaction was run in triplicate and mean Ct was averaged. Data was analysed using the $2^{-\Delta\Delta Ct}$ method to quantify fold change relative to the expression of cel-miR-39 control in each sample (Selth, Townley et al. 2012).

Results

miRNA transcripts are abundant in Müller glia EV

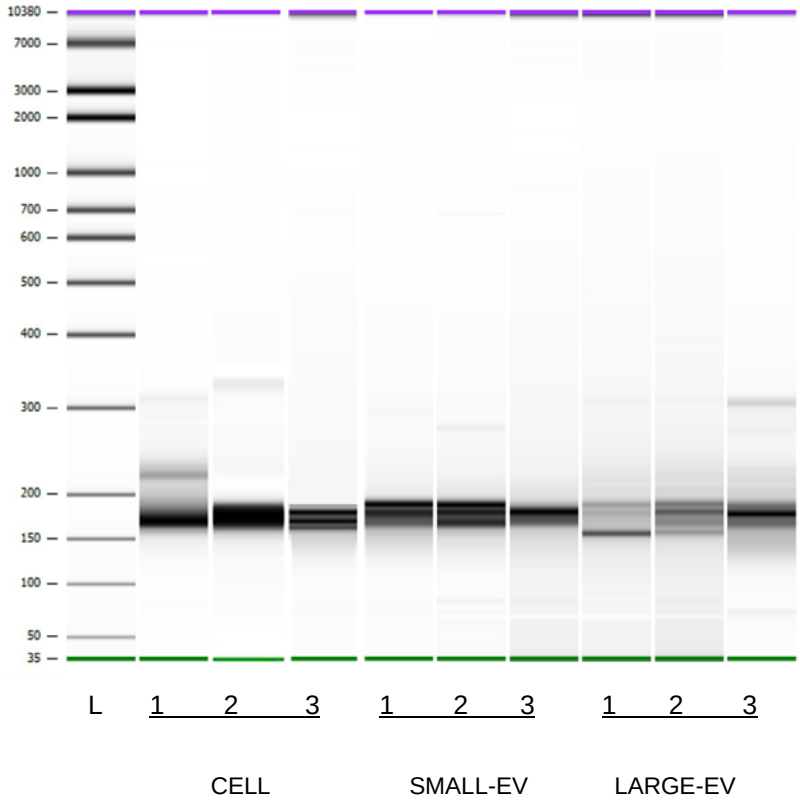

Figure 25. ***Size analysis of cDNA libraries generated for Illumina sequencing runs****. The Agilent 2100 Bioanalyzer HighSensitivity DNA chip was used to characterize the libraries of the reverse transcribed miRNA species. Bands between 160 and 200 represent the miRNA population. The lane marked L denotes the ladder and size in nucleotides is listed, as are purple (upper) and green (lower) markers.*

Yield and size distribution of cDNA libraries generated from each sample were validated using Agilent 2100 Bioanalyser on a high-sensitivity DNA assay (Agilent Technologies, United States) as detailed in the methods section above. Prior to generation of cDNA libraries, adapters are ligated sequentially to the 3' and 5' ends of the 20 – 30 nt mature miRNA molecules present in samples. Following cDNA synthesis, each library was found to contain DNA molecules of between 160 and 200 nts length, corresponding to the miRNA population. Sequencing data underwent a quality check using FastQC prior to alignment to human miRNA database. All 9 samples passed FastQC quality control scores. Between 75 – 96 % of the small RNA reads were aligned to the reference sequences (Table 1). Despite variability in the number of reads between large EV, small EV, and cell replicates, > 90% of reads were mapped to mature human miRNAs, and were normalized for further analysis. In total, 662 miRNAs were identified in EV samples, approximately ~25% of the 2654 total human miRNAs currently annotated in the latest miRBase release (22), confirming that extracellular miRNA were abundant in EV released by Müller glia.

	Cells_1	**Cells_2**	**Cells_3**	**sEV_1**	**sEV_2**	**sEV_3**	**lEV_1**	**lEV_2**	**lEV_3**
Total raw reads	5553930	5950940	1941970	11591624	9803483	8277500	3732507	5873534	8499789
Quality score (FastQC)	Passed	Passed	Passed	Passed	Passed	Passed	Passed	Passed	Passed
Number of alignments to miRbase	5276233.5	5765467	1865497	10821587	8501356	7217571	2825149	4753448	7806377
Percentage of alignments	95.00	96.88	96.06	93.36	86.72	87.20	75.69	80.93	91.84
Number of reads for miRNAs	396025	3990900	1252144	1225541	2038635	3134561	468118	1262297	2166798
Number of identified miRNAs	586	1058	811	431	427	329	218	235	520
Number of miRNA with read=1	133	164	159	11	9	23	42	26	13

Table 1. ***A summary of full alignment for each sample library****. Total number of reads generated by sequencing with number of alignments mapped to mature human miRNA, and number of species identified in each sample replicate. Number of miRNAs identified in each sample replicate represent the number of all the total miRNA with reads more than or equal to 1.*

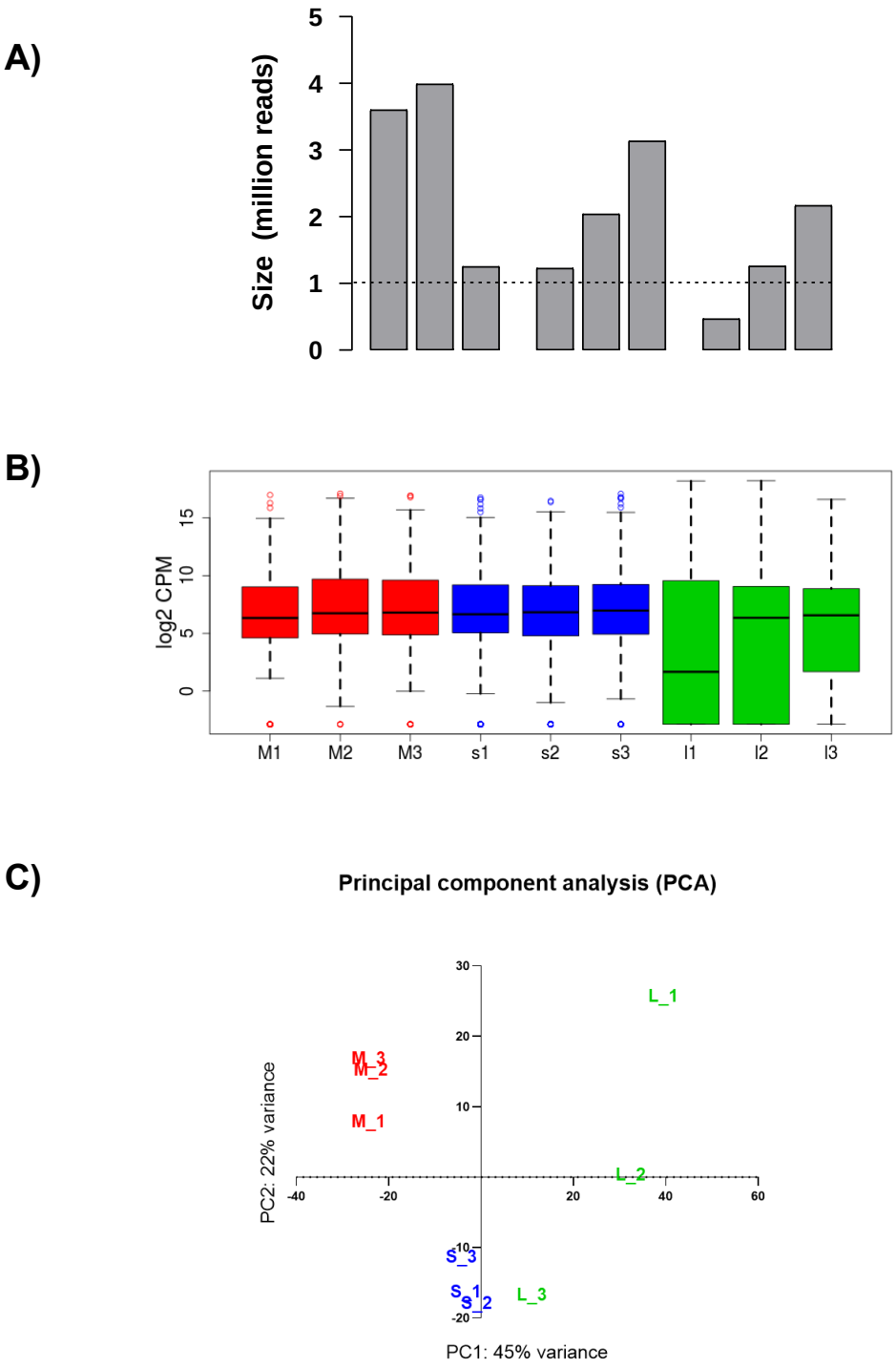

Figure 26. ***Plots summarising library depth, distribution of reads and variance between sources****. (**A**) Bar plot indicating depth of assigned reads in each library following Bowtie2 alignment. (**B**) Histogram comparing distribution of normalized samples (log2 count per million) across each library. (**C**) Principal component analysis (PCA) of log2 miRNA normalized counts visualizing variance between each sample library. A clear clustering of samples was observed, indicating strong variability in miRNA expression between preparations from different sources.*

Next generation sequencing analysis of the nine small RNA libraries derived from small and large EV, as well as whole donor MIO-M1 cells (N=3) yielded more than

101.2 million sequences (15-33 nt). After filtering, approximately 13.4, 29.6 and 18.1 million high-quality sequence reads from the whole cell, small EV and large EV libraries respectively, were available for reference genome alignment. The aligned miRNA-seq reads (mapped to miRBase (v22) using Bowtie2 -v2.2.2) were required to match the reference sequence perfectly, with one mismatch allowed in the first 32 bases of the read. In total, an average of 3.1, 2.1, and 1.3 million reads were aligned to miRNAs in libraries from the whole cell, small EV and large EV libraries respectively (table 1). One sample of large EV (EV_1) had comparatively low read depth ($4.7E^4$ assigned reads). To allow for direct comparison between samples, raw read counts were scaled by a sample-specific normalization factor reflecting individual sample depth, and expressed as log2 of counts per million (TMM) (fig. 26B). Normalized comparisons of read distribution indicated equivalence between whole cell and small EV samples, with more shallow and variable coverage in large EV libraries.

As an indicator of quality control, miRNA profiles from each of the nine libraries generated from the three different RNA sources were assessed for their correlation with biological reproducibility. Principal component analysis involves the linear transformation of a large data set, in this case the normalized miRNA expression counts, to a set of orthogonal components. The first principal component specifies the direction with the largest variability in the data, the second component is the direction with the second largest variation. The PCA plot indicated that both EV subtypes and cells displayed higher variance between the different sample groups than to their respective replicates, with significant clustering of biological replicates from the three different sample sources (fig 26:C). Whole cell libraries and those generated from small EV were tightly clustered, and distinct from each other. More variation was evident in the libraries derived from large EV RNA. Here, samples 1 and 2 were distinct from each other, as well as from the other two source clusters. Large EV sample 3 appeared closer in terms of variance to the cluster of small EV libraries than to the other large EV or whole cell samples.

A B

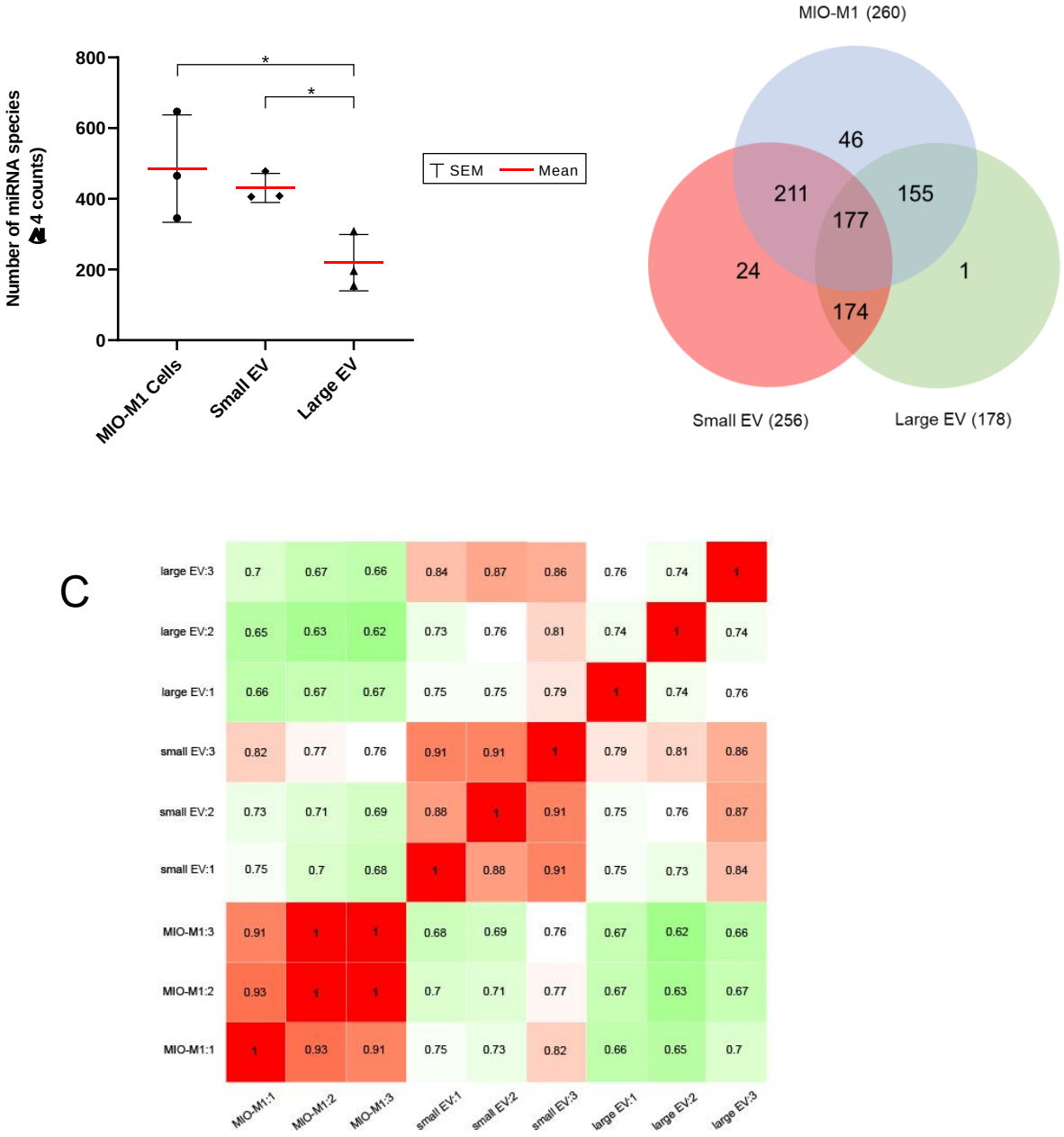

Figure 27. Summary of the number of miRNA species detected, and their overlap between libraries and relatedness between individual samples. *(A) Number of miRNA species detected with at least 5 reads mapped / million of the total library for each replicate. (B) Venn diagram showing number of unique and common miRNAs between different samples. To insure against false positive assignments, miRNA with read counts ≥5 CPM in at least 2 of the 3 biological replicates for each sample were considered true positives. (C) Correlation coefficient maps of the expression levels of miRNA species across each library.*

Alignment of pre-processed miRNA reads with the human miRNA database miRbase genome assembly GRCh38.p13, was conducted using Bowtie2. The

Sequencing of miRNAs in small EV samples yielded a mean of 430 ± 23.7 identified miRNA entries, a minimum read count cut off of 2 was used to ensure against false positive annotations (fig. 27A). This value was comparable to the number of positive assignments identified in whole cell libraries (485 ± 87.8 species). Large EV were found to contain significantly fewer miRNAs, and a more diverse range was detected between samples (223 ± 37.7).

Overlap of miRNA species detected was also compared between the EV and donor cell samples, and a minimum read count threshold was used to ensure against false-positive annotations (≥ 2 counts in at least three libraries) (fig. 27B). MIO-M1 libraries were found to contain 46 miRNAs only present in whole cells, whilst 24 unique assignments were detected in small EV samples, possibly indicating the loading of specific miRNAs into small EV. Notably, just one species was found to be unique to large EV. 177 miRNAs were found to be common between small, large, and whole cell samples. The two EV subsets shared 174 miRNA species. Collectively, this data suggests that the vesicle subsets may differ to a certain degree, but are also in positive correlation with regard to their miRNA cargo. Notably, small EV were assigned 23 miRNAs that were absent in the other samples, suggesting sorting of specific miRNAs. Large EV did not show a distinct miRNA distribution pattern per se, but were instead associated with a variable combination of the species detected in the whole cell and small EV libraries.

To gain more insight into possible disparities between miRNA distribution in cells versus EV, a correlation matrix was generated using the *cor* function in R to conduct a correlation coefficient test for association between the top 75% of miRNAs by expression level. The matrix depicted in fig. 27C indicates that whole cell samples were highly similar (r = ≥0.91), as were those isolated from small EV (r = 0.88 – 0.91). Large EV replicates had a much lower correlation coefficient (r = ≤0.76), and similar to the small EV samples (r = 0.73 – 0.87), than to each other. Large EV and whole cell libraries were the least alike (r = 0.62 – 0.7). Taken together, these data suggest that whilst small EV clearly represent a distinct subset of extracellular RNA population, large EV are more variable.

A heatmap was generated by first ranking miRNAs by standard deviation of log2 transformed counts across each of the samples (fig. 28). The data was centered by subtracting average expression for each species, and the average linkage was used. The heatmap allows for a general overview of the data, where green indicates comparatively low expression of a miRNA in a given library, and red where that miRNA was comparatively abundant. Of note are the blocks of abundant miRNAs in small EV samples (s_1,2,3) where expression is upregulated relative to the whole cells (M_1,2,2), as well as the large areas of low expression or absence in the large EV samples (l_1,23) in the columns to the left of the plot (fig. 28). Small EV and intracellular miRNA profiles within each cell type are clearly distinct, further supporting the hypothesis that the loading of EV cargo is an active and regulated mechanism rather than a passive process that merely reflects cellular content.

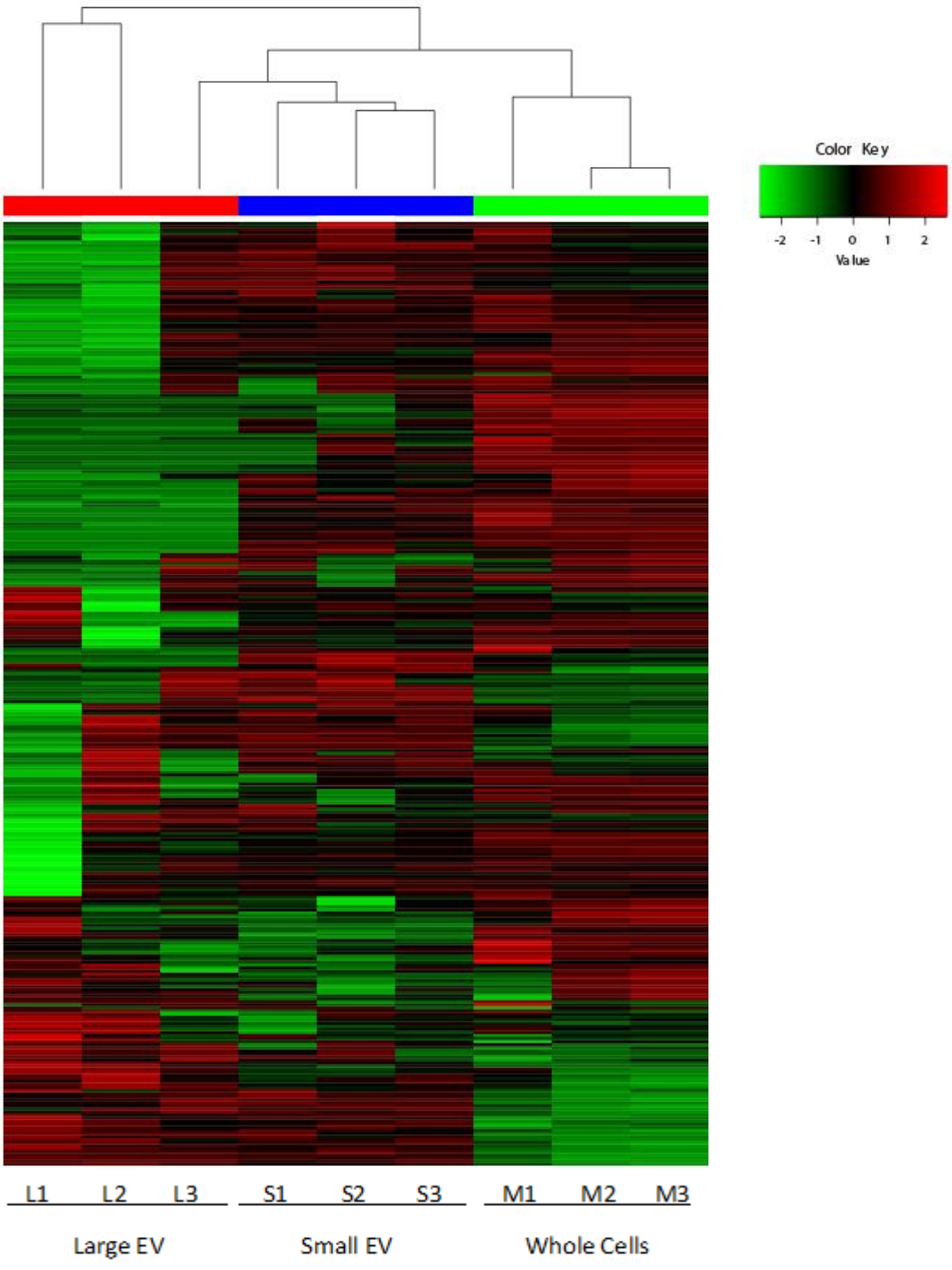

Figure 28. ***Hierarchical clustering heatmap displaying high variability in normalized level of expression of miRNA species between sample libraries.***

Differential enrichment of microRNAs when comparing whole cells and different EV samples

Differential expression (DE) analysis was conducted using the R software package DESeq2, and allowed identification of a quantity of miRNAs that were significantly enriched or depleted between samples of different origin. The data summarized by a histogram in figure 29 presents the log-fold change in relative abundance of microRNAs in pairwise comparisons between the different libraries. Positive values in red represent enriched transcripts, whilst negative fold changes in blue represent those relatively depleted.

In total, 40 miRNAs (~7%) were found to be differentially expressed in comparisons between small EV and donor MIO-M1 cells. 31 transcripts were specifically enriched in small EV, whilst analysis also identified 9 miRNAs that were significantly depleted in EV and consequently upregulated in whole cells (figs. 29, 30; A). Greater variability was detected between large EV and whole cells. A total of 120 transcripts (~22%) were found to be differentially expressed, of which 78 were significantly upregulated in cells and 42 in large vesicles (fig. 30; B). Interestingly, 26 of the 31 miRNA highly abundant in small EV when compared to cells, were also highly represented in large EV (fig. 27; B).

DESeq2 analysis also revealed 51 microRNA (~9%) differentially expressed in comparisons between small and large EV. Of these, the vast majority were found to be significantly enriched in small vesicles (49), whilst only two miRNAs (767-3p, 3656) were comparatively abundant in large vesicles (figs 29, 30; C). Together, the non-random distribution of miRNAs in Müller glia and EV derived from these cells is consistent with a sorting mechanism for disposal of “unused” small RNAs or for communication with the surrounding environment as shown in other cell types.

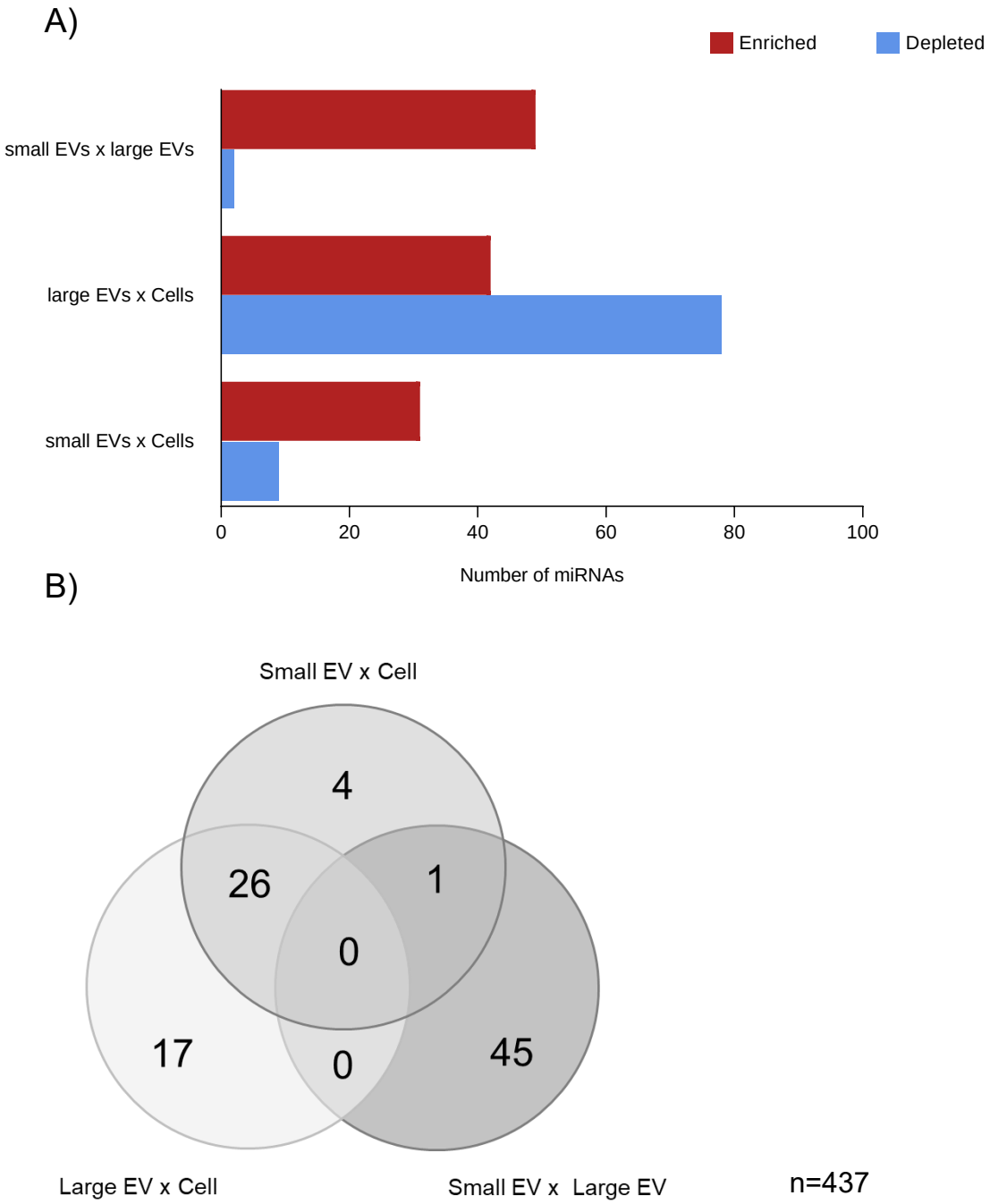

Figure 29. ***Summary of the results of DEseq2 differential enrichment analysis*** *(**A**) Histogram presenting the numbers of differentially enriched miRNA transcripts when comparing small EV, large EV, and whole cell sequencing libraries. (**B**) Venn diagram shows unique and shared miRNAs significantly enriched between the different preparations.*

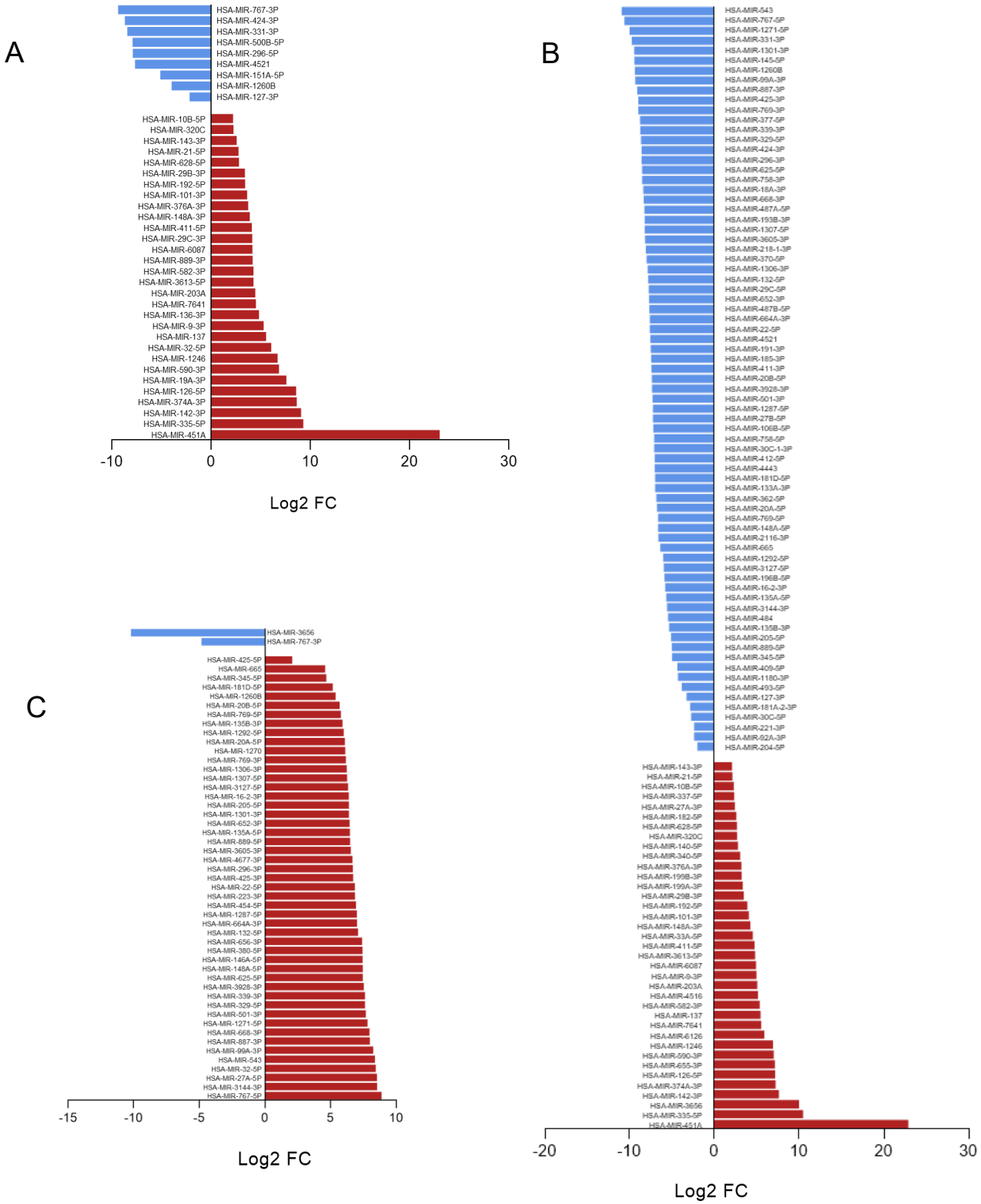

Figure 30. ***Identification of genes differentially expressed (DE) amongst preparations.*** *Histograms list the genes found differentially expressed by DEseq2 differential enrichment analysis. (**A**) 40 miRNAs DE in small EV and (**B**) 120 miRNAs DE in large EV compared with whole cell samples. (**C**) 51 miRNAs DE in small EV compared to large EV libraries (fold change ≥ 2 / ≤ -2 and FDR P-values < 0.01).*

KEGG pathways enriched by small EV microRNA	p-value	genes	miRNAs	KEGG pathways enriched by whole cell microRNA	p-value	genes	miRNAs
ECM-receptor interaction (hsa04512)	1.93E-20	49	23	**Lysine degradation (hsa00310)**	4.97E-07	22	13
FoxO signaling pathway (hsa04068)	3.64E-06	85	27	**GABAergic synapse (hsa04727)**	2.76E-04	27	8
Hippo signaling pathway (hsa04390)	1.41E-05	85	29	2-Oxocarboxylic acid metabolism (hsa01210)	5.74E-04	8	6
Focal adhesion (hsa04510)	1.41E-05	125	28	Glutamatergic synapse (hsa04724)	5.74E-04	40	11
TGF-beta signaling pathway (hsa04350)	7.46E-05	51	25	**Glycosaminoglycan biosynthesis - heparan sulfate / heparin (hsa00534)**	5.93E-04	11	7
Ras signaling pathway (hsa04014)	2.86E-04	123	28	Axon guidance (hsa04360)	1.58E-03	42	12
Rap1 signaling pathway (hsa04015)	5.12E-04	183	28	**Hippo signaling pathway (hsa04390)**	1.70E-03	45	13
PI3K-Akt signaling pathway (hsa04151)	5.12E-04	118	29	**ErbB signaling pathway (hsa04012)**	2.02E-03	33	11
Adherens junction (hsa04520)	7.30E-04	48	23	**Signaling pathways regulating pluripotency of stem cells (hsa04550)**	5.46E-03	44	11
Phosphatidylinositol signaling system (hsa04070)	1.11E-03	47	25	Gap junction (hsa04540)	8.37E-03	30	11
Signaling pathways regulating pluripotency of stem cells (hsa04550)	1.42E-03	79	28	MAPK signaling pathway (hsa04010)	8.37E-03	81	13
mTOR signaling pathway (hsa04150)	4.27E-03	70	25	**Cell adhesion molecules (CAMs) (hsa04514)**	8.47E-03	39	12
Axon guidance (hsa04360)	4.27E-03	40	26	Wnt signaling pathway (hsa04310)	9.49E-03	46	13
Endocytosis (hsa04144)	5.29E-03	108	27	**FoxO signaling pathway (hsa04068)**	1.13E-02	47	8
GABAergic synapse (hsa04727)	9.06E-03	50	25	Endocytosis (hsa04144)	1.25E-02	60	13
Neurotrophin signaling pathway (hsa04722)	1.02E-02	70	29	TGF-beta signaling pathway (hsa04350)	1.25E-02	30	11
cAMP signaling pathway (hsa04024)	1.12E-02	107	27	Regulation of actin cytoskeleton (hsa04810)	1.67E-02	66	10
Long-term potentiation (hsa04720)	1.25E-02	42	26	Adherens junction (hsa04520)	1.74E-02	25	10
Glutamatergic synapse (hsa04724)	1.55E-02	63	26	Long-term depression (hsa04730)	1.79E-02	18	11
Lysine degradation (hsa00310)	2.21E-02	24	23	mTOR signaling pathway (hsa04150)	1.79E-02	24	10
ErbB signaling pathway (hsa04012)	2.22E-02	53	26	Neurotrophin signaling pathway (hsa04722)	2.12E-02	41	14
Glycosaminoglycan biosynthesis - heparan sulfate / heparin (hsa00534)	3.00E-02	14	11	Estrogen signaling pathway (hsa04915)	2.15E-02	32	12
Tight junction (hsa04530)	3.50E-02	76	27	Retrograde endocannabinoid signaling (hsa04723)	3.08E-02	33	12
Estrogen signaling pathway (hsa04915)	3.50E-02	53	27	cGMP-PKG signaling pathway (hsa04022)	4.06E-02	51	12
MAPK signaling pathway (hsa04010)	4.57E-02	129	30				

Table 2. ***Biological pathways enriched by differentially regulated microRNAs in small EV and whole cell samples****. KEGG pathways ranked by order of significance. Unique annotations are highlighted in bold. Gene targets were predicted by Tarbase, FDR-corrected P value <0.05.*

Differentially enriched miRNA present in small EV and Müller glia cells target genes are involved in nervous system functional processes and stem cell potency

To better understand the functions of up and down-regulated genes revealed by DE analysis of miRNAs enriched in small EV and whole cells, in silico investigations were conducted to predict Kyoto Encyclopaedia of Genes and Genomes (KEGG) pathways significantly regulated by miRNAs. The DIANA miRPath, a powerful tool for analysis of the combinational effects of miRNA gene silencing on signalling pathways was used for this study. Pathway

predictions were made using experimentally validated and computationally predicted gene targets of relevant miRNAs, and filtered to remove those associated with functions not related to the eye or nervous system (table 2). In total, the 31 miRNAs enriched in small EV samples had 1892 predicted gene targets in 25 significantly regulated biological pathways, whilst the 9 miRNAs comparatively enriched in whole cell samples had 982 gene targets in 24 significant pathways (FDR-corrected P <0.05).

Identification of significant pathways shared between miRNAs present in whole cells and small EV revealed an insight into key processes regulated by Muller glia. Interestingly, the genes targeted by miRNA in both groups were associated with pathways relating to nervous tissue maintenance: glutamatergic synapse, GABAergic synapse, and axon guidance, as well as non-specific cellular processes like endocytosis, adherens junction, and lysine degradation. Shared pathways also included those relating to secreted growth factors including neurotrophin signalling, TGF-β, and ErbB, as well as the intrinsic growth pathways mTOR, and MAPK. Several of the shared pathways related to tissue development and maintenance of stem cell pluripotency (Hippo signalling, FoxO signalling), whilst Wnt signalling was uniquely associated with enriched whole cell miRNA.

Small EV miRNA targets were most significantly associated with ECM-receptor interactions. Interestingly, small EV miRNA but not whole cell microRNA were significantly associated with the cell growth pathways PI3K/AKT (p = 5.12E-4), Rap1 (p = 5.30E-4), and Ras1 (p = 2.86E-4), as well as cAMP signalling (1.12E-2). Small EV libraries were also comparatively enriched in miRNA targeting genes in nerve growth-related pathways including axon guidance (p = 4.27E-3), neurotrophin signalling (p = 1.02E-2), mTOR (p = 4.27E-3), MAPK (p = 4.57E-2), and TGF-B (7.46E-5).

The most significant pathway interactions predicted for whole cell enriched miRNA targets were for cellular processes, including Lysine degradation (p =

4.97E-7), GABAergic synapse (p = 2.76E-4), 2-Oxocarboxylic acid metabolism (5.74E-4), and Glutamergic synapse (p = 5.74E-4). Muller glia cell-only enriched miRNAs also targeted pathways associated with nervous system processes such as retrograde endocannabinoid signalling (p = 3.08E-2), and long term depression (p = 1.79E-2), and regulation of actin cytoskeleton (p = 1.67E-2), as well as cell adhesion molecules (p = 8.47E-3).

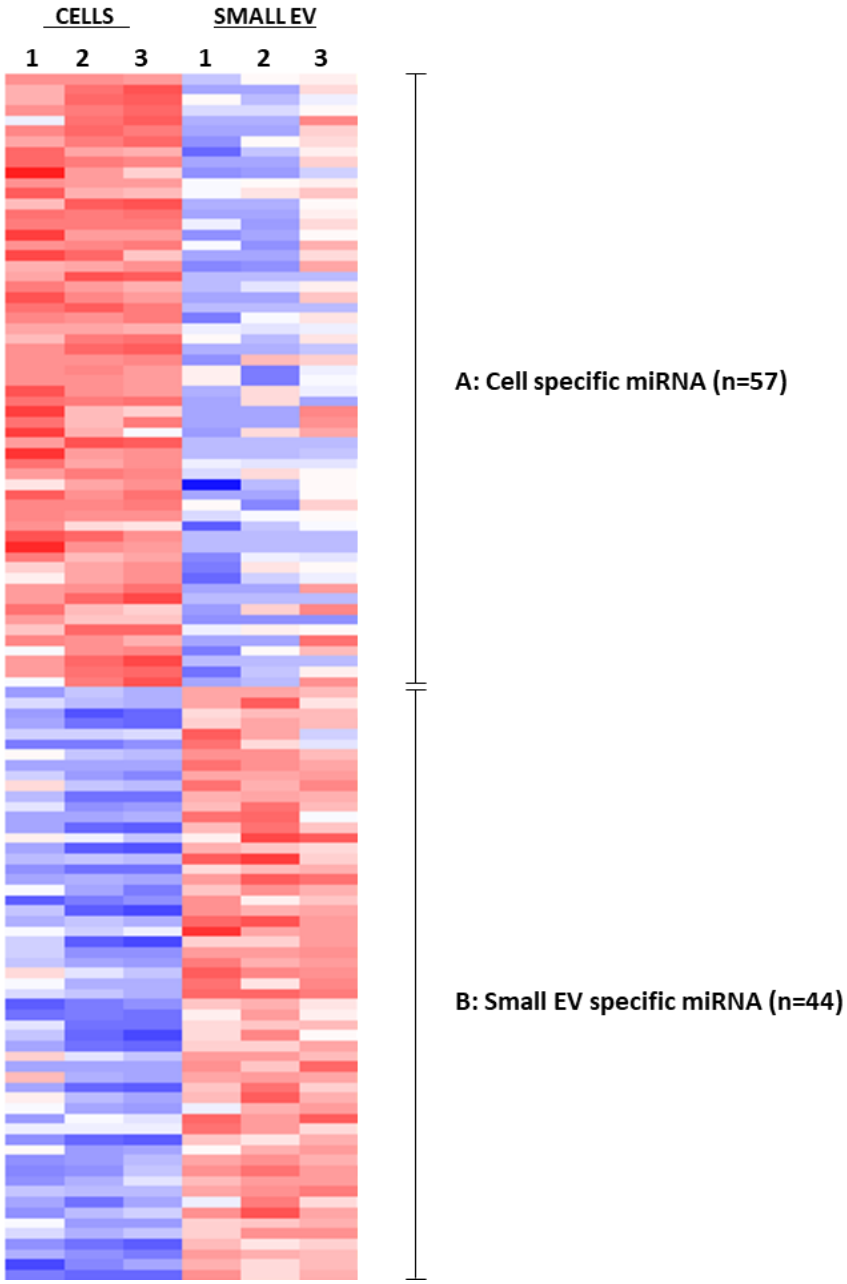

Figure 31. ***K-means clustering of miRNA transcript expression.*** *A cluster of 57 miRNAs abundant in donor cells compared to small EV were identified (**A**), as were a cluster of 44 enriched in small EV compared to donor cells (**B**).*

K-means clustering identifies a large set of small EV-abundant microRNA for functional enrichment analysis

Next, unsupervised K-means clustering was performed on the sequencing dataset with the intention of identifying more microRNA highly abundant in small EV that may contribute towards the neuroprotective secretions attributed to Müller glia cells in whole-cell transplantation studies.

K-means clustering fits microRNA into defined groups based upon expression pattern across all three sample sources. microRNA were first ranked by standard deviation of expression, and the top 200 most variable were selected, before separation into four clearly defined clusters. 44 small-EV specific microRNA were identified that were highly abundant in small EV but under-represented in cells, as well as 57 transcripts enriched in cells but lacking in small and large vesicles (fig. 31). Each of these groups also contained the miRNAs previously identified by DE analysis respectively.

To assess the potential functional impact of the miRNAs most abundant in secreted vesicles, the subset of 44 small EV-enriched microRNA identified by K-means clustering underwent *in silico* analysis by Ingenuity Pathway Analysis (IPA) software (version 8.8, Ingenuity Systems, Redwood City, CA, USA) using the microRNA filter and Core Analysis features. A total of 33 pathways were predicted to be significantly regulated by the miRNA enriched in Müller-secreted vesicles, following filtering to remove those associated with a specific disease, or functions not relating to the eye or central nervous system. Interestingly, 15 of these (45%) related to signalling pathways, including those regulating cell growth and survival (fig. 32; A).

Amongst the most highly modulated pathways were PI3K-AKT (hsa04151), Ras (hsa04014), Rap1 (hsa04015), MAPK signaling (hsa04010), as well as regulation of actin cytoskeleton (hsa04810), and focal adhesion (hsa04510). Comparatively fewer interactions were predicted for pathways involved with cellular processes

like Fatty acid biosynthesis (hsa00061), Glycosaminoglycan biosynthesis (hsa00534), Fatty acid metabolism (hsa01212), lysine degradation (hsa00310), and N-glycan biosythnesis (hsa00510). All of the miRNA investigated had significant numbers of gene targets predicted within the pathways listed. In particular, miR-137, miR-182-5p, miR-27a-3p, miR-30e-5p, miR-340-5p, and miR-590-3p had >400 predicted interactions.

Gene targets predicted for the set of 44 small EV-enriched microRNAs were subjected to GO biological process enrichment analysis using the IPA microRNA target filter (fig. 32, B). The analysis returned a number of biological processes predicted to be regulated by Müller glia-abundant microRNAs, the most highly enriched of which were “Signal transduction” (24.8%), “Cell communication” (23.1%), “Regulation of nucleic acid metabolism” (18.35%), and “Transport” (7.92%). Of particular relevance given the neuroprotective action of Müller glia signalling, 6.54% of the genes targeted by miRNA were associated with “Cell growth and/or maintenance” processes, and 1.56% with “Apoptosis”.

Given the significance of PI3K/AKT pathway enrichment interactions predicted for small EV-abundant microRNAs, an *in silico* analysis was conducted in order to identify potential mechanisms for neuroprotection related to the modulation of PI3K-associated genes. IPA software was used to generate a network of experimentally observed microRNA interactions within the pathway (fig. 33, B), and it was observed that the master inhibitor ‘Phosphatase and tensin homolog’ (PTEN) was the target of several of the most abundant microRNA transcripts identified in small EV libraries: miR-21-5p, miR-148a-3p, miR-221-3p, and miR-29b-3p.

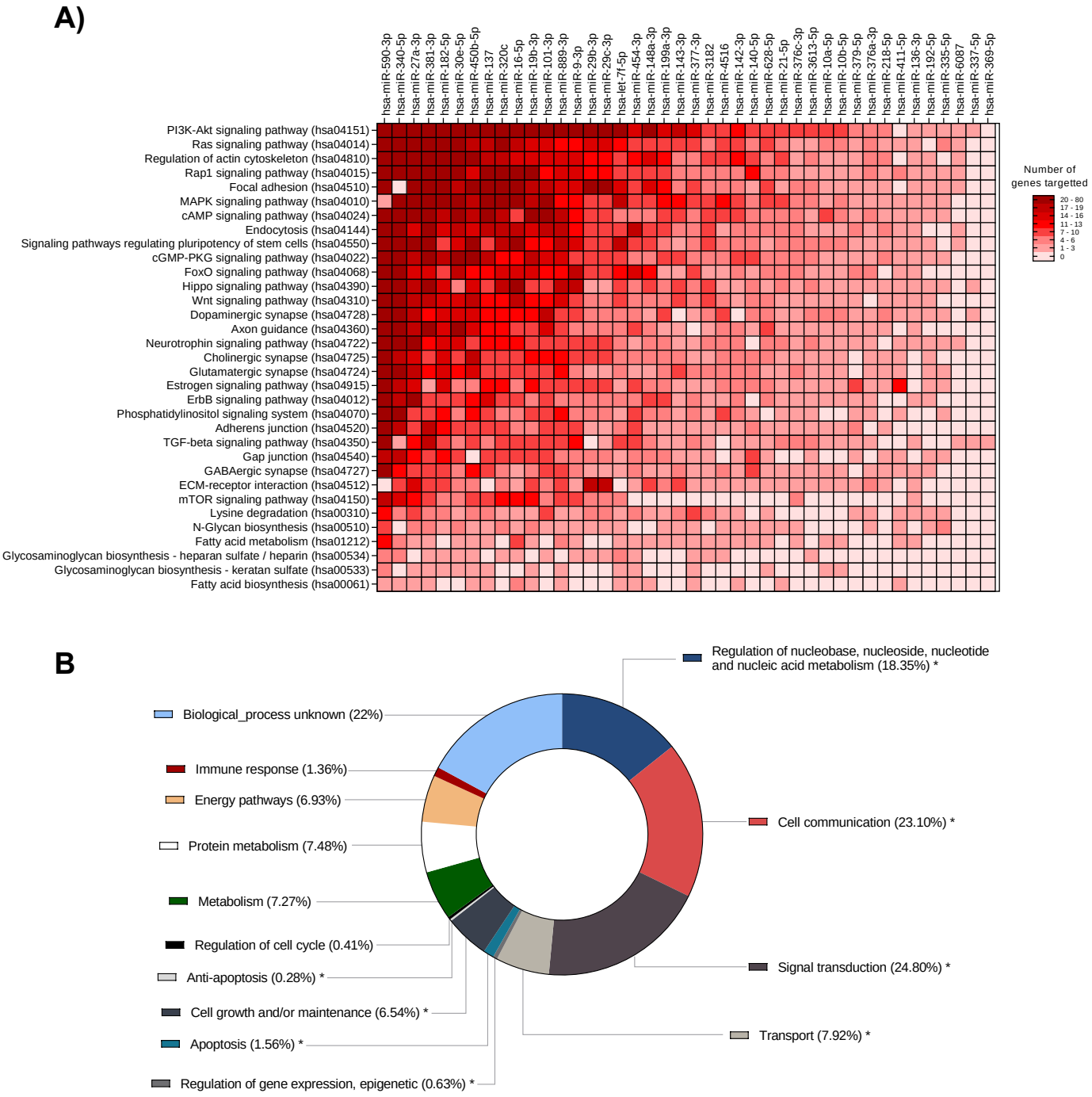

Figure 32. ***IPA functional analysis of small EV-enriched microRNAs.*** *(**A**) Pathway annotation heatmap presenting significant pathways on the Y-axis (p<0.05), and small EV-enriched miRNAs on the X-axis. The color code represents the number of experimentally observed gene targets. (**B**) Pie chart presenting results of GO Biological process enrichment analysis. The most significantly enriched processes are shown, with the associated percentage of total microRNA gene interactions. Processes marked * were determined statistically significant by hypergeometric testing (p = < 0.05).*

A

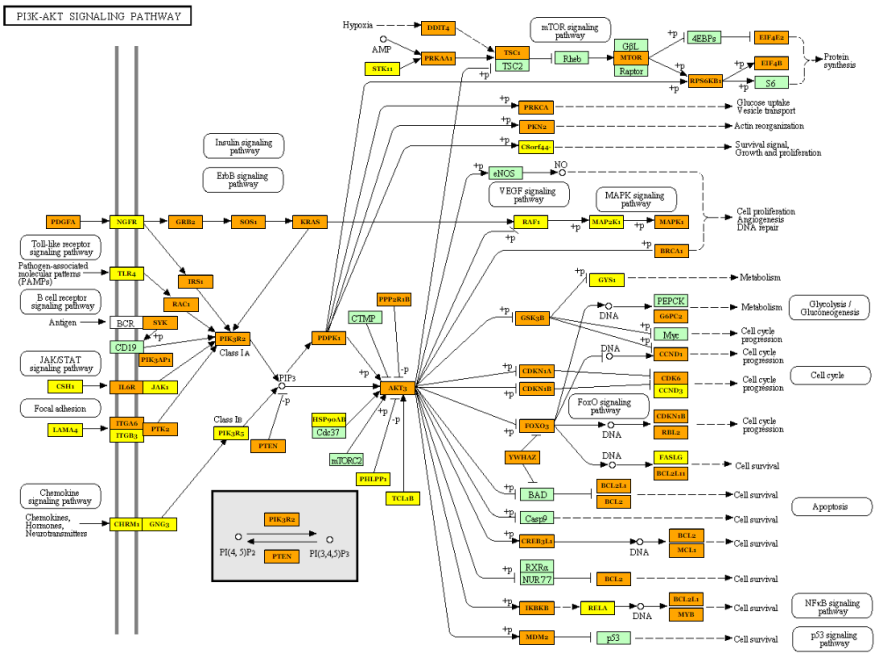

B

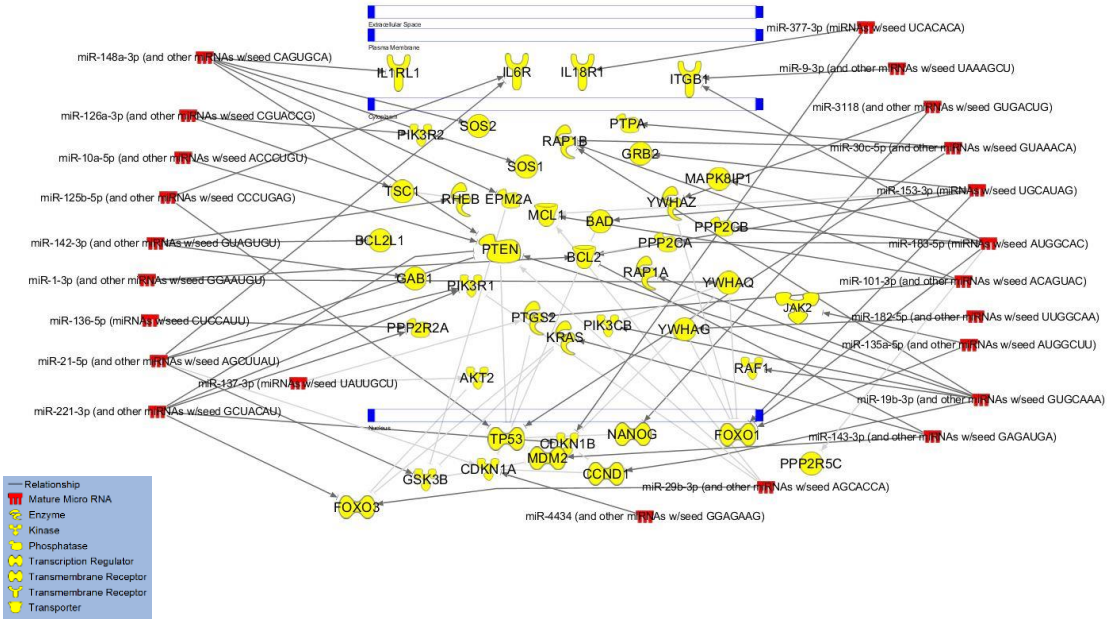

Figure 33. ***small EV-enriched microRNAs in the PI3k/AKT pathway****. (**A**) KEGG diagram of the PI3K/AKT signalling pathway (hsa04151), genes in yellow have predicted interactions with one miRNA and those in orange with more than one. (**B**) miRNA network generated by IPA. Schematic diagram displaying 23 miRNAs abundant in small EV and their experimentally observed targets within the PI3K / AKT intrinsic growth pathway. In red are mature microRNAs, in yellow are gene targets.*

Real-time quantitative PCR validated the presence of PTEN-targeting microRNA transcripts in Müller glia EV

Four miRNA of interest were. Three PTEN-targeting microRNA abundant in small EV were selected for validation by real-time quantitative PCR (qPCR), miR-21-5p, miR-29b-5p and miR-10a-5p. In addition, one miRNA predicted to be differentially depleted in sEV compared to whole cells, miR-767-3p, was also included (fig. 34). For purposes of comparison, RNA samples recovered from small EV released by Müller glia that had been differentiated from stem cell retinal organoids in the lab were also included (referred to here as PSC1). All four of the validation set were found to be robustly expressed in small EV from both of the Müller glia cell cultures investigated, as well as in the donor cells themselves (fig. 34; A, and supplementary table 5).

When normalised to the detection of an internal spike-in sequence (cel-miR-39), miR-21-5p was found to be specifically abundant in MIO-M1 small EV compared to whole cells (FC = 2.47), as was miR-29b-5p (FC = 2.78), findings that are in agreement with the results of DEseq2 analysis previously reported in this thesis (table 6). Similarly, miR-767-3p was found to be depleted in MIO-M1 EV compared to whole cells, although to a lesser extent than predicted (FC = -4.93). Interestingly, miR-767-3p was not found to be significantly downregulated in EV derived from PSC1 cells (FC = 0.29). Neither of the Müller derived EV were found to be differentially enriched in miR-10a-5p compared to donor cells.

miRNA	Fold change predicted (DEseq2)	Fold change observed (2^-ΔΔCt)
hsa-miR-21-5p	2.78	2.47
has-miR-29b-5p	3.40	2.78
has-miR-10a-5p	1.70	-1.46
has-miR-767-3p	-9.37	-4.93

Table 3. ***Comparing differential log2 fold changes in expression predicted by miRNA sequencing and DEseq2 analysis with data observed from qPCR validation experiments.***

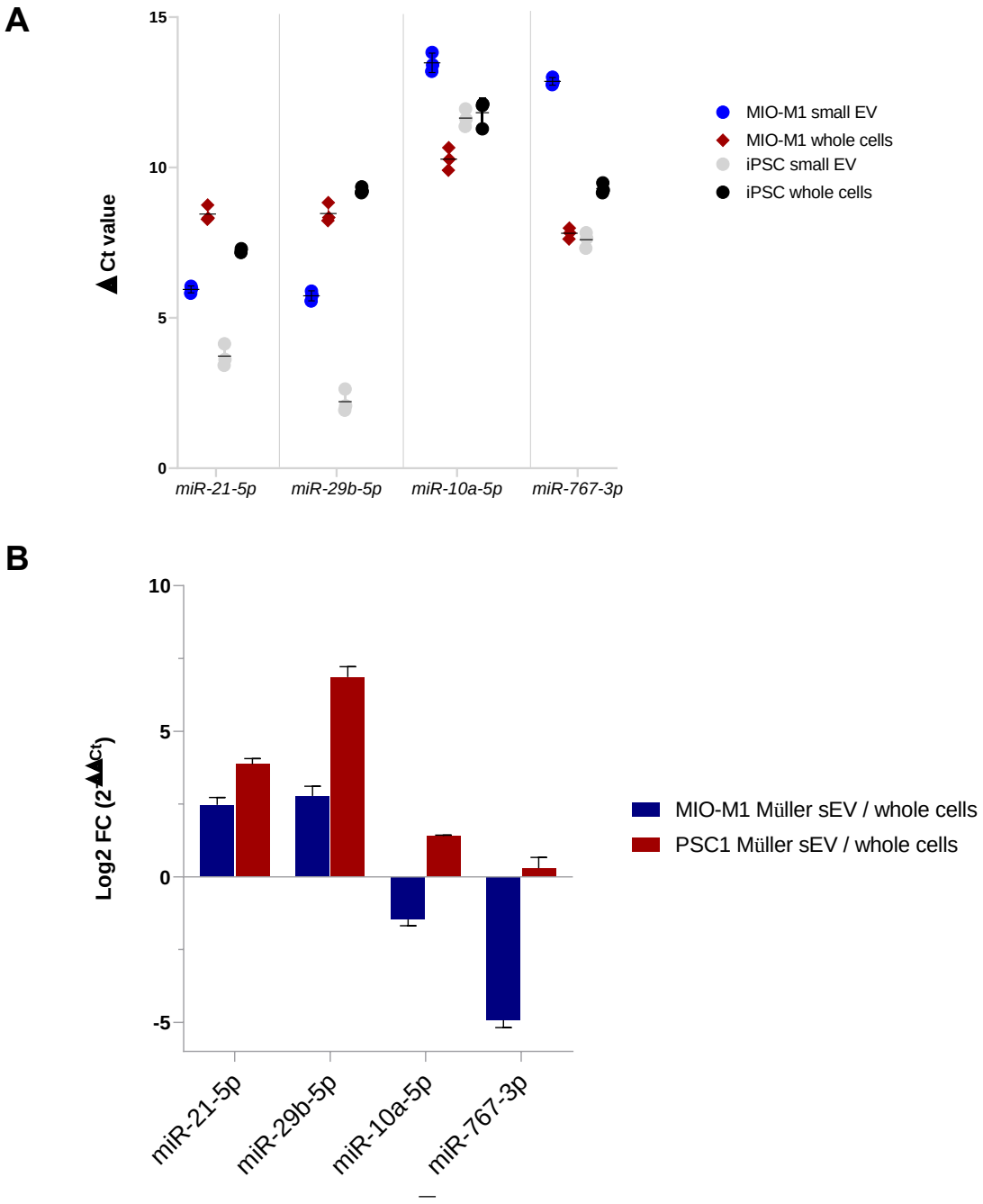

Figure 34. ***Validation of miRNA expression by real-time PCR.*** *(**A**) The relative expression of miR-21-5p, miR-29b-5p, miR-10a-5p, and miR-767-3p compared to an internal spike-in control sequence (cel-miR-39). For purposes of comparison, small EV refined from Muller glia cultures differentiated from stem-cell retinal organoids in the lab (PSC1) were also included in the experiment. One numeric difference in ΔCt represents a 2-fold difference in miRNA quantity detected, and each point represents the mean of three technical replicates. (**B**) The relative difference in expression of the validated miRNAs between EV and donor cells, data represent mean ± SEM normalized to cel-miR-39 control by the ΔΔC t method (n = 3).*

Discussion

Müller glia EV are abundant in microRNA transcripts

This study investigated the expression profile of EV derived from Müller glia cells *in vitro,* to get insight into an under-appreciated mechanism of cell communication and investigate variations in the microRNA content between EV subtypes. High-throughput next generation sequencing and an integrative bioinformatics pipeline (fig.24), allowed for the profiling of microRNAs present in populations of small and large extracellular vesicles isolated from Müller glia cell culture supernatants, as well as those present within donor cells. *In silico* analysis revealed significant differential enrichment of transcripts between sample sources, and miRNA:mRNA target-prediction software suggested the modulation of biological pathways and processes associated with cell growth and survival signalling pathways. miRNAs of interest were validated by quantitative PCR, where an exogenous miRNA spike-in (cel-miR-39) was used as internal control. Together this data suggest a potential mechanism of action for the known neuroprotective effects of Müller cells. These observations may contribute towards the development of regenerative strategies using EV to overcome the potential complications of cell-based therapy.

89.5% percent of the total number of raw reads generated by Illumina sequencing successfully aligned to the miRbase index of human mature transcripts. Despite this work focusing on miRNA molecules, fragmented mRNA and short non-coding species such as t-RNA and y-RNA have also been reported in EV and can also be captured by the cDNA library preparation (Nolte-'t Hoen, Buermans et al. 2012). This data confirms that Müller glia-derived EV are abundant in mature microRNA molecules, deepening the literature with regard to the encapsulation of these molecules as first described by Valadi and colleagues, as well as in more recent publications (Valadi, Ekström et al. 2007, Chiba, Kimura et al. 2012, Eirin, Riester et al. 2014).

Despite numerous reports of miRNA internalisation within EV and transfer to neighbouring cells in various experimental settings, whether or not this exchange occurs in functionally significant quantities *in situ* to illicit response in a physiological context is far from proven (Skog, Würdinger et al. 2008, Mittelbrunn, Gutiérrez-Vázquez et al. 2011). Thus far, plausible and convincing evidence for a physiological role of miRNA encapsulated within EV is yet to emerge, and it is possible that some of the responses attributed to miRNA may depend on a different functional cargo, or even ligand-binding interactions stimulated by proteins present on EV membranes during endocytosis (Shelke, Yin et al. 2019). This is suggested by a recent investigation showing that a stoichiometry of less than one miRNA molecule per vesicle was present in five diverse cellular sources, although a comparatively small number of highly-enriched vesicles could account for a relatively large proportion of the total miRNA yield. (Chevillet, Kang et al. 2014). New strategies for identifying, characterising, and purifying these disproportionately enriched EV – perhaps by specific membrane markers or protein components - would greatly reduce experimental noise and provide insight into mechanisms of miRNA sorting.

Variation in number of miRNA species detected between EV and whole cell libraries

Sequencing of microRNAs revealed a significant difference between the number of species identified in small and large vesicle populations. Large EV libraries also had lower inter-sample correlation than small and whole cells, and PCA indicated replicates failed to cluster. The large EV preparations used in this study had a mean diameter of 312 nm (±7) which is significantly larger than that typically described for endosome-derived exosomes (30 – 150 nm) (Johnstone, Adam et al. 1987). Despite this, a small but not-insignificant quantity of smaller particles co-segregated with the large EV, as seen by nano-particle tracking analysis and western blot assays probing for endosomal markers (Figs. 19, 20). Approximately equivalent quantities of RNA were recovered from large and small vesicle preparations and both were enriched in small non-coding species, but only large EV contained traces of rRNA subunits and longer coding transcripts. Also of

interest are the analyses of differential microRNA abundance between the vesicle subtypes, which revealed many more (49) transcripts comparatively enriched in small EV than in the large EV libraries (2). It is also significant that when each was compared to whole cells, the vast majority (87%) of the small EV-enriched miRNAs, were also enriched in large EV (fig. 29). Together, this evidence is suggestive of a model where variable quantities of small EV contamination in large EV purifications contribute to the majority of the miRNA species present in these samples, which would account for their variable expression profile and limited abundance.

Sparse evidence suggests that plasma membrane shed vesicles are enriched in microRNA (Hunter, Ismail et al. 2008, Muralidharan-Chari, Clancy et al. 2009, Lv, Cao et al. 2013). Due to a lack of consensus in the literature with regard to nomenclature of vesicle subtypes and methods for their purification however, care must be taken when interpreting these findings in relation to previously published work. In particular the term “microvesicle”, which is generally used to describe “large” cell membrane-shed vesicles, has previously been used as a catch-all term for all membrane vesicles as well as to describe endosome-derived exosomes (Hunter, Ismail et al. 2008, Waldenström, Gennebäck et al. 2012). Comparisons can be made, however, with studies that have purified EV subsets using an equivalent methodology; i.e. centrifugal sedimentation at 10’000 – 20’000 x g. The results of these experiments are comparable to those reported by Lunavat and colleagues (2015) who used small RNA sequencing to attempt to differentiate between vesicle subsets isolated by differential centrifugation from melanoma cells. In this study, particles sedimented at 16’00 x g also contained ribosomal RNA subunits, but failed to reveal a distinct miRNA distribution pattern when compared to small EV precipitated at 120,000 x g or whole donor cells (Lunavat, Cheng et al. 2015). Interestingly the same study reported significant overlap with regard to miRNA expression between microvesicles and apoptotic bodies (collected at 2,000 x g) as well as whole cells (Lunavat, Cheng et al. 2015).

Distinct miRNA profiles have been reported in EV subtypes purified from culture supernatants of immortalized mesenchymal stem cells by density-gradient centrifugation. In agreement with the findings reported here, large vesicles

collected at 10,000 x g, as well as small vesicles of low-density were found to contain trace rRNA subunits, whilst exosomes collected from a higher-density fraction did not (Willms, Johansson et al. 2016). Interestingly, these small vesicle subpopulations showed significantly varied differential gene enrichment when incubated with H5V endothelial cells for 24 h, whilst the larger microvesicles did not, implying the absence of a functional cargo (Willms, Johansson et al. 2016). Since convincing evidence for a specific mechanism of miRNA sorting into large membrane-shed vesicles is yet to emerge, the data reported for this thesis strongly suggest that the modest quantities of miRNA transcripts detected in these organelles may be randomly encapsulated cytoplasmic molecules, captured during the blebbing process.

A subset of microRNAs are specifically abundant in extracellular vesicles compared to whole donor cells

Differential expression analysis was conducted using Deseq2 in order to identify miRNA present in the various libraries at higher abundance than would be expected due to random assortment (Love, Anders et al. 2014). Comparisons between small EV and whole cell miRNAs revealed that approximately 7% were differentially enriched, with 31 significantly abundant, and 9 significantly depleted. The relative enrichment and depletion of select miRNA species in small EV compared to whole cells was subsequently validated by quantitative PCR (fig. 34). These findings largely contribute to the body of literature suggesting that certain miRNA species are preferentially sorted into EV, although the precise process is unclear. Several potential mechanisms for sorting have been suggested, including the importance of certain short motifs in miRNA sequences that may bind preferentially to proteins involved in the formation and packaging of exosomes (Stoorvogel 2015).

A multiple alignment analysis study on the mature sequences of 30 miRNAs significantly enriched in T-cell exosomes, identified the presence of a four nucleotide motif ‘GGAG’ in the 3′ half of the miRNA sequence in 75% of

transcripts (Villarroya-Beltri, Gutiérrez-Vázquez et al. 2013). Interestingly, targeted-mutagenesis of the motif dramatically reduced the expression of miR-601 in T-cell exosomes, whilst the opposite was true of cell-enriched miR-17 following addition of the same sequence, suggesting that it's presence plays a key role in the sorting of specific miRNA into EV. In an attempt to see if the same motif identified by Villarroya-Beltri and colleagues was similarly associated with the 30 species found here to be significantly abundant in Müller glia small EV compared to cells, an alignment was performed using the MEME suite motif alignment & search tool (Bailey, Johnson et al. 2015). Surprisingly, no incidences of the GGAG motif were observed, suggesting that a separate mechanism may be controlling the sorting of miRNA in Müller cells to that in T-cells. The same alignment did, however, detect the presence of a different motif, 'CUGA', in 33% of the DE small EV microRNAs. In order to see if it was similarly prevalent in a larger set of small EV-abundant transcripts, a second alignment was performed on the set of 42 miRNA previously identified by K-means clustering. Among these, the CUGA motif was present in 25% of sequences, compared to just 5% of the 57 cell-abundant microRNA, and 9% of a control set of 500 miRNA downloaded from the miRBase index (Kozomara, Birgaoanu et al. 2019). Experiments measuring the comparative prevalence of miRNA containing this motif in EV before and after targeted mutagenesis and disruption, would allow insight into its putative role in miRNA sorting. Without this data, the significance of the 'CUGA' motif can only be a matter for speculation. It is possible that its presence within a sequence increases the likelihood of the miRNA becoming enriched in Müller glia-derived vesicles, through some as-yet undetermined interaction with ESCRT-related proteins.

Whilst there is evidence to suggest that certain miRNAs are specifically loaded into EV to facilitate extracellular processes (Becker, Thakur et al. 2016), a second school of thought postulates that EV may be a convenient carrier to purge redundant or inhibitory RNAs from cells. Support for this theory is provided by reports that miRNAs from the let-7 family were found within EV secreted by the metastatic gastric cancer cell line AZ-P7a, but not from less metastatic cell lines (Ohshima, Inoue et al. 2010). Because let-7 miRNAs are considered tumour-

suppressive, their elimination from metastatic cells may aid in maintaining their oncogenic and invasive properties. The two hypotheses are not mutually exclusive and may coexist within a cell, as recently suggested by the demonstration that the quantity of target transcript in endothelial cells modulated the availability of miRNAs for EV secretion by macrophages, and this in turn dictated which miRNAs were transferred to repress transcripts in recipient cells (Squadrito, Baer et al. 2014).

Small EV-abundant miRNA specifically target cell growth and survival pathways

In the present study, DIANA-mirPath was utilized in order to compare the predicted role of microRNAs enriched in small EV and lacking in whole cells, and vice versa. Interestingly, whole-cell enriched and small vesicle-depleted miRNA were found to target genes associated with basic cellular processes, including 2-Oxocarboxylic acid metabolism, actin cytoskeleton regulation, gap junction maintenance, and processes involving genes relevant to Müller glia function *in situ.* For example, multiple whole cell-enriched miRNA had targets predicted for the neural cell adhesion molecule protein (NCAM2) expressed on post- and pre-synaptic neurons and axon growth cones, which is also known to be enriched in Müller glial processes in the outer nuclear layer of adult zebrafish and chick retina (Drazba and Lemmon 1990, Kustermann, Hildebrandt et al. 2010).

The Müller glia cell line MIO-M1 isolated from adult retina, have numerous stem cell-like characteristics, which appear to be regulated through activation of the Wnt and Notch developmental signalling pathways. It is noteworthy, therefore, that the Wnt pathway was also predicted to be significantly modulated by the microRNA enriched in whole cells, as were genes in other processes associated with organ development and growth, including FoxO and Hippo. The miRNA identified also had interactions predicted with pathways associated with stem-cell pluripotency, tissue growth and development. These included MAPK, mTOR, and TGF-β signalling. Because the Müller glia cells used in this study are in fact a spontaneously immortalized cell line, it is difficult to ascertain whether the

presence of these miRNA relates to their innate stem cell-like characteristics or is instead an aspect of their capacity for unlimited self-renewal.

Although a full comparison between the miRNA transcriptome of primary Müller glia and those of the MIO-M1 immortalized cell line used in these experiments is beyond the scope of this study, it is of note that many of the transcripts found to be abundant in whole cell libraries have also been identified as important regulators of Müller cell functions *in vivo.* Müller cells generate retinal progenitor like cells after injury in teleost fish species, and a recent study conducted on primary zebrafish cells suggest that various let-7 microRNAs highly expressed in these cells are required to maintain a differentiated state in quiescent adult tissue, where they inhibit translation of the pro-neural transcription factor Ascl1a (Ramachandran, Fausett et al. 2010). It is therefore of significance, that let-7s were the most abundant miRNA detected in MIO-M1 whole cells (see supplementary table 4).

Also relevant are miRNA enriched in Müller glia that are comparatively depleted in the retinal neurons that they support, as these may represent miRNA Müller "markers". In freshly isolated mammalian Müller cells, seven miRNAs fitting that expression profile were uncovered by a recent publication that aimed to compare the glia miRNA transcriptome *in vitro* and *in vivo* (Wohl and Reh 2016). Each of these were present in the MIO-M1 libraries sequenced, in particular miR-125–5p, miR-204, miR-9 and miR-23a were among the top 25 most abundant transcripts detected in whole cells, whilst miR-100 and miR-99a were particularly enriched in small EV (see supplementary table 4). Further evidence to support the role of Müller-specific miRNA can be derived from observations made after targeted knockout of Dicer1 protein, required for miRNA function in mice. Deletion of this protein leads to the formation of large glial aggregations and severe disruption of normal retinal architecture (Wohl, Jorstad et al. 2017). This phenotype could be partially rescued by the overexpression of miR-9, through modulation of proteoglycan Brevican expression (*Bcan*), further emphasizing the importance of this miRNA in mammalian Müller cells. Given the similarities in miRNA

transcriptome reported in this thesis, it can be speculated that despite their immortalized nature, the Müller cells used in this study retain the most important regulatory miRNA species required for their specialised functions in the retina in vivo.

miRNA present in whole cells and EV are Müller glia-specific

Despite differential enrichment of certain species, the majority of the most abundant and functionally relevant miRNA detected in Müller cells were also present in small and large EV (see supplementary table 4). Similarly, the DE of small-EV transcripts shared many predicted pathway interactions with those enriched in whole cells; including axon guidance, growth factor signalling, and stem cell pluripotency (see table 2). It can be suggested, therefore, that the miRNA profile of Müller EV is tissue specific. This observation is of significance in the context of identifying neuroprotective Müller-derived signals, and is supported by many previous studies including those conducted using tumour-associated macrophages, which were found to shuttle a profile of invasion-potentiating miRNAs into breast cancer cells (Yang, Chen et al. 2011). That the small EV miRNAs were predicted to target similar functions as those recovered from whole donor cells implies that extracellular miRNA may be a mechanism by which these cells communicate their functions in the wider retinal environment.

Meanwhile, the significant pathways uniquely associated with abundant microRNAs in small EV related predominantly to growth factor / ECM-receptor interactions, cell survival, growth, and proliferation including signal transduction pathways. In order to further examine the potential function of the miRNA cohort present in small EV, *in silico* biological process analysis was conducted on a larger set of abundant miRNA identified by K-means clustering (fig. 32; A). A total of 33 pathways were significantly enriched by the EV-abundant miRNA set, 15 of which (45%) related to signalling pathways, including those regulating cell growth and survival. Similarly, the significant biological processes returned by GO analysis included “Signal transduction”, “Cell communication”, and “Cell growth and/or maintenance” (fig. 32; B). Together this data suggested a potential

mechanism for extracellular neuroprotective signalling that involves modulation of key growth pathways in target cells.

The IPA microRNA target filter identified the PI3K/AKT pathways as the most highly regulated by small EV miRNA, and a network of experimentally observed microRNA:mRNA interactions was drawn (fig. 33, B). Here it was evident that the master inhibitor of the pathway 'Phosphatase and tensin homolog' (PTEN) was the target of several of the most abundant microRNA transcripts identified in small EV libraries: miR-21-5p, miR-148a-3p, miR-221-3p, and miR-29b-3p. The presence of PTEN-targeting miRNAs predicted to be enriched in small EV was validated by quantitative real-time PCR (fig. 34). In addition, the same miRNA were found to be enriched in small EV derived from Müller cells that had been isolated from pluripotent stem cell-derived retinal organoids in the lab, demonstrating that the release of these miRNA was not a feature unique to the immortalised cell line MIO-M1.

PTEN silencing as a putative mechanism of miRNA neuroprotection

PTEN is the critical antagonist of the PI3K/AKT/mTOR pathway. Growth factors activate phosphatidylinositol-3 kinase (PI3K) through receptor tyrosine kinase (RTK) binding to promote cell growth and survival. RTK stimulation leads to the recruitment and activation of PI3K which is responsible for the phosphorylation and activation of phosphatidylinositol-3,4,5-trisphosphate (PIP3) (Maehama and Dixon 1998). Unchecked, PIP3 recruits a number of proteins to the membrane through binding to pleckstrin homology domains, including the serine/threonine kinase AKT and 3-phosphoinositide-dependent kinase (PDK1) (fig. 33; A) (Downward 2004). Following activation, AKT can phosphorylate many target proteins, most notably glycogen synthase kinase 3 (GSK3), tuberous sclerosis 2 (TSC2), caspase 9 and PRAS40 (AKT1S1), which accounts for its wide spectrum of downstream effects in promoting cell proliferation, differentiation, apoptosis, angiogenesis and metabolism (Thorpe, Yuzugullu et al. 2015). Unsurprisingly, the core components of the PI3K/AKT/mTOR pathway are commonly

overactivated in various types of cancer, and are therefore the focus of many studies in the oncology field (Sabatini 2006, Thorpe, Yuzugullu et al. 2015).

In nervous tissue the PI3K/AKT/mTOR pathway is essential for the regulation of axon formation and extension during development, and in adulthood PI3K signalling has been demonstrated to be responsible for the regeneration of peripheral nerve axons via the induction of the transcription factor SMAD1 (Hur, Liu et al. 2013). Expression of constitutively active Akt in embryonic chick dorsal root ganglion cells increases axon branching, cell hypertrophy and growth cone expansion, while viral vector overexpression of Akt in the rat, promotes remarkable regrowth of lesioned dopaminergic axons in vivo (Grider, Park et al. 2009, Kim, Chen et al. 2011). It may be logical, therefore, that selective activation of the PI3K/AKT/mTOR pathway in the axons of RGCs may facilitate their protection and recovery, and evidence suggests that this could be achieved through the delivery of molecules able to regulate the critical inhibitors of this pathway.

In experiments intended to identify molecular pathways that limit the intrinsic regenerative capacity of adult RGCs, Park et al. revealed that deletion of PTEN (or mTOR inhibitor TSC1) in adult RGCs promotes robust axon regeneration following optic nerve injury (Park, Liu et al. 2008). Genetic knockdown of PTEN, SOCS3, or a combination of the two was sufficient to preserve integrity and partially regenerate RGC dendrites and axons in the mouse retina following optic nerve crush. The authors observed that axon regrowth in the retina could be detected as early as one week following injury, and was sustained after 6 months (Mak, Ng et al. 2020). Interestingly, whilst PTEN and PTEN/SOCS3 knockdown also ameliorated RGC dendritic shrinkage, SOCS3 deletion alone did not, suggesting that the two signalling pathways involved in axon regrowth do not contribute equally to RGC preservation. Moreover, there is also evidence to suggest that adult retinal axons lacking PTEN and SOCS3 have not only the ability to regenerate, but are also capable of reforming functional excitatory synapses, making active connections with suprachiasmatic nucleus neurons (Li,

He et al. 2015). In order to fully evaluate the potential of PTEN-inhibition as a target for neuroprotection and neurotrophism in retinal neurodegeneration, a literature search was conducted in order to summarise existing data in relevant models (see table 4). To date nine studies have reported enhanced survival, extension, and regeneration of RGC / optic nerve axons following the targeted deletion or silencing of PTEN, or a combination of PTEN and SOCS3 *in vivo.*

Experimental data suggests, therefore, that manipulation of intrinsic growth control pathways may provide new therapeutic approaches to promote substantial axon regeneration in injured RGCs and optic nerve. It may be that part, or all of the neuroprotective influence of Müller glia cells relate to their ability to transfer miRNA capable of modulating these pathways in target RGC, and identification of these candidate molecules will allow development of targeted therapeutic approaches.

Conclusion

Illumina sequencing revealed abundant miRNA species in EV derived from Müller cells in culture, as well as transcripts present in whole cells that may be key to glia function *in vivo.* It was of special interest that small EV were differentially enriched in miRNAs predicted to target genes associated with extrinsic and intrinsic growth pathways. In particular, many of the miRNA most abundant in Müller EV, such as miR-21-5, have been shown to modulate PTEN, the master antagonist of the PI3K/AKT pathway. This strongly suggests that Müller glia EV may be able to activate intrinsic growth pathways in target cells which may contribute to the neuroprotective ability recognised in these cells.

To date, a range of studies advocate that miRNA can be transferred between different types of vertebrate cells through EV, and that they regulate expression of target genes in the recipient cells. For instance, bone marrow-derived mesenchymal stem cells secrete miRNA-containing vesicles which can be internalised by murine tubular epithelial cells, and inhibit translation of corresponding mRNA targets (Collino, Deregibus et al. 2010). Given that miRNA

target a great many different mRNAs, it is difficult to determine which molecules and pathways are responsible for the therapeutic effects observed. Many of these targets are still only predictions with only a fraction tested and experimentally observed. Within these targets however, well known instigators of RGC death including the bcl2 family (Maes, Schlamp et al. 2017), TNF (Tezel 2008), and PTEN/mTOR (Morgan-Warren, O'Neill et al. 2016) exist and further study will determine to what extent EV-derived miRNA is acting through these pathways.

Nonetheless, the ability of EV to transfer various RNA species and proteins, and to act as paracrine factors, raises exciting possibilities for therapeutic uses. Once effective miRNA or combinations of miRNA have been identified, cells could be engineered to selectively express these molecules so that they can deliver them to local cellular environments via EV. Engineered miRNA mimics could be encapsulated to provide sustained local delivery, or EV could be purified and added exogenously to tissue. As current techniques for gene transfer typically use viral or synthetic agents as delivery vehicles, the potential of EV released from engineered cells would offer the advantage of a virus-free approach and make the prospects of gene or cell-based therapies safer.

Approach	Model	Effect	Citation
Deletion by IV AAV Cre injection into conditional knockout neonates	Optic nerve crush	**Enhanced RGC survival**	(Park et al. 2008)
Down-regulation by overexpression of Nedd4 protein	Embryonic Xenopus RGC cultures	**Increased RGC axon branching**	(Drinjakovic et al. 2010)
Deletion by intravitreal AAV cre injection, combined with oncomodulin and cAMP treatments	Optic nerve crush	**Optic axon regeneration (long distance)**	(Kurimoto et al. 2010)
Deletion of PTEN and SOCS3 by IV AAV Cre injection into neonates	Optic nerve crush	**Sustained axon regeneration**	(Sun et al. 2011)
Deletion combined with Zymosan and CPT-cAMP treatments	Optic nerve crush	**Long-distance axon regeneration**	(de Lima et al. 2012)
Deletion by IV AAV Cre injection into conditional knockout neonates	Optic nerve crush	**Promote additional optic nerve axon regeneration**	(O'Donovan et al. 2014)
PTEN silencing by AAV2-vector delivery of shRNA	Rat optic nerve crush	**RGC survival and long-distance optic nerve fibre regeneration**	(Huang et al. 2017)
Inhibition of PTEN by antagonist peptide	Rat optic nerve crush, transection, temporary retinal ischemia by ophthalmic artery ligation	**Enhanced neuron survival and functional improvement**	(Shabanzadeh et al. 2019)
Tamoxifen and genetic knockdown of PTEN/SOCS3	Mouse optic nerve crush	**Partial axon regeneration. Amelioration of RGC dendritic shrinkage**	(Mak et al. 2020)

Table 4. Summary of PTEN/SOCS3 inhibition effect on axon protection and growth in glaucoma-like models of neurodegeneration.

Chapter 5: Functional analysis of Müller glia EV in a rodent model of glaucoma

Introduction

Cell-type specific EV uptake

Although results from some studies suggest that labelled EV, particularly those that are tumour-derived, can be internalised indiscriminately by a wide variety of cells (Zech, Rana et al. 2012, Svensson, Christianson et al. 2013), other experiments have highlighted the significance of ligand and receptor interactions for the initiation of endocytosis, which is indicative of a cell type-specific process. Lymph node stroma–derived EV were found to be more effectively internalized by endothelial and pancreatic cells than by donor lymph node cells (Rana, Yue et al. 2012). The same study identified interactions between EV-expressed tetraspanin Tspan8 and plasma membrane glycoprotein CD54 as responsible for this discrepancy. Similarly EV recovered from milk can be taken up via monocyte-derived dendritic cells thanks to the interaction between DC-SIGN and MUC1, whereas EV derived from other sources and lacking MUC1 were unable to enter these cells (Näslund, Paquin-Proulx et al. 2014). Groups have also attempted to hijack the specificity of these membrane interactions in order to target EV to certain cell types within a tissue. EV derived from dendritic cells that had been engineered to express a version of the exosomal membrane protein Lamp2b fused to the neuron-specific RVG peptide, enabled the targeted delivery of siRNA specifically to neurons, microglia and oligodendrocytes in the brain following their intravenous injection. Together, this data has great significance for attempts to translate EV studies into viable therapeutic agents, particularly in the context of stem cell based therapies. Donor cells that have specificity to cell targets in tissues of interest may be internalised more efficiently than those derived from more general sources.

While the data summarised above clearly indicates an endocytosis-mediated route of cellular entry, it is also clear that no single pathway of uptake for EV exists that is universal across all cell types and tissues. While vesicles are engulfed into phagocytes by phagocytosis, other cell types appear to prioritise

CMD, CIE, or macropinocytosis. Indeed many studies have identified multiple mechanisms of entry at play simultaneously in the same cell (Tian, Zhu et al. 2014). It is therefore likely that a combination of different endocytic sub-pathways, initiated by donor cell-specific membrane-presented proteins and phospholipids, regulate EV intake in a manner that depends upon recipient cell type and tissue context. Further complicating matters is the fact that EV are not homogenous, but differ greatly in terms of size and membrane-enrichment, even within a population purified from a single cell monoculture. This heterogeneity almost certainly contributes to the differences in apparent internalization mechanisms observed in various studies, as well as the lack of a single clear uptake route in any given study.

The therapeutic potential of stem-cell derived EV in retinal neurodegeneration

Regardless of the precise underlying endocytic mechanisms, once internalised, EV release functionally active microRNAs inside the recipient cell, as confirmed by luminescent reporter assays (Montecalvo, Larregina et al. 2012). EV-miRNA can regulate gene expression through de-novo translation and post-translational regulation of target mRNAs, and the ability of EV to alter the transcriptome and signalling activity within recipient cells allows them to induce specific phenotypic changes (Valadi, Ekström et al. 2007). Whilst alterations in EV activity have been revealed as a feature of certain pathologies, including cancer (Sheehan and D'Souza-Schorey 2019), there is also interest in EV for potential therapeutics. By harnessing the capability of EV to transfer their contents into target cells it may be possible to convert these vesicles into vehicles for the delivery of RNAs and small molecules (Alvarez-Erviti, Seow et al. 2011, Besse, Charrier et al. 2016) .

The paradigm shift in the role of EV as a potential therapeutic agent can be traced back to a 1996 publication showing that vesicles derived from the endocytic compartments of B lymphocytes were able to present MHC class II molecules and induce an immune response (Raposo, Nijman et al. 1996). Shortly after, Zitvogel et al (1998) published the first report of EV with therapeutic benefit by

demonstrating that MHC-positive vesicles derived from dendritic cells were capable of priming cytotoxic T lymphocytes for the suppression of murine tumours *in vivo* (Zitvogel, Regnault et al. 1998). The promise of these studies led to the first phase I clinical trials of EV-based therapeutics in 2005, where 15 metastatic melanoma patients received four doses of autologous dendritic cell-derived EV, demonstrating the feasibility of large scale exosome production and the safety of vesicle administration (Escudier, Dorval et al. 2005).

Several pre-clinical studies have examined the effects of exosomes and small-EV derived from cells with presumed therapeutic influence in a variety of disease models, including neurodegeneration. Evidence from *in vitro* studies suggests that stem cell-derived EV are capable of protecting and even promoting axon growth in cultured neurons. Human menstrual MSC exosomes, and those derived from bone marrow stem cells (BMSC) promoted significant neuritic outgrowth in primary cerebro-cortical cultures (Lopez-Verrilli, Caviedes et al. 2016). In addition, application of BMSC exosomes to human retinal cultures derived from embryonic stem cells enhanced neuroprotection following treatment with the microtubule poison colchicine (Mead, Chamling et al. 2020). Thus far, as reviewed in Chapter 1, many of the therapeutic benefits of stem cell-derived EV have been ascribed to their ability to transfer neuroprotective miRNA. This is further demonstrated by observations that BMSC treated with ischemic brain extracts have been shown to secrete vesicles with an increased payload of neuroprotective miR-133b (Xin, Li et al. 2012). Subsequent experiments have shown that when these miR133b containing EV are applied to neuronal cultures, the number of branching neurites as well as total neurite length increase (Xin, Li et al. 2013).

EV derived from various stem cell sources have also proven efficacious in several *in vivo* models of CNS degeneration. Delivery of siRNA to the mouse brain by systemic injection of EV was capable of effecting a 62% knockdown of BACE1 protein, a therapeutic target in Alzheimer's disease, in wild-type mice (Alvarez-Erviti, Seow et al. 2011). Intravenous injection of BMSC EV induced increase in

axonal density and synaptogenesis in a rodent model of stroke, along with locomotor recovery (Xin, Li et al. 2013). An analogous study reported enhanced angiogenesis and neurogenesis, as well as cognitive and sensorimotor benefits when injected systemically after traumatic brain injury (Zhang, Chopp et al. 2015).

Müller cell derived extracellular vesicles in the eye

As interest in therapeutic strategies based upon EV signalling has developed for neurodegenerative diseases of the CNS, so too has their potential as a candidate treatment for conditions affecting the eye. Several groups have demonstrated the efficacy of EV based interventions in animal models of ocular diseases: Periocular injection of EV purified from mesenchymal stem cell supernatants significantly ameliorated experimental autoimmune uveoretinitis in rats. This effect was shown to be due to inhibition of the migration of inflammatory cells, and was equivalent to that observed following transplantation of parent cells (Bai, Shao et al. 2017). Similarly, it has been demonstrated that intravenous injections of small-EV in a mouse model of autoimmune uveitis attenuated retinal damage, which was accompanied by a reduction in inflammatory cell infiltration and cytokine production (Shigemoto-Kuroda, Oh et al. 2017).

Importantly, in the context of retinal neurodegenerative conditions like glaucoma, BMSC-derived small EV pre-loaded with fluorescent label have been shown to deliver their cargo to RGC following transplantation into the vitreous, as demonstrated by the detection of fluorescent signal in the nerve fibre layer (Mead and Tomarev 2017). The same study also reported significant neuroprotection and preservation of RGC function in the rat following optic nerve crush. No neuroprotective benefit was observed when fibroblast EV were substituted by BMSC, implying that the therapeutic benefits related to specific agents contained within these cells, rather than the action of EV internalisation. Surprisingly, a separate study utilizing fibroblast EV in an *in vitro* experiment conducted on cortical neurons did report significant axon regeneration, although no neuroprotective effect was reported (Tassew, Charish et al. 2017). Similar data suggests that alternative sources of pluripotent stem cells may also be efficacious

when administered to retinal neurons. Transplantation of small EV derived from umbilical cord MSC after optic nerve crush in the rat resulted in improved survival of RGCs and promoted glia cell activation (Pan, Chang et al. 2019).

In an effort to model glaucomatous RGC damage, a recent study administered BMSC EV into the vitreous of rats after induction of artificially elevated IOP, reporting significant neuroprotection of RGC while preventing degenerative thinning of the nerve fibre layer (Mead, Amaral et al. 2018). The same group conducted analogous experiments in the DBA/2J mouse model of progressive eye degeneration, and observed that monthly transplantation of EV preserved RGC numbers and reduced axonal degeneration (Mead, Ahmed et al. 2018). In both of these reports, efficacy of EV was reduced following knockdown of the RNA-induced silencing complex protein AGO2, strongly indicates that miRNA activity is responsible for the therapeutic effects described.

Together, the data summarised above strongly suggests the efficacy of stem-cell derived EV in the protection and even regeneration of degenerated neurons, both in the retina and in the wider CNS. Like mesenchymal stem cells, Müller glia have progenitor characteristics and can protect RGC and partially restore retinal function following intravitreal transplantation (Becker, Eastlake et al. 2016, Eastlake, Wang et al. 2019). It is logical, therefore, that EV derived from these cells may be similarly efficacious, with the possible advantage of being retinal cell specific, and so benefiting from enhanced endocytosis.

Chapter summary and objectives

Whilst EV uptake has been demonstrated in a wide range of different cell types and lines, no evidence of their internalisation *in vitro* into primary RGCs has yet been reported. Since any therapeutic benefit provided by Müller glia-derived EV would rely on their fusion and transfer of neuroprotective molecules to target cells, it is important to clarify their propensity for internalisation into RGC prior to *in vivo* administration.

Previous reports from our lab have demonstrated that Müller glia cells protect retinal ganglion cells, and preserve their function following transplantation in an NMDA glaucoma model (Eastlake, Wang et al. 2019). This process appears to rely on the extracellular transfer of secreted molecules, which is significant given the discovery that that small EV derived from Müller glia are enriched in miRNA species with potential neuroprotective function. It is logical, therefore, that these particles be trialled in an equivalent *in vivo* design as that employed previously for whole cell transplant, in order to better evaluate the contribution of EV to the restoration of RGC function.

On this basis, the experimental aims for Chapter 5 of this thesis were:

1. To examine the internalisation of human Müller glia-derived EV into primary rodent RGCs and other retinal cells.

2. To evaluate the tolerance and efficacy of these particles as a potential therapeutic agent in a preliminary *in vivo* study of experimental glaucoma.

Materials and methods

Preparation of primary RGC suspensions for in vitro studies

RGC were isolated from new born pups using a two-step immunopanning protocol previously published (Winzeler and Wang 2013). Pregnant female Sprague Dawley (SD) rats were obtained from Charles Rivers Fish facility and the new-born postnatal pups were maintained at the UCL Biological Service Unit at the Institute of Ophthalmology. Procedures involving animals were performed in accordance to the guidelines described in the ARVO Statement for the Use of Animals in Ophthalmic and Vision Research. The use of animals for this study was approved by the Ethics Committee at University College London Institute of Ophthalmology and the U.K. Home Office.

Retinae were collected from pups at postnatal day 4, following euthanasia by cervical dislocation. Under a dissection microscope, the skin overlaying the eyeball was cut away aseptically to reveal the eye. Using and a surgical scalpel (VWR; Cat no. 233-5364), the lens and vitreous humour were removed using the back of the scalpel to reveal the retinae, which were then gently detached using a flat spatula and transferred to a 6-cm Petri dish containing pre-warmed Earle's balanced salt solution (EBSS). Retinae were examined under the dissection microscope, and the surrounding membranes containing blood vessels were removed using forceps. Retinae were then transferred to 10 mL of papain dissociation solution (Worthington Biochemicals; Cat no. LK003178) containing 100 µL of DNase I (0.4%) (Worthington Biochemicals; Cat no. LS006342), and incubated at 37°C for 30 minutes. At 15 minute intervals, the dissociative solution was disrupted by gentle rocking.

Digestion was ceased by 4 mL of low-ovomucoid solution comprised of Earle's balanced salt solution (Worthington Biochem), 1.1 mg/mL of reconstituted albumin ovomucoid inhibitor (150 µL; Worthington Biochem), and 100 µL of DNase I (0.4%), which was added to the retinal cell suspension, and incubated

for 1 minute. The cell suspension was then centrifuged at 300 x g for 5 minutes, and the pellet then re-eluted in a further 4 mL of low-ovomucoid suspension, also containing 80 µL of rabbit anti-rat macrophage polyclonal antibody (Cedarlane; Cat no. CLAD51240). After gentle trituration using a 1 mL pipette, retinae were incubated for 10 minutes at room temperature to allow for antibody binding to cells. After a final mechanical dissociation by pipetting the cell suspension several times, it was passed through a sterile 40-µm nylon mesh (Corning; Cat no. 352340). The suspension was then centrifuged at 500 x g for 12 minutes at room temperature. Supernatant was aspirated and the cell pellet resuspended in high concentration ovo solution, followed by centrifugation at 1000 rpm for 12 minutes at 25°C.

Preparation of negative and positive immuno-panning plates and culture chambers

Two antibody-coated, 15-cm negative selection plates were prepared for removal of macrophages by adding 60 µl of goat anti-rabbit IgM (H + L) (Invitrogen ™; A27033) and 20 mL of 50 mM Tris-HCl (pH 9.5) (Invitrogen™; Cat no. 15567027) per dish. A single 10 cm positive selection petri dish was prepared by adding 30 µL of goat anti-mouse IgM (µ-chain specific) and 10 mL of 50 mM Tris-HCl (pH 9.5). Plates were swirled gently for even coating with antibody-Tris solution, before incubation overnight at 4 °C.

Prior to use, the positive selection plate was rinsed once with Dulbecco's PBS (Gibco; Cat no. 14190144), and 10 mL of rabbit anti-rat Thy-1 antibody (Abcam, Cat no. ab92574) in 9 mL of DPBS and 1mL of 0.2% BSA was added and swirled gently to coat the plate evenly. Plates were left at room temperature for at least 2 hours.

100 µl of 1×Poly-D-lysine stock (PDL, Sigma-Aldrich; Cat no. A3890401) was added to 16-well culture chambers (Invitrogen™; C37000), which were incubated overnight at room temperature in order to coat them. After incubation, chambers were rinsed three to four times with sterile H2O and aspirated to dryness.

Mouse laminin (1 mg/ml, Sigma-Aldrich; Cat no. CC095) was diluted to a final concentration of 50 µg/ml by adding 10 µl of the laminin stock to 5 ml of Neurobasal™ medium (Gibco; Cat no. 21103049). The diluted laminin solution was mixed well, and 100 µL was added to the dried cell culture chambers, and incubated in a 37 °C incubator for 2 h. Immediately prior to use, the plates were rinsed with D-PBS three times.

Enrichment of RGCs from retinal cell suspensions

The digested cell suspension was transferred to the 1st negative panning plate, which was placed on a flat surface and incubated for 20 minutes. The unbound cell suspension was then recovered, and transferred to the 2nd negative panning plate, and incubated for 45 minutes. The plate was agitated every 15 minutes. During this incubation, the positive panning plate was aspirated to remove the Thy1 antibody solution and rinsed with D-PBS three times. The cell suspension was transferred to the positive panning plate by 10 mL stripette, and incubated for a further 45 minutes, with gentle agitation every 15 minutes. After incubation, the plate was washed six times with DPBS, and then a solution consisting of 100 µL of trypsin stock (30,000 U/mL, Sigma-Aldrich; Cat no. T9935), and 4 mL of pre-warmed Earl's balanced salt solution (EBSS) (Gibco™; 14155063) was added, and incubated for 4 minutes in order to dissociate adherent cells.

2 mL of DPBS containing 30% FCS (Biosera, Boussens, France) was added to the plate in order to quench the reaction, and the dissociated cells were collected into a 50 mL Falcon tube. The cell suspension was gently homogenised and then pelleted by centrifugation at 1000 x g for 12 minutes. The cell pellet was resuspended in prewarmed RGC Complete Medium as previously defined

(Winzeler and Wang 2013) and cell counts were conducted using trypan blue. Cells were seeded at 10,000 cells / well into the 16-well culture chambers, and were cultured at 37 °C under normoxic conditions.

Labelling of extracellular vesicles with the lipophilic dye PKH26

Small EV suspensions were prepared as previously described in Chapter three of this thesis. EV in DPBS suspension were stained with PKH26 using PKH26 Red Fluorescent Cell Linker Kits for General Cell Membrane Labelling (Sigma-Aldrich; Cat no. PKH26GL). Prior to staining, PKH26 in diluent C was incubated in an ultrasonic water bath at 37 °C for 15 min. Alternatively, for the control sample, particle-free Dulbecco's phosphate-buffered saline (DPBS; Sigma-Aldrich) was used as the input instead of the exosome standard. Exosome and control samples were stained according to the following procedures.

PKH26 dye was diluted in 100 µL diluent C to a final concentration of 8 µM. Then 1x 10^9 exosomes (as determined by nanoparticle tracking analysis) suspended in 20 µL particle-depleted DPBS were incubated with 80 µL of the dye solution for 5 minutes at room temperature and mixed with gentle pipetting. Next, excess dye was bound with 100 µL of 10% BSA in Dulbecco's modified Eagle's medium (Gibco™; Cat no. A9576) to quench the binding process. In order to separate labelled-EV from unbound dye, EV were then diluted with 400 µL DPBS and layered onto a 20% to 60% discontinuous sucrose gradient (Sigma Aldrich; Cat no. S8501) in 34mL polypropylene ultracentrifugation tubes (Beckman Coulter; Cat no. 326823). The gradient was centrifuged at 100’000 ×g for 12 h at 4 °C in an Optima® XE-90 preparative centrifuge (Beckman Coulter; Cat no. A94471). Fractions 3 to 6 (density range 1.08–1.15 g/mL as measured by refractometer), were combined, and diluted to 30 mL with DPBS. Finally EV were pelleted by ultracentrifugation at 100’000 ×g for 1 h at 4 °C. The pellets were gently resuspended in 50 µL DPBS, and samples were taken for analysis and confirmation of labelling by nanoparticle tracking analysis (NanoSight Ltd; LM10).

$1x10^8$ labelled EV were added to primary RGC-enriched retinal cultures and incubated for 4 h at 37°C.

Confocal microscopy and image analysis

Fluorescence images were acquired using a Zeiss confocal laser scanning microscope (LSM 700/710). The objectives 10X, 20X and 40X (oil immersion for LSM 700 and water immersion for LSM 710) were used according to the resolution acquired. Exposure times in milliseconds were set for individual filters without bleaching. Images were taken using Zeiss Zen Imaging Software and were analysed using ImageJ software. The results were processed using Excel and GraphPad Prism as described previously (see Chapter 2).

Imaging of primary retinal cultures by confocal microscopy

After incubation with PKH26-labelled EV, primary RGC cell cultures were fixed with 4% PFA for 5 minutes, cryoprotected in 30% sucrose for 30 minutes, and allowed to dry before freezing. For use, cells were defrosted and 500 µl of tris-buffered saline (TBS) + 0.3% triton X was added. Cells were blocked for 1 hour in TBS + 0.3% triton + 5% donkey serum before the addition of the primary antibody (diluted in blocking buffer). RGCs were stained with primary antibodies specific to markers β-III tubulin (TUJ), and DAPI (Abcam; Cat no. ab18207). A non-specific actin filament stain (Phalloidin 488, Invitrogen™; A12379) was also used to identify TUJ-negative cells. Primary antibodies (see supplementary table 3) were incubated overnight at 4°C. Cells were then washed with TBS three times for 5 minutes. Secondary antibodies (Alexa flour, Invitrogen, U.K. 1:500 in TBS + 0.3% triton) were incubated for 3 hours at room temperature in the dark. Fluorescence images utilizing Z-stacks were acquired using the Zeiss Zen Imaging Software on a Zeiss confocal laser scanning microscope (LSM 700/710) and image analyses were performed on images processed for maximum intensity projection. PKH26 was excited using a 555-nm solid state laser line, and emission fluorescence was filtered with a 565-nm to 605-nm band-pass filter.

Intraocular injection of EV into a rat model of RGC depletion

A total of 20 wild-type Lister hooded rats were used in this study. Animals were maintained according to the U.K. Home Office regulations for the care and use of laboratory animals (Scientific Procedures Act 1986). 10 male and 10 female rats were matched, and separated in control groups containing equal numbers of each. The use of the animal species for the study was approved by the local ethics committee at University College London, Institute of Ophthalmology and the U.K. Home Office. The animals were given access to food and water *ad libitum* and kept under 12-hour light/12-hourdark cycles. Immunosuppression started 2 days before cell transplantations, was administered daily in drinking water, and consisted of 25 mg azathioprine, 5 mg prednisolone, and 210 mg cyclosporin per litre.

Induction of RGC Damage by NMDA

Four weeks old rats were anaesthetized using ketamine (60 mg/kg) and xylazine (7.5 mg/kg). Prior to intraocular injections, pupils were treated with tropicamide (1% w/v, Minims; Bausch and Lomb, Kingston-upon-Thames, Surrey, U.K.), phenylephrine hydrochloride (2.5% w/v, Minims; Bausch and Lomb, Kingston-upon-Thames, Surrey,U.K.) and oxybuprocaine hydrochloride (0.4% w/v; Minims Bausch and Lomb, Kingston-upon-Thames, Surrey, U.K.) drops. Lubricating drops (Viscotears™, Bausch and Lomb) were used to make sure the fellow eye did not dry out. Procedures were performed using a 5 µl Hamilton syringe and a 32G needle. RGC damage was induced by injection of 2 µl of a mixture of NMDA (80 µM) and triamcinolone (80 mg/ml) into the intravitreal space of the left eye (Lam, Abler et al. 1999).

Administration of Müller glia small EV

Müller glia cells obtained from retinal organoids formed by pluripotent stem cells were provided by Dr Karen Eastlake, using techniques previously described in publications by our lab (Eastlake, Wang et al. 2019). Small EV were isolated from

Müller glia cell cultures and EV were isolated as described previously (see chapter two, p). EV suspended in sterile PBS were administered two weeks after the induction of RGC damage. Animals were anaesthetized as described above, and a 2 µL volume containing 3 x 10^9 EV were injected into the vitreous of the right eye of test animals, just posterior to the limbus using a glass micropipette. EV were injected slowly, and the needle was retracted after a 1-minute delay to minimize backflow. Control animals received an equivalent dose containing PBS-alone.

Scotopic ERG Recordings

Retinal function was assessed by scotopic full field electroretinogram (ERG). An individual masked to the treatment groups performed all readings and analysis. Intravitreal treatment with NMDA results in excitotoxic damage to RGCs that reliably and reproducibly depresses the negative scotopic threshold response in rats (Bui and Fortune 2004). Before ERG, animals were dark adapted overnight and anaesthetized as described above. Both eyes were treated with oxybuprocaine hydrochloride anaesthetic (0.4% w/v), as well as tropicamide (1% w/v) and phenylephrine hydrochloride (2.5% w/v) in order to dilate the pupils. Viscotears lubricating drops were also used to ensure the cornea remained hydrated. Animals were placed onto a heated table to control body temperature, which was positioned inside a Faraday cage to minimise noise, and corneal ring electrodes were positioned onto cornea of both eyes. ERG recordings were made using a Ganzfeld stimulator (Colordome.; http://diagnosysllc.com). Flash stimuli (4-millisecond duration, repetition rate of 0.13 Hz) were presented in the Ganzfeld colourdome by light-emitting diode stimulator at intensities of −6.5 to −2 log cd second/m2. The flash stimulus was repeated 30 times for each light intensity. The responses near scotopic ERG threshold always consisted of a positive potential (pSTR) followed by a slow negative component (nSTR). NMDA does not influence the pSTR of the rat full field ERG and so it was disregarded for these experiments (Bui and Fortune 2004). The responses were measured using the Espion Diagnosys V6 software. Measurements for nSTR analysis were analysed by determination and recording of the maximal negative response in the range of 160–230 milliseconds (for nSTR) at each light intensity.

Analysis of ERG measurements

All analyses were made using R version 3.4.0 (The R Foundation for Statistical Computing). An analysis of variance model was fitted to each intensity, which took into account any confounding effects in which the measurements were taken, and the treatment group. Least square (LS) means were obtained for each treatment group, and differences in mean response to the control group were presented together with corresponding 95% confidence intervals (CI). As an additional exploration, a mixed effects model was fitted to data for intensities −4.5 to – 3.5 combined. The fixed effects included in the model were day, intensity, treatment, and treatment by intensity interaction. Animal was fitted as a random effect. The LS means were obtained as an averaged for each treatment across the intensities used in the test, and differences in average response to the control group were presented, together with 95% CI.

As a field, EV biology and therapeutics is very much in it's infancy, and this is especially true with regard to diseases of the eye and retina. As a result, hugely significant questions relating to their potential use are still to be resolved, including the optimum route and timing of administration, the dosage and frequency required for effect, the routes of metabolism and clearance after injection, potential toxicity and host immune response. The design of studies to assess EV functionality is therefore challenging, as all of these issues must be taken into account. For this reason, it was decided that the *in vivo* experiments conducted for this work would follow an identical design to that previously used by colleagues investigating the efficacy of whole cell transplant. In this way. Animals were unilaterally injected with NMDA in order to deplete the ganglion cell layer, which depresses the nSTR. Outcome of the transplantation was evaluated by assessing the negative scotopic threshold response (nSTR) of the electroretinogram (ERG).

Results

Primary rat retinal ganglion cells internalise Müller glia-derived EV in vitro

In order to evaluate the uptake and internalisation of EV by retinal cells, RGC-enriched primary retinal cell cultures isolated from 5-day post-natal rats were incubated for 4 hours at 37°C with small EV derived from human Müller glia cells labelled with PKH26. Confocal microscopy analysis of immunostained cells showed EV internalization, with EV localized around the nuclei and scattered throughout the cytoplasm of RGC staining for β-III-tubulin (TUJ antibody) (fig. 35). At higher magnifications, immunofluorescent EV could be detected in RGC axons, suggesting that EV can be internalised into different neuronal compartments (fig. 35).

Labelled EV were also observed surrounding the nuclei of primary cells that were negative for TUJ staining, as judged by immunostaining for the non-specific actin filament marker phalloidin. Analysis of the size and morphology of the stained cells suggested that the enriched RGC preparations contained non-neuronal cells, which were also able to internalize EV. These cells appeared to have sequestered EV around the soma, suggesting an endocytic mechanism of uptake, possibly by microglia (fig. 35: A), as these primary cell cultures are known to be enriched in these cells (Winzeler and Wang 2013). Importantly, no signal could be detected in retinal cultures treated with unlabelled-EV, negating the possibility that the signal originated from autofluorescent artefacts (figs. 35: B and 36: B).

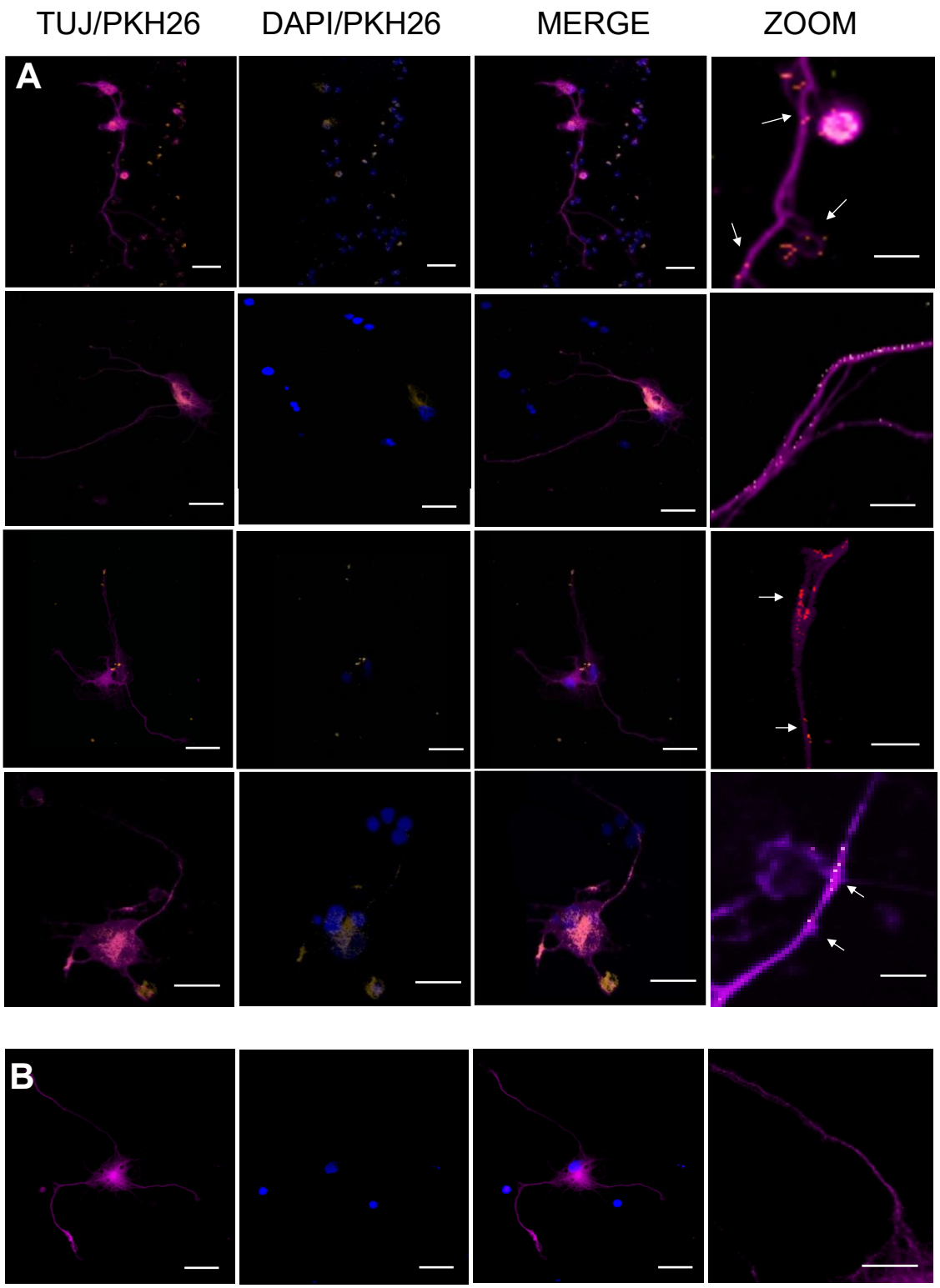

Figure 35. ***Representative phase microscopy images demonstrating internalisation of EV into retinal ganglion cells****. (**A**) EV labelled with PKH26 dye excited at λ 555 nm (yellow) surrounding primary retinal culture nuclei and scattered throughout the axonal cytoplasm, as evidenced by TJU staining (λ 488 nm, magenta). Scale bar = 100 μm. Images on the right column show a magnification of a section corresponding to the images on the left columns, scale bar = 25 μm. EV internalization is indicated by white arrows. (**B**) No EV were detected in control cultures treated with unlabelled EV.*

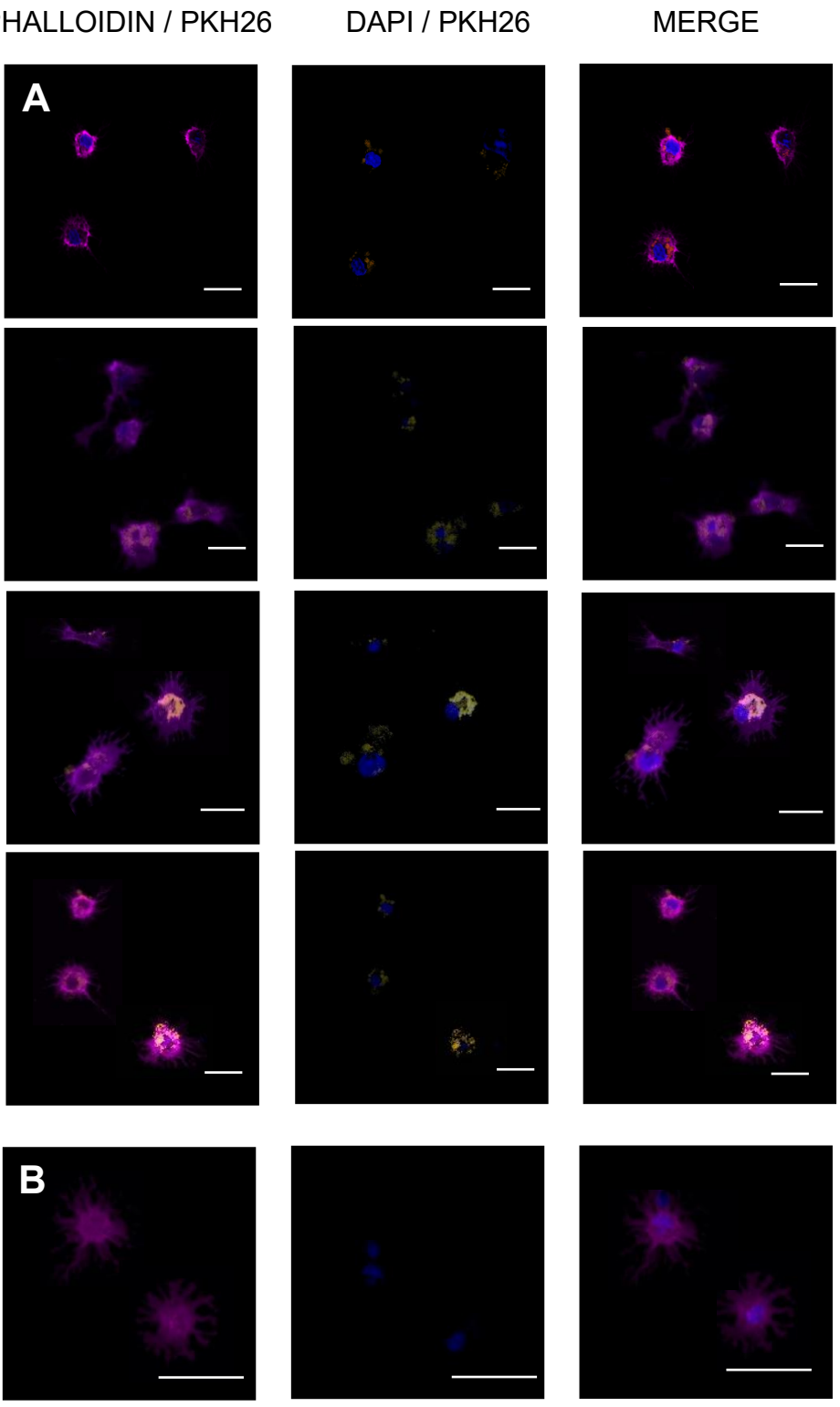

Figure 36. ***Representative phase microscopy images demonstrating internalisation of EV into primary retinal cells.*** *Scale bar = 50 µm. (**A**) Labelled EV (yellow, λ 555 nm) localised around the nuclei of primary retinal cells in culture that do not have RGC morphology or express neural markers (likely to be microglia) (magenta, λ 488 nm). (**B**) No PKH26 stain was detected in control cultures treated with unlabelled EV.*

Small EV preserve RGC function in an animal model of glaucoma-like disease

A preliminary *in vivo* study was conducted in order to assess whether Müller-derived EV were able to improve RGC function as that observed when Müller cells are transplanted into the same model. Following intravitreal transplantation of 1x 10^9 small EV into animals depleted of RRC by NMDA, RGC function was assessed by electroretinogram (ERG) 2 weeks and 4 weeks after EV injection. At high stimulus intensities (−3 to −1 log cd m−2), control eyes showed a characteristic initial negative a-wave followed by a positive b-wave, whereas at lower stimulus levels (<−4 log cd m−2) a small positive wave (forming the positive STR (pSTR) was generated. This was followed by the generation of a negative wave (forming the negative STR (nSTR) (fig. 37).

Two weeks post-intervention a non-significant ($p = 0.107$) trend was evident where control animals that received NMDA treatment but no EV, exhibited a reduced nSTR at luminance −4.5 through to −3.5 log cd second/m^{-2}, in comparison to animals in the test group (fig. 37: A). This trend suggested that animals that had received the EV injection had superior RGC responses following NMDA- excitotoxicity than those that had received the sham. At four weeks post-intervention, 2-way matched pairs ANOVA indicated that this superior response indicated a significant recovery of the nSTR in treated animals compared to control ($p = .047$), suggesting that Müller-small EV may be capable of preserving RGC function following the onset of retinal neurodegeneration (fig. 37: B).

A

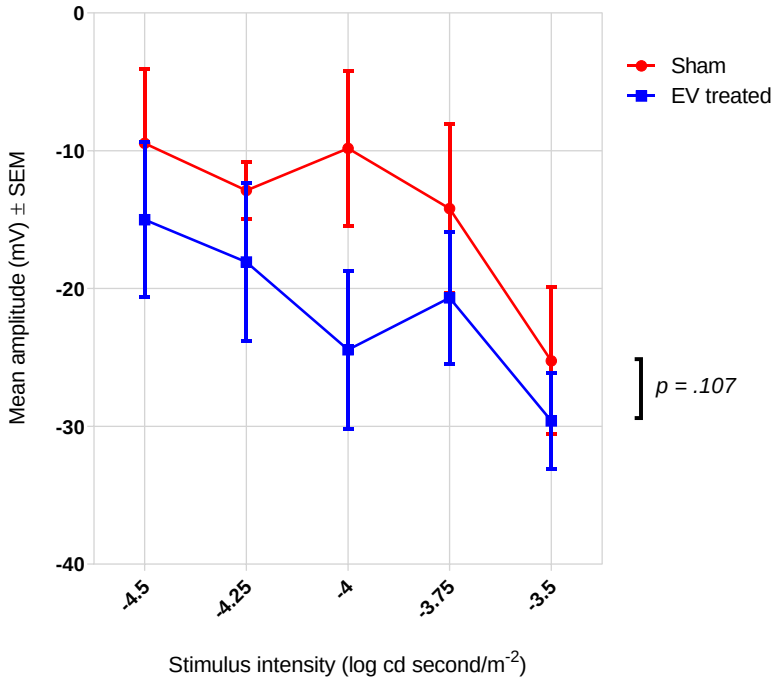

B

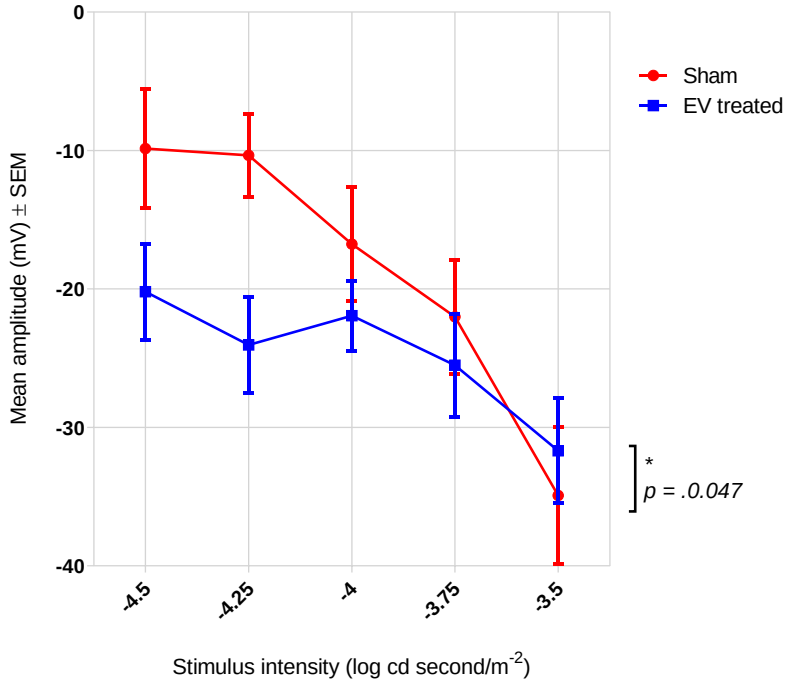

Figure 37. ***Electroretinogram (ERG) responses following application of EV in the NMDA damaged rat eye****. Comparison of the effects of Muller-derived sEV treatment with control treatment on the nSTR amplitude across light intensities from −4.75 to −3.5 log cd seconds/m-*$^{2.}$ *. (**A**) Average nSTR response 2 weeks post-treatment. (**B**) Average nSTR response 4 weeks post-treatment (n = 10 for each experimental group.*

Discussion

Retinal ganglion cells internalise Müller cell EV

The present study demonstrates that sEV derived from Müller glia cells can be internalised by RGC, and preliminary transplantation studies suggest that they might be able to preserve RGC function in a rodent model of RGC damage by NMDA. Taken together with the results of previous studies indicating that the signalling ability of EV is largely dependent on the transfer of small-non coding RNAs (Bai, Shao et al. 2017), and the data presented in Chapter 3 of this work demonstrating that Müller EV are enriched in miRNAs known to regulate pro-growth and survival cascades, these findings suggest that EV represent part of the neuroprotective secretome of Müller glia cells.

While strong evidence from a range of published reports suggest that EV can be endocytosed by recipient cells, the intricacies of the plasma membrane-localized molecular interactions that regulate EV internalisation appear to vary between different cell types. Evidence for the importance of these interactions can be seen from the fact that EV can be engineered to target specific cell types in a tissue through modifications to proteins expressed on their external membranes (Kumar, Wu et al. 2007), as well as in reports that exosomes expressing certain tetraspanin complexes are preferentially taken up by endothelial and pancreas cells than those that do not (Rana, Yue et al. 2012). Any neuroprotective function that Müller glia derived-EV may bestow upon RGCs would inevitably require their internalisation, and so it is highly significant that EV labelled with PKH26 were found to localize intracellularly in primary RGC cells, four hours after their addition to cell cultures.

To the author's knowledge, this is the first study to demonstrate direct internalisation of EV by RGCs in vitro. Other studies, however, have reported *in vivo* internalization of EV in the retinal nerve fibre layer following intravitreal injection of fluorescently tagged particles (Mead and Tomarev 2017), and

BMSC derived vesicles have been shown to integrate into cortical neuron cell bodies and axons (Zhang, Chopp et al. 2017). Whilst little is known about the role that EV play in intracellular communication between Müller glia and retinal neurons *in situ*, macroglia of the CNS have been demonstrated to secrete EV that have been implicated in the transfer of relevant molecules to neurons, both in normal physiological conditions and in the context of certain neurodegenerative conditions. Astrocytes expressing the mutant SOD1 protein associated with motor neuron disease release EV that are capable of transferring this peptide to primary spinal neurons, inducing subsequent motor neuron cell death (Basso, Pozzi et al. 2013). Similarly, oligodendrocytes release EV that contain myelin proteins such as PLP, CNP, MAG, and MOG, all of which are associated with the process of axon myelination (Krämer-Albers, Bretz et al. 2007). Labelled oligodendrocyte derived EV have also been detected within primary cortical neurons following their co-culture, and their uptake has been shown to improve neuronal viability under stress conditions (Frühbeis, Fröhlich et al. 2013). It is likely therefore, that internalization of EV by neurons represents an important component of the trophic and functional support that Müller glia provide to retinal neurons *in situ*, and so it is logical that EV released by these cells may express membrane proteins and lipids that would facilitate their internalisation by recipient cells of the retina. This retinal specificity may mean that Müller glia EV represent a more efficient vehicle for delivery of neuroprotective molecules to RGCs than alternative approaches that have looked to use lipid vectors, or vesicles released from pluripotent cells of mesenchymal origin.

EV appeared to be internalised by distal ganglion axons

Because the methods used in this study were not capable of detecting EV fusion to cell membranes, it is not possible to say definitively where EV entered the cells. Confocal microscopy analysis of RGCs suggested that labelled EV accumulated around the nuclei, although small numbers of EV could also be identified within the axons and dendrites of RGC. With this in mind it is logical that EV enter RGCs at the point where receptor-ligand interactions are made, and are then subjected to axonal transport in endocytic compartments to the cell body for processing. On

this basis, it is possible to suggest that EV-mediated communication by retinal neurons may be analogous to the process of endocytosis and retrograde transport of Trk-neurotrophin complexes which convey Trk signals from distal axons to the cell body (Butowt and von Bartheld 2001).

One potential issue with tracking vesicle internalisation using membrane-associated dyes such as PKH26 is that the presence of the labelling molecules could affect the normal behaviour of EV. The fact that EV uptake has been observed despite labelling with many different lipid-binding dyes suggests that these molecules do not hinder their uptake; however the interactions underlying these processes are still to be revealed and further experimentation is needed to verify whether the precise biological behaviour of internalised EV is affected. Further work to confirm the precise location of internalised EV would require a study design involving EV tagged with a specific reporter molecule such as luciferase, as well as electron-microscopy analysis. Therapies based on the supply of neuroprotective agents to the RGC typically involve their delivery into the vitreous, where they can be received by RGC axons in the nerve fibre layer. It is important, therefore, that Müller-EV are capable of internalisation into these compartments. This is particularly true given that distal RGC axons are the site of localised damage to the optic nerve in the glaucomatous retina. The results of this study suggest the possibility of EV internalisation by RGCs adjacent to the point of intravitreal delivery, where they could then be trafficked via endosomal compartments to the cell body or even to distal axons as required.

EV are also internalised by non-neural retinal cells

Analysis of primary retinal cultures that had been incubated with labelled-EV also suggested that many non-neuronal cells internalised these particles. Cells were counterstained with phalloidin in order to visualise cell bodies, and assessment of their morphology and size suggested that they were microglia (Ashwell, Holländer et al. 1989). In these cells, EV appeared to be sequestered around the soma region, as opposed to the more diffuse distribution pattern evident in the RGC cytoplasm and axons (Figs 36, A). While this may simply reflect the

underlying morphology of the different cell types, it may also indicate variability in the specific mode of endocytosis utilised for EV internalisation. While both neurons and microglia exhibit clathrin-dependent and clathrin-independent forms of endocytosis, microglia are uniquely capable of phagocytosis (Napoli and Neumann 2009). Without further analysis to identify the nature of the EV-labelled compartments, it is not possible to confirm their specific endosomal nature, however the distribution of EV identified in non-RGC cells in this study is highly comparable to that seen from analogous studies using phagocytes as the recipient cells (Feng, Zhao et al. 2010). A possible confounding issue with the use of lipophilic dyes such as PKH26 for the labelling of vesicles in internalisation studies is the potential for leaching of the fluorescent agent onto recipient cell membranes, leading to a false pattern of internalisation that is due to normal membrane recycling rather than indicating EV uptake. This is unlikely, however, given the many studies that demonstrate prevention of internalisation following the addition of various molecular inhibitors (Svensson, Christianson et al. 2013, Franzen, Simms et al. 2014). Additional experiments, involving incubation of cells with excess unlabelled EV and measurement of the rate of transfer of fluorescence between EV also support the notion that the increased fluorescence in recipient cells is due to specific uptake of EV rather than non-specific dye leaching.

The current observations that Müller-derived vesicles are internalised by both neural and non-neural cells, is consistent with the hypothesis that EV-mediated communication represents a hitherto underappreciated mode of Müller cell function in the retina. In the wider CNS, a growing body of literature reports evidence for functional regulation of microglia by EV secreted by neurons and macroglial cells (Fitzner, Schnaars et al. 2011). For example, exosomes released by neurons have been shown to facilitate microglial removal of degenerating neurites, by inducing up-regulation of the complement molecule C3 in microglia (Bahrini, Song et al. 2015). Neuronal EV containing Amyloid-β have also been shown to be internalised by microglia for degradation (Yuyama, Sun et al. 2012). In addition, EV derived from mesenchymal stromal cells modulate astrocytic and microglial activity, decreasing pro-inflammatory factors such as TNF-α and IL-1β

(Cui, Wu et al. 2018). The intake of Müller-derived EV into microglia and other non-neuron cells as suggested by the current results, is therefore likely to be typical of both normal cellular activity within the retina, as well as in stress or disease states.

That Müller EV can be internalized indiscriminately by different retinal cells is also significant in the context of EV as a potential therapeutic agent for retinal neurodegenerative conditions. While this work has attempted to identify miRNAs present in EV that may have a neuroprotective function on RGCs, these internalisation experiments suggest that molecules present within EV may also be delivered to the various glial populations that support them. Further experiments must be conducted, to ensure that the activation of signalling cascades that enhance RGC survival, do not result in less desirable consequences when initiated in other retinal cells. This may, however, represent another advantage for the use of EV derived from retina-specific cells, rather than those secreted by adult stem cells from different organs and tissues. It can be assumed that EV released by Müller glia are routinely released into the retinal microenvironment and taken up by the various retinal cell types that they neighbour *in situ* without adverse effect.

Alvarez-Erviti et al. have shown that it is possible to engineer EV that express specific proteins that facilitate their specific internalisation by selected cells, including brain neurons (Alvarez-Erviti, Seow et al. 2011). In order to specifically target retinal neurons in the same manner, it would be necessary to identify the specific ligands and receptors that control the entry of EV into these cells. The results of such studies would allow for the design of RGC-specific EV capable of delivering target molecules to support their recovery in the glaucomatous retina. Alternatively, since glaucoma and related diseases of the retina have a complex and multifactorial nature, with multiple non-mutually exclusive theories explaining their cause and progression, an efficacious therapy may aim to target multiple mechanisms, rather than focusing on one pathway or molecule. The fact that EV can be internalised by different retinal cell types suggests that they would be able

to deliver their bioactive cargos to the diverse cell types involved with progressive degeneration in the glaucomatous retina. This raises the possibility of neuroprotection through both direct, and indirect mechanisms.

It is important to note that the experiments reported here suggest that rat retinal cells are capable of internalising EV secreted by human Müller glia. Although not unexpected, these findings provide further evidence for a lack of species specificity in the process of EV uptake, and support findings from previous studies demonstrating the transfer of mouse exosomal RNA to human mast cells (Valadi, Ekström et al. 2007), and the uptake of bovine EV by human H1299 cells (Munagala, Aqil et al. 2016). Although it may seem counterintuitive that EV entry into recipients is cell-type but not species specific, the membrane-bound ligands and receptors thought to initiate this process are highly conserved between mammalian species, but differ significantly between the specialised cell types of different organs. For example, the tetraspanins CD9 and CD63 that are frequently used as markers of MVB-derived EV share >90% amino acid homology between mouse and human orthologues.

Limitations of the study design

While the use of fluorescent labels allows for direct visualisation of EV internalisation, it should be appreciated that studies utilising traditional light microscopy suffer from limited resolution and as such, are unable to detect single EV. This is because the minimum wavelength of visible light is approximately 390 nm, therefore single vesicles or particle clusters that are less than 390 nm in diameter cannot be visualized. This should not affect the assessment of EV uptake in general but may affect the visualization and dynamic localization analysis of individual EV. It is important to note that even the smallest signals present in confocal images of labelled EV represents an accumulation of several individual particles. For this reason, images where none or minimal presence of EV is indicated are not necessarily demonstrating their complete absence.

EV may be visualized in a more specific way via the use of fluorescent protein tags fused with membrane-exposed vesicular proteins and by electron-microscopy. For example, CD9 and CD63 are tetraspanin proteins found enriched in EV which, when tagged with GFP, can be used to show uptake and processing of vesicles in cells (Piao, Kim et al. 2018). Because the precise receptor-ligand interactions underlying EV uptake by cells are still to be revealed, a possible limitation of this strategy is the assumption that the fluorescent tag will not affect the normal function or trafficking of the tetraspanin protein, and does not therefore alter the behaviour of the EV during uptake. Also worthy of consideration is the fact that that no singular tetraspanin has yet been identified as a universal EV marker, and EV with variable protein cargos are commonly identified even within relatively homogenous preparations (Barranco, Padilla et al. 2019).

A range of techniques can be used in conjunction with EV uptake assays in order to enhance their specificity and limit some of the challenges in their use noted above. Blocking antibodies can be used to test the role of specific ligands or receptors, and the use of chemical inhibitors to block specific uptake pathways. The results of such studies, would shed further light upon the processes underlying the intake of EV in RGCs, for which identifying non neuron-specific receptors may allow for the design of EV able to directly target recipient cells.

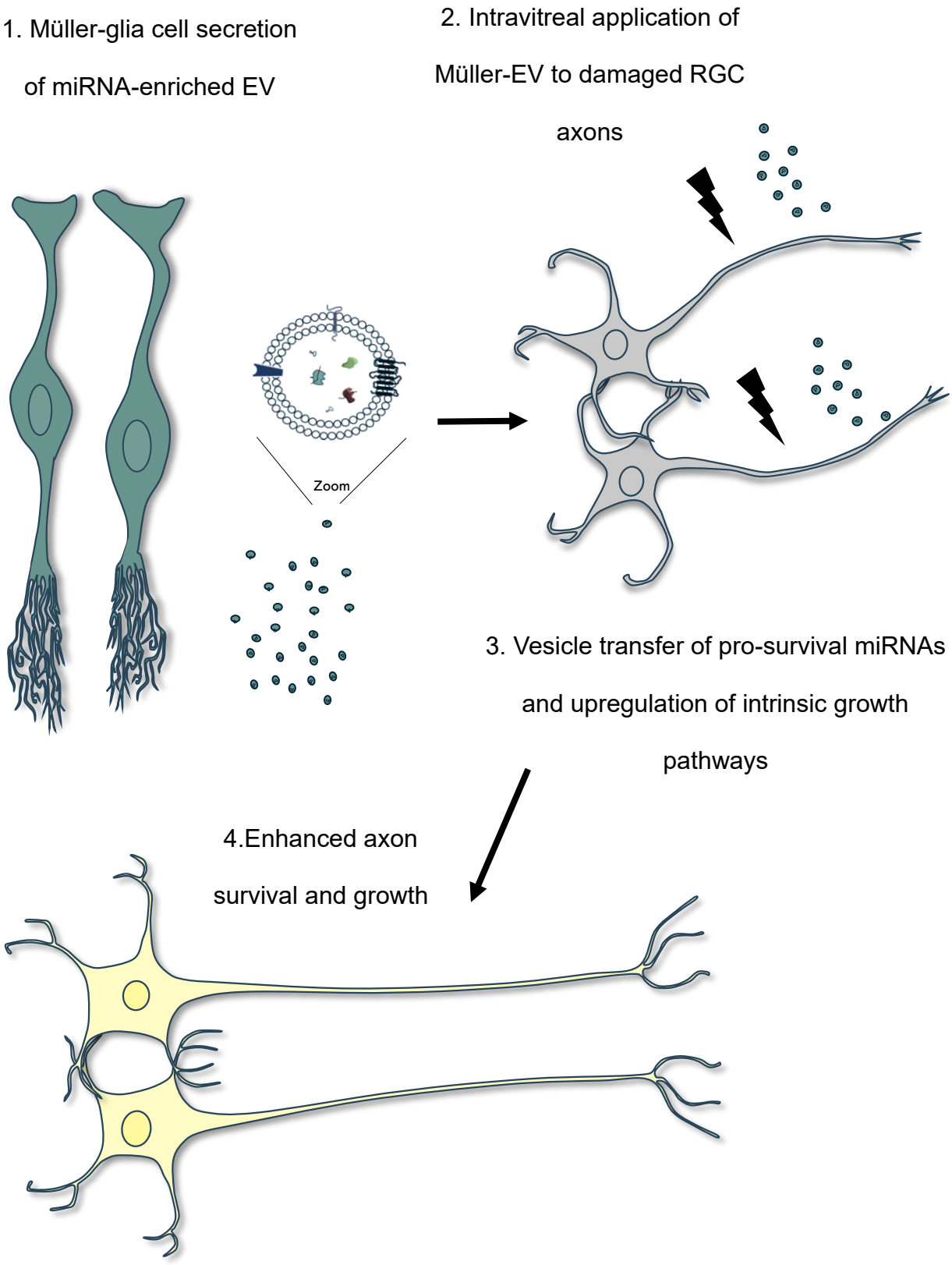

Figure 38. ***Putative mechanism of neuroprotection for a Müller glia EV glaucoma therapy****. Extracellular vesicles enriched in pro-neurotrophic miRNAs may represent effective therapeutic agents capable of protecting degenerated retinal ganglion cells.*

Intravitreal injection of Müller glia-derived EV partially restores RGC function in a rat model of RGC depletion

After identifying that EV derived from Müller glia cells could be internalised by rat RGCs, a test of their potential neuroprotective function was conducted using an *in vivo* model of glaucoma-like damage in the rat. RGC degenerative disease and optic nerve transection cause a specific decline in the scotopic threshold response (STR) of the electroretinogram (ERG), which reflects RGC function. In the rat, NMDA induced excitotoxicity has been shown to substantially depress the nSTR (Bui and Fortune 2004). In this study, assessment of retinal function by ERG following intravitreal injection of 3×10^9 EV in animals with NMDA induced RGC damage, showed significant improvement of the nSTR four weeks after the EV injection ($p = 0.04$). A small improvement, although not significant, was also evident at two weeks post injection. These results are comparable with, and build upon previous publications by our group, that reported rescue of RGC function following transplant of $1x10^5$ Müller cells (Eastlake, Wang et al. 2019). It may be assumed that EV do, therefore, represent a significant component of the neuroprotective mechanisms attributed to these cells, most likely in addition to the release of other molecules such as neurotrophic factors and antioxidants. To identify the precise effects mediated by EV will require further clarification, and could be achieved by knocking-down RAB proteins (RAB27A and RAB27B) in transplant cells in order to inhibit exosome secretion, and evaluating any subsequent loss in neuroprotective function.

As a field, extracellular vesicle biology and their potential role as therapeutic agents is very much in its infancy, this is especially true with regard to diseases of the eye and retina. As a result, hugely significant questions relating to their use are still to be resolved, including the optimum route and timing of administration, the dosage size and frequency required for effect and maintenance of function, as well as the routes of metabolism and clearance after injection. In this study, it was of interest that the greatest improvement in nSTR was detected four weeks after EV treatment, rather than at two weeks. Tracking of EV following injection into host tissue is extremely challenging due to their very small size, and as a

result it is impossible to say how long EV remained present and viable once delivered. Ideally, ocular treatments should be long lasting to minimize repeat injections and while there is a precedent for trialled retinal cell therapies to have medium lasting effects (Kuppermann, Boyer et al. 2018), no studies have thus far assessed the longevity of transplanted small EV. Whether the improvements in RGC function detected result from a cumulative effect caused by 4 week-extended exposure to EV, or whether a quick, initial “spike” of EV signal is simply required to manifest as improvements in the ERG, is a matter for clarifying in further studies. It is encouraging, however, that EV-mediated improvements were observed at four weeks, which would potentially reduce the need for frequent repeat injections. These results are comparable with previous work reporting no change in therapeutic efficacy between weekly and monthly administration of BMSC-derived exosomes in a microbead ocular hypertension glaucoma model, although in that study EV were delivered at the time of induction of IOP elevation (Mead, Ahmed et al. 2018), as opposed to two weeks following RGC depletion in the present study. Interestingly, a separate study used a single intravenous administration of 15×10^9 EV in an experimental autoimmune uveitis model, and reported a therapeutic effect that was evident 21 days later (Shigemoto-Kuroda, Oh et al. 2017).

Although it is unclear how long EV remain after administration into biological tissues, a purported advantage of their use as vehicles for the transfer of therapeutic molecules like RNAs, and proteins is that the lipid bilayer membrane is able to protect their cargo from degradation. While glaucoma therapies based upon direct delivery of neurotrophic factors, or RNA-based molecules like siRNA to the vitreous have been shown capable of producing a beneficial response, they suffer from rapid clearance and degradation and require frequent repeat injections which are poorly tolerated (del Amo, Rimpelä et al. 2017). In contrast, exosomes are constitutively present as a component of the vitreous in healthy eyes, and are able to diffuse readily through the ~500nm meshwork and remain stable for extended periods following injection (Peeters, Sanders et al. 2005, Mead, Amaral et al. 2018, Zhao, Weber et al. 2018). In this way, EV could be considered as organic nanoparticular liposomes, with the added ability to resist

complement lysis (Clayton, Harris et al. 2003) and endonuclease degradation, allowing in vivo stability and protection of their nucleic acid content (Valadi, Ekström et al. 2007).

The effect reported in this study suggest that recipient cells are able to make use of EV-derived neuroprotective signals for weeks after administration, however care must be taken when extrapolating data from disease-models, in particular for a complex and multifactorial condition such as glaucoma. While NMDA treatment effectively depletes the RGC layer, this excitotoxin injection model is effective in damaging RGC but may not fully represent the complex damage observed in the glaucomatous retina. Moreover, because the damage to RGCs stabilises after the initial insult and does not progressively deteriorate, as is typically the case with elevated-IOP glaucoma models, the potential for their preservation and recovery may be greater. In this way the model represents a 'best case' scenario for RGC damage, which may account for some of the partial recovery of function. Similarly, while NMDA induced excitotoxicity is known to cause reproducible and fast RGC death, and the rat nSTR is known to depend upon ganglion cell contributions, it is impossible to say definitively that improvements in the treated group related to enhanced RGC survival, or regeneration of axons based upon ERG data alone. Since the internalisation experiments observed *in vitro* suggest that Müller EV can be taken up by both neuronal and non-neuronal retinal cells, it is not clear if the therapeutic response observed was via a direct effect on the RGC or through macro or microglial intermediaries. In a study investigating the neuroprotective potential of mesenchymal stem cells exosomes, Mead & Tomarev reported improved density of RGCs in retinal wholemounts from transplanted animals, for which it is tempting to speculate than a similar mechanism of action is likely responsible for the therapeutic effect reported in this study. A more comprehensive study to validate the results of this preliminary work should include analysis of retinal architecture by immunohistochemistry and optical coherence tomography, in order to better understand the retinal function preservation.

For this study $3x10^9$ EV were injected intravitreally in a 2 µL volume of vehicle. Precise figures on the numbers of EV required to initiate functionally relevant responses in recipient cells are yet to be clarified. Previous studies conducting stoichiometric analyses of exosome-mediated miRNA communication are yet to find a consensus, with some researchers suggesting that even the most abundant miRNAs are only present in less than one copy per EV (Chevillet, Kang et al. 2014), whilst others reporting certain species present in numbers greater than 10 copies per EV (Stevanato, Thanabalasundaram et al. 2016). Recent experiments in the field of RNAi have shed some light on the dose-response requirements for the clinical relevance of miRNAs and siRNAs. A study investigating the therapeutic potential of a novel siRNA compound for glaucoma treatment demonstrated efficacy in monkeys with an intravitreal dose of 100 nM (Martínez, González et al. 2014), although much smaller (143 pM) doses may be effective when delivered directly to the transected optic nerve in SD rats (Lingor, Koeberle et al. 2005). The efficacy of miRNA-based delivery by EV would depend on both the quantity of functional transcripts delivered, as well as the relative quantity of mRNA target. While it may be tempting, therefore, to simply over-saturate target cells in functional experiments, some in vitro evidence suggests that exosomes delivered in very high concentrations may prove cytotoxic for hippocampal neurons, although this effect also seemed to be dependent upon the cell passage from which they were derived (Venugopal, Shamir et al. 2017). Adding to the uncertainty are reports that the relative make-up of MSC-EV cargo varies between cell passages, and MSC-donor sources, and so using the same number of EV does not guarantee that the therapeutic cargo is being correctly dosed.

Despite these challenges, the data reported here indicate that $3x10^9$ EV were sufficient for promoting partial recovery of RGC function, and was well tolerated by recipient animals, in which no evidence of inflammation or toxicity were identified. This is largely in keeping with previous in vitro and in vivo toxicology reports which detail their safety after culture treatment or systemic delivery (Maji, Yan et al. 2017, Zhu, Badawi et al. 2017), although it is important to note that neither of these were conducted in the eye. While no evidence from related studies involving intravitreal injection of EV report complications arising from their

delivery into the eye (Mead and Tomarev 2017, Mead, Ahmed et al. 2018, Mead, Amaral et al. 2018), extensive toxicology studies are still required. A possible benefit on the use of EV rather than whole cell transplant may be an opportunity to bypass issues surrounding safety and immunogenicity that may complicate the translation of these therapies to the clinic, particularly with regard to injections of dividing or differentiating cells into the eye. A recent report detailed three patients who received intravitreal injections of adipose-derived MSC as a treatment for AMD. Unfortunately, these patients subsequently suffered complications involving retinal detachment and haemorrhage, thought to relate to the formation of a monolayer on the inner limiting membrane of the retina (Kuriyan, Albini et al. 2017). A study involving transplantation of MSC into rat vitreous also demonstrated a significant inflammatory response (Huang, Kolibabka et al. 2019). Since EV appear to comprise a large proportion of the efficacious secretome of Müller glia, administering these in their place may constitute a safer approach.

Conclusion

In conclusion, the data presented here demonstrates that EV derived from human Müller glia cells can be internalised by primary rat RGCs, and are capable of significant preservation of RGC function in an animal model of glaucoma. While the precise mechanism of action is still to be revealed, the fact that EV are enriched in miRNA known to target genes responsible for the survival and plasticity of neurons is highly promising. Further study is required to determine precisely which miRNA, and through which mRNA targets, the greatest therapeutic efficacy can be exerted.

Together, this data recommends Müller-derived EV as a potential treatment for ocular diseases like glaucoma, possibly as an adjunctive therapy to IOP-lowering interventions. While whole cell transplant may yet prove the most effective way to supply the cells of the glaucomatous retina with neuroprotective molecules, there are still many challenges inherent to their use to be overcome, particularly regarding their large-scale manufacture, storage and delivery. Since, EV are

stable, non-replicative, and have the added benefit of displaying little or no deterioration after long term storage, these organelles may represent a new therapeutic paradigm for cell-based therapies with decreased risk (Kusuma, Barabadi et al. 2018).

Chapter 6: General discussion

Background

Glaucoma is the most common neurodegenerative disease in the world, affecting approximately 64 million people or 3.5% of the global population aged 40-80 years (Tham, Li et al. 2014). Current therapeutic interventions are based upon controlling some of the primary risk factors associated with the disease, namely elevated intraocular pressure, but are unable to replace or regenerate damaged neural cells, and often fail to prevent progression of the disease. As a result, new strategies are required that could act as an adjunct to IOP-lowering therapies, and help to protect and preserve function of the retinal neurons.

Currently, stem cell-based therapies may be considered the only hope for restoration or maintenance of visual function in patients affected by severe disease. Thus far, most studies in the retina regenerative field have been aimed at replacing neurons by cell transplantation. However, neural replacement by cell grafting has not been successfully achieved as this process requires integration of transplanted cells within major neural networks. Nonetheless, promising protection of cells and restoration of certain aspects of retinal function have been observed after experimental stem cell grafting, suggesting that a paracrine signalling mechanism involving the release of various neuroprotective agents is capable of repairing neural damage. This is a subject of current investigations in the field (Ramsden, Powner et al. 2013).

Whilst several sub-types of pluripotent cell are currently under investigation, it has been recently revealed that a population of Müller glia cells represent an adult stem cell niche in the eye, raising the possibility for a retinal-specific approach. Our lab have previously identified Müller glia with progenitor-like characteristics in the adult human retina, which can be induced to express markers of retinal neurons in vitro to generate neural precursors capable of inducing a significant recovery of function following sub-retinal transplantation (Singhal, Bhatia et al. 2012, Jayaram, Jones et al. 2014) Moreover, Muller glia differentiated from PSC-derived retinal organoids partially restore visual function in rats following NMDA-

induced cytotoxicity, as determined by improvements in the negative scotopic threshold response of the electroretinogram (Eastlake, Wang et al. 2019).

Building upon these previous observations, this thesis looked to investigate the nature of the neuroprotective molecules secreted by Müller glia, with the aim of elucidating mechanisms by which these cells restore visual function, as well as to investigating the potential for the development of new and effective cell-based therapies that could potentially restore or maintain vision in individuals with retinal neurodegenerative conditions.

Müller glia synthesise and secrete neurotrophic factors

The initial experiments conducted for this work demonstrated that human Müller glia constitutively express neurotrophins and other neurotrophic factors which have been previously shown to prolong neural survival and even promote axon outgrowth in RGCs (Meyer-Franke, Kaplan et al. 1995, Di Polo, Aigner et al. 1998, Liang, Yu et al. 2019). These observations are of particular interest given that deprivation of neurotrophic factor supply to the RGCs is known to contribute to their apoptosis in the glaucomatous retina. These experiments revealed a considerable modulation of neurotrophin gene expression following the addition of exogenous cytokines to Müller glia cultures, although the data did not reveal whether these effects were as a direct result of cytokine signalling or if the mechanism at work was more indirect and complex. Although further investigations are required in order to reveal the interactions underlying cytokine and neurotrophin signalling in Müller glia, this data have significant implications for the fate and behaviour of cells transplanted into the vitreous of glaucomatous eyes, which have been previously shown to be enriched in TNF-αand TGF-β compared to healthy eyes (Ochiai and Ochiai 2002).

The present study also highlighted some of the challenges associated with therapeutic strategies based upon the supply of soluble factors. Although capable of stimulating beneficial responses in the short-term, these are known to have a

short half-life and a transient and flattened effect which is not boosted by repeat applications (Chan, Love et al. 2017). Indeed, while attempts to treat glaucoma with neurotrophic factor-based interventions have had mixed success, the increased availability of factors appears to result in a negative feedback loop involving downregulation of the receptor on neuron membranes (Chen and Weber 2004). In conclusion, whilst the production and release of neurotrophins is likely to be key to the process by which transplanted Müller cells have been shown to ameliorate neurodegeneration and restore RGC function, it is also likely that secondary sources of communication are involved with this process. Since glaucoma is a complex and multifactorial disease, it is also logical that a combination of several different secretions is likely to prove more effective as a long-term therapeutic strategy.

Recently it has been demonstrated that cells are capable of communicating via the release and receipt of nano-sized membrane-bound organelles, known as extracellular vesicles (EV). These contain cargos of proteins and nucleic acids capable of influencing sustained phenotypic alterations following their internalisation into recipient cells. A large proportion of the exciting protective and restorative effects reported for cell-based therapies in various disease contexts can be attributed to their secretion of EV, as demonstrated by the fact that inhibition of exosome production in donor cells limits their ability to stimulate regeneration and functional improvement in infarcted mouse myocardium (Ibrahim, Cheng et al. 2014). Moreover, injection of purified exosomes is often sufficient to reproduce beneficial effects reported following stem cell transplant (Kooijmans, Aleza et al. 2016, Mead, Amaral et al. 2018).

Increasingly, the therapeutic potential of EV's is being recognised and investigated in a range of disease contexts, often as an extension to whole stem-cell based approaches. Since the content of EV appears to be specific to their donor cells, it has been suggested that these represent a more general and sustainable mechanism of neuroprotective signalling which may be taken advantage of in the context of retinal neurodegenerative conditions. Unlike cells,

soluble factors or oligo-based therapies, EV are highly stable in a long-term, non-replicative, and simple to produce and purify, making them a potentially effective and simplified platform for the treatment of a wide range of disease conditions (Choi, Kim et al. 2013). On this basis, the present study aimed to establish a protocol by which EV derived from Müller glia cells could be purified and analysed, and to investigate their potential role in the neuroprotective signalling previously ascribed to these cells.

Müller glia secrete extracellular vesicles

Using a combination of micro-filtration and differential ultracentrifugation involving separation and purification by density gradients, a protocol was established in order to reproducibly purify two sub-populations of cell-derived particles from Müller glia cultures. These consisted of i) small EV with an average diameter of ~100 nm, which were relatively enriched in proteins present on endosomal membranes and deficient in whole cell markers, suggesting enrichment in endosome-derived “exosomes”, and ii) large EV with an average diameter greater than >250 nm, which contained higher quantities of Müller plasma membrane and cytoskeleton markers, suggesting enrichment in membrane-derived “microvesicles”. One challenge facing the still-young field of EV research is the inability to effectively discriminate between sub-populations that share many overlapping characteristics. Although techniques based upon selecting vesicles with regard to the presence of individual proteins on surface membranes allows for the purification of highly homogenous populations, no comprehensive “exosome marker” has yet been recognised (Théry, Amigorena et al. 2006) . As such, the use of these strategies risks discriminating against certain EV, whilst biasing purifications for others. For this reason, the more inclusive collection protocol described above was used for these experiments, which looked to evaluate the Müller EV secretome as a whole.

Both large and small EV populations had a distinctive bi-layer membrane evident by electron microscopy, and lacked of apoptotic markers. In addition, no evidence

of neurotrophic factors was detected in either EV cohort, although admittedly the technique used for their investigation was western blotting, which is of limited sensitivity. A more exhaustive investigation of the protein content of Müller-derived EV would require the employment of mass-spectrometry, and should be a subject for future studies. Collectively, the data presented in this thesis satisfy the International Society for Extracellular Vesicle (ISEV) requirements to claim the presence of cell-derived EV (Théry, Witwer et al. 2018).

Both EV populations were found to be enriched in small RNAs, whilst lacking for evidence of larger coding transcripts. This was of particular interest since previous studies have demonstrated that the transfer of RNAs by exosomes represents a mechanism of genetic transfer between cells, and there is evidence that small non-coding RNAs contained within vesicles are capable of regulating the translation of specific gene targets and moderate diverse signalling pathways (Valadi, Ekström et al. 2007). On the basis of previous observations that paracrine cytoprotective functions reported following stem cell-transplantation could be arrested by knockdown of proteins required for miRNA function (Mead and Tomarev 2017), it is important to investigate the miRNA profile of Müller glia EV and its regulation of neural function within the retina

Müller glia EV are enriched in microRNA with neuroprotective potential

The present study provides the first report regarding the miRNA profile of EV derived from Müller glia cells. These experiments were conducted with the intention of gaining insight into this under-appreciated mechanism of intracellular communication, as well as allowing further investigation of the neuroprotective secretome ascribed to these cells. High-throughput sequencing and an integrative bioinformatics pipeline (fig.24), revealed the extent of miRNAs present in populations of both small and large EV, and allowed comparison with those miRNAs expressed by donor cells. It was remarkable that rather than merely representing the cell in miniature, bioinformatic analysis revealed significant

differential enrichment of transcripts between sample sources. This discovery was suggestive of a specific mechanism by which certain transcripts were preferentially sorted into cells, although the details of this are still to be resolved and may be the subject of future investigations. Alignment of miRNA sequences revealed that a particular motif “CUGA” was present in 33% of miRNAs enriched in small EV, in comparison with just 9% in whole cells and 5% in a randomised control data set. While it may be speculated that interactions between miRNA-associated proteins and this sequence motif may increase the likelihood of a transcript being loaded into an EV, further experimentation is required.

Software predicting miRNA:mRNA target interactions based upon previously published data suggested that small EV-enriched transcripts were capable of regulating biological pathways and processes associated with cell growth and survival, hinting at potential mechanisms of neuroprotection. Of particular interest was the PI3K/AKT pathway, which had many tens of experimentally validated interactions predicted for a subset of small EV-abundant miRNAs (fig. 32). While this pathway is highly upregulated in developing tissue, and is the source of axon regeneration in the peripheral nervous system (Hur, Liu et al. 2013, Zhang, Liu et al. 2014) it is tightly controlled in quiescent cells by the master inhibitor of this pathway, PTEN. It has been speculated that a transient reduction of PTEN mRNA in targeted neurons could facilitate the survival and regeneration of these cells through increased AKT signalling, as previously demonstrated in a range of pre-clinical models using a variety of knockdown strategies (Ohtake, Hayat et al. 2015).

It was encouraging, therefore, that many of the most abundant miRNA present in Müller glia EV have been previously demonstrated to directly target PTEN, including miR-21-5p, miR-29b-5p, and miR-10a-5p (Wang, Guan et al. 2015, Luo, Tan et al. 2017, Tu, Cheung et al. 2018). Since sequencing is not considered a quantitative technique, each of these miRNAs was subsequently confirmed in Müller glia EV by qRT-PCR, where an exogenous spike-in (cel-miR-39) was used as internal control. Together this data suggests a potential mechanism of action

for the known neuroprotective effects of Müller cells. Future studies may use *in vitro* culture assays in order to identify the precise miRNA, or combination of species, that most efficiently protects and regenerates primary neurons. Production of these could then be upregulated in Müller glia to produce an optimised gene-transfer based therapeutic with the added advantage of a retinal-specific vehicle. Alternatively, viral or non-viral delivery strategies combined with miRNA mimics could represent a more standardised and synthetic product.

Muller glia EV as a vehicle for neuroprotection RGCs

Because any therapeutic benefit provided by Müller glia EV cargos must surely involve their receipt by target neurons, experiments were conducted to evaluate the ability of RGCs to internalise Müller-derived EV in culture. EV populations were labelled with a membrane-specific lipophilic dye, and immunocytochemistry and confocal microscopy were used in order to identify their uptake by RGC-enriched primary cultures. To the author's knowledge, this work is the first to demonstrate the direct internalisation of EV into cultured RGCs. Of particular interest was the observation that EV uptake could occur in the distal axons, which is significant given that these are the site of degeneration in glaucoma. Since the RGC axons form the retinal nerve fibre layer which is directly adjacent to the vitreous (and presumed point of delivery), it is important that these compartments are able to internalise EV, whereby it appears that they are transported in endocytic compartments to the cell body for processing.

A wealth of literature describes the many and varied sub-types of EV endocytosis, and it is clear that this process is not uniform and standard for all cells and tissues, but instead depends on as yet unresolved interactions between surface-membrane molecules (Horibe, Tanahashi et al. 2018). Certain cell types appear to be selective in their ability to internalise EV of specific origin (Feng, Zhao et al. 2010), while others engineered to express certain surface molecules are internalised with a greater efficiency (Horibe, Tanahashi et al. 2018). In this study, EV derived from Müller glia may have an innate advantage in therapeutic terms for the retina, compared to a vesicle of non-retinal origin. This is particularly valid

given that the transfer of EV has been revealed as yet another mechanism by which glia and neurons communicate within the nervous system (Bahrini, Song et al. 2015, Men, Yelick et al. 2019). Further experiments involving comparison of the rate of intake between Müller EV and alternative stem cell sources would be required to confirm this hypothesis, and may be the topic of future studies in this area.

This thesis also provides reports of the first *in vivo* trials of Müller glia-derived extracellular vesicles. Here, an NMDA-model of RGC depletion was used in order to evaluate the therapeutic potential of an intravitreal injection of small EV, which was administered two weeks following induction of RGC damage. Compared to a control group receiving sham injection only, EV-treated rats had significantly improved RGC function four weeks after intervention, as determined by the negative scotopic threshold response of the full field electroretinogram. These preliminary results were particularly encouraging as the experimental design was chosen to mimic the EV content of Müller cells used in whole-cell transplants (Eastlake, Wang et al. 2019), which allowed for a direct comparison between the two strategies. The data suggests that injection of EV secreted by Müller glia, are similarly efficacious as transplant of the whole cells, which is of great significance for the future development of cell-based therapies for retinal neuroprotection.

Without evidence of direct internalisation into the NFL *in vivo,* it is impossible to say with certainty that EV administered in this study were taken up by target RGC. Similarly, without engineering specific reporter genes into Müller EV, we are not able to proof that the restoration of RGC function observed here was as a result of RNA transfer. Future studies would benefit from the examination of retinal tissue at relevant time-points, from which it could be ascertained that enhanced RGC survival was due to miRNA modulation of RGC function. This would also permit analysis of the relative expression of target genes, for example PTEN, and would provide insight into the mechanisms responsible for the effects observed.

Because many studies investigating the therapeutic application of EV have often used a cross-species experimental design, in particular, human-derived EV in rodent disease models, it is still unclear what interactions and effects may be being omitted as a result. For example, it is not yet known to what extent human-miRNA are compatible with rodent mRNA. More studies using human EV on human cells would help to refine the mechanisms at work or even yield new candidates. To this end, further *in vitro* investigations could be planned using retinal organoids derived from human pluripotent stem cells in order to investigate the effect of putative genetic transfer between Müller-derived EV in a human retinal model.

Since vesicle take-up is cell type specific, it seems likely that Müller glia derived EV express membrane molecules that facilitate this internalisation, providing appealing prospects as vehicles for the delivery of neuroprotective molecules to retinal neurons. Once internalised, EV make an attractive delivery vehicle for therapeutic miRNAs owing to their ability to protect them from ribonucleases, increased stability in circulation and high biocompatibility, as well as their low immunogenicity and toxicity profiles.

Challenges facing the translation of EV into the clinic

Unarguably, extracellular vesicles have emerged as biological agents that are central to intercellular communication and have therapeutic potential. However, despite intense investigations during the past decade aimed at elucidating EV biology, many properties and mechanisms currently remain elusive. In fact, some reports describe contradictory results, even with extracellular vesicles derived from the same cell types. For example, MSC-derived exosomes have been shown to both inhibit and promote tumour growth (Zhu, Huang et al. 2012, Bruno, Collino et al. 2013). Such discrepancies are probably a consequence of differences in cell culture conditions before extracellular vesicles are harvested, differences in the purification protocols used or due to a lack of robust extracellular vesicle characterization. As such, these results highlight some of the most significant challenges currently inhibiting the development of EV for clinical

application. For example, the large-scale production of a homogeneous and specific EV subpopulation from heterogenous cell supernatants. Overall, EV comprise a wide variety of vesicles ranging from 30 nm to several µm in diameter, and overlap exists between the different subcategories and biogenesis pathways. Since no standards currently exist to classify the different types of vesicles, the process of isolation of EV subtypes is still controversial, and is further confused by a lack of standardized protocols for their purification (Baranyai, Herczeg et al. 2015).

Another concern is that the exact mechanisms of EV mediated pro-regenerative effects remain unknown, and more thorough investigations of EV and their components are needed. The majority of recent studies on EV function have focused primarily on miRNA and genetic transfer, however less is known about protein content and effects, exosomal lipids, and other nucleic acids which have also been shown to be present in these organelles and that exert important cell functions. More rigorous characterization of extracellular vesicles using a combination of methods — including sucrose gradient separation, electron microscopy and full RNA, lipid and protein profiling — will be therefore required to fully explore the biology of extracellular vesicles and to assess potential biohazards that may emerge as clinical translation of these therapies progresses. The detailed mechanisms of how miRNAs and other cargos are selected into extracellular milieu via EV must be better understood. Taken together, more research on EV will be necessary to fully harness the potential of these particles as therapeutics for future clinical application.

Therapeutic potential of Müller glia EV

The results presented in this thesis suggest that the release of miRNA-enriched EV represents a significant proportion of the therapeutic effect observed following transplantation of whole Müller cells. This data provides further evidence of the potential of EV as a therapeutic tool for retinal degenerative conditions, and may serve as the foundation to the translation of new neuroprotective tools with potential for therapeutic applications, where their utility may hold several

advantages over other cell-based strategies. Unlike cells, EV do not elicit acute immune rejection and may also have the advantage of stability and the potential for long-term storage without a reduction in potency (Ge, Zhou et al. 2014). As a result, it is logical that their manufacture would be less complex and relatively inexpensive when compared to the preparation of viable cells for transplantation. Thanks to their ability to be enriched with various bioactive agents, and potential to be targeted to specific cells, EV may also represent a more directed and efficient therapeutic strategy when compared to the transplant of whole cells into damaged tissues (Sun, Zhuang et al. 2010, Alvarez-Erviti, Seow et al. 2011).

Human Müller glia isolated from stem cell-derived retinal organoids are relatively simple to produce and are highly expansible in culture, as shown by previous experiments conducted in our laboratory (Eastlake, Wang et al. 2019). These cells secrete plentiful EV, and are viable for extended periods in FBS-depleted conditions, allowing for efficient harvesting of their secreted vesicles from culture supernatants. It could be suggested therefore, that such cells constitute a valuable resource for isolation of retinal-specific EV, that could be potentially translated into the clinic. Importantly, these cells are not immortalised, and undergo finite numbers of cell divisions before senescence. Further investigations will need to ascertain whether the secretome of these cells alters as they age, which would have significance for the development of EV-based therapies.

Despite the challenges inherent to the translation of EV-based therapies to the clinic, the data presented in this thesis recommends vesicles derived from Müller glia as a neuroprotective agent that could play a future role in the treatment of retinal neurodegenerative conditions like glaucoma. In the healthy and diseased retina, Müller glia support the survival of retinal neurons via numerous direct and indirect mechanisms, and it is logical that their vesicle secretome is a key component of this function. Results of early trials of intravitreal EV delivery to the retina for the treatment of macular holes suggests that such treatments are safe and well tolerated (Zhang, Liu et al. 2018), although data on the durability of EV

in the vitreous, the dosage required for functional effect, the mechanisms of their clearance, and the required frequency of repeat injections is still to be established.

The experiments investigating the functionality of Müller-EV presented in Chapter 5 of this thesis suggest that in the rat eye, the effects of their administration may be evident up to one month after injection, however, the major anatomical differences between the human and rodent eye make it difficult to extrapolate these findings. It is also relevant that while the NMDA excitotoxicity model of RGC damage follows a predictable course of onset and damage, human glaucoma is a hugely multifactorial condition involving several converging pathways. The stage of progression at which a neuroprotective “boost” of EV may be most likely to have significant beneficial effects during the course of such a disease must be established.

Since glaucoma is also most-commonly associated with the structural changes that come with aging, the issues underlying the cause of disease may be impossible to fully address in many cases, and interventions designed to preserve RGC function must take that into account. It may be that the most efficacious and well-tolerated time to deliver such a therapy would be during the surgical interventions currently used to reduce elevated IOP, such as routine trabeculectomies. Further studies may evaluate whether such a strategy would be capable of preserving remaining RGCs, and preventing any further loss of vision following these treatments.

Conclusions

In summary, the work presented in this thesis provides new insights into the neuroprotective secretome of Müller glia cells, adding further support to previous studies demonstrating their potential for retinal therapies. In addition to the constitutive production of soluble neurotrophins, including BDNF, Müller glia were

found to release large quantities of EV, and a protocol was designed for the efficient purification of these based upon size.

Although EV have been demonstrated to transfer a wide range of potentially trophic molecules between cells, much of their protective ability appears to be mediated by short non-coding RNAs (Tomasoni, Longaretti et al. 2012, Chowdhury, Webber et al. 2015, Vallabhaneni, Penfornis et al. 2015). The current investigations revealed that Müller glia small EV were enriched in miRNAs that target genes involved with cell growth and survival, including PTEN, the master inhibitor of the AKT/mTOR pathway. In this way, a putative mechanism for the pro-survival and neurotrophic functions previously ascribed to these cells was revealed, and further reinforced by the fact that these EV were readily internalised by retinal ganglion cells in vitro and were capable of partially restoring retinal function in an animal model of glaucoma-like disease.

Future studies should be aimed to further investigate the nature of this neuroprotective effect. *In vitro* experiments using human retinal organoids or whole rodent retina will allow clarification of the miRNA-based mechanism of action proposed. In addition, a larger, and longer *in vivo* study would have greater power to determine the magnitude of EV benefit to RGCs, and may confirm the therapeutic potential of these particles – as well as answering significant questions regarding the dosage and timing of administration for optimum effect.

As a field, EV research is still in its infancy, particularly with regard to their use as agents for tissue regeneration, and many questions surrounding the precise pathways and factors underlying the results of studies like this, and others are still to be resolved. Further investigations are also required to determine exactly which miRNA or miRNAs (and through which mRNA targets) exert their greatest therapeutic efficacy. Analysis of the effect of individual or combinations of miRNA species may allow for the identification and “cherry picking” of active molecules, as well as the removal of non-relevant or potentially deleterious transcripts, allowing for a far more direct and potent therapeutic agent. EV engineered in this

way would have the added advantage of greater uniformity, making them a more attractive prospect for commercialisation.

Chapter 7: References

1. Absalon, S., D. M. Kochanek, V. Raghavan and A. M. Krichevsky (2013). "MiR-26b, upregulated in Alzheimer's disease, activates cell cycle entry, tau-phosphorylation, and apoptosis in postmitotic neurons." Journal of Neuroscience **33**(37): 14645-14659.
2. Adell, A. Y. and D. Teis (2011). "Assembly and disassembly of the ESCRT-III membrane scission complex." FEBS letters **585**(20): 3191-3196.
3. Aderem, A. and D. M. Underhill (1999). "Mechanisms of phagocytosis in macrophages." Annual review of immunology **17**(1): 593-623.
4. Ahmed, F., H. R. Ansari and G. P. Raghava (2009). "Prediction of guide strand of microRNAs from its sequence and secondary structure." BMC bioinformatics **10**(1): 105.
5. Al-Nedawi, K., B. Meehan, J. Micallef, V. Lhotak, L. May, A. Guha and J. Rak (2008). "Intercellular transfer of the oncogenic receptor EGFRvIII by microvesicles derived from tumour cells." Nature cell biology **10**(5): 619-624.
6. Ali, B. and M. Seabra (2005). Targeting of Rab GTPases to cellular membranes, Portland Press Limited.
7. Alvarez-Erviti, L., Y. Seow, H. Yin, C. Betts, S. Lakhal and M. J. Wood (2011). "Delivery of siRNA to the mouse brain by systemic injection of targeted exosomes." Nature biotechnology **29**(4): 341-345.
8. Anderson, W., D. Kozak, V. A. Coleman, Å. K. Jämting and M. Trau (2013). "A comparative study of submicron particle sizing platforms: accuracy, precision and resolution analysis of polydisperse particle size distributions." Journal of colloid and interface science **405**: 322-330.
9. Andreazzoli, M. (2009). "Molecular regulation of vertebrate retina cell fate." Birth Defects Research Part C: Embryo Today: Reviews **87**(3): 284-295.
10. Andreeva, K. and N. G. Cooper (2014). "MicroRNAs in the neural retina." International journal of genomics **2014**.
11. Andrews, S. (2017). FastQC: a quality control tool for high throughput sequence data. 2010.
12. Androutsellis-Theotokis, A., R. R. Leker, F. Soldner, D. J. Hoeppner, R. Ravin, S. W. Poser, M. A. Rueger, S.-K. Bae, R. Kittappa and R. D. McKay (2006). "Notch signalling regulates stem cell numbers in vitro and in vivo." Nature **442**(7104): 823-826.
13. Aramant, R. and M. Seiler (1991). "Cryopreservation and transplantation of immature rat retina into adult rat retina." Brain Res Dev Brain Res **61**(2): 151-159.
14. Ashwell, K., H. Holländer, W. Streit and J. Stone (1989). "The appearance and distribution of microglia in the developing retina of the rat." Visual neuroscience **2**(5): 437-448.
15. Babst, M. (2011). "MVB vesicle formation: ESCRT-dependent, ESCRT-independent and everything in between." Current opinion in cell biology **23**(4): 452-457.
16. Babst, M., D. J. Katzmann, W. B. Snyder, B. Wendland and S. D. Emr (2002). "Endosome-associated complex, ESCRT-II, recruits transport machinery for protein sorting at the multivesicular body." Developmental cell **3**(2): 283-289.
17. Bae, H. W., N. Lee, G. J. Seong, S. Rho, S. Hong and C. Y. Kim (2016). "Protective effect of etanercept, an inhibitor of tumor necrosis factor-α, in a rat model of retinal ischemia." BMC ophthalmology **16**(1): 75.
18. Bahrini, I., J.-h. Song, D. Diez and R. Hanayama (2015). "Neuronal exosomes facilitate synaptic pruning by up-regulating complement factors in microglia." Scientific reports **5**: 7989.
19. Bai, L., H. Shao, H. Wang, Z. Zhang, C. Su, L. Dong, B. Yu, X. Chen, X. Li and X. Zhang (2017). "Effects of mesenchymal stem cell-derived exosomes on experimental autoimmune uveitis." Scientific reports **7**(1): 1-11.
20. Bai, Y., J. x. Ma, J. Guo, J. Wang, M. Zhu, Y. Chen and Y. Z. Le (2009). "Müller cell-derived VEGF is a significant contributor to retinal neovascularization." The Journal of Pathology: A Journal of the Pathological Society of Great Britain and Ireland **219**(4): 446-454.
21. Baietti, M. F., Z. Zhang, E. Mortier, A. Melchior, G. Degeest, A. Geeraerts, Y. Ivarsson, F. Depoortere, C. Coomans and E. Vermeiren (2012). "Syndecan–syntenin–ALIX regulates the biogenesis of exosomes." Nature cell biology **14**(7): 677.
22. Bailey, T. L., J. Johnson, C. E. Grant and W. S. Noble (2015). "The MEME suite." Nucleic acids research **43**(W1): W39-W49.
23. Baj-Krzyworzeka, M., R. Szatanek, K. Węglarczyk, J. Baran, B. Urbanowicz, P. Brański, M. Z. Ratajczak and M. Zembala (2006). "Tumour-derived microvesicles carry several surface determinants and mRNA of tumour cells and transfer some of these determinants to monocytes." Cancer Immunology, Immunotherapy **55**(7): 808-818.

24. Baker, S. J. and E. P. Reddy (1998). "Modulation of life and death by the TNF receptor superfamily." Oncogene **17**(25): 3261.
25. Baneke, A. J., K. S. Lim and M. Stanford (2016). "The pathogenesis of raised intraocular pressure in uveitis." Current eye research **41**(2): 137-149.
26. Banin, E., A. Obolensky, M. Idelson, I. Hemo, E. Reinhardtz, E. Pikarsky, T. Ben-Hur and B. Reubinoff (2006). "Retinal incorporation and differentiation of neural precursors derived from human embryonic stem cells." Stem cells **24**(2): 246-257.
27. Baranyai, T., K. Herczeg, Z. Onódi, I. Voszka, K. Módos, N. Marton, G. Nagy, I. Mäger, M. J. Wood and S. El Andaloussi (2015). "Isolation of exosomes from blood plasma: qualitative and quantitative comparison of ultracentrifugation and size exclusion chromatography methods." PloS one **10**(12): e0145686.
28. Barde, Y.-A., D. Edgar and H. Thoenen (1982). "Purification of a new neurotrophic factor from mammalian brain." The EMBO journal **1**(5): 549-553.
29. Bari, R., Q. Guo, B. Xia, Y. H. Zhang, E. E. Giesert, S. Levy, J. J. Zheng and X. A. Zhang (2011). "Tetraspanins regulate the protrusive activities of cell membrane." Biochemical and biophysical research communications **415**(4): 619-626.
30. Barranco, I., L. Padilla, I. Parrilla, A. Álvarez-Barrientos, C. Pérez-Patiño, F. J. Peña, E. A. Martínez, H. Rodriguez-Martínez and J. Roca (2019). "Extracellular vesicles isolated from porcine seminal plasma exhibit different tetraspanin expression profiles." Scientific reports **9**(1): 1-9.
31. Barrès, C., L. Blanc, P. Bette-Bobillo, S. André, R. Mamoun, H.-J. Gabius and M. Vidal (2010). "Galectin-5 is bound onto the surface of rat reticulocyte exosomes and modulates vesicle uptake by macrophages." Blood **115**(3): 696-705.
32. Basso, M., S. Pozzi, M. Tortarolo, F. Fiordaliso, C. Bisighini, L. Pasetto, G. Spaltro, D. Lidonnici, F. Gensano and E. Battaglia (2013). "Mutant Copper-Zinc Superoxide Dismutase (SOD1) Induces Protein Secretion Pathway Alterations and Exosome Release in Astrocytes IMPLICATIONS FOR DISEASE SPREADING AND MOTOR NEURON PATHOLOGY IN AMYOTROPHIC LATERAL SCLEROSIS." Journal of Biological Chemistry **288**(22): 15699-15711.
33. Baye, L. M. and B. A. Link (2007). "Interkinetic nuclear migration and the selection of neurogenic cell divisions during vertebrate retinogenesis." Journal of Neuroscience **27**(38): 10143-10152.
34. Beaudoin, A. R. and G. Grondin (1991). "Shedding of vesicular material from the cell surface of eukaryotic cells: different cellular phenomena." Biochimica et Biophysica Acta (BBA)-Reviews on Biomembranes **1071**(3): 203-219.
35. Becker, A., B. K. Thakur, J. M. Weiss, H. S. Kim, H. Peinado and D. Lyden (2016). "Extracellular vesicles in cancer: cell-to-cell mediators of metastasis." Cancer cell **30**(6): 836-848.
36. Becker, S., K. Eastlake, H. Jayaram, M. F. Jones, R. A. Brown, G. J. McLellan, D. G. Charteris, P. T. Khaw and G. A. Limb (2016). "Allogeneic Transplantation of Muller-Derived Retinal Ganglion Cells Improves Retinal Function in a Feline Model of Ganglion Cell Depletion." Stem Cells Transl Med **5**(2): 192-205.
37. Becker, S., K. Eastlake, H. Jayaram, M. F. Jones, R. A. Brown, G. J. McLellan, D. G. Charteris, P. T. Khaw and G. A. Limb (2016). "Allogeneic Transplantation of Müller-Derived Retinal Ganglion Cells Improves Retinal Function in a Feline Model of Ganglion Cell Depletion." Stem cells translational medicine **5**(2): 192-205.
38. Bellingham, S. A., B. M. Coleman and A. F. Hill (2012). "Small RNA deep sequencing reveals a distinct miRNA signature released in exosomes from prion-infected neuronal cells." Nucleic acids research **40**(21): 10937-10949.
39. Bengtsson, B. (1976). "The variation and covariation of cup and disc diameters." Acta ophthalmologica **54**(6): 804-818.
40. Benmerah, A., M. Bayrou, N. Cerf-Bensussan and A. Dautry-Varsat (1999). "Inhibition of clathrin-coated pit assembly by an Eps15 mutant." Journal of cell science **112**(9): 1303-1311.
41. Bernardos, R. L., L. K. Barthel, J. R. Meyers and P. A. Raymond (2007). "Late-stage neuronal progenitors in the retina are radial Müller glia that function as retinal stem cells." Journal of Neuroscience **27**(26): 7028-7040.
42. Bernstein, E., S. Y. Kim, M. A. Carmell, E. P. Murchison, H. Alcorn, M. Z. Li, A. A. Mills, S. J. Elledge, K. V. Anderson and G. J. Hannon (2003). "Dicer is essential for mouse development." Nature genetics **35**(3): 215-217.
43. Besse, B., M. Charrier, V. Lapierre, E. Dansin, O. Lantz, D. Planchard, T. Le Chevalier, A. Livartoski, F. Barlesi and A. Laplanche (2016). "Dendritic cell-derived exosomes as maintenance

immunotherapy after first line chemotherapy in NSCLC." Oncoimmunology **5**(4): e1071008.
44. Bevers, E. M., P. Comfurius, D. W. Dekkers and R. F. Zwaal (1999). "Lipid translocation across the plasma membrane of mammalian cells." Biochimica et Biophysica Acta (BBA)-Molecular and Cell Biology of Lipids **1439**(3): 317-330.
45. Bezzi, P., M. Domercq, L. Brambilla, R. Galli, D. Schols, E. De Clercq, A. Vescovi, G. Bagetta, G. Kollias and J. Meldolesi (2001). "CXCR4-activated astrocyte glutamate release via TNFα: amplification by microglia triggers neurotoxicity." Nature neuroscience **4**(7): 702-710.
46. Bhatia, B., H. Jayaram, S. Singhal, M. F. Jones and G. A. Limb (2011). "Differences between the neurogenic and proliferative abilities of Muller glia with stem cell characteristics and the ciliary epithelium from the adult human eye." Exp Eye Res **93**(6): 852-861.
47. Bhattacharyya, S. N., R. Habermacher, U. Martine, E. I. Closs and W. Filipowicz (2006). "Relief of microRNA-mediated translational repression in human cells subjected to stress." Cell **125**(6): 1111-1124.
48. Bieniasz, P. D. (2009). "The cell biology of HIV-1 virion genesis." Cell host & microbe **5**(6): 550-558.
49. Bobrie, A., M. Colombo, S. Krumeich, G. Raposo and C. Théry (2012). "Diverse subpopulations of vesicles secreted by different intracellular mechanisms are present in exosome preparations obtained by differential ultracentrifugation." Journal of extracellular vesicles **1**(1): 18397.
50. Bonini, S., L. Aloe, S. Bonini, P. Rama, A. Lamagna and A. Lambiase (2002). Nerve growth factor (NGF): an important molecule for trophism and healing of the ocular surface. Lacrimal Gland, Tear Film, and Dry Eye Syndromes 3, Springer**:** 531-537.
51. Bratton, D. L., V. A. Fadok, D. A. Richter, J. M. Kailey, L. A. Guthrie and P. M. Henson (1997). "Appearance of phosphatidylserine on apoptotic cells requires calcium-mediated nonspecific flip-flop and is enhanced by loss of the aminophospholipid translocase." Journal of Biological Chemistry **272**(42): 26159-26165.
52. Bringmann, A., A. Grosche, T. Pannicke and A. Reichenbach (2013). "GABA and glutamate uptake and metabolism in retinal glial (Müller) cells." Frontiers in endocrinology **4**: 48.
53. Bringmann, A., I. Iandiev, T. Pannicke, A. Wurm, M. Hollborn, P. Wiedemann, N. N. Osborne and A. Reichenbach (2009). "Cellular signaling and factors involved in Müller cell gliosis: neuroprotective and detrimental effects." Progress in retinal and eye research **28**(6): 423-451.
54. Bringmann, A., T. Pannicke, J. Grosche, M. Francke, P. Wiedemann, S. N. Skatchkov, N. N. Osborne and A. Reichenbach (2006). "Muller cells in the healthy and diseased retina." Prog Retin Eye Res **25**(4): 397-424.
55. Bringmann, A. and P. Wiedemann (2012). "Müller glial cells in retinal disease." Ophthalmologica **227**(1): 1-19.
56. Bruno, M. A. and A. C. Cuello (2006). "Activity-dependent release of precursor nerve growth factor, conversion to mature nerve growth factor, and its degradation by a protease cascade." Proceedings of the National Academy of Sciences **103**(17): 6735-6740.
57. Bruno, S., F. Collino, M. C. Deregibus, C. Grange, C. Tetta and G. Camussi (2013). "Microvesicles derived from human bone marrow mesenchymal stem cells inhibit tumor growth." Stem cells and development **22**(5): 758-771.
58. Bui, B. V. and B. Fortune (2004). "Ganglion cell contributions to the rat full-field electroretinogram." The Journal of physiology **555**(1): 153-173.
59. Bull, N. D., K.-A. Irvine, R. J. Franklin and K. R. Martin (2009). "Transplanted oligodendrocyte precursor cells reduce neurodegeneration in a model of glaucoma." Investigative ophthalmology & visual science **50**(9): 4244-4253.
60. Busk, P. K. (2014). "A tool for design of primers for microRNA-specific quantitative RT-qPCR." BMC bioinformatics **15**(1): 1-9.
61. Butowt, R. and C. S. von Bartheld (2001). "Sorting of internalized neurotrophins into an endocytic transcytosis pathway via the Golgi system: ultrastructural analysis in retinal ganglion cells." Journal of Neuroscience **21**(22): 8915-8930.
62. Cai, F., W. M. Campana, D. R. Tomlinson and P. Fernyhough (1999). "Transforming growth factor-β1 and glial growth factor 2 reduce neurotrophin-3 mRNA expression in cultured Schwann cells via a cAMP-dependent pathway." Molecular brain research **71**(2): 256-264.
63. Calin, G. A., C. D. Dumitru, M. Shimizu, R. Bichi, S. Zupo, E. Noch, H. Aldler, S. Rattan, M. Keating and K. Rai (2002). "Frequent deletions and down-regulation of micro-RNA genes miR15 and miR16 at 13q14 in chronic lymphocytic leukemia." Proceedings of the national academy of

sciences **99**(24): 15524-15529.
64. Canossa, M., O. Griesbeck, B. Berninger, G. Campana, R. Kolbeck and H. Thoenen (1997). "Neurotrophin release by neurotrophins: implications for activity-dependent neuronal plasticity." Proceedings of the National Academy of Sciences **94**(24): 13279-13286.
65. Caputo, V., L. Sinibaldi, A. Fiorentino, C. Parisi, C. Catalanotto, A. Pasini, C. Cogoni and A. Pizzuti (2011). "Brain derived neurotrophic factor (BDNF) expression is regulated by microRNAs miR-26a and miR-26b allele-specific binding." PloS one **6**(12): e28656.
66. Carthew, R. W. and E. J. Sontheimer (2009). "Origins and mechanisms of miRNAs and siRNAs." Cell **136**(4): 642-655.
67. Casaccia-Bonnefil, P., C. Gu and M. Chao (1999). Neurotrophins in cell survival/death decisions. The functional roles of glial cells in health and disease, Springer**:** 275-282.
68. Castillo Jr, B., M. Del Cerro, X. Breakefield, D. Frim, C. Barnstable, D. Dean and M. Bohn (1994). "Retinal ganglion cell survival is promoted by genetically modified astrocytes designed to secrete brain-derived neurotrophic factor (BDNF)." Brain research **647**(1): 30-36.
69. Chan, S. J., C. Love, M. Spector, S. M. Cool, V. Nurcombe and E. H. Lo (2017). "Endogenous regeneration: Engineering growth factors for stroke." Neurochemistry international **107**: 57-65.
70. Chao, M. V. and B. L. Hempstead (1995). "p75 and Trk: a two-receptor system." Trends in neurosciences **18**(7): 321-326.
71. Chargaff, E. and R. West (1946). "The biological significance of the thromboplastic protein of blood." J Biol Chem **166**(1): 189-197.
72. Chen, H. and A. Weber (2004). "Brain-derived neurotrophic factor (BDNF) reduces tyrosine kinase B (trkB) receptor protein in the normal rat retina and following optic nerve damage." Brain Res **1011**: 99-106.
73. Cheng, L., R. A. Sharples, B. J. Scicluna and A. F. Hill (2014). "Exosomes provide a protective and enriched source of miRNA for biomarker profiling compared to intracellular and cell-free blood." Journal of extracellular vesicles **3**(1): 23743.
74. Chevillet, J. R., Q. Kang, I. K. Ruf, H. A. Briggs, L. N. Vojtech, S. M. Hughes, H. H. Cheng, J. D. Arroyo, E. K. Meredith and E. N. Gallichotte (2014). "Quantitative and stoichiometric analysis of the microRNA content of exosomes." Proceedings of the National Academy of Sciences **111**(41): 14888-14893.
75. Chiba, M., M. Kimura and S. Asari (2012). "Exosomes secreted from human colorectal cancer cell lines contain mRNAs, microRNAs and natural antisense RNAs, that can transfer into the human hepatoma HepG2 and lung cancer A549 cell lines." Oncology reports **28**(5): 1551-1558.
76. Choi, D. S., D. K. Kim, Y. K. Kim and Y. S. Gho (2013). "Proteomics, transcriptomics and lipidomics of exosomes and ectosomes." Proteomics **13**(10-11): 1554-1571.
77. Chowdhury, R., J. P. Webber, M. Gurney, M. D. Mason, Z. Tabi and A. Clayton (2015). "Cancer exosomes trigger mesenchymal stem cell differentiation into pro-angiogenic and pro-invasive myofibroblasts." Oncotarget **6**(2): 715.
78. Christianson, H. C., K. J. Svensson, T. H. van Kuppevelt, J.-P. Li and M. Belting (2013). "Cancer cell exosomes depend on cell-surface heparan sulfate proteoglycans for their internalization and functional activity." Proceedings of the National Academy of Sciences **110**(43): 17380-17385.
79. Clark, A., W.-H. Wang and L. McNatt (2006). RNAi inhibition of serum amyloid a for treatment of glaucoma, Google Patents.
80. Clayton, A., C. L. Harris, J. Court, M. D. Mason and B. P. Morgan (2003). "Antigen-presenting cell exosomes are protected from complement-mediated lysis by expression of CD55 and CD59." European journal of immunology **33**(2): 522-531.
81. Cochella, L. and O. Hobert (2012). Diverse functions of microRNAs in nervous system development. Current topics in developmental biology, Elsevier. **99:** 115-143.
82. Cohen, S. and R. Levi-Montalcini (1957). "Purification and properties of a nerve growth-promoting factor isolated from mouse sarcoma 180." Cancer research **17**(1): 15-20.
83. Collins, A., D. Li, S. B. McMahon, G. Raisman and Y. Li (2017). "Transplantation of cultured olfactory bulb cells prevents abnormal sensory responses during recovery from dorsal root avulsion in the rat." Cell transplantation **26**(5): 913-924.
84. Conde-Vancells, J., E. Rodriguez-Suarez, N. Embade, D. Gil, R. Matthiesen, M. Valle, F. Elortza, S. C. Lu, J. M. Mato and J. M. Falcon-Perez (2008). "Characterization and comprehensive proteome profiling of exosomes secreted by hepatocytes." Journal of proteome research **7**(12): 5157-5166.
85. Cooper, J. M., P. O. Wiklander, J. Z. Nordin, R. Al-Shawi, M. J. Wood, M. Vithlani, A. H. Schapira, J.

P. Simons, S. El-Andaloussi and L. Alvarez-Erviti (2014). "Systemic exosomal siRNA delivery reduced alpha-synuclein aggregates in brains of transgenic mice." Movement Disorders **29**(12): 1476-1485.
86. Coordinators, N. R. (2017). "Database resources of the national center for biotechnology information." Nucleic acids research **45**(Database issue): D12.
87. Crescitelli, R., C. Lässer, T. G. Szabó, A. Kittel, M. Eldh, I. Dianzani, E. I. Buzás and J. Lötvall (2013). "Distinct RNA profiles in subpopulations of extracellular vesicles: apoptotic bodies, microvesicles and exosomes." Journal of extracellular vesicles **2**(1): 20677.
88. Cui, G. H., J. Wu, F. F. Mou, W. H. Xie, F. B. Wang, Q. L. Wang, J. Fang, Y. W. Xu, Y. R. Dong and J. R. Liu (2018). "Exosomes derived from hypoxia-preconditioned mesenchymal stromal cells ameliorate cognitive decline by rescuing synaptic dysfunction and regulating inflammatory responses in APP/PS1 mice." The FASEB Journal **32**(2): 654-668.
89. Dajas-Bailador, F., B. Bonev, P. Garcez, P. Stanley, F. Guillemot and N. Papalopulu (2012). "microRNA-9 regulates axon extension and branching by targeting Map1b in mouse cortical neurons." Nature neuroscience **15**(5): 697.
90. Das, A. V., K. B. Mallya, X. Zhao, F. Ahmad, S. Bhattacharya, W. B. Thoreson, G. V. Hegde and I. Ahmad (2006). "Neural stem cell properties of Müller glia in the mammalian retina: regulation by Notch and Wnt signaling." Developmental biology **299**(1): 283-302.
91. de Melo Reis, R. A., A. L. M. Ventura, C. S. Schitine, M. C. F. de Mello and F. G. de Mello (2008). "Müller glia as an active compartment modulating nervous activity in the vertebrate retina: neurotransmitters and trophic factors." Neurochemical research **33**(8): 1466-1474.
92. de Miguel-Beriain, I. (2015). "The ethics of stem cells revisited." Adv Drug Deliv Rev **82-83**: 176-180.
93. del Amo, E. M., A.-K. Rimpelä, E. Heikkinen, O. K. Kari, E. Ramsay, T. Lajunen, M. Schmitt, L. Pelkonen, M. Bhattacharya and D. Richardson (2017). "Pharmacokinetic aspects of retinal drug delivery." Progress in retinal and eye research **57**: 134-185.
94. del Cerro, M., M. F. Notter, C. del Cerro, S. J. Wiegand, D. A. Grover and E. Lazar (1989). "Intraretinal transplantation for rod-cell replacement in light-damaged retinas." J Neural Transplant **1**(1): 1-10.
95. Delaune, E., P. Lemaire and L. Kodjabachian (2005). "Neural induction in Xenopus requires early FGF signalling in addition to BMP inhibition." Development **132**(2): 299-310.
96. Denli, A. M., B. B. Tops, R. H. Plasterk, R. F. Ketting and G. J. Hannon (2004). "Processing of primary microRNAs by the Microprocessor complex." Nature **432**(7014): 231-235.
97. Denzer, K., M. J. Kleijmeer, H. Heijnen, W. Stoorvogel and H. J. Geuze (2000). "Exosome: from internal vesicle of the multivesicular body to intercellular signaling device." Journal of cell science **113**(19): 3365-3374.
98. Di Polo, A., L. J. Aigner, R. J. Dunn, G. M. Bray and A. J. Aguayo (1998). "Prolonged delivery of brain-derived neurotrophic factor by adenovirus-infected Müller cells temporarily rescues injured retinal ganglion cells." Proceedings of the National Academy of Sciences **95**(7): 3978-3983.
99. Dinger, M. E., T. R. Mercer and J. S. Mattick (2008). "RNAs as extracellular signaling molecules." Journal of molecular endocrinology **40**(4): 151-159.
100. Doherty, G. J. and H. T. McMahon (2009). "Mechanisms of endocytosis." Annual review of biochemistry **78**: 857-902.
101. Donaldson, J. G. (2003). "Multiple roles for Arf6: sorting, structuring, and signaling at the plasma membrane." Journal of Biological Chemistry **278**(43): 41573-41576.
102. Downward, J. (2004). PI 3-kinase, Akt and cell survival. Seminars in cell & developmental biology, Elsevier.
103. Dozio, V. and J.-C. Sanchez (2017). "Characterisation of extracellular vesicle-subsets derived from brain endothelial cells and analysis of their protein cargo modulation after TNF exposure." Journal of extracellular vesicles **6**(1): 1302705.
104. Drazba, J. and V. Lemmon (1990). "The role of cell adhesion molecules in neurite outgrowth on Müller cells." Developmental biology **138**(1): 82-93.
105. Eastlake, K., W. E. Heywood, D. Tracey-White, E. Aquino, E. Bliss, G. R. Vasta, K. Mills, P. T. Khaw, M. Moosajee and G. A. Limb (2017). "Comparison of proteomic profiles in the zebrafish retina during experimental degeneration and regeneration." Scientific reports **7**: 44601.
106. Eastlake, K., W. Wang, H. Jayaram, C. Murray-Dunning, A. J. Carr, C. M. Ramsden, A. Vugler, K. Gore, N. Clemo and M. Stewart (2019). "Phenotypic and functional characterization of Müller glia

isolated from induced pluripotent stem cell-derived retinal organoids: Improvement of retinal ganglion cell function upon transplantation." Stem cells translational medicine **8**(8): 775-784.
107. Edbauer, D., J. R. Neilson, K. A. Foster, C.-F. Wang, D. P. Seeburg, M. N. Batterton, T. Tada, B. M. Dolan, P. A. Sharp and M. Sheng (2010). "Regulation of synaptic structure and function by FMRP-associated microRNAs miR-125b and miR-132." Neuron **65**(3): 373-384.
108. Eden, E. R., T. Burgoyne and C. E. Futter (2016). "Multivesicular Bodies: Roles in Intracellular and Intercellular Signaling." Lysosomes: Biology, Diseases, and Therapeutics: Biology, Diseases, and Therapeutics: 33-49.
109. Eirin, A., S. M. Riester, X.-Y. Zhu, H. Tang, J. M. Evans, D. O'Brien, A. J. van Wijnen and L. O. Lerman (2014). "MicroRNA and mRNA cargo of extracellular vesicles from porcine adipose tissue-derived mesenchymal stem cells." Gene **551**(1): 55-64.
110. Englund-Johansson, U., C. Mohlin, I. Liljekvist-Soltic, P. Ekström and K. Johansson (2010). "Human neural progenitor cells promote photoreceptor survival in retinal explants." Experimental eye research **90**(2): 292-299.
111. Erickson, J. T., J. C. Conover, V. Borday, J. Champagnat, M. Barbacid, G. Yancopoulos and D. M. Katz (1996). "Mice lacking brain-derived neurotrophic factor exhibit visceral sensory neuron losses distinct from mice lacking NT4 and display a severe developmental deficit in control of breathing." Journal of Neuroscience **16**(17): 5361-5371.
112. Escrevente, C., S. Keller, P. Altevogt and J. Costa (2011). "Interaction and uptake of exosomes by ovarian cancer cells." BMC cancer **11**(1): 108.
113. Escudier, B., T. Dorval, N. Chaput, F. André, M.-P. Caby, S. Novault, C. Flament, C. Leboulaire, C. Borg and S. Amigorena (2005). "Vaccination of metastatic melanoma patients with autologous dendritic cell (DC) derived-exosomes: results of thefirst phase I clinical trial." Journal of translational medicine **3**(1): 10.
114. Eulalio, A., E. Huntzinger and E. Izaurralde (2008). "GW182 interaction with Argonaute is essential for miRNA-mediated translational repression and mRNA decay." Nature structural & molecular biology **15**(4): 346.
115. Fadok, V. A., D. Voelker, P. Campbell, J. Cohen, D. Bratton and P. Henson (1992). "Exposure of phosphatidylserine on the surface of apoptotic lymphocytes triggers specific recognition and removal by macrophages." The Journal of Immunology **148**(7): 2207-2216.
116. Fahnestock, M., B. Michalski, B. Xu and M. D. Coughlin (2001). "The precursor pro-nerve growth factor is the predominant form of nerve growth factor in brain and is increased in Alzheimer's disease." Molecular and Cellular Neuroscience **18**(2): 210-220.
117. Fahy, E. T., V. Chrysostomou and J. G. Crowston (2016). "Mini-review: impaired axonal transport and glaucoma." Current eye research **41**(3): 273-283.
118. Fan, G., C. Egles, Y. Sun, L. Minichiello, J. J. Renger, R. Klein, G. Liu and R. Jaenisch (2000). "Knocking the NT4 gene into the BDNF locus rescues BDNF deficient mice and reveals distinct NT4 and BDNF activities." Nature neuroscience **3**(4): 350.
119. Fausett, B. V. and D. Goldman (2006). "A role for α1 tubulin-expressing Müller glia in regeneration of the injured zebrafish retina." Journal of Neuroscience **26**(23): 6303-6313.
120. Feng, D., W. L. Zhao, Y. Y. Ye, X. C. Bai, R. Q. Liu, L. F. Chang, Q. Zhou and S. F. Sui (2010). "Cellular internalization of exosomes occurs through phagocytosis." Traffic **11**(5): 675-687.
121. Ferreira, A. F., G. A. Calin, V. Picanço-Castro, S. Kashima, D. T. Covas and F. A. de Castro (2018). "Hematopoietic stem cells from induced pluripotent stem cells–considering the role of microRNA as a cell differentiation regulator." J Cell Sci **131**(4): jcs203018.
122. Ferrer, I., E. Goutan, C. Marın, M. Rey and T. Ribalta (2000). "Brain-derived neurotrophic factor in Huntington disease." Brain research **866**(1-2): 257-261.
123. Filipe, V., A. Hawe and W. Jiskoot (2010). "Critical evaluation of Nanoparticle Tracking Analysis (NTA) by NanoSight for the measurement of nanoparticles and protein aggregates." Pharmaceutical research **27**(5): 796-810.
124. Fimbel, S. M., J. E. Montgomery, C. T. Burket and D. R. Hyde (2007). "Regeneration of inner retinal neurons after intravitreal injection of ouabain in zebrafish." Journal of Neuroscience **27**(7): 1712-1724.
125. Fink, S. L. and B. T. Cookson (2005). "Apoptosis, pyroptosis, and necrosis: mechanistic description of dead and dying eukaryotic cells." Infection and immunity **73**(4): 1907-1916.
126. Fiore, R., S. Khudayberdiev, M. Christensen, G. Siegel, S. W. Flavell, T. K. Kim, M. E. Greenberg and G. Schratt (2009). "Mef2-mediated transcription of the miR379–410 cluster regulates activity-

dependent dendritogenesis by fine-tuning Pumilio2 protein levels." The EMBO journal **28**(6): 697-710.
127. Fitzner, D., M. Schnaars, D. van Rossum, G. Krishnamoorthy, P. Dibaj, M. Bakhti, T. Regen, U.-K. Hanisch and M. Simons (2011). "Selective transfer of exosomes from oligodendrocytes to microglia by macropinocytosis." Journal of cell science **124**(3): 447-458.
128. Flaxman, S. R., R. R. Bourne, S. Resnikoff, P. Ackland, T. Braithwaite, M. V. Cicinelli, A. Das, J. B. Jonas, J. Keeffe and J. H. Kempen (2017). "Global causes of blindness and distance vision impairment 1990–2020: a systematic review and meta-analysis." The Lancet Global Health **5**(12): e1221-e1234.
129. Fortune, B., B. V. Bui, J. C. Morrison, E. C. Johnson, J. Dong, W. O. Cepurna, L. Jia, S. Barber and G. A. Cioffi (2004). "Selective ganglion cell functional loss in rats with experimental glaucoma." Investigative ophthalmology & visual science **45**(6): 1854-1862.
130. Franze, K., J. Grosche, S. N. Skatchkov, S. Schinkinger, C. Foja, D. Schild, O. Uckermann, K. Travis, A. Reichenbach and J. Guck (2007). "Müller cells are living optical fibers in the vertebrate retina." Proceedings of the National Academy of Sciences **104**(20): 8287-8292.
131. Franzen, C. A., P. E. Simms, A. F. Van Huis, K. E. Foreman, P. C. Kuo and G. N. Gupta (2014). "Characterization of uptake and internalization of exosomes by bladder cancer cells." BioMed research international **2014**.
132. Freund-Michel, V., C. Bertrand and N. Frossard (2006). "TrkA signalling pathways in human airway smooth muscle cell proliferation." Cellular signalling **18**(5): 621-627.
133. Friedman, R. C., K. K.-H. Farh, C. B. Burge and D. P. Bartel (2009). "Most mammalian mRNAs are conserved targets of microRNAs." Genome research **19**(1): 92-105.
134. Frühbeis, C., D. Fröhlich, W. P. Kuo, J. Amphornrat, S. Thilemann, A. S. Saab, F. Kirchhoff, W. Möbius, S. Goebbels and K.-A. Nave (2013). "Neurotransmitter-triggered transfer of exosomes mediates oligodendrocyte–neuron communication." PLoS Biol **11**(7): e1001604.
135. Fuentealba, L. C., S. B. Rompani, J. I. Parraguez, K. Obernier, R. Romero, C. L. Cepko and A. Alvarez-Buylla (2015). "Embryonic origin of postnatal neural stem cells." Cell **161**(7): 1644-1655.
136. Fukuchi, T., J. Ueda, T. Hanyu, H. Abe and S. Sawaguchi (2001). "Distribution and Expression of Transforming Growth Factor-β and Platelet-derived Growth Factor in the Normal and Glaucomatous Monkey Optic Nerve Heads." Japanese journal of ophthalmology **45**(6): 592-599.
137. Gadient, R., K. Cron and U. Otten (1990). "Interleukin-1 β and tumor necrosis factor-α synergistically stimulate nerve growth factor (NGF) release from cultured rat astrocytes." Neuroscience letters **117**(3): 335-340.
138. Gan, L., S. W. Wang, Z. Huang and W. H. Klein (1999). "POU domain factor Brn-3b is essential for retinal ganglion cell differentiation and survival but not for initial cell fate specification." Developmental biology **210**(2): 469-480.
139. García, M., V. Forster, D. Hicks and E. Vecino (2002). "Müller glia enhance ganglion cells survival and neuritogenesis in adult pig retina in vitro." Invest. Ophthalmol. Vis. Sci **43**: 3735-3743.
140. García, M. n., V. Forster, D. Hicks and E. Vecino (2002). "Effects of muller glia on cell survival and neuritogenesis in adult porcine retina in vitro." Investigative ophthalmology & visual science **43**(12): 3735-3743.
141. Garharta, C. and V. Lakshminarayananb (2015). "Anatomy of the Eye."
142. Gasser, O. and J. r. A. Schifferli (2004). "Activated polymorphonuclear neutrophils disseminate anti-inflammatory microparticles by ectocytosis." Blood **104**(8): 2543-2548.
143. Ge, Q., Y. Zhou, J. Lu, Y. Bai, X. Xie and Z. Lu (2014). "miRNA in plasma exosome is stable under different storage conditions." Molecules **19**(2): 1568-1575.
144. Gillespie, D. C., M. C. Crair and M. P. Stryker (2000). "Neurotrophin-4/5 alters responses and blocks the effect of monocular deprivation in cat visual cortex during the critical period." Journal of Neuroscience **20**(24): 9174-9186.
145. Glebova, N. O. and D. D. Ginty (2005). "Growth and survival signals controlling sympathetic nervous system development." Annu. Rev. Neurosci. **28**: 191-222.
146. Goldie, B. J., M. D. Dun, M. Lin, N. D. Smith, N. M. Verrills, C. V. Dayas and M. J. Cairns (2014). "Activity-associated miRNA are packaged in Map1b-enriched exosomes released from depolarized neurons." Nucleic acids research **42**(14): 9195-9208.
147. Goldman, D. (2014). "Müller glial cell reprogramming and retina regeneration." Nature Reviews Neuroscience **15**(7): 431.
148. Gonzalez-Cordero, A., K. Kruczek, A. Naeem, M. Fernando, M. Kloc, J. Ribeiro, D. Goh, Y. Duran, S.

J. I. Blackford, L. Abelleira-Hervas, R. D. Sampson, I. O. Shum, M. J. Branch, P. J. Gardner, J. C. Sowden, J. W. B. Bainbridge, A. J. Smith, E. L. West, R. A. Pearson and R. R. Ali (2017). "Recapitulation of Human Retinal Development from Human Pluripotent Stem Cells Generates Transplantable Populations of Cone Photoreceptors." Stem Cell Reports **9**(3): 820-837.

149. Grider, M., D. Park, D. Spencer and H. Shine (2009). "Lipid raft-targeted Akt promotes axonal branching and growth cone expansion via mTOR and Rac1, respectively." Journal of neuroscience research **87**(14): 3033-3042.
150. Groth, S. L. (2018). "Prospects for Neuroprotection in Glaucoma." Review of Optometry **155**(2): 68-72.
151. Gruber, H., G. Hoelscher, S. Bethea and E. Hanley Jr (2012). "Interleukin 1-beta upregulates brain-derived neurotrophic factor, neurotrophin 3 and neuropilin 2 gene expression and NGF production in annulus cells." Biotechnic & Histochemistry **87**(8): 506-511.
152. Guduric-Fuchs, J., A. O'Connor, B. Camp, C. L. O'Neill, R. J. Medina and D. A. Simpson (2012). "Selective extracellular vesicle-mediated export of an overlapping set of microRNAs from multiple cell types." BMC genomics **13**(1): 357.
153. Guescini, M., S. Genedani, V. Stocchi and L. F. Agnati (2010). "Astrocytes and Glioblastoma cells release exosomes carrying mtDNA." Journal of neural transmission **117**(1): 1.
154. Guo, H., N. T. Ingolia, J. S. Weissman and D. P. Bartel (2010). "Mammalian microRNAs predominantly act to decrease target mRNA levels." Nature **466**(7308): 835-840.
155. Guo, L., S. E. Moss, R. A. Alexander, R. R. Ali, F. W. Fitzke and M. F. Cordeiro (2005). "Retinal ganglion cell apoptosis in glaucoma is related to intraocular pressure and IOP-induced effects on extracellular matrix." Investigative ophthalmology & visual science **46**(1): 175-182.
156. Guo, L., T. E. Salt, A. Maass, V. Luong, S. E. Moss, F. W. Fitzke and M. F. Cordeiro (2006). "Assessment of neuroprotective effects of glutamate modulation on glaucoma-related retinal ganglion cell apoptosis in vivo." Investigative ophthalmology & visual science **47**(2): 626-633.
157. Gupta, V., Y. You, J. Li, V. Gupta, M. Golzan, A. Klistorner, M. van den Buuse and S. Graham (2014). "BDNF impairment is associated with age-related changes in the inner retina and exacerbates experimental glaucoma." Biochimica et Biophysica Acta (BBA)-Molecular Basis of Disease **1842**(9): 1567-1578.
158. Ha, M. and V. N. Kim (2014). "Regulation of microRNA biogenesis." Nature reviews Molecular cell biology **15**(8): 509-524.
159. Hagiwara, S., P. Kantharidis and M. E Cooper (2014). "MicroRNA as biomarkers and regulator of cardiovascular development and disease." Current pharmaceutical design **20**(14): 2347-2370.
160. Halkein, J., S. P. Tabruyn, M. Ricke-Hoch, A. Haghikia, M. Scherr, K. Castermans, L. Malvaux, V. Lambert, M. Thiry and K. Sliwa (2013). "MicroRNA-146a is a therapeutic target and biomarker for peripartum cardiomyopathy." The Journal of clinical investigation **123**(5): 2143-2154.
161. Hallböök, F., C. F. Ibáñez and H. Persson (1991). "Evolutionary studies of the nerve growth factor family reveal a novel member abundantly expressed in Xenopus ovary." Neuron **6**(5): 845-858.
162. Hankin, M. H. and R. D. Lund (1987). "Specific target-directed axonal outgrowth from transplanted embryonic rodent retinae into neonatal rat superior colliculus." Brain Res **408**(1-2): 344-348.
163. Hankin, M. H. and R. D. Lund (1990). "Directed early axonal outgrowth from retinal transplants into host rat brains." J Neurobiol **21**(8): 1202-1218.
164. Harada, C., X. Guo, K. Namekata, A. Kimura, K. Nakamura, K. Tanaka, L. F. Parada and T. Harada (2011). "Glia-and neuron-specific functions of TrkB signalling during retinal degeneration and regeneration." Nature communications **2**(1): 1-9.
165. Harada, T., C. Harada, S. Kohsaka, E. Wada, K. Yoshida, S. Ohno, H. Mamada, K. Tanaka, L. F. Parada and K. Wada (2002). "Microglia–Müller glia cell interactions control neurotrophic factor production during light-induced retinal degeneration." Journal of Neuroscience **22**(21): 9228-9236.
166. Harraz, M. M., S. M. Eacker, X. Wang, T. M. Dawson and V. L. Dawson (2012). "MicroRNA-223 is neuroprotective by targeting glutamate receptors." Proceedings of the National Academy of Sciences **109**(46): 18962-18967.
167. He, X., Q. Zhang, Y. Liu and X. Pan (2007). "Cloning and identification of novel microRNAs from rat hippocampus." Acta biochimica et biophysica Sinica **39**(9): 708-714.
168. Hemler, M. E. (2003). "Tetraspanin proteins mediate cellular penetration, invasion, and fusion events and define a novel type of membrane microdomain." Annual review of cell and

developmental biology **19**(1): 397-422.
169. Henderson, C. E. (1996). "Role of neurotrophic factors in neuronal development." Current opinion in neurobiology **6**(1): 64-70.
170. Hergenreider, E., S. Heydt, K. Tréguer, T. Boettger, A. J. Horrevoets, A. M. Zeiher, M. P. Scheffer, A. S. Frangakis, X. Yin and M. Mayr (2012). "Atheroprotective communication between endothelial cells and smooth muscle cells through miRNAs." Nature cell biology **14**(3): 249.
171. Heusermann, W., J. Hean, D. Trojer, E. Steib, S. Von Bueren, A. Graff-Meyer, C. Genoud, K. Martin, N. Pizzato and J. Voshol (2016). "Exosomes surf on filopodia to enter cells at endocytic hot spots, traffic within endosomes, and are targeted to the ER." Journal of Cell Biology **213**(2): 173-184.
172. Hildebrand, G. D. and A. R. Fielder (2011). Anatomy and physiology of the retina. Pediatric retina, Springer**:** 39-65.
173. Hitchcock, P. F., K. J. L. Myhr, S. S. Easter Jr, R. Mangione-Smith and D. D. Jones (1992). "Local regeneration in the retina of the goldfish." Journal of neurobiology **23**(2): 187-203.
174. Homma, K., S. Okamoto, M. Mandai, N. Gotoh, H. K. Rajasimha, Y. S. Chang, S. Chen, W. Li, T. Cogliati, A. Swaroop and M. Takahashi (2013). "Developing rods transplanted into the degenerating retina of Crx-knockout mice exhibit neural activity similar to native photoreceptors." Stem Cells **31**(6): 1149-1159.
175. Honjo, M., H. Tanihara, N. Kido, M. Inatani, K. Okazaki and Y. Honda (2000). "Expression of ciliary neurotrophic factor activated by retinal Muller cells in eyes with NMDA-and kainic acid–induced neuronal death." Investigative ophthalmology & visual science **41**(2): 552-560.
176. Horibe, S., T. Tanahashi, S. Kawauchi, Y. Murakami and Y. Rikitake (2018). "Mechanism of recipient cell-dependent differences in exosome uptake." BMC cancer **18**(1): 47.
177. Howells, D., M. J. Porritt, J. Wong, P. Batchelor, R. Kalnins, A. Hughes and G. Donnan (2000). "Reduced BDNF mRNA expression in the Parkinson's disease substantia nigra." Experimental neurology **166**(1): 127-135.
178. Hu, Z.-L., N. Li, X. Wei, L. Tang, T.-H. Wang and X.-M. Chen (2017). "Neuroprotective effects of BDNF and GDNF in intravitreally transplanted mesenchymal stem cells after optic nerve crush in mice." International journal of ophthalmology **10**(1): 35.
179. Huang, H., M. Kolibabka, R. Eshwaran, A. Chatterjee, A. Schlotterer, H. Willer, K. Bieback, H. P. Hammes and Y. Feng (2019). "Intravitreal injection of mesenchymal stem cells evokes retinal vascular damage in rats." The FASEB Journal **33**(12): 14668-14679.
180. Hunter, M. P., N. Ismail, X. Zhang, B. D. Aguda, E. J. Lee, L. Yu, T. Xiao, J. Schafer, M.-L. T. Lee and T. D. Schmittgen (2008). "Detection of microRNA expression in human peripheral blood microvesicles." PloS one **3**(11).
181. Huntzinger, E. and E. Izaurralde (2011). "Gene silencing by microRNAs: contributions of translational repression and mRNA decay." Nature Reviews Genetics **12**(2): 99-110.
182. Hur, E.-M., C.-M. Liu, Z. Jiao, W.-L. Xu and F.-Q. Zhou (2013). "PI3K–GSK3 signalling regulates mammalian axon regeneration by inducing the expression of Smad1." Nature communications **4**: 2690.
183. Hurley, J. H. (2010). "The ESCRT complexes." Critical reviews in biochemistry and molecular biology **45**(6): 463-487.
184. Hutzinger, R., R. Feederle, J. Mrazek, N. Schiefermeier, P. J. Balwierz, M. Zavolan, N. Polacek, H.-J. Delecluse and A. Hüttenhofer (2009). "Expression and processing of a small nucleolar RNA from the Epstein-Barr virus genome." PLoS pathogens **5**(8).
185. Hwang, H. and J. Mendell (2006). "MicroRNAs in cell proliferation, cell death, and tumorigenesis." British journal of cancer **94**(6): 776-780.
186. Iavello, A., V. S. Frech, C. Gai, M. C. Deregibus, P. J. Quesenberry and G. Camussi (2016). "Role of Alix in miRNA packaging during extracellular vesicle biogenesis." International journal of molecular medicine **37**(4): 958-966.
187. Ibáñez, C. F. (1996). "Neurotrophin-4: the odd one out in the neurotrophin family." Neurochemical research **21**(7): 787-793.
188. Ibrahim, A. G.-E., K. Cheng and E. Marbán (2014). "Exosomes as critical agents of cardiac regeneration triggered by cell therapy." Stem cell reports **2**(5): 606-619.
189. Ikeda, K., H. Tanihara, Y. Honda, T. Tatsuno, H. Noguchi and C. Nakayama (1999). "BDNF attenuates retinal cell death caused by chemically induced hypoxia in rats." Investigative ophthalmology & visual science **40**(9): 2130-2140.
190. Imai, T., Y. Takahashi, M. Nishikawa, K. Kato, M. Morishita, T. Yamashita, A. Matsumoto, C.

Charoenviriyakul and Y. Takakura (2015). "Macrophage-dependent clearance of systemically administered B16BL6-derived exosomes from the blood circulation in mice." Journal of extracellular vesicles **4**(1): 26238.
191. Ivanisevic, L., W. Zheng, S. B. Woo, K. E. Neet and H. U. Saragovi (2007). "TrkA receptor "hot spots" for binding of NT-3 as a heterologous ligand." Journal of Biological Chemistry **282**(23): 16754-16763.
192. Iwabe, S., N. A. Moreno-Mendoza, F. Trigo-Tavera, C. Crowder and G. A. García-Sánchez (2007). "Retrograde axonal transport obstruction of brain-derived neurotrophic factor (BDNF) and its TrkB receptor in the retina and optic nerve of American Cocker Spaniel dogs with spontaneous glaucoma." Veterinary ophthalmology **10**: 12-19.
193. Izumi, Y., K. Shimamoto, A. M. Benz, S. B. Hammerman, J. W. Olney and C. F. Zorumski (2002). "Glutamate transporters and retinal excitotoxicity." Glia **39**(1): 58-68.
194. Jayaram, H., M. F. Jones, K. Eastlake, P. B. Cottrill, S. Becker, J. Wiseman, P. T. Khaw and G. A. Limb (2014). "Transplantation of photoreceptors derived from human Muller glia restore rod function in the P23H rat." Stem Cells Transl Med **3**(3): 323-333.
195. Jayaram, H., M. F. Jones, K. Eastlake, P. B. Cottrill, S. Becker, J. Wiseman, P. T. Khaw and G. A. Limb (2014). "Transplantation of photoreceptors derived from human Müller glia restore rod function in the P23H rat." Stem cells translational medicine **3**(3): 323-333.
196. Ji, J. Z., W. Elyaman, H. K. Yip, V. W. Lee, L. W. Yick, J. Hugon and K. F. So (2004). "CNTF promotes survival of retinal ganglion cells after induction of ocular hypertension in rats: the possible involvement of STAT3 pathway." European Journal of Neuroscience **19**(2): 265-272.
197. Ji, S., S. Lin, J. Chen, X. Huang, C.-C. Wei, Z. Li and S. Tang (2018). "Neuroprotection of transplanting human umbilical cord mesenchymal stem cells in a microbead induced ocular hypertension rat model." Current eye research **43**(6): 810-820.
198. Jiang, J., C. Liu, B. Zhang, X. Wang, M. Zhang, S. Zhang, P. Hall, Y. Hu and F. Zhou (2015). "MicroRNA-26a supports mammalian axon regeneration in vivo by suppressing GSK3 β expression." Cell death & disease **6**(8): e1865-e1865.
199. Jin, Y., K. Chen, Z. Wang, Y. Wang, J. Liu, L. Lin, Y. Shao, L. Gao, H. Yin and C. Cui (2016). "DNA in serum extracellular vesicles is stable under different storage conditions." BMC cancer **16**(1): 753.
200. Joachim, S. C., J. Reichelt, S. Berneiser, N. Pfeiffer and F. H. Grus (2008). "Sera of glaucoma patients show autoantibodies against myelin basic protein and complex autoantibody profiles against human optic nerve antigens." Graefe's Archive for Clinical and Experimental Ophthalmology **246**(4): 573-580.
201. Johnson, E. C., L. M. Deppmeier, S. K. Wentzien, I. Hsu and J. C. Morrison (2000). "Chronology of optic nerve head and retinal responses to elevated intraocular pressure." Investigative ophthalmology & visual science **41**(2): 431-442.
202. Johnson, L. F., H. T. Abelson, S. Penman and H. Green (1977). "The relative amounts of the cytoplasmic RNA species in normal, transformed and senescent cultured cell lines." Journal of cellular physiology **90**(3): 465-470.
203. Johnson, T. V., N. D. Bull, D. P. Hunt, N. Marina, S. I. Tomarev and K. R. Martin (2010). "Neuroprotective effects of intravitreal mesenchymal stem cell transplantation in experimental glaucoma." Investigative ophthalmology & visual science **51**(4): 2051-2059.
204. Johnstone, R. M., M. Adam, J. Hammond, L. Orr and C. Turbide (1987). "Vesicle formation during reticulocyte maturation. Association of plasma membrane activities with released vesicles (exosomes)." Journal of Biological Chemistry **262**(19): 9412-9420.
205. Jones, B. W., C. B. Watt, J. M. Frederick, W. Baehr, C. K. Chen, E. M. Levine, A. H. Milam, M. M. Lavail and R. E. Marc (2003). "Retinal remodeling triggered by photoreceptor degenerations." J Comp Neurol **464**(1): 1-16.
206. Jones, R. S., M. Pedisich, R. C. Carroll and S. Nawy (2014). "Spatial organization of AMPAR subtypes in ON RGCs." Journal of Neuroscience **34**(2): 656-661.
207. Ju, W.-K., K.-Y. Kim, M. Angert, K. X. Duong-Polk, J. D. Lindsey, M. H. Ellisman and R. N. Weinreb (2009). "Memantine blocks mitochondrial OPA1 and cytochrome c release and subsequent apoptotic cell death in glaucomatous retina." Investigative ophthalmology & visual science **50**(2): 707-716.
208. Katoh-Semba, R., I. K. Takeuchi, R. Semba and K. Kato (1997). "Distribution of brain-derived neurotrophic factor in rats and its changes with development in the brain." Journal of neurochemistry **69**(1): 34-42.

209. Kawasaki, A., Y. Otori and C. J. Barnstable (2000). "Muller cell protection of rat retinal ganglion cells from glutamate and nitric oxide neurotoxicity." Investigative ophthalmology & visual science **41**(11): 3444-3450.
210. Keerthikumar, S., D. Chisanga, D. Ariyaratne, H. Al Saffar, S. Anand, K. Zhao, M. Samuel, M. Pathan, M. Jois and N. Chilamkurti (2016). "ExoCarta: a web-based compendium of exosomal cargo." Journal of molecular biology **428**(4): 688-692.
211. Kerr, M. C. and R. D. Teasdale (2009). "Defining macropinocytosis." Traffic **10**(4): 364-371.
212. Kettenmann, H., U.-K. Hanisch, M. Noda and A. Verkhratsky (2011). "Physiology of microglia." Physiological reviews **91**(2): 461-553.
213. Kim, D.-K., J. Lee, R. J. Simpson, J. Lötvall and Y. S. Gho (2015). EVpedia: A community web resource for prokaryotic and eukaryotic extracellular vesicles research. Seminars in cell & developmental biology, Elsevier.
214. Kim, M. S., M. J. Haney, Y. Zhao, D. Yuan, I. Deygen, N. L. Klyachko, A. V. Kabanov and E. V. Batrakova (2018). "Engineering macrophage-derived exosomes for targeted paclitaxel delivery to pulmonary metastases: in vitro and in vivo evaluations." Nanomedicine: Nanotechnology, Biology and Medicine **14**(1): 195-204.
215. Kim, S. R., X. Chen, T. F. Oo, T. Kareva, O. Yarygina, C. Wang, M. During, N. Kholodilov and R. E. Burke (2011). "Dopaminergic pathway reconstruction by Akt/Rheb-induced axon regeneration." Annals of neurology **70**(1): 110-120.
216. Kim, Y.-K., B. Kim and V. N. Kim (2016). "Re-evaluation of the roles of DROSHA, Exportin 5, and DICER in microRNA biogenesis." Proceedings of the National Academy of Sciences **113**(13): E1881-E1889.
217. Kirwan, R. P., J. K. Crean, C. H. Fenerty, A. F. Clark and C. J. O'Brien (2004). "Effect of cyclical mechanical stretch and exogenous transforming growth factor-β1 on matrix metalloproteinase-2 activity in lamina cribrosa cells from the human optic nerve head." Journal of glaucoma **13**(4): 327-334.
218. Knox, D. L., R. C. Eagle and W. R. Green (2007). "Optic nerve hydropic axonal degeneration and blocked retrograde axoplasmic transport: histopathologic features in human high-pressure secondary glaucoma." Archives of ophthalmology **125**(3): 347-353.
219. Kobayashi, H. and Y. Tomari (2016). "RISC assembly: Coordination between small RNAs and Argonaute proteins." Biochimica et Biophysica Acta (BBA)-Gene Regulatory Mechanisms **1859**(1): 71-81.
220. Kolodny, G. (1971). "Evidence for transfer of macromolecular RNA between mammalian cells in culture." Experimental cell research **65**(2): 313-324.
221. Kong, Y. X. G., A. Gibbins and A. Brooks (2019). "Glaucoma in perspective." Medical Journal of Australia **210**(4): 150-152. e151.
222. Kooijmans, S. A., C. G. Aleza, S. R. Roffler, W. W. van Solinge, P. Vader and R. M. Schiffelers (2016). "Display of GPI-anchored anti-EGFR nanobodies on extracellular vesicles promotes tumour cell targeting." Journal of extracellular vesicles **5**(1): 31053.
223. Koppers-Lalic, D., M. Hackenberg, I. V. Bijnsdorp, M. A. van Eijndhoven, P. Sadek, D. Sie, N. Zini, J. M. Middeldorp, B. Ylstra and R. X. de Menezes (2014). "Nontemplated nucleotide additions distinguish the small RNA composition in cells from exosomes." Cell reports **8**(6): 1649-1658.
224. Kosaka, N., H. Iguchi, K. Hagiwara, Y. Yoshioka, F. Takeshita and T. Ochiya (2013). "Neutral sphingomyelinase 2 (nSMase2)-dependent exosomal transfer of angiogenic microRNAs regulate cancer cell metastasis." Journal of Biological Chemistry: jbc. M112. 446831.
225. Kowal, J., G. Arras, M. Colombo, M. Jouve, J. P. Morath, B. Primdal-Bengtson, F. Dingli, D. Loew, M. Tkach and C. Théry (2016). "Proteomic comparison defines novel markers to characterize heterogeneous populations of extracellular vesicle subtypes." Proceedings of the National Academy of Sciences **113**(8): E968-E977.
226. Kozomara, A., M. Birgaoanu and S. Griffiths-Jones (2019). "miRBase: from microRNA sequences to function." Nucleic acids research **47**(D1): D155-D162.
227. Krabbe, K., A. Nielsen, R. Krogh-Madsen, P. Plomgaard, P. Rasmussen, C. Erikstrup, C. Fischer, B. Lindegaard, A. Petersen and S. Taudorf (2007). "Brain-derived neurotrophic factor (BDNF) and type 2 diabetes." Diabetologia **50**(2): 431-438.
228. Krämer-Albers, E. M., N. Bretz, S. Tenzer, C. Winterstein, W. Möbius, H. Berger, K. A. Nave, H. Schild and J. Trotter (2007). "Oligodendrocytes secrete exosomes containing major myelin and stress-protective proteins: Trophic support for axons?" PROTEOMICS–Clinical Applications **1**(11): 1446-

1461.
229. Kriegstein, A. and A. Alvarez-Buylla (2009). "The glial nature of embryonic and adult neural stem cells." Annual review of neuroscience **32**: 149-184.
230. Kuang, Y., Q. Liu, X. Shu, C. Zhang, N. Huang, J. Li, M. Jiang and H. Li (2012). "Dicer1 and MiR-9 are required for proper Notch1 signaling and the Bergmann glial phenotype in the developing mouse cerebellum." Glia **60**(11): 1734-1746.
231. Kuehn, M. H., C. Y. Kim, J. Ostojic, M. Bellin, W. L. Alward, E. M. Stone, D. S. Sakaguchi, S. D. Grozdanic and Y. H. Kwon (2006). "Retinal synthesis and deposition of complement components induced by ocular hypertension." Experimental eye research **83**(3): 620-628.
232. Kumar, P., H. Wu, J. L. McBride, K.-E. Jung, M. H. Kim, B. L. Davidson, S. K. Lee, P. Shankar and N. Manjunath (2007). "Transvascular delivery of small interfering RNA to the central nervous system." Nature **448**(7149): 39-43.
233. Kuno, R., Y. Yoshida, A. Nitta, T. Nabeshima, J. Wang, Y. Sonobe, J. Kawanokuchi, H. Takeuchi, T. Mizuno and A. Suzumura (2006). "The role of TNF-alpha and its receptors in the production of NGF and GDNF by astrocytes." Brain research **1116**(1): 12-18.
234. Kuppermann, B. D., D. S. Boyer, B. Mills, J. Yang and H. J. Klassen (2018). "Safety and Activity of a Single, Intravitreal Injection of Human Retinal Progenitor Cells (jCell) for Treatment of Retinitis Pigmentosa (RP)." Investigative Ophthalmology & Visual Science **59**(9): 2987-2987.
235. Kuriyan, A. E., T. A. Albini, J. H. Townsend, M. Rodriguez, H. K. Pandya, R. E. Leonard, M. B. Parrott, P. J. Rosenfeld, H. W. Flynn Jr and J. L. Goldberg (2017). "Vision loss after intravitreal injection of autologous "stem cells" for AMD." New England journal of medicine **376**(11): 1047-1053.
236. Kustermann, S., H. Hildebrandt, S. Bolz, K. Dengler and K. Kohler (2010). "Genesis of rods in the zebrafish retina occurs in a microenvironment provided by polysialic acid-expressing Müller glia." Journal of Comparative Neurology **518**(5): 636-646.
237. Kusuma, G. D., M. Barabadi, J. L. Tan, D. A. Morton, J. E. Frith and R. Lim (2018). "To protect and to preserve: novel preservation strategies for extracellular vesicles." Frontiers in pharmacology **9**: 1199.
238. Kuzuoğlu-Öztürk, D., D. Bhandari, E. Huntzinger, M. Fauser, S. Helms and E. Izaurralde (2016). "miRISC and the CCR4–NOT complex silence mRNA targets independently of 43S ribosomal scanning." The EMBO journal **35**(11): 1186-1203.
239. Kwon, S. C., T. A. Nguyen, Y.-G. Choi, M. H. Jo, S. Hohng, V. N. Kim and J.-S. Woo (2016). "Structure of human DROSHA." Cell **164**(1-2): 81-90.
240. Lai, R. C., T. S. Chen and S. K. Lim (2011). "Mesenchymal stem cell exosome: a novel stem cell-based therapy for cardiovascular disease." Regenerative medicine **6**(4): 481-492.
241. Lam, T. T., A. S. Abler, J. M. Kwong and M. O. Tso (1999). "N-methyl-D-aspartate (NMDA)–induced apoptosis in rat retina." Investigative ophthalmology & visual science **40**(10): 2391-2397.
242. Lamballe, F., R. Klein and M. Barbacid (1991). "trkC, a new member of the trk family of tyrosine protein kinases, is a receptor for neurotrophin-3." Cell **66**(5): 967-979.
243. Lambiase, A., L. Aloe, M. Centofanti, V. Parisi, F. Mantelli, V. Colafrancesco, G. L. Manni, M. G. Bucci, S. Bonini and R. Levi-Montalcini (2009). "Experimental and clinical evidence of neuroprotection by nerve growth factor eye drops: Implications for glaucoma." Proceedings of the National Academy of Sciences **106**(32): 13469-13474.
244. Lambiase, A., M. Centofanti, A. Micera, G. L. Manni, E. Mattei, A. De Gregorio, G. De Feo, M. G. Bucci and L. Aloe (1997). "Nerve growth factor (NGF) reduces and NGF antibody exacerbates retinal damage induced in rabbit by experimental ocular hypertension." Graefe's archive for clinical and experimental ophthalmology **235**(12): 780-785.
245. Lamriben, L., J. B. Graham, B. M. Adams and D. N. Hebert (2016). "N-Glycan-based ER Molecular Chaperone and Protein Quality Control System: The Calnexin Binding Cycle." Traffic **17**(4): 308-326.
246. Lancaster, G. I. and M. A. Febbraio (2005). "Exosome-dependent trafficking of HSP70 A novel secretory pathway for cellular stress proteins." Journal of Biological Chemistry **280**(24): 23349-23355.
247. Langmead, B. and S. Salzberg (2013). "Langmead. 2013. Bowtie2." Nature Methods **9**: 357-359.
248. Lawrence, J. M., S. Singhal, B. Bhatia, D. J. Keegan, T. A. Reh, P. J. Luthert, P. T. Khaw and G. A. Limb (2007). "MIO-M1 cells and similar muller glial cell lines derived from adult human retina exhibit neural stem cell characteristics." Stem Cells **25**(8): 2033-2043.
249. Lebrun-Julien, F., B. Morquette, A. Douillette, H. U. Saragovi and A. Di Polo (2009). "Inhibition of

p75 NTR in glia potentiates TrkA-mediated survival of injured retinal ganglion cells." Molecular and Cellular Neuroscience **40**(4): 410-420.
250. Lee, A. H., C. Lange, R. Ricken, R. Hellweg and U. E. Lang (2011). "Reduced brain-derived neurotrophic factor serum concentrations in acute schizophrenic patients increase during antipsychotic treatment." Journal of clinical psychopharmacology **31**(3): 334-336.
251. Lee, J.-Y., J.-M. Shin, M.-H. Chun and S.-J. Oh (2014). "Morphological analyses on retinal glial responses to glaucomatous injury evoked by venous cauterization." Applied Microscopy **44**(1): 21-29.
252. Lee, Y., S. El Andaloussi and M. J. Wood (2012). "Exosomes and microvesicles: extracellular vesicles for genetic information transfer and gene therapy." Human molecular genetics **21**(R1): R125-R134.
253. Lengner, C. J. (2010). "iPS cell technology in regenerative medicine." Ann N Y Acad Sci **1192**: 38-44.
254. Leventis, P. A. and S. Grinstein (2010). "The distribution and function of phosphatidylserine in cellular membranes." Annual review of biophysics **39**: 407-427.
255. Lévesque, K., M. Halvorsen, L. Abrahamyan, L. Chatel-Chaix, V. Poupon, H. Gordon, L. DesGroseillers, A. Gatignol and A. J. Mouland (2006). "Trafficking of HIV-1 RNA is mediated by heterogeneous nuclear ribonucleoprotein A2 expression and impacts on viral assembly." Traffic **7**(9): 1177-1193.
256. Levkovitch-Verbin, H., O. Sadan, S. Vander, M. Rosner, Y. Barhum, E. Melamed, D. Offen and S. Melamed (2010). "Intravitreal injections of neurotrophic factors secreting mesenchymal stem cells are neuroprotective in rat eyes following optic nerve transection." Investigative ophthalmology & visual science **51**(12): 6394-6400.
257. Li, G., C. Luna, P. B. Liton, I. Navarro, D. L. Epstein and P. Gonzalez (2007). "Sustained stress response after oxidative stress in trabecular meshwork cells." Molecular vision **13**: 2282.
258. Li, S., Q. He, H. Wang, X. Tang, K. W. Ho, X. Gao, Q. Zhang, Y. Shen, A. Cheung and F. Wong (2015). "Injured adult retinal axons with Pten and Socs3 co-deletion reform active synapses with suprachiasmatic neurons." Neurobiology of disease **73**: 366-376.
259. Li, X. J., Z. J. Ren, J. H. Tang and Q. Yu (2017). "Exosomal MicroRNA MiR-1246 promotes cell proliferation, invasion and drug resistance by targeting CCNG2 in breast cancer." Cellular Physiology and Biochemistry **44**(5): 1741-1748.
260. Li, Y., P. Jung and A. Brown (2012). "Axonal transport of neurofilaments: a single population of intermittently moving polymers." Journal of Neuroscience **32**(2): 746-758.
261. Liang, Y., Y. Yu, H. Yu and L. Ma (2019). "Effect of BDNF-TrKB pathway on apoptosis of retinal ganglion cells in glaucomatous animal model." European review for medical and pharmacological sciences **23**(9): 3561-3568.
262. Limb, G. A., T. E. Salt, P. M. Munro, S. E. Moss and P. T. Khaw (2002). "In vitro characterization of a spontaneously immortalized human Muller cell line (MIO-M1)." Investigative ophthalmology & visual science **43**(3): 864-869.
263. Lingor, P., P. Koeberle, S. Kügler and M. Bähr (2005). "Down-regulation of apoptosis mediators by RNAi inhibits axotomy-induced retinal ganglion cell death in vivo." Brain **128**(3): 550-558.
264. Lonfat, N. and C. Cepko (2017). "Epigenomics of Retinal Development in Mice and Humans." Neuron **94**(3): 420-423.
265. Lopez-Verrilli, M. A., A. Caviedes, A. Cabrera, S. Sandoval, U. Wyneken and M. Khoury (2016). "Mesenchymal stem cell-derived exosomes from different sources selectively promote neuritic outgrowth." Neuroscience **320**: 129-139.
266. Lötvall, J., A. F. Hill, F. Hochberg, E. I. Buzás, D. Di Vizio, C. Gardiner, Y. S. Gho, I. V. Kurochkin, S. Mathivanan and P. Quesenberry (2014). Minimal experimental requirements for definition of extracellular vesicles and their functions: a position statement from the International Society for Extracellular Vesicles, Taylor & Francis.
267. Love, M., S. Anders and W. Huber (2014). "Differential analysis of count data–the DESeq2 package." Genome Biol **15**(550): 10-1186.
268. Love, M. I., S. Anders and W. Huber (2019). Analyzing RNA-seq data with DESeq2.
269. Lunavat, T. R., L. Cheng, D.-K. Kim, J. Bhadury, S. C. Jang, C. Lässer, R. A. Sharples, M. D. López, J. Nilsson and Y. S. Gho (2015). "Small RNA deep sequencing discriminates subsets of extracellular vesicles released by melanoma cells–Evidence of unique microRNA cargos." RNA biology **12**(8): 810-823.

270. Lund, R. D., S. Wang, B. Lu, S. Girman, T. Holmes, Y. Sauve, D. J. Messina, I. R. Harris, A. J. Kihm, A. M. Harmon, F. Y. Chin, A. Gosiewska and S. K. Mistry (2007). "Cells isolated from umbilical cord tissue rescue photoreceptors and visual functions in a rodent model of retinal disease." Stem Cells **25**(3): 602-611.
271. Luo, M., X. Tan, L. Mu, Y. Luo, R. Li, X. Deng, N. Chen, M. Ren, Y. Li and L. Wang (2017). "MiRNA-21 mediates the antiangiogenic activity of metformin through targeting PTEN and SMAD7 expression and PI3K/AKT pathway." Scientific reports **7**: 43427.
272. Lv, L.-L., Y. Cao, D. Liu, M. Xu, H. Liu, R.-N. Tang, K.-L. Ma and B.-C. Liu (2013). "Isolation and quantification of microRNAs from urinary exosomes/microvesicles for biomarker discovery." International journal of biological sciences **9**(10): 1021.
273. Ma, Y.-T., T. Hsieh, M. E. Forbes, J. E. Johnson and D. O. Frost (1998). "BDNF injected into the superior colliculus reduces developmental retinal ganglion cell death." Journal of Neuroscience **18**(6): 2097-2107.
274. MacLaren, R. E. and R. A. Pearson (2007). "Stem cell therapy and the retina." Eye (Lond) **21**(10): 1352-1359.
275. MacLaren, R. E., R. A. Pearson, A. MacNeil, R. H. Douglas, T. E. Salt, M. Akimoto, A. Swaroop, J. C. Sowden and R. R. Ali (2006). "Retinal repair by transplantation of photoreceptor precursors." Nature **444**(7116): 203-207.
276. Maehama, T. and J. E. Dixon (1998). "The tumor suppressor, PTEN/MMAC1, dephosphorylates the lipid second messenger, phosphatidylinositol 3, 4, 5-trisphosphate." Journal of Biological Chemistry **273**(22): 13375-13378.
277. Maes, M. E., C. L. Schlamp and R. W. Nickells (2017). "BAX to basics: How the BCL2 gene family controls the death of retinal ganglion cells." Progress in retinal and eye research **57**: 1-25.
278. Magill, S. T., X. A. Cambronne, B. W. Luikart, D. T. Lioy, B. H. Leighton, G. L. Westbrook, G. Mandel and R. H. Goodman (2010). "microRNA-132 regulates dendritic growth and arborization of newborn neurons in the adult hippocampus." Proceedings of the National Academy of Sciences **107**(47): 20382-20387.
279. Maisonpierre, P. C., L. Belluscio, S. Squinto, N. Y. Ip, M. E. Furth, R. M. Lindsay and G. D. Yancopoulos (1990). "Neurotrophin-3: a neurotrophic factor related to NGF and BDNF." Science **247**(4949): 1446-1451.
280. Maji, S., I. K. Yan, M. Parasramka, S. Mohankumar, A. Matsuda and T. Patel (2017). "In vitro toxicology studies of extracellular vesicles." Journal of Applied Toxicology **37**(3): 310-318.
281. Mak, H. K., S. H. Ng, T. Ren, C. Ye and C. K.-s. Leung (2020). "Impact of PTEN/SOCS3 deletion on amelioration of dendritic shrinkage of retinal ganglion cells after optic nerve injury." Experimental Eye Research **192**: 107938.
282. Malik, J., Z. Shevtsova, M. Bähr and S. Kügler (2005). "Long-term in vivo inhibition of CNS neurodegeneration by Bcl-XL gene transfer." Molecular Therapy **11**(3): 373-381.
283. Mandel, P. and P. Metais (1948). "Les acides nucleiques du plasma sanguine chez l'homme."
284. Martin, K. R., H. A. Quigley, D. J. Zack, H. Levkovitch-Verbin, J. Kielczewski, D. Valenta, L. Baumrind, M. E. Pease, R. L. Klein and W. W. Hauswirth (2003). "Gene therapy with brain-derived neurotrophic factor as a protection: retinal ganglion cells in a rat glaucoma model." Investigative ophthalmology & visual science **44**(10): 4357-4365.
285. Martin, M. (2011). "Cutadapt removes adapter sequences from high-throughput sequencing reads." EMBnet. journal **17**(1): 10-12.
286. Martínez, T., M. V. González, I. Roehl, N. Wright, C. Pañeda and A. I. Jiménez (2014). "In vitro and in vivo efficacy of SYL040012, a novel siRNA compound for treatment of glaucoma." Molecular Therapy **22**(1): 81-91.
287. Mathys, H., J. Basquin, S. Ozgur, M. Czarnocki-Cieciura, F. Bonneau, A. Aartse, A. Dziembowski, M. Nowotny, E. Conti and W. Filipowicz (2014). "Structural and biochemical insights to the role of the CCR4-NOT complex and DDX6 ATPase in microRNA repression." Molecular cell **54**(5): 751-765.
288. Matsumoto, A., Y. Takahashi, M. Nishikawa, K. Sano, M. Morishita, C. Charoenviriyakul, H. Saji and Y. Takakura (2017). "Role of phosphatidylserine-derived negative surface charges in the recognition and uptake of intravenously injected B16BL6-derived exosomes by macrophages." Journal of pharmaceutical sciences **106**(1): 168-175.
289. McHugh, K. J., M. Saint-Geniez and S. L. Tao (2013). "Topographical control of ocular cell types for tissue engineering." J Biomed Mater Res B Appl Biomater **101**(8): 1571-1584.

290. Mead, B., Z. Ahmed and S. Tomarev (2018). "Mesenchymal Stem Cell–Derived Small Extracellular Vesicles Promote Neuroprotection in a Genetic DBA/2J Mouse Model of Glaucoma." Investigative ophthalmology & visual science **59**(13): 5473-5480.
291. Mead, B., J. Amaral and S. Tomarev (2018). "Mesenchymal Stem Cell–Derived Small Extracellular Vesicles Promote Neuroprotection in Rodent Models of Glaucoma." Investigative ophthalmology & visual science **59**(2): 702-714.
292. Mead, B., X. Chamling, D. J. Zack, Z. Ahmed and S. Tomarev (2020). "TNFα-Mediated Priming of Mesenchymal Stem Cells Enhances Their Neuroprotective Effect on Retinal Ganglion Cells." Investigative ophthalmology & visual science **61**(2): 6-6.
293. Mead, B., A. Logan, M. Berry, W. Leadbeater and B. A. Scheven (2013). "Intravitreally transplanted dental pulp stem cells promote neuroprotection and axon regeneration of retinal ganglion cells after optic nerve injury." Investigative ophthalmology & visual science **54**(12): 7544-7556.
294. Mead, B. and B. A. Scheven (2015). "Mesenchymal stem cell therapy for retinal ganglion cell neuroprotection and axon regeneration." Neural regeneration research **10**(3): 371.
295. Mead, B. and S. Tomarev (2017). "Bone Marrow-Derived Mesenchymal Stem Cells-Derived Exosomes Promote Survival of Retinal Ganglion Cells Through miRNA-Dependent Mechanisms." Stem cells translational medicine **6**(4): 1273-1285.
296. Meares, G. P., R. Rajbhandari, M. Gerigk, C. L. Tien, C. Chang, S. C. Fehling, A. Rowse, K. C. Mulhern, S. Nair and G. K. Gray (2018). "MicroRNA-31 is required for astrocyte specification." Glia **66**(5): 987-998.
297. Men, Y., J. Yelick, S. Jin, Y. Tian, M. S. R. Chiang, H. Higashimori, E. Brown, R. Jarvis and Y. Yang (2019). "Exosome reporter mice reveal the involvement of exosomes in mediating neuron to astroglia communication in the CNS." Nature communications **10**(1): 1-18.
298. Mensinger, A. F. and M. K. Powers (1999). "Visual function in regenerating teleost retina following cytotoxic lesioning." Visual neuroscience **16**(2): 241-251.
299. Merkle, F. T., A. D. Tramontin, J. M. García-Verdugo and A. Alvarez-Buylla (2004). "Radial glia give rise to adult neural stem cells in the subventricular zone." Proceedings of the National Academy of Sciences **101**(50): 17528-17532.
300. Mesentier-Louro, L. A., C. Zaverucha-do-Valle, A. J. da Silva-Junior, G. Nascimento-dos-Santos, F. Gubert, A. B. P. de Figueirêdo, A. L. Torres, B. D. Paredes, C. Teixeira and F. Tovar-Moll (2014). "Distribution of mesenchymal stem cells and effects on neuronal survival and axon regeneration after optic nerve crush and cell therapy." PLoS One **9**(10).
301. Mey, J. and S. Thanos (1993). "Intravitreal injections of neurotrophic factors support the survival of axotomized retinal ganglion cells in adult rats in vivo." Brain research **602**(2): 304-317.
302. Meyer-Franke, A., M. R. Kaplan, F. W. Pfieger and B. A. Barres (1995). "Characterization of the signaling interactions that promote the survival and growth of developing retinal ganglion cells in culture." Neuron **15**(4): 805-819.
303. Meza-Sosa, K. F., D. Valle-García, G. Pedraza-Alva and L. Pérez-Martínez (2012). "Role of microRNAs in central nervous system development and pathology." Journal of neuroscience research **90**(1): 1-12.
304. Michaelidis, T. M. and D. C. Lie (2008). "Wnt signaling and neural stem cells: caught in the Wnt web." Cell and tissue research **331**(1): 193-210.
305. Michlewski, G. and J. F. Cáceres (2019). "Post-transcriptional control of miRNA biogenesis." Rna **25**(1): 1-16.
306. Miklič, Š., D. M. Jurič and M. Čaman-Kržan (2004). "Differences in the regulation of BDNF and NGF synthesis in cultured neonatal rat astrocytes." International journal of developmental neuroscience **22**(3): 119-130.
307. Miller, R. and J. Dowling (1970). "Intracellular responses of the Müller (glial) cells of mudpuppy retina: their relation to b-wave of the electroretinogram." Journal of neurophysiology **33**(3): 323-341.
308. Minciacchi, V. R., S. You, C. Spinelli, S. Morley, M. Zandian, P.-J. Aspuria, L. Cavallini, C. Ciardiello, M. R. Sobreiro and M. Morello (2015). "Large oncosomes contain distinct protein cargo and represent a separate functional class of tumor-derived extracellular vesicles." Oncotarget **6**(13): 11327.
309. Mitchell, P. S., R. K. Parkin, E. M. Kroh, B. R. Fritz, S. K. Wyman, E. L. Pogosova-Agadjanyan, A. Peterson, J. Noteboom, K. C. O'Briant and A. Allen (2008). "Circulating microRNAs as stable blood-based markers for cancer detection." Proceedings of the National Academy of Sciences **105**(30):

10513-10518.
310. Mittelbrunn, M., C. Gutiérrez-Vázquez, C. Villarroya-Beltri, S. González, F. Sánchez-Cabo, M. Á. González, A. Bernad and F. Sánchez-Madrid (2011). "Unidirectional transfer of microRNA-loaded exosomes from T cells to antigen-presenting cells." Nature communications **2**: 282.
311. Mo, X., A. Yokoyama, T. Oshitari, H. Negishi, M. Dezawa, A. Mizota and E. Adachi-Usami (2002). "Rescue of axotomized retinal ganglion cells by BDNF gene electroporation in adult rats." Investigative ophthalmology & visual science **43**(7): 2401-2405.
312. Mollick, T., C. Mohlin and K. Johansson (2016). "Human neural progenitor cells decrease photoreceptor degeneration, normalize opsin distribution and support synapse structure in cultured porcine retina." Brain research **1646**: 522-534.
313. Montecalvo, A., A. T. Larregina, W. J. Shufesky, D. Beer Stolz, M. L. Sullivan, J. M. Karlsson, C. J. Baty, G. A. Gibson, G. Erdos and Z. Wang (2012). "Mechanism of transfer of functional microRNAs between mouse dendritic cells via exosomes." Blood **119**(3): 756-766.
314. Montgomery, J. E., M. J. Parsons and D. R. Hyde (2010). "A novel model of retinal ablation demonstrates that the extent of rod cell death regulates the origin of the regenerated zebrafish rod photoreceptors." Journal of Comparative Neurology **518**(6): 800-814.
315. Morel, L., M. Regan, H. Higashimori, S. K. Ng, C. Esau, S. Vidensky, J. Rothstein and Y. Yang (2013). "Neuronal exosomal miRNA-dependent translational regulation of astroglial glutamate transporter GLT1." Journal of Biological Chemistry **288**(10): 7105-7116.
316. Morelli, A. E., A. T. Larregina, W. J. Shufesky, M. L. Sullivan, D. B. Stolz, G. D. Papworth, A. F. Zahorchak, A. J. Logar, Z. Wang and S. C. Watkins (2004). "Endocytosis, intracellular sorting, and processing of exosomes by dendritic cells." Blood **104**(10): 3257-3266.
317. Morgan-Warren, P. J., J. O'Neill, F. De Cogan, I. Spivak, H. Ashush, H. Kalinski, Z. Ahmed, M. Berry, E. Feinstein and R. A. Scott (2016). "siRNA-mediated knockdown of the mTOR inhibitor RTP801 promotes retinal ganglion cell survival and axon elongation by direct and indirect mechanisms." Investigative ophthalmology & visual science **57**(2): 429-443.
318. Müller, A., T. G. Hauk, M. Leibinger, R. Marienfeld and D. Fischer (2009). "Exogenous CNTF stimulates axon regeneration of retinal ganglion cells partially via endogenous CNTF." Molecular and Cellular Neuroscience **41**(2): 233-246.
319. Munagala, R., F. Aqil, J. Jeyabalan and R. C. Gupta (2016). "Bovine milk-derived exosomes for drug delivery." Cancer letters **371**(1): 48-61.
320. Murakami, S., H. Imbe, Y. Morikawa, C. Kubo and E. Senba (2005). "Chronic stress, as well as acute stress, reduces BDNF mRNA expression in the rat hippocampus but less robustly." Neuroscience research **53**(2): 129-139.
321. Muralidharan-Chari, V., J. Clancy, C. Plou, M. Romao, P. Chavrier, G. Raposo and C. D'Souza-Schorey (2009). "ARF6-regulated shedding of tumor cell-derived plasma membrane microvesicles." Current Biology **19**(22): 1875-1885.
322. Muralidharan-Chari, V., J. W. Clancy, A. Sedgwick and C. D'Souza-Schorey (2010). "Microvesicles: mediators of extracellular communication during cancer progression." Journal of cell science **123**(10): 1603-1611.
323. Murphy, D. E., O. G. de Jong, M. Brouwer, M. J. Wood, G. Lavieu, R. M. Schiffelers and P. Vader (2019). "Extracellular vesicle-based therapeutics: natural versus engineered targeting and trafficking." Experimental & molecular medicine **51**(3): 1-12.
324. Nabhan, J. F., R. Hu, R. S. Oh, S. N. Cohen and Q. Lu (2012). "Formation and release of arrestin domain-containing protein 1-mediated microvesicles (ARMMs) at plasma membrane by recruitment of TSG101 protein." Proceedings of the National Academy of Sciences **109**(11): 4146-4151.
325. Nagelhus, E. A., Y. Horio, A. Inanobe, A. Fujita, F. m. Haug, S. Nielsen, Y. Kurachi and O. P. Ottersen (1999). "Immunogold evidence suggests that coupling of K+ siphoning and water transport in rat retinal Müller cells is mediated by a coenrichment of Kir4. 1 and AQP4 in specific membrane domains." Glia **26**(1): 47-54.
326. Nakazawa, T., C. Nakazawa, A. Matsubara, K. Noda, T. Hisatomi, H. She, N. Michaud, A. Hafezi-Moghadam, J. W. Miller and L. I. Benowitz (2006). "Tumor necrosis factor-α mediates oligodendrocyte death and delayed retinal ganglion cell loss in a mouse model of glaucoma." Journal of Neuroscience **26**(49): 12633-12641.
327. Nanbo, A., E. Kawanishi, R. Yoshida and H. Yoshiyama (2013). "Exosomes derived from Epstein-Barr virus-infected cells are internalized via caveola-dependent endocytosis and promote

phenotypic modulation in target cells." Journal of virology **87**(18): 10334-10347.
328. Napoli, I. and H. Neumann (2009). "Microglial clearance function in health and disease." Neuroscience **158**(3): 1030-1038.
329. Näslund, T. I., D. Paquin-Proulx, P. T. Paredes, H. Vallhov, J. K. Sandberg and S. Gabrielsson (2014). "Exosomes from breast milk inhibit HIV-1 infection of dendritic cells and subsequent viral transfer to CD4+ T cells." Aids **28**(2): 171-180.
330. Nazari, H., L. Zhang, D. Zhu, G. J. Chader, P. Falabella, F. Stefanini, T. Rowland, D. O. Clegg, A. H. Kashani, D. R. Hinton and M. S. Humayun (2015). "Stem cell based therapies for age-related macular degeneration: The promises and the challenges." Prog Retin Eye Res **48**: 1-39.
331. Nentwich, M. M. and M. W. Ulbig (2015). "Diabetic retinopathy-ocular complications of diabetes mellitus." World journal of diabetes **6**(3): 489.
332. Newman, E. and A. Reichenbach (1996). "The Müller cell: a functional element of the retina." Trends in neurosciences **19**(8): 307-312.
333. Nguyen, S. M., C. N. Alexejun and L. A. Levin (2003). "Amplification of a reactive oxygen species signal in axotomized retinal ganglion cells." Antioxidants and Redox Signaling **5**(5): 629-634.
334. Nolte-'t Hoen, E., T. Cremer, R. C. Gallo and L. B. Margolis (2016). "Extracellular vesicles and viruses: Are they close relatives?" Proc Natl Acad Sci U S A **113**(33): 9155-9161.
335. Nolte-'t Hoen, E. N., H. P. Buermans, M. Waasdorp, W. Stoorvogel, M. H. Wauben and P. A. 't Hoen (2012). "Deep sequencing of RNA from immune cell-derived vesicles uncovers the selective incorporation of small non-coding RNA biotypes with potential regulatory functions." Nucleic acids research **40**(18): 9272-9285.
336. Nuschke, A. C., S. R. Farrell, J. M. Levesque and B. C. Chauhan (2015). "Assessment of retinal ganglion cell damage in glaucomatous optic neuropathy: axon transport, injury and soma loss." Experimental eye research **141**: 111-124.
337. Obregon, C., B. Rothen-Rutishauser, P. Gerber, P. Gehr and L. P. Nicod (2009). "Active uptake of dendritic cell-derived exovesicles by epithelial cells induces the release of inflammatory mediators through a TNF-α-mediated pathway." The American journal of pathology **175**(2): 696-705.
338. Ochiai, Y. and H. Ochiai (2002). "Higher concentration of transforming growth factor-β in aqueous humor of glaucomatous eyes and diabetic eyes." Japanese journal of ophthalmology **46**(3): 249-253.
339. Oddone, F., G. Roberti, A. Micera, A. Busanello, S. Bonini, L. Quaranta, L. Agnifili and G. Manni (2017). "Exploring serum levels of brain derived neurotrophic factor and nerve growth factor across glaucoma stages." PLoS One **12**(1).
340. Ohshima, K., K. Inoue, A. Fujiwara, K. Hatakeyama, K. Kanto, Y. Watanabe, K. Muramatsu, Y. Fukuda, S.-i. Ogura and K. Yamaguchi (2010). "Let-7 microRNA family is selectively secreted into the extracellular environment via exosomes in a metastatic gastric cancer cell line." PloS one **5**(10).
341. Ohtake, Y., U. Hayat and S. Li (2015). "PTEN inhibition and axon regeneration and neural repair." Neural regeneration research **10**(9): 1363.
342. Okisaka, S., A. Murakami, A. Mizukawa and J. Ito (1997). "Apoptosis in retinal ganglion cell decrease in human glaucomatous eyes." Japanese journal of ophthalmology **41**(2): 84-88.
343. Oppenheim, R. W. (1991). "Cell death during development of the nervous system." Annual review of neuroscience **14**(1): 453-501.
344. Ortin-Martinez, A., E. L. Tsai, P. E. Nickerson, M. Bergeret, Y. Lu, S. Smiley, L. Comanita and V. A. Wallace (2017). "A Reinterpretation of Cell Transplantation: GFP Transfer From Donor to Host Photoreceptors." Stem Cells **35**(4): 932-939.
345. Ostrowski, M., N. B. Carmo, S. Krumeich, I. Fanget, G. Raposo, A. Savina, C. F. Moita, K. Schauer, A. N. Hume and R. P. Freitas (2010). "Rab27a and Rab27b control different steps of the exosome secretion pathway." Nature cell biology **12**(1): 19.
346. Oushy, S., J. E. Hellwinkel, M. Wang, G. J. Nguyen, D. Gunaydin, T. A. Harland, T. J. Anchordoquy and M. W. Graner (2018). "Glioblastoma multiforme-derived extracellular vesicles drive normal astrocytes towards a tumour-enhancing phenotype." Phil. Trans. R. Soc. B **373**(1737): 20160477.
347. Oyagi, A., S. Moriguchi, A. Nitta, K. Murata, Y. Oida, K. Tsuruma, M. Shimazawa, K. Fukunaga and H. Hara (2011). "Heparin-binding EGF-like growth factor is required for synaptic plasticity and memory formation." Brain research **1419**: 97-104.
348. Pan, B.-T. and R. M. Johnstone (1983). "Fate of the transferrin receptor during maturation of

sheep reticulocytes in vitro: selective externalization of the receptor." Cell **33**(3): 967-978.
349. Pan, D., X. Chang, M. Xu, M. Zhang, S. Zhang, Y. Wang, X. Luo, J. Xu, X. Yang and X. Sun (2019). "UMSC-derived exosomes promote retinal ganglion cells survival in a rat model of optic nerve crush." Journal of chemical neuroanatomy **96**: 134-139.
350. Pang, P. T., H. K. Teng, E. Zaitsev, N. T. Woo, K. Sakata, S. Zhen, K. K. Teng, W.-H. Yung, B. L. Hempstead and B. Lu (2004). "Cleavage of proBDNF by tPA/plasmin is essential for long-term hippocampal plasticity." Science **306**(5695): 487-491.
351. Parisi, V., M. Centofanti, S. Gandolfi, D. Marangoni, L. Rossetti, L. Tanga, M. Tardini, S. Traina, N. Ungaro and M. Vetrugno (2014). "Effects of coenzyme Q10 in conjunction with vitamin E on retinal-evoked and cortical-evoked responses in patients with open-angle glaucoma." Journal of glaucoma **23**(6): 391-404.
352. Park, K. K., K. Liu, Y. Hu, P. D. Smith, C. Wang, B. Cai, B. Xu, L. Connolly, I. Kramvis and M. Sahin (2008). "Promoting axon regeneration in the adult CNS by modulation of the PTEN/mTOR pathway." Science **322**(5903): 963-966.
353. Park, S. S., S. Caballero, G. Bauer, B. Shibata, A. Roth, P. G. Fitzgerald, K. I. Forward, P. Zhou, J. McGee, D. G. Telander, M. B. Grant and J. A. Nolta (2012). "Long-term effects of intravitreal injection of GMP-grade bone-marrow-derived CD34+ cells in NOD-SCID mice with acute ischemia-reperfusion injury." Invest Ophthalmol Vis Sci **53**(2): 986-994.
354. Parolini, I., C. Federici, C. Raggi, L. Lugini, S. Palleschi, A. De Milito, C. Coscia, E. Iessi, M. Logozzi and A. Molinari (2009). "Microenvironmental pH is a key factor for exosome traffic in tumor cells." Journal of Biological Chemistry **284**(49): 34211-34222.
355. Pasha, S. P. B. S., R. Münch, P. Schäfer, P. Oertel, A. M. Sykes, Y. Zhu and M. O. Karl (2017). "Retinal cell death dependent reactive proliferative gliosis in the mouse retina." Scientific reports **7**(1): 1-16.
356. Patapoutian, A. and L. F. Reichardt (2001). "Trk receptors: mediators of neurotrophin action." Current opinion in neurobiology **11**(3): 272-280.
357. Pathan, M., P. Fonseka, S. V. Chitti, T. Kang, R. Sanwlani, J. Van Deun, A. Hendrix and S. Mathivanan (2019). "Vesiclepedia 2019: a compendium of RNA, proteins, lipids and metabolites in extracellular vesicles." Nucleic acids research **47**(D1): D516-D519.
358. Paulson, O. B. and E. A. Newman (1987). "Does the release of potassium from astrocyte endfeet regulate cerebral blood flow?" Science **237**(4817): 896-898.
359. Pearson, R. A., A. Gonzalez-Cordero, E. L. West, J. R. Ribeiro, N. Aghaizu, D. Goh, R. D. Sampson, A. Georgiadis, P. V. Waldron, Y. Duran, A. Naeem, M. Kloc, E. Cristante, K. Kruczek, K. Warre-Cornish, J. C. Sowden, A. J. Smith and R. R. Ali (2016). "Donor and host photoreceptors engage in material transfer following transplantation of post-mitotic photoreceptor precursors." Nat Commun **7**: 13029.
360. Pease, M. E., S. J. McKinnon, H. A. Quigley, L. A. Kerrigan–Baumrind and D. J. Zack (2000). "Obstructed axonal transport of BDNF and its receptor TrkB in experimental glaucoma." Investigative ophthalmology & visual science **41**(3): 764-774.
361. Peeters, L., N. N. Sanders, K. Braeckmans, K. Boussery, J. Van de Voorde, S. C. De Smedt and J. Demeester (2005). "Vitreous: a barrier to nonviral ocular gene therapy." Investigative ophthalmology & visual science **46**(10): 3553-3561.
362. Pena, J. D., A. W. Taylor, C. S. Ricard, I. Vidal and M. R. Hernandez (1999). "Transforming growth factor β isoforms in human optic nerve heads." British journal of ophthalmology **83**(2): 209-218.
363. Peng, Y. and C. M. Croce (2016). "The role of MicroRNAs in human cancer." Signal transduction and targeted therapy **1**(1): 1-9.
364. Pera, E. M., O. Wessely, S.-Y. Li and E. De Robertis (2001). "Neural and head induction by insulin-like growth factor signals." Developmental cell **1**(5): 655-665.
365. Peterziel, H., K. Unsicker and K. Krieglstein (2002). "TGFβ induces GDNF responsiveness in neurons by recruitment of GFRα1 to the plasma membrane." The Journal of cell biology **159**(1): 157-167.
366. Phillips, H. S., J. M. Hains, M. Armanini, G. R. Laramee, S. A. Johnson and J. W. Winslow (1991). "BDNF mRNA is decreased in the hippocampus of individuals with Alzheimer's disease." Neuron **7**(5): 695-702.
367. Piao, Y. J., H. S. Kim, E. H. Hwang, J. Woo, M. Zhang and W. K. Moon (2018). "Breast cancer cell-derived exosomes and macrophage polarization are associated with lymph node metastasis." Oncotarget **9**(7): 7398.

368. Pichi, F., A. Lembo, M. Morara, C. Veronese, M. Alkabes, P. Nucci and A. P. Ciardella (2014). "Early and late inner retinal changes after inner limiting membrane peeling." International ophthalmology **34**(2): 437-446.
369. Pinet, S., B. Bessette, N. Vedrenne, A. Lacroix, L. Richard, M.-O. Jauberteau, S. Battu and F. Lalloué (2016). "TrkB-containing exosomes promote the transfer of glioblastoma aggressiveness to YKL-40-inactivated glioblastoma cells." Oncotarget **7**(31): 50349.
370. Poitry-Yamate, C. L., S. Poitry and M. Tsacopoulos (1995). "Lactate released by Muller glial cells is metabolized by photoreceptors from mammalian retina." Journal of Neuroscience **15**(7): 5179-5191.
371. Pols, M. S. and J. Klumperman (2009). "Trafficking and function of the tetraspanin CD63." Experimental cell research **315**(9): 1584-1592.
372. Ponomarev, E. D., T. Veremeyko, N. Barteneva, A. M. Krichevsky and H. L. Weiner (2011). "MicroRNA-124 promotes microglia quiescence and suppresses EAE by deactivating macrophages via the C/EBP-α–PU. 1 pathway." Nature medicine **17**(1): 64-70.
373. Pow, D. and D. Crook (1996). "Direct immunocytochemical evidence for the transfer of glutamine from glial cells to neurons: Use of specific antibodies directed against thed-stereoisomers of glutamate and glutamine." Neuroscience **70**(1): 295-302.
374. Proenca, C. C., M. Song and F. S. Lee (2016). "Differential effects of BDNF and neurotrophin 4 (NT 4) on endocytic sorting of TrkB receptors." Journal of neurochemistry **138**(3): 397-406.
375. Proia, P., G. Schiera, M. Mineo, A. M. R. Ingrassia, G. Santoro, G. Savettieri and I. Di Liegro (2008). "Astrocytes shed extracellular vesicles that contain fibroblast growth factor-2 and vascular endothelial growth factor." International journal of molecular medicine **21**(1): 63-67.
376. Quigley, H. A., E. M. Addicks, W. R. Green and A. Maumenee (1981). "Optic nerve damage in human glaucoma: II. The site of injury and susceptibility to damage." Archives of ophthalmology **99**(4): 635-649.
377. Quigley, H. A., S. J. McKinnon, D. J. Zack, M. E. Pease, L. A. Kerrigan–Baumrind, D. F. Kerrigan and R. S. Mitchell (2000). "Retrograde axonal transport of BDNF in retinal ganglion cells is blocked by acute IOP elevation in rats." Investigative ophthalmology & visual science **41**(11): 3460-3466.
378. Quigley, H. A., R. W. Nickells, L. A. Kerrigan, M. E. Pease, D. J. Thibault and D. J. Zack (1995). "Retinal ganglion cell death in experimental glaucoma and after axotomy occurs by apoptosis." Investigative ophthalmology & visual science **36**(5): 774-786.
379. Qureshi, I. A. and M. F. Mehler (2012). "Emerging roles of non-coding RNAs in brain evolution, development, plasticity and disease." Nature Reviews Neuroscience **13**(8): 528-541.
380. Raff, M. C., B. A. Barres, J. F. Burne, H. S. Coles, Y. Ishizaki and M. D. Jacobson (1993). "Programmed cell death and the control of cell survival: lessons from the nervous system." Science **262**(5134): 695-700.
381. Raju, T. and M. R. Bennett (1986). "Retinal ganglion cell survival requirements: A major but transient dependence on Mu¨ ller glia during development." Brain research **383**(1-2): 165-176.
382. Ramachandran, R., B. V. Fausett and D. Goldman (2010). "Ascl1a regulates Müller glia dedifferentiation and retinal regeneration through a Lin-28-dependent, let-7 microRNA signalling pathway." Nature cell biology **12**(11): 1101-1107.
383. Ramachandran, R., X.-F. Zhao and D. Goldman (2011). "Ascl1a/Dkk/β-catenin signaling pathway is necessary and glycogen synthase kinase-3β inhibition is sufficient for zebrafish retina regeneration." Proceedings of the National Academy of Sciences **108**(38): 15858-15863.
384. Ramsden, C. M., M. B. Powner, A.-J. F. Carr, M. J. Smart, L. da Cruz and P. J. Coffey (2013). "Stem cells in retinal regeneration: past, present and future." Development **140**(12): 2576-2585.
385. Rana, S., S. Yue, D. Stadel and M. Zöller (2012). "Toward tailored exosomes: the exosomal tetraspanin web contributes to target cell selection." The international journal of biochemistry & cell biology **44**(9): 1574-1584.
386. Raposo, G., H. W. Nijman, W. Stoorvogel, R. Liejendekker, C. V. Harding, C. Melief and H. J. Geuze (1996). "B lymphocytes secrete antigen-presenting vesicles." Journal of Experimental Medicine **183**(3): 1161-1172.
387. Raposo, G., H. W. Nijman, W. Stoorvogel, R. Liejendekker, C. V. Harding, C. J. Melief and H. J. Geuze (1996). "B lymphocytes secrete antigen-presenting vesicles." Journal of Experimental Medicine **183**(3): 1161-1172.
388. Raposo, G. and W. Stoorvogel (2013). "Extracellular vesicles: exosomes, microvesicles, and friends." Journal of Cell Biology **200**(4): 373-383.

389. Ratajczak, J., K. Miekus, M. Kucia, J. Zhang, R. Reca, P. Dvorak and M. Ratajczak (2006). "Embryonic stem cell-derived microvesicles reprogram hematopoietic progenitors: evidence for horizontal transfer of mRNA and protein delivery." Leukemia **20**(5): 847-856.
390. Raymond, P. A. and P. F. Hitchcock (2000). How the neural retina regenerates. Vertebrate eye development, Springer**:** 197-218.
391. Reese, B. E. (2011). "Development of the retina and optic pathway." Vision research **51**(7): 613-632.
392. Reggiori, F. and H. R. Pelham (2001). "Sorting of proteins into multivesicular bodies: ubiquitin-dependent and-independent targeting." The EMBO journal **20**(18): 5176-5186.
393. Reichenbach, A. and A. Bringmann (2010). Müller cells in the healthy retina. Müller Cells in the Healthy and Diseased Retina, Springer**:** 35-214.
394. Reichenbach, A. and S. R. Robinson (1995). The involvement of Müller cells in the outer retina. Neurobiology and clinical aspects of the outer retina, Springer**:** 395-416.
395. Reichenbach, A., M. Ziegert, J. Schnitzer, S. Pritz-Hohmeier, P. Schaaf, W. Schober and H. Schneider (1994). "Development of the rabbit retina. V. The question of 'columnar units'." Developmental brain research **79**(1): 72-84.
396. Reis, R. A., M. C. Cabral da Silva, N. E. Loureiro dos Santos, E. Bampton, J. S. Taylor, F. G. de Mello and R. Linden (2002). "Sympathetic neuronal survival induced by retinal trophic factors." Journal of neurobiology **50**(1): 13-23.
397. Ren, X. and J. H. Hurley (2010). "VHS domains of ESCRT-0 cooperate in high-avidity binding to polyubiquitinated cargo." The EMBO journal **29**(6): 1045-1054.
398. Rich, A. and U. RajBhandary (1976). "Transfer RNA: molecular structure, sequence, and properties." Annual review of biochemistry **45**(1): 805-860.
399. Riera, M., L. Fontrodona, S. Albert, D. M. Ramirez, A. Seriola, A. Salas, Y. Munoz, D. Ramos, M. P. Villegas-Perez, M. A. Zapata, A. Raya, J. Ruberte, A. Veiga and J. Garcia-Arumi (2016). "Comparative study of human embryonic stem cells (hESC) and human induced pluripotent stem cells (hiPSC) as a treatment for retinal dystrophies." Mol Ther Methods Clin Dev **3**: 16010.
400. Robbins, P. D. and A. E. Morelli (2014). "Regulation of immune responses by extracellular vesicles." Nature Reviews Immunology **14**(3): 195.
401. Roberti, G., F. Mantelli, I. Macchi, M. Massaro-Giordano and M. Centofanti (2014). "Nerve growth factor modulation of retinal ganglion cell physiology." Journal of cellular physiology **229**(9): 1130-1133.
402. Robinson, M. D., D. J. McCarthy and G. K. Smyth (2010). "edgeR: a Bioconductor package for differential expression analysis of digital gene expression data." Bioinformatics **26**(1): 139-140.
403. Rocchi, A., D. Moretti, G. Lignani, E. Colombo, J. Scholz-Starke, P. Baldelli, T. Tkatch and F. Benfenati (2019). "Neurite-enriched microRNA-218 stimulates translation of the GluA2 subunit and increases excitatory synaptic strength." Molecular neurobiology **56**(8): 5701-5714.
404. Rodgers, H., V. Huffman, V. Voronina, M. Lewandoski and P. Mathers (2018). "The role of the Rx homeobox gene in retinal progenitor proliferation and cell fate specification." Mechanisms of development **151**: 18-29.
405. Rohrer, B., M. M. LaVail, K. R. Jones and L. F. Reichardt (2001). "Neurotrophin receptor TrkB activation is not required for the postnatal survival of retinal ganglion cells in vivo." Experimental neurology **172**(1): 81-91.
406. Rufino-Ramos, D., P. R. Albuquerque, V. Carmona, R. Perfeito, R. J. Nobre and L. P. de Almeida (2017). "Extracellular vesicles: novel promising delivery systems for therapy of brain diseases." Journal of Controlled Release **262**: 247-258.
407. Saba, R., P. H. Störchel, A. Aksoy-Aksel, F. Kepura, G. Lippi, T. D. Plant and G. M. Schratt (2012). "Dopamine-regulated microRNA MiR-181a controls GluA2 surface expression in hippocampal neurons." Molecular and cellular biology **32**(3): 619-632.
408. Sabatini, D. M. (2006). "mTOR and cancer: insights into a complex relationship." Nature Reviews Cancer **6**(9): 729-734.
409. Saha, R. N., X. Liu and K. Pahan (2006). "Up-regulation of BDNF in astrocytes by TNF-α: a case for the neuroprotective role of cytokine." Journal of Neuroimmune Pharmacology **1**(3): 212-222.
410. Santos-Ferreira, T., S. Llonch, O. Borsch, K. Postel, J. Haas and M. Ader (2016). "Retinal transplantation of photoreceptors results in donor-host cytoplasmic exchange." Nat Commun **7**: 13028.
411. Schiera, G., P. Proia, C. Alberti, M. Mineo, G. Savettieri and I. Di Liegro (2007). "Neurons produce

FGF2 and VEGF and secrete them at least in part by shedding extracellular vesicles." Journal of cellular and molecular medicine **11**(6): 1384-1394.
412. Schratt, G. (2009). "microRNAs at the synapse." Nature Reviews Neuroscience **10**(12): 842-849.
413. Schuettauf, F., C. Vorwerk, R. Naskar, A. Orlin, K. Quinto, D. Zurakowski, N. S. Dejneka, R. L. Klein, E. M. Meyer and J. Bennett (2004). "Adeno-associated viruses containing bFGF or BDNF are neuroprotective against excitotoxicity." Current eye research **29**(6): 379-386.
414. Seki, M., T. Tanaka, Y. Sakai, T. Fukuchi, H. Abe, H. Nawa and N. Takei (2005). "Muller Cells as a source of brain-derived neurotrophic factor in the retina: noradrenaline upregulates brain-derived neurotrophic factor levels in cultured rat Muller cells." Neurochem Res **30**(9): 1163-1170.
415. Seki, M., T. Tanaka, Y. Sakai, T. Fukuchi, H. Abe, H. Nawa and N. Takei (2005). "Müller cells as a source of brain-derived neurotrophic factor in the retina: noradrenaline upregulates brain-derived neurotrophic factor levels in cultured rat Müller cells." Neurochemical research **30**(9): 1163-1170.
416. Selth, L. A., S. Townley, J. L. Gillis, A. M. Ochnik, K. Murti, R. J. Macfarlane, K. N. Chi, V. R. Marshall, W. D. Tilley and L. M. Butler (2012). "Discovery of circulating microRNAs associated with human prostate cancer using a mouse model of disease." International Journal of Cancer **131**(3): 652-661.
417. Sempere, L. F., S. Freemantle, I. Pitha-Rowe, E. Moss, E. Dmitrovsky and V. Ambros (2004). "Expression profiling of mammalian microRNAs uncovers a subset of brain-expressed microRNAs with possible roles in murine and human neuronal differentiation." Genome biology **5**(3): R13.
418. Sheehan, C. and C. D'Souza-Schorey (2019). "Tumor-derived extracellular vesicles: molecular parcels that enable regulation of the immune response in cancer." Journal of Cell Science **132**(20).
419. Shelke, G. V., Y. Yin, S. C. Jang, C. Lässer, S. Wennmalm, H. J. Hoffmann, L. Li, Y. S. Gho, J. A. Nilsson and J. Lötvall (2019). "Endosomal signalling via exosome surface TGFβ-1." Journal of extracellular vesicles **8**(1): 1650458.
420. Shen, W., M. Fruttiger, L. Zhu, S. H. Chung, N. L. Barnett, J. K. Kirk, S. Lee, N. J. Coorey, M. Killingsworth and L. S. Sherman (2012). "Conditional Müller cell ablation causes independent neuronal and vascular pathologies in a novel transgenic model." Journal of Neuroscience **32**(45): 15715-15727.
421. Sherpa, T., S. M. Fimbel, D. E. Mallory, H. Maaswinkel, S. D. Spritzer, J. A. Sand, L. Li, D. R. Hyde and D. L. Stenkamp (2008). "Ganglion cell regeneration following whole-retina destruction in zebrafish." Developmental neurobiology **68**(2): 166-181.
422. Shibata, M., H. Nakao, H. Kiyonari, T. Abe and S. Aizawa (2011). "MicroRNA-9 regulates neurogenesis in mouse telencephalon by targeting multiple transcription factors." Journal of Neuroscience **31**(9): 3407-3422.
423. Shigemoto-Kuroda, T., J. Y. Oh, D.-k. Kim, H. J. Jeong, S. Y. Park, H. J. Lee, J. W. Park, T. W. Kim, S. Y. An and D. J. Prockop (2017). "MSC-derived extracellular vesicles attenuate immune responses in two autoimmune murine models: type 1 diabetes and uveoretinitis." Stem cell reports **8**(5): 1214-1225.
424. Shirai, H., M. Mandai, K. Matsushita, A. Kuwahara, S. Yonemura, T. Nakano, J. Assawachananont, T. Kimura, K. Saito, H. Terasaki, M. Eiraku, Y. Sasai and M. Takahashi (2016). "Transplantation of human embryonic stem cell-derived retinal tissue in two primate models of retinal degeneration." Proc Natl Acad Sci U S A **113**(1): E81-90.
425. Shiratsuchi, A., M. Kaido, T. Takizawa and Y. Nakanishi (2000). "Phosphatidylserine-mediated phagocytosis of influenza A virus-infected cells by mouse peritoneal macrophages." Journal of Virology **74**(19): 9240-9244.
426. Shurtleff, M. J., M. M. Temoche-Diaz, K. V. Karfilis, S. Ri and R. Schekman (2016). "Y-box protein 1 is required to sort microRNAs into exosomes in cells and in a cell-free reaction." elife **5**: e19276.
427. Shurtleff, M. J., M. M. Temoche-Diaz and R. Schekman (2018). "Extracellular vesicles and cancer: caveat lector." Annual Review of Cancer Biology **2**: 395-411.
428. Siddique, S. S., A. M. Suelves, U. Baheti and C. S. Foster (2013). "Glaucoma and uveitis." Survey of ophthalmology **58**(1): 1-10.
429. Singhal, S., B. Bhatia, H. Jayaram, S. Becker, M. F. Jones, P. B. Cottrill, P. T. Khaw, T. E. Salt and G. A. Limb (2012). "Human Muller glia with stem cell characteristics differentiate into retinal ganglion cell (RGC) precursors in vitro and partially restore RGC function in vivo following transplantation." Stem Cells Transl Med **1**(3): 188-199.
430. Singhal, S., B. Bhatia, H. Jayaram, S. Becker, M. F. Jones, P. B. Cottrill, P. T. Khaw, T. E. Salt and G. A.

Limb (2012). "Human Müller glia with stem cell characteristics differentiate into retinal ganglion cell (RGC) precursors in vitro and partially restore RGC function in vivo following transplantation." Stem cells translational medicine **1**(3): 188-199.
431. Skog, J., T. Würdinger, S. Van Rijn, D. H. Meijer, L. Gainche, W. T. Curry, B. S. Carter, A. M. Krichevsky and X. O. Breakefield (2008). "Glioblastoma microvesicles transport RNA and proteins that promote tumour growth and provide diagnostic biomarkers." Nature cell biology **10**(12): 1470-1476.
432. Sodha, S., K. Wall, S. Redenti, H. Klassen, M. J. Young and S. L. Tao (2011). "Microfabrication of a three-dimensional polycaprolactone thin-film scaffold for retinal progenitor cell encapsulation." J Biomater Sci Polym Ed **22**(4-6): 443-456.
433. Sometani, A., H. Kataoka, A. Nitta, H. Fukumitsu, H. Nomoto and S. Furukawa (2001). "Transforming growth factor-β1 enhances expression of brain-derived neurotrophic factor and its receptor, TrkB, in neurons cultured from rat cerebral cortex." Journal of neuroscience research **66**(3): 369-376.
434. Soto, I. and G. R. Howell (2014). "The complex role of neuroinflammation in glaucoma." Cold Spring Harbor perspectives in medicine **4**(8): a017269.
435. Sottile, V., M. Li and P. J. Scotting (2006). "Stem cell marker expression in the Bergmann glia population of the adult mouse brain." Brain research **1099**(1): 8-17.
436. Sposato, V., V. Parisi, L. Manni, M. T. Antonucci, V. Di Fausto, F. Sornelli and L. Aloe (2009). "Glaucoma alters the expression of NGF and NGF receptors in visual cortex and geniculate nucleus of rats: effect of eye NGF application." Vision research **49**(1): 54-63.
437. Squadrito, M. L., C. Baer, F. Burdet, C. Maderna, G. D. Gilfillan, R. Lyle, M. Ibberson and M. De Palma (2014). "Endogenous RNAs modulate microRNA sorting to exosomes and transfer to acceptor cells." Cell reports **8**(5): 1432-1446.
438. Stachowiak, J. C., E. M. Schmid, C. J. Ryan, H. S. Ann, D. Y. Sasaki, M. B. Sherman, P. L. Geissler, D. A. Fletcher and C. C. Hayden (2012). "Membrane bending by protein–protein crowding." Nature cell biology **14**(9): 944.
439. Stahl, P. D. and G. Raposo (2019). "Extracellular vesicles: exosomes and microvesicles, integrators of homeostasis." Physiology **34**(3): 169-177.
440. Sterling, P., R. G. Smith, R. Rao and N. Vardi (1995). Functional architecture of mammalian outer retina and bipolar cells. Neurobiology and clinical aspects of the outer retina, Springer**:** 325-348.
441. Stevanato, L., L. Thanabalasundaram, N. Vysokov and J. D. Sinden (2016). "Investigation of content, stoichiometry and transfer of miRNA from human neural stem cell line derived exosomes." PLoS One **11**(1): e0146353.
442. Stone, J. and Z. Dreher (1987). "Relationship between astrocytes, ganglion cells and vasculature of the retina." Journal of Comparative Neurology **255**(1): 35-49.
443. Stoorvogel, W. (2015). "Resolving sorting mechanisms into exosomes." Cell research **25**(5): 531-532.
444. Strauss, O. (2005). "The retinal pigment epithelium in visual function." Physiological reviews **85**(3): 845-881.
445. Strettoi, E. and R. H. Masland (1995). "The organization of the inner nuclear layer of the rabbit retina." Journal of Neuroscience **15**(1): 875-888.
446. Sun, D., X. Zhuang, X. Xiang, Y. Liu, S. Zhang, C. Liu, S. Barnes, W. Grizzle, D. Miller and H.-G. Zhang (2010). "A novel nanoparticle drug delivery system: the anti-inflammatory activity of curcumin is enhanced when encapsulated in exosomes." Molecular Therapy **18**(9): 1606-1614.
447. Svensson, K. J., H. C. Christianson, A. Wittrup, E. Bourseau-Guilmain, E. Lindqvist, L. M. Svensson, M. Mörgelin and M. Belting (2013). "Exosome uptake depends on ERK1/2-heat shock protein 27 signaling and lipid Raft-mediated endocytosis negatively regulated by caveolin-1." Journal of Biological Chemistry **288**(24): 17713-17724.
448. Tafreshi, A., X.-F. Zhou and R. Rush (1998). "Endogenous nerve growth factor and neurotrophin-3 act simultaneously to ensure the survival of postnatal sympathetic neurons in vivo." Neuroscience **83**(2): 373-380.
449. Tan, C. Y., R. C. Lai, W. Wong, Y. Y. Dan, S.-K. Lim and H. K. Ho (2014). "Mesenchymal stem cell-derived exosomes promote hepatic regeneration in drug-induced liver injury models." Stem cell research & therapy **5**(3): 76.
450. Tassew, N. G., J. Charish, A. P. Shabanzadeh, V. Luga, H. Harada, N. Farhani, P. D'Onofrio, B. Choi, A. Ellabban and P. E. Nickerson (2017). "Exosomes mediate mobilization of autocrine Wnt10b to

promote axonal regeneration in the injured CNS." Cell reports **20**(1): 99-111.
451. Tauro, B. J., D. W. Greening, R. A. Mathias, H. Ji, S. Mathivanan, A. M. Scott and R. J. Simpson (2012). "Comparison of ultracentrifugation, density gradient separation, and immunoaffinity capture methods for isolating human colon cancer cell line LIM1863-derived exosomes." Methods **56**(2): 293-304.
452. Taylor, S., B. Srinivasan, R. J. Wordinger and R. S. Roque (2003). "Glutamate stimulates neurotrophin expression in cultured Müller cells." Molecular brain research **111**(1-2): 189-197.
453. Temchura, V. V., M. Tenbusch, G. Nchinda, G. Nabi, B. Tippler, M. Zelenyuk, O. Wildner, K. Überla and S. Kuate (2008). "Enhancement of immunostimulatory properties of exosomal vaccines by incorporation of fusion-competent G protein of vesicular stomatitis virus." Vaccine **26**(29-30): 3662-3672.
454. Tessarollo, L., P. Tsoulfas, M. J. Donovan, M. E. Palko, J. Blair-Flynn, B. L. Hempstead and L. F. Parada (1997). "Targeted deletion of all isoforms of the trkC gene suggests the use of alternate receptors by its ligand neurotrophin-3 in neuronal development and implicates trkC in normal cardiogenesis." Proceedings of the National Academy of Sciences **94**(26): 14776-14781.
455. Tezel, G. (2008). "TNF-α signaling in glaucomatous neurodegeneration." Progress in brain research **173**: 409-421.
456. Tezel, G. (2013). "Immune regulation toward immunomodulation for neuroprotection in glaucoma." Current opinion in pharmacology **13**(1): 23-31.
457. Tezel, G. and M. B. Wax (2000). "Increased production of tumor necrosis factor-α by glial cells exposed to simulated ischemia or elevated hydrostatic pressure induces apoptosis in cocultured retinal ganglion cells." Journal of Neuroscience **20**(23): 8693-8700.
458. Tezel, G. l. n., L. Y. Li, R. V. Patil and M. B. Wax (2001). "TNF-α and TNF-α receptor-1 in the retina of normal and glaucomatous eyes." Investigative ophthalmology & visual science **42**(8): 1787-1794.
459. Tham, Y.-C., X. Li, T. Y. Wong, H. A. Quigley, T. Aung and C.-Y. Cheng (2014). "Global prevalence of glaucoma and projections of glaucoma burden through 2040: a systematic review and meta-analysis." Ophthalmology **121**(11): 2081-2090.
460. Théry, C., S. Amigorena, G. Raposo and A. Clayton (2006). "Isolation and characterization of exosomes from cell culture supernatants and biological fluids." Current protocols in cell biology **30**(1): 3.22. 21-23.22. 29.
461. Théry, C., M. Boussac, P. Véron, P. Ricciardi-Castagnoli, G. Raposo, J. Garin and S. Amigorena (2001). "Proteomic analysis of dendritic cell-derived exosomes: a secreted subcellular compartment distinct from apoptotic vesicles." The Journal of Immunology **166**(12): 7309-7318.
462. Théry, C., K. W. Witwer, E. Aikawa, M. J. Alcaraz, J. D. Anderson, R. Andriantsitohaina, A. Antoniou, T. Arab, F. Archer and G. K. Atkin-Smith (2018). "Minimal information for studies of extracellular vesicles 2018 (MISEV2018): a position statement of the International Society for Extracellular Vesicles and update of the MISEV2014 guidelines." Journal of extracellular vesicles **7**(1): 1535750.
463. Théry, C., L. Zitvogel and S. Amigorena (2002). "Exosomes: composition, biogenesis and function." Nature reviews immunology **2**(8): 569-579.
464. Thorpe, L. M., H. Yuzugullu and J. J. Zhao (2015). "PI3K in cancer: divergent roles of isoforms, modes of activation and therapeutic targeting." Nature Reviews Cancer **15**(1): 7-24.
465. Thummel, R., S. C. Kassen, J. M. Enright, C. M. Nelson, J. E. Montgomery and D. R. Hyde (2008). "Characterization of Müller glia and neuronal progenitors during adult zebrafish retinal regeneration." Experimental eye research **87**(5): 433-444.
466. Tian, T., Y.-L. Zhu, Y.-Y. Zhou, G.-F. Liang, Y.-Y. Wang, F.-H. Hu and Z.-D. Xiao (2014). "Exosome uptake through clathrin-mediated endocytosis and macropinocytosis and mediating miR-21 delivery." Journal of Biological Chemistry **289**(32): 22258-22267.
467. Tomasoni, S., L. Longaretti, C. Rota, M. Morigi, S. Conti, E. Gotti, C. Capelli, M. Introna, G. Remuzzi and A. Benigni (2012). "Transfer of growth factor receptor mRNA via exosomes unravels the regenerative effect of mesenchymal stem cells." Stem cells and development **22**(5): 772-780.
468. Tomita, M., E. Lavik, H. Klassen, T. Zahir, R. Langer and M. J. Young (2005). "Biodegradable polymer composite grafts promote the survival and differentiation of retinal progenitor cells." Stem Cells **23**(10): 1579-1588.
469. Tong, M. and L. Chamley (2015). "Placental extracellular vesicles and feto-maternal communication." Cold Spring Harbor perspectives in medicine: a023028.
470. Tout, S., T. Chan-Ling, H. Holländer and J. Stone (1993). "The role of Müller cells in the formation

of the blood-retinal barrier." Neuroscience **55**(1): 291-301.
471. Trajkovic, K., C. Hsu, S. Chiantia, L. Rajendran, D. Wenzel, F. Wieland, P. Schwille, B. Brügger and M. Simons (2008). "Ceramide triggers budding of exosome vesicles into multivesicular endosomes." Science **319**(5867): 1244-1247.
472. Tsacopoulos, M. and P. J. Magistretti (1996). "Metabolic coupling between glia and neurons." Journal of Neuroscience **16**(3): 877-885.
473. Tsui, N. B., E. K. Ng and Y. D. Lo (2002). "Stability of endogenous and added RNA in blood specimens, serum, and plasma." Clinical chemistry **48**(10): 1647-1653.
474. Tsutsumi, A., T. Kawamata, N. Izumi, H. Seitz and Y. Tomari (2011). "Recognition of the pre-miRNA structure by Drosophila Dicer-1." Nature structural & molecular biology **18**(10): 1153.
475. Tu, J., H.-H. Cheung, G. Lu, Z. Chen and W.-Y. Chan (2018). "MicroRNA-10a promotes granulosa cells tumor development via PTEN-AKT/Wnt regulatory axis." Cell Death & Disease **9**(11).
476. Turchinovich, A., O. Drapkina and A. Tonevitsky (2019). "Transcriptome of extracellular vesicles: State-of-the-art." Frontiers in immunology **10**.
477. Valadi, H., K. Ekström, A. Bossios, M. Sjöstrand, J. J. Lee and J. O. Lötvall (2007). "Exosome-mediated transfer of mRNAs and microRNAs is a novel mechanism of genetic exchange between cells." Nature cell biology **9**(6): 654.
478. Vallabhaneni, K. C., P. Penfornis, S. Dhule, F. Guillonneau, K. V. Adams, Y. Y. Mo, R. Xu, Y. Liu, K. Watabe and M. C. Vemuri (2015). "Extracellular vesicles from bone marrow mesenchymal stem/stromal cells transport tumor regulatory microRNA, proteins, and metabolites." Oncotarget **6**(7): 4953.
479. Van Bergen, N. J., J. P. Wood, G. Chidlow, I. A. Trounce, R. J. Casson, W.-K. Ju, R. N. Weinreb and J. G. Crowston (2009). "Recharacterization of the RGC-5 retinal ganglion cell line." Investigative ophthalmology & visual science **50**(9): 4267-4272.
480. Van der Pol, E., F. Coumans, A. Grootemaat, C. Gardiner, I. Sargent, P. Harrison, A. Sturk, T. Van Leeuwen and R. Nieuwland (2014). "Particle size distribution of exosomes and microvesicles determined by transmission electron microscopy, flow cytometry, nanoparticle tracking analysis, and resistive pulse sensing." Journal of Thrombosis and Haemostasis **12**(7): 1182-1192.
481. Ventura, L. M. and V. Porciatti (2006). "Pattern electroretinogram in glaucoma." Current opinion in ophthalmology **17**(2): 196.
482. Venugopal, C., C. Shamir, S. Senthilkumar, J. V. Babu, P. K. Sonu, K. J. Nishtha, K. S. Rai and A. Dhanushkodi (2017). "Dosage and passage dependent neuroprotective effects of exosomes derived from rat bone marrow mesenchymal stem cells: an in vitro analysis." Current gene therapy **17**(5): 379-390.
483. Verdera, H. C., J. J. Gitz-Francois, R. M. Schiffelers and P. Vader (2017). "Cellular uptake of extracellular vesicles is mediated by clathrin-independent endocytosis and macropinocytosis." Journal of Controlled Release **266**: 100-108.
484. Vihtelic, T. S. and D. R. Hyde (2000). "Light-induced rod and cone cell death and regeneration in the adult albino zebrafish (Danio rerio) retina." Journal of neurobiology **44**(3): 289-307.
485. Villarroya-Beltri, C., F. Baixauli, C. Gutiérrez-Vázquez, F. Sánchez-Madrid and M. Mittelbrunn (2014). Sorting it out: regulation of exosome loading. Seminars in cancer biology, Elsevier.
486. Villarroya-Beltri, C., C. Gutiérrez-Vázquez, F. Sánchez-Cabo, D. Pérez-Hernández, J. Vázquez, N. Martin-Cofreces, D. J. Martinez-Herrera, A. Pascual-Montano, M. Mittelbrunn and F. Sánchez-Madrid (2013). "Sumoylated hnRNPA2B1 controls the sorting of miRNAs into exosomes through binding to specific motifs." Nature communications **4**: 2980.
487. Vlachos, I. S., K. Zagganas, M. D. Paraskevopoulou, G. Georgakilas, D. Karagkouni, T. Vergoulis, T. Dalamagas and A. G. Hatzigeorgiou (2015). "DIANA-miRPath v3. 0: deciphering microRNA function with experimental support." Nucleic acids research **43**(W1): W460-W466.
488. Vorwerk, C. K., M. S. Gorla and E. B. Dreyer (1999). "An experimental basis for implicating excitotoxicity in glaucomatous optic neuropathy." Survey of ophthalmology **43**: S142-S150.
489. Vrabec, J. and L. Levin (2007). "The neurobiology of cell death in glaucoma." Eye **21**(1): S11-S14.
490. Waldenström, A., N. Gennebäck, U. Hellman and G. Ronquist (2012). "Cardiomyocyte microvesicles contain DNA/RNA and convey biological messages to target cells." PloS one **7**(4): e34653.
491. Walker, J. C. and R. M. Harland (2009). "microRNA-24a is required to repress apoptosis in the developing neural retina." Genes & development **23**(9): 1046-1051.
492. Wang, H., X. Guan, Y. Tu, S. Zheng, J. Long, S. Li, C. Qi, X. Xie, H. Zhang and Y. Zhang (2015).

"MicroRNA-29b attenuates non-small cell lung cancer metastasis by targeting matrix metalloproteinase 2 and PTEN." Journal of experimental & clinical cancer research **34**(1): 1-12.
493. Wang, J.-S. and V. J. Kefalov (2011). "The cone-specific visual cycle." Progress in retinal and eye research **30**(2): 115-128.
494. Wang, N., C. Chen, D. Yang, Q. Liao, H. Luo, X. Wang, F. Zhou, X. Yang, J. Yang and C. Zeng (2017). "Mesenchymal stem cells-derived extracellular vesicles, via miR-210, improve infarcted cardiac function by promotion of angiogenesis." Biochimica et Biophysica Acta (BBA)-Molecular Basis of Disease **1863**(8): 2085-2092.
495. Wang, R. Y., R. Z. Phang, P. H. Hsu, W. H. Wang, H. T. Huang and I. Y. Liu (2013). "In vivo knockdown of hippocampal miR-132 expression impairs memory acquisition of trace fear conditioning." Hippocampus **23**(7): 625-633.
496. Wang, S. and K. Li (2014). "MicroRNA-96 regulates RGC-5 cell growth through caspase-dependent apoptosis." International journal of clinical and experimental medicine **7**(10): 3694.
497. Wang, W.-H., L. G. McNatt, I.-H. Pang, P. E. Hellberg, J. H. Fingert, M. D. McCartney and A. F. Clark (2008). "Increased expression of serum amyloid A in glaucoma and its effect on intraocular pressure." Investigative ophthalmology & visual science **49**(5): 1916-1923.
498. Wang, X., W. Huang, G. Liu, W. Cai, R. W. Millard, Y. Wang, J. Chang, T. Peng and G.-C. Fan (2014). "Cardiomyocytes mediate anti-angiogenesis in type 2 diabetic rats through the exosomal transfer of miR-320 into endothelial cells." Journal of molecular and cellular cardiology **74**: 139-150.
499. Wässle, H. (2004). "Parallel processing in the mammalian retina." Nature Reviews Neuroscience **5**(10): 747.
500. Wax, M. B., G. Tezel, J. Yang, G. Peng, R. V. Patil, N. Agarwal, R. M. Sappington and D. J. Calkins (2008). "Induced autoimmunity to heat shock proteins elicits glaucomatous loss of retinal ganglion cell neurons via activated T-cell-derived fas-ligand." Journal of Neuroscience **28**(46): 12085-12096.
501. Wayman, G. A., M. Davare, H. Ando, D. Fortin, O. Varlamova, H.-Y. M. Cheng, D. Marks, K. Obrietan, T. R. Soderling and R. H. Goodman (2008). "An activity-regulated microRNA controls dendritic plasticity by down-regulating p250GAP." Proceedings of the National Academy of Sciences **105**(26): 9093-9098.
502. Weber, J. A., D. H. Baxter, S. Zhang, D. Y. Huang, K. How Huang, M. Jen Lee, D. J. Galas and K. Wang (2010). "The microRNA spectrum in 12 body fluids." Clinical chemistry **56**(11): 1733-1741.
503. Webster, M., M. Herman, J. Kleinman and C. S. Weickert (2006). "BDNF and trkB mRNA expression in the hippocampus and temporal cortex during the human lifespan." Gene Expression Patterns **6**(8): 941-951.
504. Weinreb, R. N., C. K. Leung, J. G. Crowston, F. A. Medeiros, D. S. Friedman, J. L. Wiggs and K. R. Martin (2016). "Primary open-angle glaucoma." Nature Reviews Disease Primers **2**(1): 1-19.
505. West, A., P. Pruunsild and T. Timmusk (2014). Neurotrophins: transcription and translation. Neurotrophic Factors, Springer**:** 67-100.
506. West, E. L., R. A. Pearson, M. Tschernutter, J. C. Sowden, R. E. MacLaren and R. R. Ali (2008). "Pharmacological disruption of the outer limiting membrane leads to increased retinal integration of transplanted photoreceptor precursors." Exp Eye Res **86**(4): 601-611.
507. Wiklander, O. P., R. B. Bostancioglu, J. A. Welsh, A. M. Zickler, F. Murke, G. Corso, U. Felldin, D. W. Hagey, B. Evertsson and X.-M. Liang (2018). "Systematic methodological evaluation of a multiplex bead-based flow cytometry assay for detection of extracellular vesicle surface signatures." Frontiers in immunology **9**: 1326.
508. Williams, G. and W. Tao (2009). "A phase II study of encapsulated CNTF secreting cell implant (NT-501) in patients with visual acuity impairment associated with atrophic macular degeneration." Investigative Ophthalmology & Visual Science **50**(13): 5003-5003.
509. Willis, G. R., A. Fernandez-Gonzalez, S. H. Vitali, X. Liu, S. A. Mitsialis and S. Kourembanas (2017). Mesenchymal stem cell exosome treatment restores lung architecture and ameliorates pulmonary hypertension associated with bronchopulmonary dysplasia. C16. BRONCHOPULMONARY DYSPLASIA TURNS 50, American Thoracic Society**:** A4934-A4934.
510. Willms, E., H. J. Johansson, I. Mäger, Y. Lee, K. E. M. Blomberg, M. Sadik, A. Alaarg, C. E. Smith, J. Lehtiö and S. E. Andaloussi (2016). "Cells release subpopulations of exosomes with distinct molecular and biological properties." Scientific reports **6**(1): 1-12.
511. Wilson, S. W. and C. Houart (2004). "Early steps in the development of the forebrain." Developmental cell **6**(2): 167-181.

512. Winzeler, A. and J. T. Wang (2013). "Purification and culture of retinal ganglion cells from rodents." Cold Spring Harbor Protocols **2013**(7): pdb. prot074906.
513. Wohl, S. G., N. L. Jorstad, E. M. Levine and T. A. Reh (2017). "Müller glial microRNAs are required for the maintenance of glial homeostasis and retinal architecture." Nature communications **8**(1): 1-15.
514. Wohl, S. G. and T. A. Reh (2016). "The microRNA expression profile of mouse Müller glia in vivo and in vitro." Scientific reports **6**: 35423.
515. Wolf, P. (1967). "The nature and significance of platelet products in human plasma." British journal of haematology **13**(3): 269-288.
516. Wollensak, G. and E. Spoerl (2004). "Biomechanical characteristics of retina." Retina **24**(6): 967-970.
517. Xin, H., Y. Li, B. Buller, M. Katakowski, Y. Zhang, X. Wang, X. Shang, Z. G. Zhang and M. Chopp (2012). "Exosome-mediated transfer of miR-133b from multipotent mesenchymal stromal cells to neural cells contributes to neurite outgrowth." Stem cells **30**(7): 1556-1564.
518. Xin, H., Y. Li, Z. Liu, X. Wang, X. Shang, Y. Cui, Z. G. Zhang and M. Chopp (2013). "MiR-133b promotes neural plasticity and functional recovery after treatment of stroke with multipotent mesenchymal stromal cells in rats via transfer of exosome-enriched extracellular particles." Stem cells **31**(12): 2737-2746.
519. Xu, H., M. Chen and J. V. Forrester (2009). "Para-inflammation in the aging retina." Progress in retinal and eye research **28**(5): 348-368.
520. Yan, Q., J. Wang, C. R. Matheson and J. L. Urich (1999). "Glial cell line–derived neurotrophic factor (GDNF) promotes the survival of axotomized retinal ganglion cells in adult rats: Comparison to and combination with brain-derived neurotrophic factor (BDNF)." Journal of neurobiology **38**(3): 382-390.
521. Yan, X., G. Tezel, M. B. Wax and D. P. Edward (2000). "Matrix metalloproteinases and tumor necrosis factor α in glaucomatous optic nerve head." Archives of Ophthalmology **118**(5): 666-673.
522. Yang, J.-S., H. Gad, S. Y. Lee, A. Mironov, L. Zhang, G. V. Beznoussenko, C. Valente, G. Turacchio, A. N. Bonsra and G. Du (2008). "A role for phosphatidic acid in COPI vesicle fission yields insights into Golgi maintenance." Nature cell biology **10**(10): 1146.
523. Yang, J., S. Wu, L. Hou, D. Zhu, S. Yin, G. Yang and Y. Wang (2020). "Therapeutic effects of simultaneous delivery of nerve growth factor mrna and protein via exosomes on cerebral ischemia." Molecular Therapy-Nucleic Acids **21**: 512-522.
524. Yang, J., X. Zhang, X. Chen, L. Wang and G. Yang (2017). "Exosome mediated delivery of miR-124 promotes neurogenesis after ischemia." Molecular Therapy-Nucleic Acids **7**: 278-287.
525. Yang, M., J. Chen, F. Su, B. Yu, F. Su, L. Lin, Y. Liu, J.-D. Huang and E. Song (2011). "Microvesicles secreted by macrophages shuttle invasion-potentiating microRNAs into breast cancer cells." Molecular cancer **10**(1): 117.
526. Yau, K.-W., T. Lamb and D. Baylor (1977). "Light-induced fluctuations in membrane current of single toad rod outer segments." Nature **269**(5623): 78-80.
527. Yücel, Y. H., N. Gupta, Q. Zhang, A. P. Mizisin, M. W. Kalichman and R. N. Weinreb (2006). "Memantine protects neurons from shrinkage in the lateral geniculate nucleus in experimental glaucoma." Archives of ophthalmology **124**(2): 217-225.
528. Yuyama, K., H. Sun, S. Mitsutake and Y. Igarashi (2012). "Sphingolipid-modulated exosome secretion promotes clearance of amyloid-β by microglia." Journal of Biological Chemistry **287**(14): 10977-10989.
529. Zech, D., S. Rana, M. W. Büchler and M. Zöller (2012). "Tumor-exosomes and leukocyte activation: an ambivalent crosstalk." Cell Communication and Signaling **10**(1): 37.
530. Zhang, B.-Y., C.-M. Liu, R.-Y. Wang, Q. Zhu, Z. Jiao and F.-Q. Zhou (2014). "Akt-independent GSK3 inactivation downstream of PI3K signaling regulates mammalian axon regeneration." Biochemical and biophysical research communications **443**(2): 743-748.
531. Zhang, L., S. Zhang, J. Yao, F. J. Lowery, Q. Zhang, W.-C. Huang, P. Li, M. Li, X. Wang and C. Zhang (2015). "Microenvironment-induced PTEN loss by exosomal microRNA primes brain metastasis outgrowth." Nature **527**(7576): 100-104.
532. Zhang, Q.-l., W. Wang, J. Li, S.-Y. Tian and T.-Z. Zhang (2015). "Decreased miR-187 induces retinal ganglion cell apoptosis through upregulating SMAD7 in glaucoma." Biomedicine & Pharmacotherapy **75**: 19-25.
533. Zhang, X., J. Liu, B. Yu, F. Ma, X. Ren and X. Li (2018). "Effects of mesenchymal stem cells and their

exosomes on the healing of large and refractory macular holes." Graefe's Archive for Clinical and Experimental Ophthalmology **256**(11): 2041-2052.
534. Zhang, Y., M. Chopp, X. S. Liu, M. Katakowski, X. Wang, X. Tian, D. Wu and Z. G. Zhang (2017). "Exosomes derived from mesenchymal stromal cells promote axonal growth of cortical neurons." Molecular neurobiology **54**(4): 2659-2673.
535. Zhang, Y., M. Chopp, Y. Meng, M. Katakowski, H. Xin, A. Mahmood and Y. Xiong (2015). "Effect of exosomes derived from multipluripotent mesenchymal stromal cells on functional recovery and neurovascular plasticity in rats after traumatic brain injury." Journal of neurosurgery **122**(4): 856-867.
536. Zhang, Y., D. Liu, X. Chen, J. Li, L. Li, Z. Bian, F. Sun, J. Lu, Y. Yin and X. Cai (2010). "Secreted monocytic miR-150 enhances targeted endothelial cell migration." Molecular cell **39**(1): 133-144.
537. Zhao, T., Y. Li, L. Tang, Y. Li, F. Fan and B. Jiang (2011). "Protective effects of human umbilical cord blood stem cell intravitreal transplantation against optic nerve injury in rats." Graefes Arch Clin Exp Ophthalmol **249**(7): 1021-1028.
538. Zhao, Y., S. R. Weber, J. Lease, M. Russo, C. A. Siedlecki, L.-C. Xu, H. Chen, W. Wang, M. Ford and R. Simo (2018). "Liquid biopsy of vitreous reveals an abundant vesicle population consistent with the size and morphology of exosomes." Translational vision science & technology **7**(3): 6-6.
539. Zhou, X.-F., D. Cameron and R. Rush (1998). "Endogenous neurotrophin-3 supports the survival of a subpopulation of sensory neurons in neonatal rat." Neuroscience **86**(4): 1155-1164.
540. Zhu, W., L. Huang, Y. Li, X. Zhang, J. Gu, Y. Yan, X. Xu, M. Wang, H. Qian and W. Xu (2012). "Exosomes derived from human bone marrow mesenchymal stem cells promote tumor growth in vivo." Cancer letters **315**(1): 28-37.
541. Zhu, X., M. Badawi, S. Pomeroy, D. S. Sutaria, Z. Xie, A. Baek, J. Jiang, O. A. Elgamal, X. Mo and K. L. Perle (2017). "Comprehensive toxicity and immunogenicity studies reveal minimal effects in mice following sustained dosing of extracellular vesicles derived from HEK293T cells." Journal of Extracellular Vesicles **6**(1): 1324730.
542. Zitvogel, L., A. Regnault, A. Lozier, J. Wolfers, C. Flament, D. Tenza, P. Ricciardi-Castagnoli, G. Raposo and S. Amigorena (1998). "Eradication of established murine tumors using a novel cell-free vaccine: dendritic cell derived exosomes." Nature medicine **4**(5): 594.
543. Zomer, A., T. Vendrig, E. S. Hopmans, M. van Eijndhoven, J. M. Middeldorp and D. M. Pegtel (2010). "Exosomes: fit to deliver small RNA." Communicative & integrative biology **3**(5): 447-450.
544. Zuber, M. E., G. Gestri, A. S. Viczian, G. Barsacchi and W. A. Harris (2003). "Specification of the vertebrate eye by a network of eye field transcription factors." Development **130**(21): 5155-5167.
545. Zwaal, R. F. and A. J. Schroit (1997). "Pathophysiologic implications of membrane phospholipid asymmetry in blood cells." Blood, The Journal of the American Society of Hematology **89**(4): 1121-1132.

Chapter 8: Appendices

Supplementary table 1: Primers used for expression analysis of neurotrophin genes by reverse-transcription PCR

Gene name	Sequence	Source
Actin-beta (β-actin)	FWD: CATGTACGTTGCTATCCAGGC REV: CTCCTTAATGTCACGCACGAT	Sigma Aldrich
Nerve Growth Factor (NGF)	FWD: TGTGGGTTGGGGATAAGACCA REV: GCTGTCAACGGGATTTGGGT	Sigma Aldrich
Brain-derived Neurotrophic Factor (BDNF)	FWD: CTACGAGACCAAGTGCAATCC REV: AATCGCCAGCCAATTCTCTTT	Sigma Aldrich
Neurotrophin 3 (NT3)	FWD: CGTGGTGGCGAACAGAACAT REV: GGCCGATGACTTGTCGGTC	Sigma Aldrich
Neurotrophin 4 (NT4)	FWD: CTGTGTGCGATGCAGTCAGT REV: TGCAGCGGGTTTCAAAGAAGT	Sigma Aldrich
Glia-derived Neurotrophic Factor (GDNF)	FWD: GGCAGTGCTTCCTAGAAGAGA REV: AAGACACAACCCCGGTTTTTG	Invitrogen

Supplementary table 2: Primers used for validation of miRNA in quantitative real-time PCR

miRNA target	Sequence	Annealing temperature	Source
HSA-MIR-21-5P	FWD: GCAGTAGCTTATCAGACTGATG REV: GGTCCAGTTTTTTTTTTTTTTCAAC	60°C	Sigma Aldrich
HSA-MIR-29B-5P	FWD: CAGTAGCACCATTTGAAATCAG REV: GGTCCAGTTTTTTTTTTTTTTAACAC	60°C	Sigma Aldrich
HSA-MIR-10A-5P	FWD: CGCTACCCTGTAGATCCGAA REV: GGTCCAGTTTTTTTTTTTTTTCATAG	60°C	Sigma Aldrich
HSA-MIR-767-3P	FWD: TCCATTTGTTTTGATGATGGACT REV: TCCAGTTTTTTTTTTTTTTGTGGT	60°C	Sigma Aldrich

Supplementary table 3: Antibodies used for western blot, immunocytochemistry, and immunopanning protocols

Antibody target	Host	Dilution	Technique used	Source
Monoclonal anti-β-actin	Mouse	1:5000	Western blot / Immunocytochemistry	Sigma Aldrich A2228
Monoclonal anti-NGF	Rabbit	1:1000	Western blot	Abcam Ab52918
Monoclonal anti-BDNF	Rabbit	1:1500	Western blot	Abcam Ab108319
Polyclonal anti-NT-3	Rabbit	1:1000	Western blot	Abcam Ab65804
Monoclonal anti-NT-4	Rabbit	1:750	Western blot	Abcam Ab150437
Polyclonal anti-GDNF	Rabbit	1:1000	Western blot	Abcam Ab18956
Monoclonal anti-CD9 antigen	Rabbit	1:2000	Western blot	Abcam Ab92726
Monoclonal anti-CD63 antigen	Mouse	1:1000	Western blot	Abcam Ab8219
Monoclonal anti-ALIX	Mouse	1:1500	Western blot	Abcam Ab117600
Monoclonal anti-Calnexin	Rabbit	1:1000	Western blot	Abcam Ab10286
Polyclonal anti-Calreticulin	Rabbit	1:1000	Western blot	Abcam Ab2907
Monoclonal anti-CD44	Rabbit	1:750	Western blot	Abcam Ab189524
Polyclonal anti-Beta-III-tubulin	Rabbit	1:1000	Immunocytochemistry	Abcam Ab18207
Anti-rat Macrophage polyclonal antibody	Rabbit	1:50	Macrophage depletion	Cedarlane CLAD51240
Anti-rabbit IgG (H+L)	Goat	1:0	Immunopanning negative selection	Invitrogen: A27033
anti-rat Thy-1 antibody	Rabbit	1:500	Immunopanning positive selection	Abcam ab92574

Supplementary table 4: 20 most abundant miRNAs detected in each specimen. Abundance displayed as Log2 of counts per million (CPM) following normalization by library-specific factors. miRNA annotated with * were significantly differentially enriched (FDR-adjusted p = < 0.01) in pairwise comparisons between whole cells and small EV libraries.

MIO-M1 cells	Log2CPM	Small EV	Log2CPM	Large EV	Log2CPM
hsa-let-7a-5p	17	**hsa-miR-21-5p***	17	hsa-let-7b-5p	18
hsa-miR-125b-5p	17	hsa-miR-16-5p	17	hsa-let-7a-5p	18
hsa-let-7b-5p	17	hsa-let-7a-5p	17	hsa-miR-16-5p	17
hsa-miR-125a-5p	16	hsa-let-7b-5p	17	hsa-let-7f-5p	17
hsa-let-7i-5p	15	hsa-let-7f-5p	16	hsa-let-7i-5p	17
hsa-miR-342-3p	15	hsa-let-7i-5p	16	hsa-miR-21-5p	16
hsa-miR-16-5p	15	hsa-miR-342-3p	15	hsa-let-7c-5p	16
hsa-miR-127-3p*	15	hsa-miR-125b-5p	15	hsa-miR-125b-5p	15
hsa-miR-9-5p	15	hsa-let-7c-5p	15	hsa-miR-342-3p	15
hsa-miR-92a-3p*	15	hsa-miR-125a-5p	14	hsa-miR-125a-5p	15
hsa-miR-221-3p	15	hsa-miR-9-5p	14	hsa-miR-9-5p	14
hsa-let-7f-5p	15	hsa-miR-29a-3p	14	hsa-miR-382-5p	14
hsa-let-7c-5p	14	hsa-miR-100-5p	14	hsa-miR-27b-3p	14
hsa-miR-30d-5p	14	hsa-miR-30d-5p	13	hsa-let-7e-5p	14
hsa-miR-181a-5p	14	hsa-miR-26a-5p	13	hsa-miR-148a-3p	14
hsa-let-7e-5p	14	**hsa-miR-148a-3p***	13	hsa-miR-409-3p	14
hsa-miR-409-3p	14	hsa-miR-30a-5p	13	hsa-miR-379-5p	14
hsa-miR-21-5p	14	hsa-miR-221-3p	13	hsa-miR-432-5p	14
hsa-miR-92b-3p	14	hsa-miR-191-5p	13	hsa-miR-151a-3p	13
hsa-miR-25-3p	14	hsa-miR-25-3p	13	hsa-miR-26b-5p	13
hsa-miR-23a-3p	13	hsa-miR-151a-3p	13	hsa-miR-24-3p	13
hsa-miR-103a-3p	13	hsa-miR-26b-5p	13	hsa-miR-26a-5p	13
hsa-miR-204-5p	13	hsa-miR-127-3p	13	hsa-miR-99b-5p	12
hsa-miR-26a-5p	13	hsa-miR-99a-5p	13	hsa-miR-191-5p	12
hsa-miR-26b-5p	13	hsa-miR-27b-3p	13	hsa-miR-423-5p	12

Supplementary table 5: Mean Ct values (averaged of three technical replicates) generated by qRT-PCR for each of the four-miRNA investigated, and the c.elegans spike-in gene that was used as an internal control

	miR-21-5p	miR-29B-5p	miR-10a-5p	miR-767-3p	Cel-miR-39
MIO-M1 EV (1)	25.55	25.62	32.93	32.73	19.73
MIO-M1 EV (2)	25.99	25.40	33.25	32.59	19.84
MIO-M1 EV (3)	25.84	25.28	33.58	32.45	19.99
MIO-M1 (1)	28.80	28.85	32.47	28.34	20.52
MIO-M1 (2)	29.01	28.34	32.36	28.59	20.29
MIO-M1 (3)	28.85	28.63	32.77	28.34	20.28
PSC1 EV (1)	23.50	21.80	30.56	27.19	19.87
PSC1 EV (2)	22.95	22.35	30.37	27.55	19.71
PSC1 EV (3)	23.01	22.19	30.68	27.60	19.55
PSC1 (1)	27.33	29.21	32.09	28.06	20.03
PSC1 (2)	27.58	29.19	32.15	28.31	19.92
PSC1 (3)	27.84	29.37	32.13	27.97	19.82

PUBLICATIONS

Published Conference Abstracts

- **Lamb, W. D,** Eastlake, K., Williams, G., Khaw, P. T., & Limb, G. A. (2019). Neuroprotective potential of Müller glia-derived Extracellular Vesicles. Investigative Ophthalmology & Visual Science, 60(9), 621.

- **Lamb, W. D**., Eastlake, K., Khaw, P. T., & Limb, G. A. (2018). Identification of extracellular vesicles released by Müller glial cells in vitro. Investigative Ophthalmology & Visual Science, 59(9), 1496

Book Chapter

- Eastlake, K., Wang, W., **Lamb, W. D**., & Limb, G. A. (2018). Stem Cell Therapies for Retinal Repair and Regeneration. Chapter 12- *Therapies for Retinal Degeneration: Targeting Common Processes*, (66), 196-215. Eds Enrique de la Rosa, Thomas G Cotter. Publisher, Royal Society of Chemistry. (https://doi.org/10.1039/9781788013666)

Book Chapter in press

- **Lamb, W. D**., Limb, G. A. (2020). Müller glia-derived exosomes and their micro-RNA cargo- potential for glaucoma therapies. Handbook of Basic and Clinical Ocular Pharmacology.

Manuscript in revision

- **Lamb W.D,** Luis J, Eastlake K, Khaw PT, Williams G, Limb GA. Potential of Muller glia-derived extracellular vesicles for retinal neuroprotection. Progress in Retinal and Eye Research.